

**Innovative Approaches to Natural Killer Cell Engineering:  
Overcoming Challenges in CRISPR-Cas9 Genome Editing,  
Transgene Expression, and Cryopreservation**

**Dong-Hyeon Jo**

**Thesis submitted to the University of Ottawa  
in partial fulfillment of the requirements for the  
Doctorate of Philosophy in Microbiology and Immunology**

**Department of Biochemistry, Microbiology, and Immunology  
Faculty of Medicine  
University of Ottawa**

## Abstract

Natural killer (NK) cells, crucial players in the innate immune system, hold immense potential for cancer immunotherapy due to their ability to target malignant cells without prior antigen sensitization and their low risk of adverse effects such as graft-versus-host disease (GvHD), cytokine release syndrome (CRS), and neurotoxicity. Despite these advantages, challenges such as suboptimal gene-editing techniques, transgene silencing, and cryopreservation-induced dysfunctions have hindered their clinical application. Here, I addressed these hurdles by integrating innovative approaches: a one-step CRISPR-Cas9-mediated gene knockout paired with therapeutic genes such as chimeric antigen receptor (CAR) and interleukin (IL)-15 transgenesis, achieving simultaneously modified NK cell populations. To counteract transgene silencing, histone deacetylase inhibitors (HDACis) were employed, resulting in sustained CAR expression and enhanced anti-tumor efficacy against multiple myeloma *in vitro* and *in vivo*. Furthermore, optimized cryopreservation protocols implemented during the early expansion phase significantly improved NK cell recovery, viability, and versatility for therapeutic applications. By integrating advanced genetic engineering, epigenetic modulation, and optimized cryopreservation strategies, my thesis establishes a scalable and durable foundation for effective NK cell-based immunotherapies to treat a wide range of cancers.

## Acknowledgment

First and foremost, I would like to express my deepest gratitude to my supervisor, Dr. Seung-Hwan Lee, for his support throughout my Ph.D. journey. Dr. Lee always fosters the success of his students. His guidance and encouragement have been invaluable to me, and I am truly fortunate to have had him as my mentor.

I sincerely thank my Thesis Advisory Committee (TAC) members, Dr. Kevin A. Henry, Dr. Scott McComb, and Dr. Jean-Simon Diallo, for their feedback, encouragement, and priceless support throughout my thesis work. Their time and expertise were an immense source of strength during my journey.

I would also like to acknowledge the members of Dr. Seung-Hwan Lee's lab. In particular, I am deeply thankful to Dr. Abrar Ul Haq Khan and Shelby Kaczmarek, with whom I began this journey. Together, we have witnessed the growth of the lab and shared both the highs and lows of the experience. I am truly fortunate to have had such genuine and supportive colleagues throughout this journey. I wish them, along with all the members of the Lee lab, continued success in their scientific endeavors.

I would also like to thank the University of Ottawa and the Ontario government for their scholarly support throughout my Ph.D. journey. Without the scholarships, I wouldn't have a chance to pursue this degree. I am truly grateful to have had the opportunity to study at the University of Ottawa.

Lastly, I want to express my deepest appreciation to my parents, Un-Jung Jo and Yeon-Suk Kim, my sister, A-Hyeon Jo, my husband, Gordon Tyler Bristow, and his family. My parents and Tyler have been my constant source of support, showing incredible patience and understanding throughout the many long years of work this journey has required. His family, too, has offered me unlimited kindness and support. As an immigrant from South Korea, their acceptance has been invaluable to me, and I would not have been able to reach this point without them.

## Table of Contents

<b>Abstract</b>	<b>ii</b>
<b>Acknowledgment</b>	<b>iii</b>
<b>List of Abbreviations</b>	<b>vii</b>
<b>List of Figures</b>	<b>xii</b>
<b>Chapter 1: General Introduction</b>	<b>1</b>
<b>1.1 Natural killer cells and NK cell receptors</b>	<b>2</b>
1.1.1 Natural killer cells	2
1.1.2 Activating receptors	4
1.1.3 Inhibitory receptors	6
1.1.4 Cytokine receptors	8
<b>1.2 NK cell immunotherapy</b>	<b>10</b>
1.2.1 NK cell sources	13
1.2.2 Chimeric antigen receptor (CAR): CAR-T and CAR-NK cells	14
<b>1.3 NK cell engineering using viral vectors</b>	<b>18</b>
<b>1.4 NK cell expansion</b>	<b>23</b>
<b>1.5 NK cell cryopreservation.</b>	<b>24</b>
<b>1.6 CRISPR-Cas9-mediated genome editing in NK cells</b>	<b>27</b>
<b>1.7 Viral particles loaded with CRISPR-Cas9</b>	<b>29</b>
<b>1.8 Histone deacetylase inhibitors and immunotherapy</b>	<b>33</b>
<b>1.9 Histone deacetylase inhibitors in viral promoter activity</b>	<b>35</b>
<b>1.10 Rationale and Research Objectives</b>	<b>38</b>
<b>Chapter 2. Simultaneous Engineering of Natural Killer Cells for CAR Transgenesis and CRISPR-Cas9 Knockout Using Retroviral Particles</b>	<b>40</b>
<b>2.1 Abstract</b>	<b>43</b>
<b>2.2 Introduction</b>	<b>44</b>
<b>2.3 Materials and Methods</b>	<b>46</b>
2.3.1 Culture of human cell lines	46
2.3.2 Isolation and culture of human pNK cells	47
2.3.3 Plasmid construction	47
2.3.4 BaEV pseudotyped lentiviral vector production	48
2.3.5 Cas9-RNP and transgene-loaded RP production	49
2.3.6 Flow virometry	49
2.3.7 NK92 cell transduction	50
2.3.8 Human primary NK cell transduction	51
2.3.9 Flow cytometry and antibodies	51
2.3.10 NK cell functional assay	52

2.3.11 Genomic analysis _____	53
2.3.12 <i>In vivo</i> tumor control _____	53
2.3.13 Statistical analysis and graph generation _____	54
<b>2.4 Results _____</b>	<b>54</b>
2.4.1 Efficient Cas9-sgRNA delivery to NK cells through BaEV-TR and VSV-G envelope glycoprotein pseudotyped retroviral particles _____	54
2.4.2 Cas9-sgRNA delivery to pNK cells using RPs efficiently abrogates TIGIT expression _____	58
2.4.3 Cas9-RNP-loaded RPs can induce <i>TIGIT</i> gene knockout and anti-EGFR-CAR transgenesis simultaneously _____	61
2.4.4 TIGIT knockout does not improve human NK cell function <i>in vitro</i> and <i>in vivo</i> _____	63
2.4.5 Cas9-RNP containing RPs allow site-specific CAR integration into the NK cell genome _____	66
<b>2.5 Discussion _____</b>	<b>68</b>
<b>Chapter 3: Entinostat, a Histone Deacetylase Inhibitor, Enhances CAR-NK Cell Anti-Tumor Activity by Sustaining CAR Expression _____</b>	<b>72</b>
<b>3.1 Abstract _____</b>	<b>75</b>
<b>3.2 Introduction _____</b>	<b>76</b>
<b>3.3 Materials and Methods _____</b>	<b>78</b>
3.3.1 Cancer cell line culture _____	78
3.3.2 Generation of master stocks of human primary NK cells _____	79
3.3.3 Molecular Cloning _____	79
3.3.4 Retroviral and lentiviral vector production _____	81
3.3.5 Primary NK cell transduction and expansion _____	81
3.3.6 Immunostaining _____	82
3.3.7 Puromycin staining _____	83
3.3.8 <i>In vitro</i> CD107a, IFN- $\gamma$ and TNF- $\alpha$ assays _____	83
3.3.9 <i>In vitro</i> killing assay _____	83
3.3.10 Histone deacetylase inhibitor treatment _____	84
3.3.11 <i>In vivo</i> tumor control experiments _____	85
3.3.12 Statistical analysis _____	85
<b>3.4 Results _____</b>	<b>86</b>
3.4.1 NK cells from a cryopreserved master stock are expandable <i>ex vivo</i> and suitable for CAR engineering _____	86
3.4.2 Anti-CD138 CAR enhances NK cell function <i>in vitro</i> ; however, CAR expression decreases during expansion <i>ex vivo</i> _____	89
3.4.3 Histone deacetylase inhibitors enhance GFP and CAR expression in NK cells in a dose- and promoter-dependent manner _____	93
3.4.4 Entinostat treatment reduces the background of NK cell degranulation but does not affect CAR-mediated NK cell degranulation _____	96
3.4.5 ENT treatment of CAR-pNK cells during expansion <i>ex vivo</i> upregulates CAR expression and improves target cell lysis. _____	99
3.4.6 ENT-treated CAR-overexpressing pNK cells show enhanced anti-myeloma activity <i>in vitro</i> and <i>in vivo</i> _____	102
<b>3.5 Discussion _____</b>	<b>106</b>

<b>Chapter 4: CD38 Knockout Using CRISPR-Cas9-Loaded Retroviral Particles Reduces Daratumumab-Mediated NK Cell Fratricide, Leading to Improved Multiple Myeloma Clearance</b>	<b>109</b>
<b>4.1 Abstract</b>	<b>111</b>
<b>4.2 Introduction</b>	<b>112</b>
<b>4.3 Materials and Methods</b>	<b>114</b>
4.3.1 Cancer cell line culture	114
4.3.2 Generation of master stocks of human primary NK cells	115
4.3.3 Retroviral and lentiviral vector production	115
4.3.4 Primary NK cell transduction and expansion	116
4.3.5 Immunostaining	116
4.3.6 <i>In vitro</i> apoptosis assay	116
4.3.7 <i>In vitro</i> killing assay	117
4.3.8 <i>In vivo</i> NK cell survival experiments	117
4.3.9 Statistical analysis	118
<b>4.4 Results</b>	<b>118</b>
4.4.1 CRISPR-Cas9-loaded retroviral particles successfully abrogate CD38 expression in NK cells.	118
4.4.2 CD38 <sup>KO</sup> improves NK cell cytotoxicity against multiple myeloma while reducing NK cell fratricide	121
4.4.3 CD38 <sup>KO</sup> NK cells improve NK cell survival in the presence of daratumumab, while IL-15 engineering facilitates NK cell expansion <i>in vivo</i> .	123
4.4.4 Simultaneous engineering of NK cells with GFP-IL-15 and CD38 <sup>KO</sup> significantly reduces NK cell fratricide and enhances NK cell expansion <i>in vivo</i> .	126
<b>4.5 Discussion</b>	<b>128</b>
<b>Chapter 5: Discussion and Future Directions</b>	<b>131</b>
<b>5.1 NK cell engineering and immunotherapy</b>	<b>132</b>
<b>5.2 NK cell expansion, cryopreservation, and population diversity</b>	<b>133</b>
<b>5.3 CRISPR-Cas9-loaded retroviral particles for NK cell engineering</b>	<b>136</b>
<b>5.4 Histone deacetylase inhibitors in NK cell engineering and transgene expression</b>	<b>139</b>
<b>Final Chapter: Concluding Remarks with Graphical Synopsis</b>	<b>143</b>
<b>References</b>	<b>148</b>
<b>Appendix</b>	<b>177</b>
<b>Supplementary Figures</b>	<b>177</b>
<b>Curriculum Vitae: Dong-Hyeon Jo</b>	<b>184</b>

## List of Abbreviations

<b>AAV</b>	Adeno-Associated Virus
<b>Ab</b>	Antibody
<b>Ad</b>	Adenovirus
<b>ADCC</b>	Antibody Dependent Cellular Cytotoxicity
<b>ADCP</b>	Antibody Dependent Cellular Phagocytosis
<b>ADPR</b>	Adenosine Diphosphate Ribose
<b>Allo</b>	Allogeneic
<b>AML</b>	Acute Myeloid Leukemia
<b>ASCT</b>	Alanine Serine Cysteine Transporter
<b>B7-H6</b>	B7 Homolog 6
<b>BaEV-G</b>	Baboon Endogenous Retroviral Glycoprotein
<b>BAT3</b>	HLA-B Associated Transcript 3
<b>BCL-2</b>	B-Cell Lymphoma 2
<b>BCL-XL</b>	B-Cell Lymphoma-Extra Large
<b>BCMA</b>	B Cell Maturation Antigen
<b>bENT</b>	Brief Entinostat-treatment
<b>BMP4</b>	Bone Morphogenetic Protein 4
<b>BMSC</b>	Bone Marrow Stromal Cells
<b>cADPR</b>	Cyclic ADP-Ribose
<b>CAR</b>	Chimeric Antigen Receptor
<b>Cas9</b>	CRISPR-Associated Protein 9
<b>CBP</b>	CREB Binding Protein
<b>CCR7</b>	C-C Chemokine Receptor 7
<b>CD3<math>\zeta</math></b>	CD3 Zeta Chain

<b>CDC</b>	Complement Dependent Cytotoxicity
<b>CIML</b>	Cytokine-Induced Memory-Like
<b>CLL</b>	Chronic Lymphocytic Leukemia
<b>CMV</b>	Cytomegalovirus
<b>CoREST</b>	Co-Repressor for Element-1 Silencing Transcription Factor
<b>CRi</b>	CR with Incomplete Hematological Recovery
<b>CRISPR</b>	Clustered Regularly Interspaced Short Palindromic Repeats
<b>CRRNA</b>	CRISPR RNA
<b>CRS</b>	Cytokine Release Syndrome
<b>DAP10</b>	DNAX-Activating Protein 10
<b>DAP12</b>	DNAX-Activating Protein 12
<b>DC</b>	Dendritic Cells
<b>dCAS9</b>	Catalytically Dead Cas9
<b>DS</b>	DMEM/F-12 Supplement
<b>DSB</b>	Double-Strand Break
<b>E2F</b>	Early Region 2 Binding Factor
<b>EFS</b>	Elongation Factor 1-alpha Small Promoter
<b>EGFP</b>	Enhanced Green Fluorescent Protein
<b>EGFR</b>	Epidermal Growth Factor Receptor
<b>ELISA</b>	Enzyme-Linked Immunosorbent Assay
<b>ELN</b>	European LeukemiaNet
<b>EMX1</b>	Empty Spiracles Homeobox 1
<b>ENT</b>	Entinostat
<b>ER</b>	Estrogen Receptor
<b>ERK</b>	Extracellular Signal-Regulated Kinase
<b>FcεR1-γ</b>	Fc Epsilon Receptor 1 Gamma

<b>FcγRIIIα</b>	Fc Gamma Receptor IIIα
<b>FLT3L</b>	Fms-Related Tyrosine Kinase 3 Ligand
<b>Gag-Cas9</b>	Gag-conjugated CRISPR-Associated Protein 9
<b>gDNA</b>	Genomic DNA
<b>GM-CSF</b>	Granulocyte-Macrophage Colony-Stimulating Factor
<b>GNAT</b>	GCN5-Related N-Acetyltransferase
<b>GOX/CAT</b>	Glucose Oxidase/Catalase
<b>GvHD</b>	Graft-versus-Host Disease
<b>GvL</b>	Graft-versus-Leukemia
<b>HAT</b>	Histone Acetyltransferase
<b>HbF</b>	Fetal Hemoglobin
<b>HbS</b>	Sicking Hemoglobin
<b>HCC</b>	Hepatocellular Carcinoma
<b>HCMV</b>	Human Cytomegalovirus
<b>HDAC</b>	Histone Deacetylase
<b>HDACi</b>	Histone Deacetylase Inhibitor
<b>HDR</b>	Homology-Directed Repair
<b>HER2</b>	Human Epidermal Growth Factor Receptor 2
<b>HLA</b>	Human Leukocyte Antigen
<b>HSCT</b>	Hematopoietic Stem Cell Transplantation
<b>HSPC</b>	Hematopoietic Stem and Progenitor Cells
<b>ICE</b>	Inference of CRISPR Edits
<b>IFN-γ</b>	Interferon-Gamma
<b>IgG</b>	Immunoglobulin G
<b>ILC</b>	Innate Lymphoid Cells
<b>IPSC</b>	Induced Pluripotent Stem Cells

<b>IRAK</b>	Interleukin-1 Receptor Associated Kinase
<b>ITAM</b>	Immunoreceptor Tyrosine-Based Activation Motif
<b>ITIM</b>	Immunoreceptor Tyrosine-Based Inhibition Motif
<b>ITT</b>	Immunoglobulin Tail Tyrosine
<b>iwCLL</b>	International Workshop on CLL
<b>JAK</b>	Janus Kinase
<b>KIRs</b>	Killer-Cell Immunoglobulin-Like Receptors
<b>KO</b>	Knockout
<b>LCK</b>	Lymphocyte-Specific Protein Tyrosine Kinase
<b>LCL</b>	Lymphoblastoid Cell Line
<b>LDL-R</b>	Low-Density Lipoprotein Receptor
<b>MAPK</b>	Mitogen-Activated Protein Kinase
<b>mb</b>	Membrane-Bound
<b>MDSC</b>	Myeloid-Derived Suppressor Cells
<b>MEK</b>	Mitogen-Activated Protein Kinase
<b>MHC</b>	Major Histocompatibility Complex
<b>MICA/B</b>	MHC Class I Chain-Related Proteins A and B
<b>MLV</b>	Murine Leukemia Virus
<b>MM</b>	Multiple Myeloma
<b>MOI</b>	Multiplicity of Infection
<b>MSCV</b>	Murine Stem Cell Virus
<b>mTOR</b>	Mammalian Target of Rapamycin
<b>MYD88</b>	Myeloid Differentiation Primary Response 88
<b>NaB</b>	Sodium Butyrate
<b>NAD</b>	Nicotinamide Adenine Dinucleotide
<b>NB</b>	Nanoblade

<b>NCRs</b>	Natural Cytotoxicity Receptors
<b>NF-<math>\kappa</math>B</b>	Nuclear Factor Kappa-Light-Chain-Enhancer of Activated B Cells
<b>NHEJ</b>	Non-Homologous End Joining
<b>NHL</b>	Non-Hodgkin Lymphoma
<b>NK</b>	Natural Killer
<b>KLRK1</b>	Killer Cell Lectin-Like Receptor K1
<b>NSCLC</b>	Non-Small Cell Lung Cancer
<b>NuRD</b>	Nucleosome Remodeling and Deacetylase
<b>ORR</b>	Overall Response Rate
<b>PAMP</b>	Pathogen-Associated Molecular Patterns
<b>PARP1</b>	Poly (ADP-Ribose) Polymerase 1
<b>PB</b>	Peripheral Blood
<b>PBNK</b>	Peripheral Blood-Derived Natural Killer Cells
<b>PBS</b>	Phosphate-Buffered Saline
<b>PD</b>	Progressive Disease
<b>PI3-K</b>	Phosphoinositide 3-Kinase
<b>PKB</b>	Protein Kinase B
<b>PMAIP1</b>	Phorbol-12-Myristate-13-Acetate-Induced Protein 1
<b>PPT</b>	PSMA Enhancer and the TARP Promoter
<b>PR</b>	Partial Response
<b>PRR</b>	Pattern Recognition Receptor
<b>Ras</b>	Rat Sarcoma Viral Oncogene
<b>RECIST</b>	Response Evaluation Criteria in Solid Tumors
<b>RGFP</b>	RGFP966
<b>RNP</b>	Ribonucleoprotein
<b>ROBO1</b>	Roundabout Guidance Receptor 1

## List of Figures

<b>Figure 1.1</b>	Activating and inhibitor receptor-mediated NK cell functional regulation.	<b>4</b>
<b>Figure 1.2</b>	Intracellular signaling domains of the chimeric antigen receptor (CAR) and their origins.	<b>15</b>
<b>Figure 1.3</b>	Challenges in NK cell engineering and novel strategies to enhance transduction using viral vectors.	<b>22</b>
<b>Figure 1.4.</b>	Graphical summary of the NK cell immunotherapy process.	<b>26</b>
<b>Figure 1.5</b>	Production of VLPs containing Cas9-RNPs using lentiviral or retroviral systems.	<b>32</b>
<b>Figure 1.6</b>	HDAC inhibitor (HDACi) effects on chromatin relaxation and application in viral vector-mediated transgene delivery.	<b>37</b>
<b>Figure 2.1</b>	Graphical abstract for Chapter 2	<b>42</b>
<b>Figure 2.2</b>	VSV-G and BaEV-TR envelopes pseudotyped RPs efficiently targeted the EGFP gene in EGFP-NK92 cells.	<b>57</b>
<b>Figure 2.3</b>	Anti-TIGIT RPs abrogated TIGIT expression in primary human NK cells.	<b>60</b>
<b>Figure 2.4</b>	Simultaneous <i>TIGIT</i> gene knockout and CAR integration into an NK cell genome by Cas9-RNP-loaded RPs.	<b>63</b>
<b>Figure 2.5</b>	TIGIT knockout failed to enhance the anti-tumor activity of human NK cell function <i>in vitro</i> and <i>in vivo</i> .	<b>65</b>
<b>Figure 2.6</b>	Site-specific CAR integration into an NK cell genome by Cas9-sgRNA RPs.	<b>67</b>
<b>Figure 3.1</b>	Graphical abstract for Chapter 3	<b>74</b>
<b>Figure. 3.2</b>	Cryopreserved master stock NK cells can be expanded and engineered for CAR therapy.	<b>88</b>
<b>Figure. 3.3</b>	Functionality and CAR expression of anti-CD138-CAR engineered NK cells.	<b>92</b>
<b>Figure. 3.4</b>	Enhanced CAR expression in NK cells with the treatment of histone deacetylase inhibitors.	<b>95</b>
<b>Figure. 3.5</b>	CAR maintenance, degranulation, and survival of ENT-treated NK cells <i>in vitro</i> .	<b>98</b>

<b>Figure. 3.6</b>	The CAR and NK cell phenotypes after long-term ENT treatment. _____	<b>101</b>
<b>Figure. 3.7</b>	Anti-tumor activity of CAR-NK cells treated with ENT <i>in vitro</i> and <i>in vivo</i> . _____	<b>104</b>
<b>Figure 4.1</b>	Graphical abstract for Chapter 4 _____	<b>110</b>
<b>Figure 4.2</b>	Efficient CD38 knockout (CD38 <sup>KO</sup> ) in NK cells using Cas9-RNP-loaded retroviral particles (RPs) and electroporation. _____	<b>120</b>
<b>Figure 4.3</b>	CD38 <sup>KO</sup> enhances daratumumab-mediated NK cell cytotoxicity while preventing NK cell fratricide. _____	<b>122</b>
<b>Figure 4.4</b>	CD38 <sup>KO</sup> and IL-15 enhance NK cell survival <i>in vivo</i> . _____	<b>125</b>
<b>Figure 4.5</b>	Simultaneous engineering of NK cells with GFP-IL-15 and CD38 <sup>KO</sup> enhances survival and expansion. _____	<b>127</b>
<b>Figure 5.1</b>	Post-NK cell expansion phenotypes using various culture conditions. ____	<b>136</b>
<b>Figure 5.2</b>	Flow virometry-based detection of Cas9 in viral particles. _____	<b>139</b>
<b>Figure 5.3</b>	Future directions for NK cell engineering using MSCV and CMV promoters and HDACi. _____	<b>142</b>
<b>Figure 6.1</b>	Graphical summary of Chapters 2 and 4. Simultaneous engineering of natural killer cells for CAR transgenesis and CRISPR-Cas9 knockout using retroviral particles. _____	<b>145</b>
<b>Figure 6.2</b>	Graphical summary of Chapter 3: Entinostat, a histone deacetylase inhibitor, enhances CAR-NK cell anti-tumor activity by sustaining CAR expression. _____	<b>146</b>
<b>Figure S1</b>	The number of retroviral particles (RPs) for human primary NK cell TIGIT knockout. _____	<b>177</b>
<b>Figure S2</b>	Size of RPs. _____	<b>178</b>
<b>Figure S3</b>	Determination of EGFR and TIGIT-ligand expression, CD112 and CD155, on various cancer cells. _____	<b>179</b>
<b>Figure S4</b>	NK cell population markers in continuously expanded and early cryo-preserved-expanded NK cells. _____	<b>180</b>
<b>Figure S5</b>	CD138 expression in target cells and pNK cell CAR functionality. ____	<b>181</b>
<b>Figure S6</b>	Histone deacetylase inhibitor (HDACi) toxicity. _____	<b>182</b>
<b>Figure S7</b>	Phenotypes of ENT-treated NK cells. _____	<b>183</b>

# **Chapter 1: General Introduction**

**Figures were generated using Biorender.com.**

## 1.1 Natural killer cells and NK cell receptors

### 1.1.1 Natural killer cells

Natural killer (NK) cells are essential players in the innate immune system, providing a rapid and direct response to infected or malignant cells.<sup>1</sup> They serve as a primary line of defense, utilizing two main strategies to combat infection and cancer. The first involves the targeted killing of abnormal cells through direct lysis. Perforins and granzymes are involved in this process by creating perforin-mediated membrane pores, facilitating granzyme cytosol invasion, and activating cell death pathways.<sup>2</sup> The second strategy relies on the release of pro-inflammatory cytokines such as tumor necrosis factor-alpha (TNF- $\alpha$ ), granulocyte-macrophage colony-stimulating factor (GM-CSF), and interferon- $\gamma$  (IFN- $\gamma$ ), inducing inflammation at the site of infection or malignancy.<sup>1,3</sup> These cytokines activate innate immune cells such as neutrophils and macrophages, which further activate T and B cells, bridging the innate and adaptive immune responses.<sup>1,4-7</sup>

NK cells are traditionally classified into two subsets in humans: CD56<sup>bright</sup> and CD56<sup>dim</sup>, a distinction first characterized by Lanier et al. in the 1980s.<sup>8,9</sup> CD56<sup>dim</sup> NK cells, which constitute approximately 90% of circulating NK cells in peripheral blood, are highly cytotoxic due to their elevated levels of perforin and granzymes.<sup>1,10</sup> In contrast, CD56<sup>bright</sup> NK cells, though they are less cytotoxic, express abundant cytokine receptors such as interleukin-2 receptor alpha chain (IL-2R $\alpha$ ) and IL-18R, priming them to respond robustly to cytokine stimulation.<sup>1,11</sup> This responsiveness enables them to produce large quantities of cytokines like TNF- $\alpha$ , GM-CSF, and IFN- $\gamma$ , thereby orchestrating broader immune responses.<sup>12,13</sup> Unlike CD56<sup>dim</sup> NK cells, which account for the majority of circulating NK

cells, CD56<sup>bright</sup> NK cells are predominantly found in secondary lymphoid tissues, including lymph nodes and tonsils.<sup>14</sup> Additionally, evidence suggests that CD56<sup>bright</sup> NK cells can differentiate into CD56<sup>dim</sup> NK cells, indicating a developmental relationship between these subsets.<sup>15</sup> Advancements in single-cell analysis have further refined the understanding of NK cell heterogeneity. In 2024, Rebuffet et al. employed high-dimensional single-cell techniques to identify six prominent NK cell subsets in healthy human blood with distinct molecular and functional profiles.<sup>16</sup>

The functionality of NK cells hinges on a finely tuned interplay between activating and inhibitory receptors.<sup>1</sup> This balance is crucial for preventing damage to healthy cells while allowing for the elimination of infected and stressed ones. The recognition mechanisms of NK cells rely heavily on inhibitory receptors, consistent with the “missing-self” hypothesis to identify targets.<sup>17,18</sup> NK cell inhibitory receptors widely recognize major histocompatibility complex (MHC) class I molecules.<sup>18-20</sup> Cells that downregulate MHC class I molecules, a common evasion tactic of infected or malignant cells from T cells, are flagged for destruction as activating signals overwhelm the absence of inhibitory signals.<sup>1</sup> This regulated surveillance mechanism ensures NK cells can efficiently eliminate threats while preserving the integrity of normal tissues expressing MHC class I, reinforcing their role as dynamic and essential sentinels of immune defense (**Figure 1.1**).

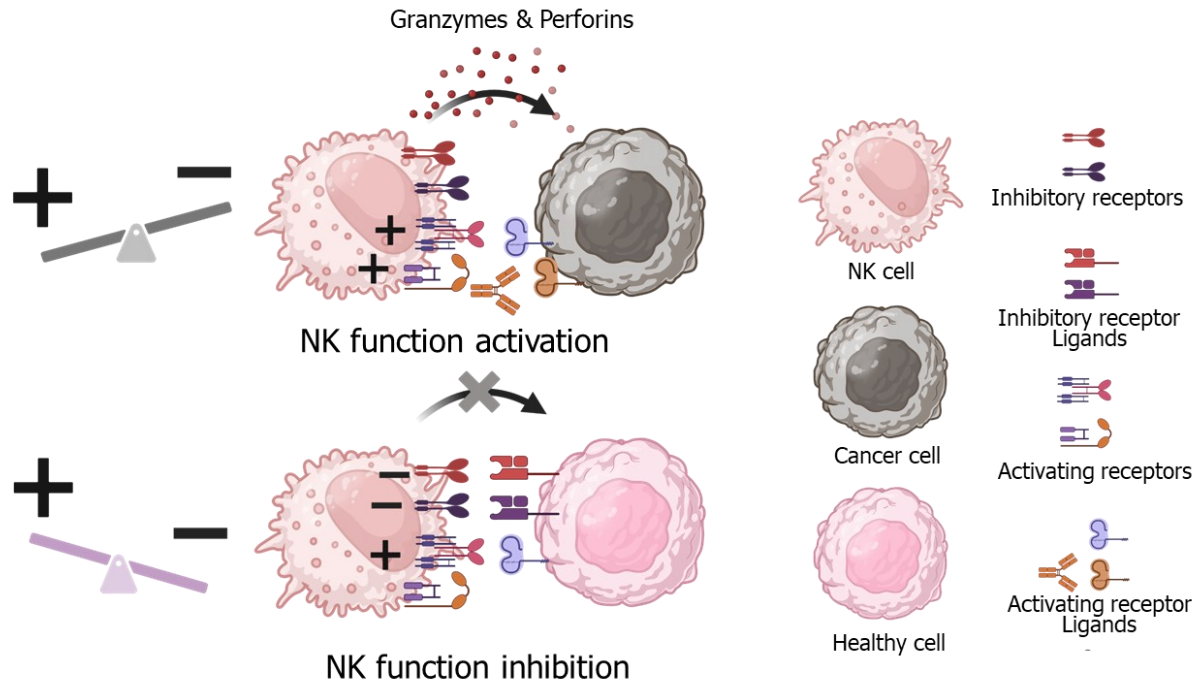


**Figure 1.1 Activating and inhibitory receptor-mediated NK cell functional regulation.** The functional regulation of NK cells is determined by the balance between activating and inhibitory receptor signals. When inhibitory signals from target cells are reduced, NK cells activate their cytolytic functions. Healthy cells expressing MHC class I molecules provide abundant inhibitory signals, preventing NK cell activation and maintaining immune tolerance.

### 1.1.2 Activating receptors

Natural cytotoxicity receptors (NCRs), such as NKp30, NKp44, and NKp46, are key drivers of NK cell activation.<sup>21,22</sup> These receptors, members of the immunoglobulin superfamily, enable NK cells to recognize and attack stressed, infected, or cancerous cells by detecting specific ligands.<sup>21</sup> NKp46 and NKp44 are mostly found on NK cells, while NKp30 also appears on many types of T cells.<sup>23,24</sup> NKp30 and NKp46 are present on resting and activated NK cells, whereas NKp44 becomes expressed when NK cells are activated.<sup>21,25</sup> Finding ligands that interact with NCRs has been challenging because of their varied

recognition abilities, but some have been identified, like B7 homolog 6 (B7-H6), which binds to NKp30 in stressed cells, and ecto-calreticulin, which serves as a ligand for NKp46 in cells experiencing endoplasmic reticulum stress.<sup>21,26</sup> Additionally, various viral and cellular factors can affect how NCRs function. For instance, the nuclear protein HLA-B-associated transcript 3 (BAT3) can either suppress NCR expression or stimulate NKp30, depending on its isoform.<sup>21,27</sup> NCRs signal through adaptor proteins that contain immunoreceptor tyrosine-based activation motifs (ITAMs). NKp30 and NKp46 use adaptors like FcεR1-gamma (FcεR1-γ) or CD3 zeta (CD3ζ), while NKp44 relies on DNAX-activating protein of 12 kDa (DAP12), another ITAM-containing protein.<sup>21,28</sup> When activated, ITAMs are phosphorylated, and zeta-chain-associated protein kinase 70 (ZAP70) is recruited to initiate a signaling cascade that involves molecules like the nuclear factor kappa-light-chain-enhancer of activated B cells (NF-κB) and the nuclear factor of activated T cells (NFAT), which promote the expression of genes for NK cell activation.<sup>28</sup>

Killer Cell Lectin-Like Receptor K1 (KLRK1, also known as NKG2D), a homodimer C-type lectin-like receptor, plays a key role in activating NK cells and cytotoxic T cells.<sup>21,28</sup> As part of the CD94/NKG2 family, NKG2D recognizes stress-induced ligands like MHC class I chain-related proteins A and B (MICA/B) and UL16 binding proteins (ULBPs), which are upregulated on infected or cancerous cells.<sup>29</sup> NKG2D utilizes a distinct signaling pathway via the adaptor molecule DNAX-activating protein 10 (DAP10), which contains a YxxM motif instead of the ITAM motif used by other activating receptors.<sup>28,30,31</sup> The YxxM motif transmits signals through phosphoinositide 3-kinases (PI3-K) and Ca<sup>2+</sup> influx.<sup>30,32</sup> This unique signaling pathway allows NKG2D to engage different downstream mechanisms critical for immune responses against cancerous and stressed cells.

Fc gamma receptor IIIa (FcγRIIIa, CD16), encoded by the *FCGR3A* gene, is pivotal in mediating antibody-dependent cellular cytotoxicity (ADCC).<sup>21,33</sup> The constant domain of an antibody on antibody-coated infected or tumor cells interacts with CD16.<sup>21,33</sup> CD16 signals through the ITAM within its associated FcεR1-γ and CD3ζ chains, activating NK cells upon recognizing antibody-coated target cells.<sup>30</sup> Unique NK cells in CMV-seropositive donors exhibit more extensive ADCC functionality than other NK cells.<sup>34</sup> These NK cells lack the expression of FcεR1-γ and instead exclusively utilize the CD3ζ chain as their primary signaling molecule. The CD3ζ chain, with its three ITAMs, induces stronger signaling pathways, whereas FcεR1-γ has only one ITAM motif, presumably explaining the superior ADCC of FcεR1-γ-lacking NK cells.<sup>35,36</sup> CD16a polymorphisms, such as the 158V/F variant, impact immunoglobulin G (IgG) binding affinity and ADCC efficacy.<sup>37</sup> The 158V variant exhibits superior IgG binding and enhanced ADCC, contributing to improved clinical outcomes in targeted therapies using the CD20-targeting antibody, rituximab.<sup>38</sup>

### 1.1.3 Inhibitory receptors

NK cells possess a wide array of innate receptors mediating cytotoxicity, raising questions about how they distinguish between healthy and abnormal cells. Central to this process is a signaling balance mechanism, where the synergistic interaction of multiple receptors is required to initiate cytotoxicity while ensuring that NK cells do not attack healthy cells.<sup>21,39</sup> Inhibitory receptors, primarily through interactions with MHC class I molecules on healthy cells, provide counterbalancing signals that override activation, preventing NK cells from attacking normal tissues.<sup>21</sup> This balance is crucial for maintaining self-tolerance and avoiding autoimmunity.<sup>40</sup> Although many activating receptor ligands are upregulated in

infected or cancerous cells, some can also be found in healthy cells, such as the ligand for NKp44 expressed by normal human articular chondrocytes.<sup>41,42</sup> However, the inhibitory signals from MHC class I molecules ensure that NK cells remain tightly regulated, preventing inappropriate cytotoxic responses even in the presence of activating ligands.<sup>21</sup>

In humans, two main classes of inhibitory receptors control NK cell activity: the killer-cell immunoglobulin-like receptors (KIRs, DL family) and the CD94-NKG2A heterodimer.<sup>19,20</sup> KIRs are transmembrane receptors with extracellular Ig-like domains that recognize human leukocyte antigens (HLA)-A/B/C molecules on target cells, while NKG2A, a single-pass type II transmembrane receptor belonging to the C-type lectin family, binds to HLA-E molecules.<sup>21,43,44</sup> KIR and NKG2A transmit inhibitory signals via immunoreceptor tyrosine-based inhibitory motifs (ITIMs) containing the conserved V/IxYxxL/V motif.<sup>22,45</sup> ITIM-bearing receptors preferentially recruit the tyrosine phosphatases the Src homology region 2 domain-containing phosphatase-1 (SHP-1) and SHP-2 in NK cells, with SHP-1 being the primary phosphatase involved in NK cell inhibition.<sup>22,45</sup> SHP-1 works by dephosphorylating key signaling molecules involved in NK cell activation.<sup>46</sup> Structurally, SHP-1 contains two tandem Src homology 2 (SH2) domains, followed by a catalytic domain and a C-terminal tail.<sup>47</sup> SHP-1 is auto-inhibited by an interaction between its N-terminal SH2 and catalytic domains. When the SH2 domains of SHP-1 interact with the phosphorylated tyrosines within the ITIMs, this interaction relieves SHP-1 from its auto-inhibited conformation and activates catalytic activity.<sup>47,48</sup> Activated SHP-1 leads to dephosphorylation of ZAP70 and lymphocyte cell-specific protein-tyrosine kinase (LCK).<sup>49,50</sup> This dephosphorylation effectively silences the activation signals from NK cell receptors, ensuring

that NK cells are regulated by cells expressing MHC class I molecules, thereby maintaining immune homeostasis.<sup>51</sup>

### 1.1.4 Cytokine receptors

The interaction between cytokines and NK cells is essential for triggering NK cell activation and promoting an effective cytotoxic response.<sup>52</sup> IL-2 and IL-15 are particularly crucial for the activation, survival, and proliferation of NK cells.<sup>52,53</sup> These cytokines bind to receptor complexes composed of two shared subunits, IL-2R $\beta$  and IL-2R $\gamma$ , with each cytokine utilizing a distinct additional subunit: IL-2R $\alpha$  for IL-2 and IL-15R $\alpha$  for IL-15.<sup>53,54</sup> Upon receptor engagement, intracellular signaling pathways are activated, including phosphorylation of Janus kinase 1 (JAK1) (via IL-2R $\beta$ ) and JAK3 (via IL-2R $\gamma$ ), leading to signal transducer and activator of transcription 5 (STAT5) dimerization and activation of the PI3-K-protein kinase B (PKB) and mitogen-activated protein kinase (MAPK) pathways.<sup>53,54</sup> These signals drive NK cell metabolism and the transcription of survival and proliferation genes like B-cell leukemia/lymphoma 2 protein (BCL-2) and BCL-x.<sup>55</sup> Additionally, IL-2 and IL-15 are critical for enhancing NK cell cytotoxicity.<sup>52,53</sup> Through IL-2 and IL-15 signaling, NK cells overexpress activating receptors such as NKG2D and NKp44, along with perforin and granzymes, amplifying their ability to eliminate target cells effectively.<sup>56</sup>

In addition to IL-2 and IL-15, IL-12 and IL-18 are critical for enhancing NK cell cytotoxic functions.<sup>57</sup> IL-12, produced by macrophages and dendritic cells (DCs), phosphorylates JAK2 and tyrosine kinase 2 (Tyk2), leading to the activation of STAT4 pathway, which is crucial for inducing IFN- $\gamma$  expression.<sup>57-59</sup> In contrast to JAK-STAT signaling, IL-18 signaling involves an unconventional pathway through myeloid

differentiation primary response 88 (MyD88), which activates the interleukin-1 receptor-associated kinase (IRAK) and tumor necrosis factor receptor-associated factor 6 (TRAF-6) pathways, leading to NF- $\kappa$ B and MAPK activation.<sup>60-62</sup> This transcriptional activation promotes NK cell metabolism and proliferation more effectively than IL-2 alone.<sup>63</sup> Notably, IL-12 and IL-18 synergistically induce robust IFN- $\gamma$  production in NK cells compared to either cytokine alone.<sup>57</sup> IL-18 also enhances NK cell migration to tumor sites by upregulating the C-C Chemokine Receptor 7 (CCR7) receptor, facilitating their localization within lymphoid tissues.<sup>64</sup>

TNF- $\alpha$  promotes NK cell proliferation and activation, especially by interacting with TNF receptor 2 (TNFR2).<sup>65</sup> The TNF $\alpha$ -TNFR2 signaling (TRAF1/2) axis enhances NK cell metabolic activity by driving aerobic glycolysis, which fuels increased proliferation and effector function.<sup>65,66</sup> This signaling upregulates CD25 expression, making NK cells more responsive to lower concentrations of IL-2. Additionally, IL-18 can upregulate TNFR2 expression on NK cells, increasing their sensitivity to TNF- $\alpha$ . When combined, IL-18 and TNF- $\alpha$  synergistically enhance NK cell proliferation, metabolism, and activation.<sup>65,67</sup> This combination promotes greater glucose uptake and nutrient transporter expression, optimizing NK cell functionality.

Although therapies that stimulate NK cells with cytokines like IL-2, IL-15, IL-12, IL-18, and TNF- $\alpha$  have shown promise in NK cell activation, their effectiveness is often compromised by the immunosuppressive cytokine, transforming growth factor-beta (TGF- $\beta$ ).<sup>68,69</sup> TGF- $\beta$  utilizes the suppressor of mothers against decapentaplegic (SMAD) signaling pathway, an immunosuppressive gene regulator that limits NK cell proliferation and

cytotoxicity by suppressing the mammalian target of rapamycin (mTOR) pathway.<sup>68,70</sup> In the presence of cytokines like IL-15, TGF- $\beta$  blocks mTOR activity, reducing NK cell metabolic activity, proliferation, and the expression of critical receptors.<sup>68,70-72</sup> This suppression reduces NK cell responses by downregulating granzyme B, leading to lowering their tumor-killing capacity.<sup>72</sup> Elevated TGF- $\beta$  concentrations in the tumor microenvironment (TME) can also convert NK cells to type 1 innate lymphoid cell (ILC1)-like cells, weakening their antitumor functions.<sup>73-75</sup>

## 1.2 NK cell immunotherapy

Adoptive cell therapies have emerged as highly effective strategies to harness the immune system's natural ability to combat cancer.<sup>1</sup> Among the diverse immune cell types, NK cells are particularly notable for their inherent capacity to recognize and eliminate tumor cells without requiring prior antigen-specific sensitization.<sup>1,76</sup> This unique capability is regulated by a finely tuned balance of activating and inhibitory signals mediated through receptors such as NKG2D, NCR, NKG2A, and KIR, which enable NK cells to target malignant cells while sparing healthy tissues selectively.<sup>19-21,28</sup> Unlike T cell-mediated therapies, often associated with substantial risks of immune-related adverse effects, NK cell therapies offer a safety profile.<sup>77,78</sup> This is largely due to their intrinsic mechanisms for distinguishing between malignant and non-malignant cells, significantly reducing the likelihood of severe complications such as cytokine release syndrome (CRS) and neurotoxicity, frequently observed in T cell-based treatments.<sup>79,80</sup> Moreover, NK cells can be derived from healthy donors for use in allogeneic settings without causing graft-versus-host disease (GvHD), a major challenge in the traditional allogeneic cell therapy.<sup>80,81</sup> This feature makes NK cells particularly well-suited for developing "off-the-shelf" products that are both

scalable and readily accessible, addressing manufacturing constraints in personalized medicine.<sup>82</sup> NK cells also have advantages with monoclonal antibodies, enhancing therapeutic efficacy through ADCC.<sup>38</sup> These properties, with their safety, scalability, and ability to integrate with other immunotherapies, potentiate NK cells for effective cancer treatment.

To understand cancer treatment outcomes, especially regarding solid tumors and hematological malignancies such as acute myeloid leukemia (AML) and chronic lymphocytic leukemia (CLL), it is essential to explore how clinical treatment outcomes are scientifically measured. For solid tumors, the Response Evaluation Criteria in Solid Tumors (RECIST 1.1) framework is commonly utilized.<sup>83</sup> According to the RECIST 1.1 guidelines, a complete response (CR) is defined as the total disappearance of all target lesions. Any pathological lymph nodes must be measured at less than 10 mm. A partial response (PR) occurs when there is at least a 30% reduction in the total diameters of target lesions, referencing the baseline total. A diagnosis of progressive disease (PD) is made when there is at least a 20% increase in the total diameters of target lesions, using the smallest sum recorded during the study as the reference, which may include the baseline sum if that is the smallest. Additionally, this 20% increase must be accompanied by an absolute rise of at least 5 mm, and the emergence of one or more new lesions also signifies disease progression. Stable disease (SD) is determined when there is insufficient shrinkage for PR or an increase for PD.<sup>83</sup>

In AML, based on European LeukemiaNet (ELN) recommendations, CR is defined by <5% leukemic blasts in the bone marrow, hematologic recovery (neutrophils  $\geq 1,000/\mu\text{L}$ , platelets  $\geq 100,000/\mu\text{L}$ ), and no extramedullary disease. CR with incomplete hematologic recovery (CRi) meets CR criteria but with persistent neutropenia (neutrophils  $< 1,000/\mu\text{L}$ ) or

thrombocytopenia (platelets  $<100,000/\mu\text{L}$ ). PR is established when bone marrow blasts are reduced to 5 - 25% with a  $\geq 50\%$  decrease in pretreatment blast count. No Response indicates a failure to meet the criteria for CR, CRi, PR, or PD.<sup>84</sup> For CLL, the International Workshop on Chronic Lymphocytic Leukemia (iwCLL) response criteria define CR as the resolution of lymphadenopathy, hepatosplenomegaly, normalization of blood counts (lymphocytes  $<4 \times 10^9/\text{L}$ ), and absence of disease in the bone marrow. PR in CLL requires a  $\geq 50\%$  decrease in lymphocyte count, lymph node size, and spleen or liver size. PD is diagnosed with a  $\geq 50\%$  increase in lymphocyte count or lymph node size over two months, new lymphadenopathy, or worsening cytopenias. SD applies when CR, PR, or PD criteria are unmet.<sup>85</sup> These standardized response criteria provide critical benchmarks for evaluating therapeutic efficacy and guiding treatment decisions.

Several clinical trials have demonstrated the therapeutic safety and potential of NK cells across various malignancies. For example, patients with malignant lymphoma or advanced and recurrent solid tumors received expanded allogeneic NK cells in a phase 1 trial (NCT01212341).<sup>86</sup> None of the patients showed GvHD with the highest planned dose,  $3 \times 10^7$  cells/kg. Eight out of 17 patients showed SD, and 9 showed PD. In neuroblastoma, combining an anti-GD2 antibody (m3F8) and haploidentical NK cells preactivated with IL-2 led to a 29% overall response rate (ORR; CR + PR) (NCT00877110).<sup>87</sup> Additionally, a phase II study (NCT02843204) found that NK cells combined with pembrolizumab (anti-PD-1 antibody) improved survival outcomes (ORR: 27.5%) for patients with advanced non-small cell lung cancer (NSCLC).<sup>88</sup> Trials in ovarian cancer (NCT00652899) and digestive cancers (NCT00529035) further validated the safety profile of NK cell infusions. NK cell therapies are also promising in treating hematologic malignancies. In a phase I trial (NCT01787474),

patients received haploidentical expanded NK cells in multiply relapsed and refractory AML.<sup>89</sup> The patients did not show any evidence of GvHD post-NK cell infusion. Seven out of 12 patients showed CR (58.3%), and one-year ORR was 41.7%.<sup>89</sup> Similarly, a study (NCT02481934) investigating autologous NK cell infusions in multiple myeloma treatment alongside anti-myeloma agents, dexamethasone, lenalidomide, and bortezomib, reported encouraging safety profiles and stable disease progression.<sup>90</sup> These clinical applications highlight the safety and effectiveness of NK cells in treating solid and liquid tumors.

### 1.2.1 NK cell sources

For generating NK cells for immunotherapy, NK cells can be derived from various sources, including peripheral blood (PB), umbilical cord blood (UCB or CB), and induced pluripotent stem cells (iPSCs).<sup>91-93</sup> Peripheral blood natural killer (PBNK) cells, sourced from adult blood, consist of 90% mature cytotoxic CD56<sup>dim</sup> CD16<sup>+</sup> NK cells, advancing tumor-killing capabilities; however, due to the highly mature NK cell composition in PB, their activities can be limited by donor variability. PBNK cells are easily obtainable from various donors and potentiate unique NK cell phenotypes such as adoptive NK cells (NKG2C<sup>+</sup> and FcεR1-γ<sup>-</sup> NK cells).<sup>94-96</sup> In contrast, CBNK cells comprise approximately 25% of immune cells in CB compared to 5 – 10% in PB, providing a more abundant source of NK cells. Most CBNK cells exhibit NKG2A<sup>+</sup> NK cell phenotypes, providing attenuated cell cytotoxicity.<sup>91,97,98</sup> With appropriate cell engineering, CBNK cells have potentially robust cancer eradication without adverse effects.<sup>99</sup> Generating NK cells from iPSCs has gained attention due to their ability to produce homogeneous, clinically scalable NK cell populations. This process involves a two-stage culture system, beginning with the differentiation of iPSCs into hematopoietic progenitors (CD34<sup>+</sup> CD45<sup>+</sup>) using stem cell factor (SCF), vascular

endothelial growth factor (VEGF), and bone morphogenetic protein 4 (BMP4). followed by further differentiation into NK cells in a medium containing SCF, Fms related tyrosine kinase 3 ligand (FLT3L), IL-3, IL-7, and IL-15.<sup>100</sup>

### 1.2.2 Chimeric antigen receptor (CAR): CAR-T and CAR-NK cells

Recent advances in immunotherapy have led to the development of chimeric antigen receptors (CARs), synthetic receptors engineered to improve therapeutic outcomes by enabling immune cells to recognize and attack specific targets. CAR constructs are composed of single-chain variable fragments (scFv) linked to a hinge region, intracellular signaling domains, and costimulatory elements derived from potent signaling proteins such as CD3 $\zeta$ , Fc $\epsilon$ R1- $\gamma$ , CD28, and 4-1BB.<sup>101</sup> This innovative design allows CAR-expressing immune cells to activate upon recognizing target cells, triggering a robust immune response. A notable breakthrough in this field was the development of CAR-T cells, first conceptualized in 1986 by Kuwana et al., who engineered murine T cells (EL4 cells) using the constant region of a T cell receptor (TCR) and the variable region of an antibody.<sup>102</sup> Engineered EL4 cells induced a calcium influx upon the antigen exposure, laying the foundation for modern CAR-T cell therapies.<sup>102</sup> Since then, in the early 1990s, the first generation of CAR structures, including CD3 $\zeta$  and Fc $\epsilon$ R1- $\gamma$  without co-stimulatory domains, was tested in T cells.<sup>103-105</sup> In the late 1990s and early 2000s, co-stimulatory domains such as CD28 and 4-1BB were introduced in CAR constructs (**Figure 1.2**).<sup>103,106-108</sup> Numerous preclinical and clinical studies have been conducted using CAR-engineered T cells; currently, there are six FDA-approved CAR-T cell treatments for various types of cancers, including lymphoma, leukemia, and multiple myeloma.<sup>109</sup> CAR-T cells significantly improved the clinical effectiveness of cell-based immunotherapy and opened up a new era of adoptive cell therapy.

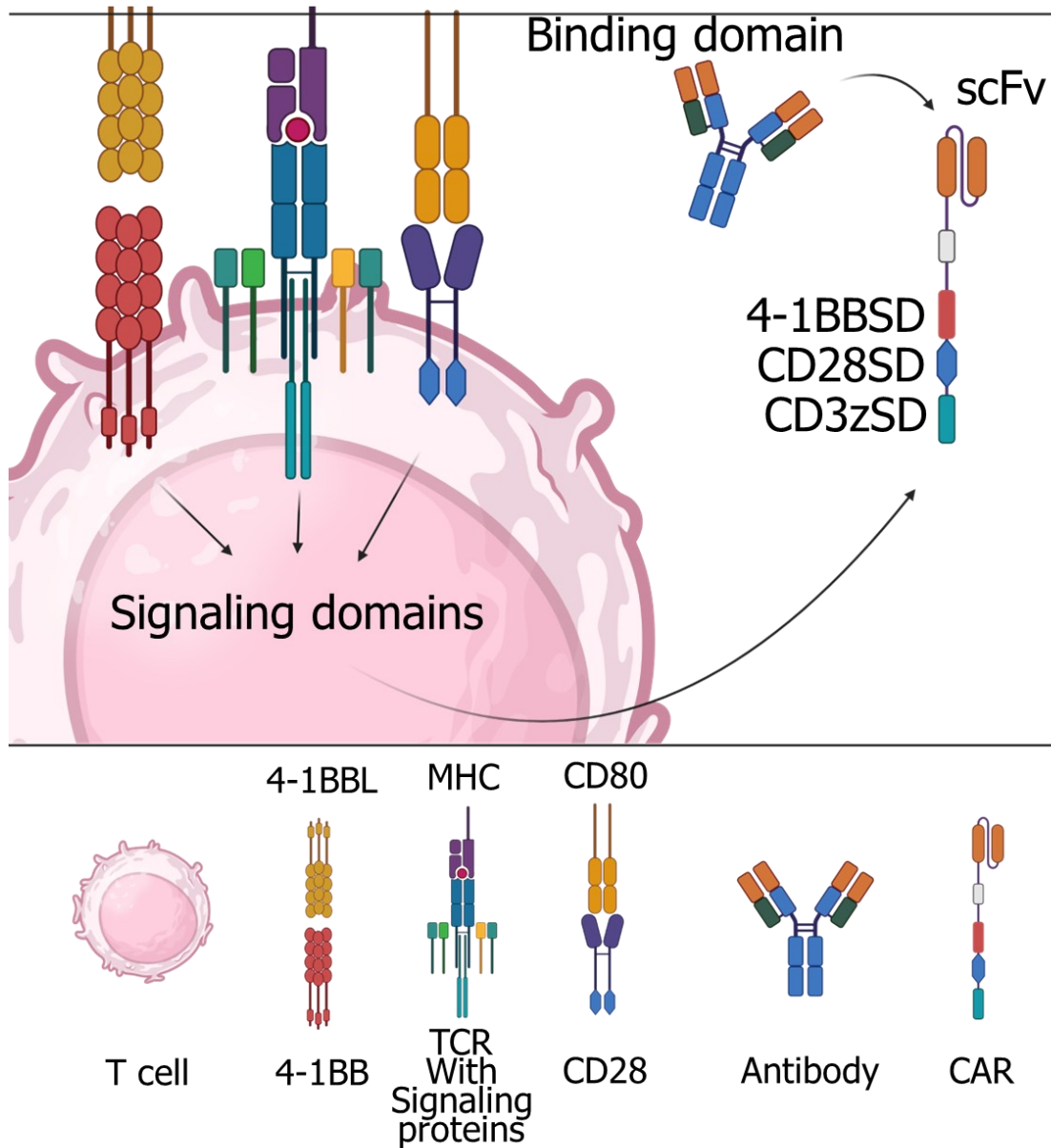


**Figure 1.2 Intracellular signaling domains of CAR and their origins.** A CAR construct contains an antigen-binding domain derived from an antibody and incorporates elements derived from T-cell activating receptors, including CD3 $\zeta$ , Fc $\epsilon$ R1- $\gamma$ , 4-1BB, and CD28. This design enables CARs to modulate immune cell functions upon binding to their target antigens; SD, signaling domain; scFv, single-chain variable fragment.

Despite their effectiveness, CAR-T cell therapies often have severe adverse effects due to their “non-self” killing, mediated by foreign peptides, and low self-regulatory machinery.<sup>110,111</sup> The most common toxicities include CRS, neurotoxicity, and GvHD, which significantly impact patient survival and require careful management.<sup>79-81</sup> GvHD frequently occurs following allogeneic hematopoietic stem cell transplantation (allo-HSCT), a procedure that involves the transfer of stem cells from a donor to a recipient.<sup>81</sup> Allo-HSCT is particularly valuable in generating a graft-versus-leukemia (GvL) effect, which can be the only curative option for patients with cancers that exhibit low levels of target antigens or are unresponsive to traditional chemotherapy or radiotherapy.<sup>112</sup> However, the allogeneic nature of the transplant introduces the risk of GvHD, where donor-derived T cells attack the recipient’s tissues. CAR-T cell therapy administered post-allo-HSCT often involves the use of allogeneic-HSCT-donor-derived T cells that are engineered to express CARs.<sup>81</sup> While these CAR-T cells offer promising outcomes for cancer treatment, they also pose a significant risk of GvHD.<sup>81</sup> To prevent GvHD and enable the use of allogeneic CAR-T cells, T-cell receptor alpha constant (TRAC) knockout was tested in a Phase 1 clinical trial of ALLO-715 for multiple myeloma and showed no GvHD in allogeneic CAR-T cell-received patients (NCT04093596).<sup>113</sup>

CRS and neurotoxicity present additional challenges associated with CAR-T cell therapies.<sup>79,80</sup> These toxicities arise from the rapid activation of immune cells, resulting in an overproduction of pro-inflammatory cytokines, particularly IL-1 and IL-6.<sup>114</sup> Norelli et al. demonstrated the critical involvement of monocytes in CAR-T cell-induced CRS using humanized mouse models, identifying monocyte-derived IL-1 and IL-6 as key drivers of both CRS and neurotoxicity.<sup>114</sup> Clinical studies have further emphasized these toxicities. Song et

al. reported that CRS occurred in all patients (58/58) treated with anti-CD19 CAR-T cells, with an impressive 93.1% (54/58) achieving complete remission by day 28.<sup>77</sup> CRS is generally manageable with interventions like tocilizumab (IL-6 receptor blocker) and corticosteroids. Tocilizumab proved ineffective in alleviating neurotoxicity symptoms. This may result from the insufficient delivery across the blood-brain barrier.<sup>79,80,115</sup> Previously, to mitigate neurotoxicity, the IL-1 receptor antagonist anakinra was tested and showed efficacy in reducing neurotoxic symptoms.<sup>116</sup> In addition, Parker et al. introduced a potential mechanism for neurotoxicity following anti-CD19 CAR-T cell therapy.<sup>117</sup> Mural cells maintain brain blood vessel integrity by directly interacting with large vessels and capillaries. Notably, mural cells express CD19, which may contribute to anti-CD19 CAR-T cell-mediated off-tumor targeting and mural cell death-induced blood-brain barrier leakage.<sup>117</sup> Emerging strategies have been reported to diminish these toxicities while preserving the anti-tumor efficacy of CAR-T cells. Optimized CAR designs, including modifications to enhance tumor-specific targeting and minimize off-target effects, are currently under active investigation.<sup>118,119</sup>

In contrast, CAR-engineered NK cells offer distinct advantages, including innate activating receptors facilitating CAR-independent cytotoxicity and naturally abundant inhibitory receptors targeting MHC class I molecules, which limit NK cell cytotoxicity against healthy tissues.<sup>77</sup> While this inhibitory pathway might reduce cancer-killing activity, it provides a critical safety advantage in post-allogeneic CAR-NK cell transfer.<sup>19,20,78</sup> The first clinical trial involving CAR-NK cells, targeting B-lineage acute lymphoblastic leukemia (ALL) with anti-CD19 CAR-NK cells, took place in 2009 (NCT00995137), though its result remains unpublished. A groundbreaking development in CAR-NK cell therapy occurred between

2017 and 2021 at the MD Anderson Cancer Center (NCT03056339),<sup>99</sup> where patients with relapsed or refractory B-cell malignancies, such as non-Hodgkin lymphoma (NHL) or CLL, received cord blood-derived anti-CD19 CAR-NK cells co-expressing IL-15 to enhance *in vivo* persistence. This trial achieved a 37.8% CR rate after one year (low-grade NHL, 83.3%; CLL, 50%; CLL-Richter's transformation, 20%; diffuse large B cell lymphoma, 29.4%).<sup>99,120</sup> Remarkably, the therapy demonstrated an excellent safety profile, with no neurotoxicity or GvHD cases, and only one patient experienced grade-1 CRS (1/37 patients).<sup>120</sup> Another clinical trial data, published in January 2025, investigated iPSC-derived anti-CD19 CAR, high-affinity CD16, and IL-15/15Ra fusion protein-expressing NK cells (FT596) for treating refractory or relapsed B cell lymphoma patients (NCT04245722).<sup>121</sup> The trial included 86 patients, with 18 receiving FT596 alone and 68 receiving FT596 + rituximab. Among the rituximab-treated group, the outcomes were 37% CR, 18% PR, and 34% PD. Grade 1 or 2 CRS was observed in 13% of patients, while no GvHD or neurotoxicity was reported.<sup>121</sup> Although CAR-NK cells have yet to receive FDA approval, numerous ongoing clinical trials are investigating their safety and efficacy against various antigens, including B cell maturation antigen (BCMA), CD22, roundabout guidance receptor 1 (ROBO1), and human epidermal growth factor receptor 2 (HER2), for targeting various cancers.<sup>122</sup>

### **1.3 NK cell engineering using viral vectors**

Viral vector-mediated transduction is a critical technique in genetic engineering. It is widely utilized for its high efficiency in gene delivery and stable integration into the host genome.<sup>123</sup> Among the available options, lentiviral and retroviral vectors are particularly favored for modifying immune cells due to their capability to enable long-term expression of therapeutic genes, such as CARs and cytokines, by integrating transgenes into the cellular

genome.<sup>124,125</sup> While this method has been instrumental in the development of CAR-T cell therapies, its application to NK cells presents unique challenges, as NK cells exhibit strong intrinsic antiviral defenses and express low levels of receptors for common viral glycoproteins, making them inherently resistant to conventional viral transduction methods.<sup>126-128</sup> Therefore, optimizing their efficiency in NK cells requires continuous advancements in viral vector engineering, including improvements in pseudotyping strategies and delivery techniques (**Figure 1.3**).

Among various viral vector production strategies, pseudotyping with the vesicular stomatitis virus glycoprotein (VSV-G) is widely employed for lentiviral and retroviral vectors due to its robust capacity to facilitate viral particle production and broad tropism across multiple cell types.<sup>129</sup> VSV-G-pseudotyped vectors efficiently transduce various cells, such as T cells, iPSCs, and common cell lines, through interaction with the low-density lipoprotein receptor (LDL-R), a key entry receptor.<sup>130-133</sup> This feature has made VSV-G the predominant pseudotype for generating clinical-grade CAR-T cells, as it supports highly efficient gene delivery.<sup>124</sup> However, its application in NK cell engineering has been limited. Unlike T cells, which highly express LDL-R upon activation, NK cells exhibit markedly low levels of this receptor, leading to poor viral entry and reduced transduction efficiency. In a study by Bari et al., NK cells activated with 500 U/mL IL-2 and 10 ng/mL IL-15 displayed only 33% surface LDL-R expression, whereas 97% of activated T cells expressed high LDL-R levels.<sup>128</sup> This stark contrast highlights a fundamental barrier in using VSV-G for NK cell modification, necessitating alternative approaches.

Several strategies have been explored to overcome the LDL-R-related inefficiency of VSV-G in NK cell transduction. One approach, evaluated by Gong et al., involves using

statins, typically prescribed to lower cholesterol levels by increasing LDL-R expression on endothelial cells.<sup>134</sup> Testing five statins and non-statin compounds demonstrated that statin treatment increased LDL-R expression on NK cells and improved the efficiency of VSV-G pseudotyped viral vector transduction. In particular, rosuvastatin enhanced VSV-G lentiviral transduction in NK cells by upregulating LDL-R expression up to three-fold.<sup>134</sup> Another approach to avoid LDL-R-mediated poor transduction is to use a different viral glycoprotein that targets proteins commonly expressed in NK cells. Baboon endogenous retroviral envelope glycoprotein (BaEV-G) targets amino acid transporters, alanine serine cysteine transporter-1 (ASCT-1) and ASCT-2, which are well expressed in activated NK cells.<sup>128,135,136</sup> BaEV-G pseudotyped viral vectors demonstrated superior 98% transduction efficiency in NK cells compared to 3% using VSV-G by Bari et al.<sup>128</sup> Despite the effectiveness of BaEV-G, producing BaEV-G pseudotyped vectors is technically challenging.<sup>135</sup> To address this, Girard-Gagnepain et al. developed two modified forms of BaEV-G: BaEV-TR, which includes the murine leukemia virus (MLV)-G intracellular domain, and BaEVRless, which has a deletion of the fusion inhibitory R-peptide.<sup>135</sup> These modified glycoproteins improved viral production and are currently the most commonly used envelope glycoprotein for NK cell engineering.<sup>137-139</sup>

In addition to overcoming low LDL-R expression, intrinsic antiviral defense mechanisms pose another challenge to viral vector-mediated transduction in NK cells.<sup>126,127</sup> NK cells play a critical role in controlling viral infections in the human body, which equips them with strong intracellular antiviral defenses. These mechanisms can hinder the efficiency of viral vector transduction. Sutlu et al. have identified the TANK-binding kinase 1/IkappaB kinase-epsilon (TBK1/IKK $\epsilon$ ) pathway as a major obstacle in VSV-G-mediated transduction of NK cells.<sup>126</sup>

This pathway is activated by pattern recognition receptor (PRR) recognition of foreign viral genomes, leading to a type I interferon response.<sup>140</sup> By inhibiting the TBK1/IKK $\epsilon$  pathway with a small molecule inhibitor, BX795, NK cell transduction was improved from 2.46% to 24%, indicating the importance of the TBK1/IKK $\epsilon$  pathway in NK cell engineering.<sup>126</sup> Similarly, amlexanox and MRT67307, TBK1/IKK $\epsilon$  inhibitors, showed significantly enhanced transduction efficiency in NK cells.<sup>127</sup>

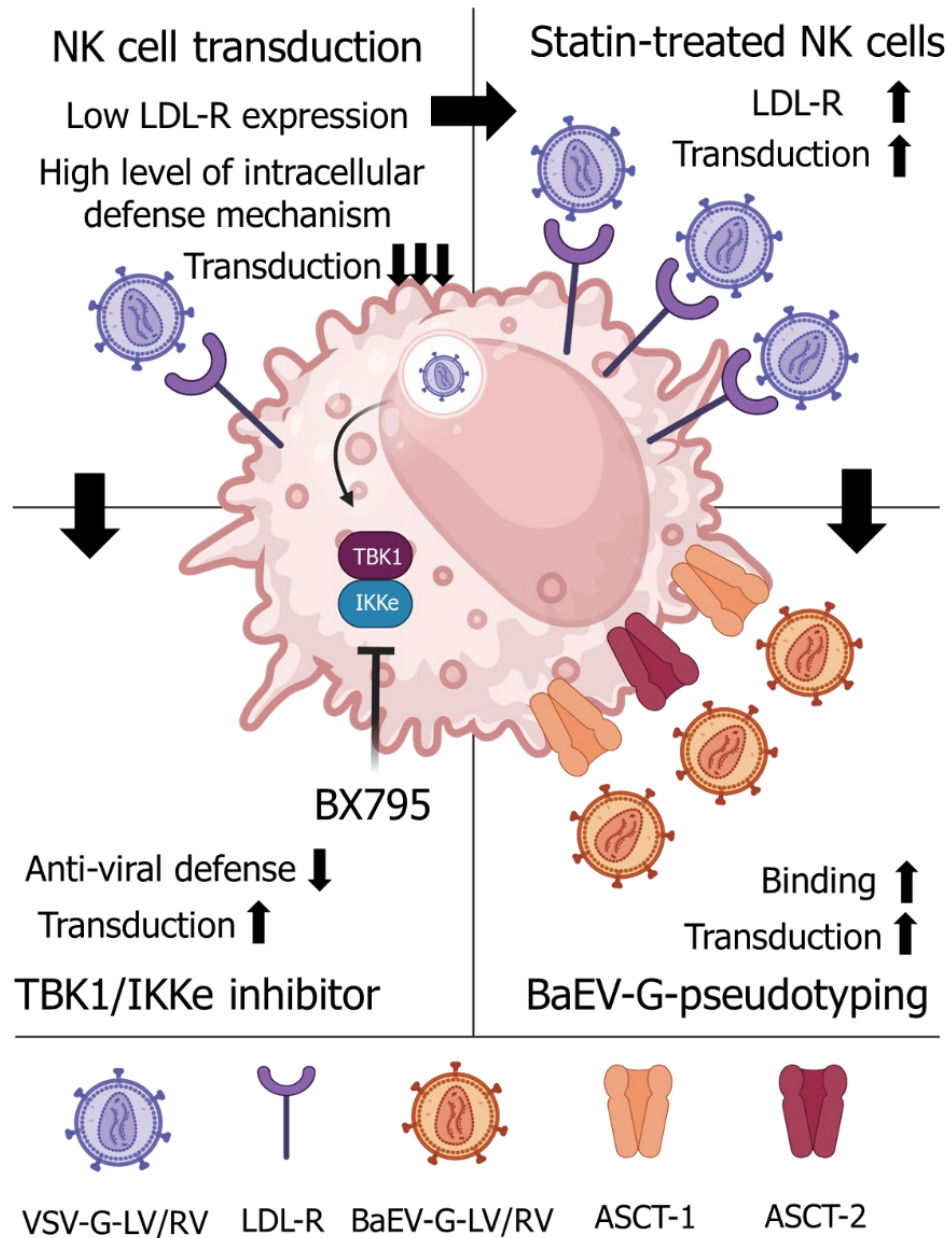


**Figure 1.3 Challenges in NK cell engineering and novel strategies to enhance transduction using viral vectors.** NK cells are resistant to VSV-G pseudotyped viral vectors due to low expression of LDL-R and robust antiviral defense mechanisms. To address these challenges, novel strategies have been explored. Statins upregulated the expression of LDL-R, improving susceptibility to VSV-G. Viral vector pseudotyping using BaEV-G, targeting amino acid transporters, ASCT-1 and ASCT-2, enhanced NK cell transduction efficiency. The TBK1/IKK $\epsilon$  inhibitor BX795 suppressed NK cell antiviral responses, facilitating effective NK cell engineering.

## 1.4 NK cell expansion

NK cell expansion is a foundation of NK cell immunotherapy to generate sufficient and highly functional NK cells for effective cancer treatment. Traditionally, NK cells are expanded using NK cell-stimulating cytokines such as IL-2 and IL-15, which promote their proliferation. Rham et al. explored the roles of IL-2 and IL-15 in NK cell expansion and demonstrated a 3-fold increase in CD56<sup>dim</sup> NK cells alongside an 18-fold expansion of CD56<sup>bright</sup> NK cells.<sup>141</sup> Interestingly, further research by Rham et al. demonstrated that adding IL-21 to IL-2 and IL-15 significantly enhanced expansion, resulting in a robust 40-fold increase in NK cell numbers.<sup>141</sup> Leong et al. examined an alternative strategy.<sup>63</sup> This strategy focused on cytokine-induced memory-like (CIML) NK cells, which were developed using IL-12, IL-15, and IL-18. These CIML NK cells showed enhanced proliferation and a superior ability to target cancer cells.<sup>63</sup> Additionally, CIML NK cells expressed higher levels of IL-2R $\alpha$  (CD25), allowing them to respond more effectively to IL-2 stimulation and leading to stronger STAT5 activation. Post-stimulation, CIML NK cells produced robust levels of cytokines such as IFN- $\gamma$  and TNF- $\alpha$ , further underscoring their therapeutic potential.<sup>63</sup> Optimal cytokine combinations that maximize NK cell expansion are continuously under investigation.<sup>142</sup>

Feeder-cell-based systems have emerged as a preferred choice for achieving high NK cell expansion rates, surpassing the limited yields of cytokine-only systems. Feeder cells, such as the HLA-negative myeloid-derived K562 and lymphoblastoid (LCL) cell lines, are selected for their ability to stimulate NK cells and are often genetically modified to improve the NK cell expansion.<sup>143,144</sup> K562 cells engineered to express membrane-bound IL-15 (mbIL-15) and the co-stimulatory molecule 4-1BBL have demonstrated robust NK cell

proliferation. NK cells cultured with these cells achieved a median recovery of 2030% after one week, compared to 250% with control K562 cells.<sup>143,145</sup> Over three weeks, the combination of mbIL-15 and 4-1BBL resulted in a 1089-fold NK cell expansion.<sup>143</sup> Introducing membrane-bound IL-21 (mbIL-21) has further advanced NK cell research by enabling even greater expansion and maintaining telomere integrity.<sup>146</sup> K562 cells modified to express mbIL-21 alongside 4-1BBL achieved a 47,967-fold NK cell expansion over three weeks.<sup>146</sup> Beyond K562 cells, EBV-transformed LCLs have also shown significant success. Yang et al. compared K562 cells expressing mbIL-21 with LCL-721.221-mbIL-21 cells and found significantly improved NK cell expansion using the modified LCL cell lines.<sup>144</sup> While these developments are promising, feeder-cell-based systems must meet strict regulatory requirements, including irradiation of the transformed feeder cells, necessitating careful consideration of their application in therapeutic contexts.

## 1.5 NK cell cryopreservation.

Conventional CAR-T cell therapies, which utilize autologous alpha-beta TCR-T cells, require personalized manufacturing processes that depend on the patient's immune cells.<sup>147</sup> This individualized approach necessitates close coordination between patient care and manufacturing, often resulting in delays that can worsen the patient's condition.<sup>147</sup> In contrast, allogeneic cell therapies using NK cells offer a more efficient alternative by enabling the production of cryopreserved off-the-shelf NK cell products (**Figure 1.4**).<sup>148</sup> However, preserving NK cells has been challenging due to their sensitivity to cryoinjury, which can lead to reduced viability and impaired functionality post-thaw.<sup>148</sup> A study published in 2020 by Damodharan et al. indicated that post-thaw NK cells exhibited critical changes in cytokine production and cytotoxic activity, limiting their clinical potential.<sup>149</sup>

Recent studies by Berjis et al. focused on optimizing cryopreservation protocols to improve NK cell viability and functionality post-thaw.<sup>150</sup> They identified cryopreservation-induced apoptosis, primarily caused by granzyme B-mediated autolysis, as a major factor contributing to NK cell damage. Post-cryopreservation, granzyme B leaked from cytotoxic granules, initiating apoptosis and reducing the number of viable NK cells. To address this, Berjis et al. employed a pre-treatment strategy using IL-15 and IL-18 before cryopreservation. IL-18 induced degranulation in NK cells, promoting the release of intracellular granzyme B before freezing. Additionally, IL-18 upregulated anti-apoptotic genes such as *BCL2-like 1*, encoding the survival protein B-cell lymphoma-extra large (Bcl-xL), further protecting NK cells against apoptosis. As a result, NK cells pre-treated with IL-15 and IL-18 showed nearly 100% recovery post-thaw while maintaining cytotoxic functionality *in vitro* and *in vivo*.<sup>150</sup> This approach enabled tumor control comparable to freshly expanded NK cells in xenograft lymphoma models, demonstrating its potential for clinical application.

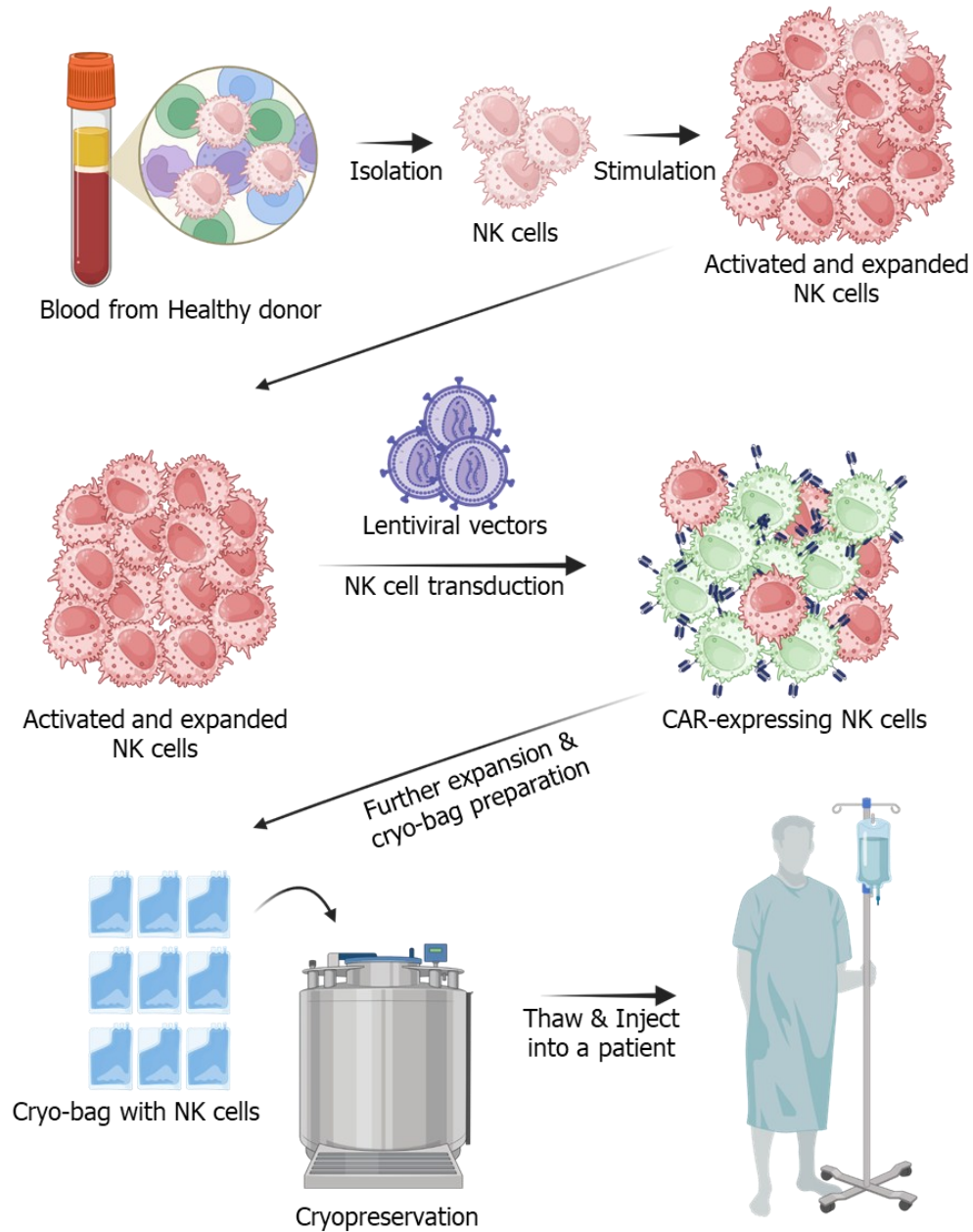


**Figure 1.4. Graphical summary of the CAR-NK cell immunotherapy process.** Allogeneic NK cell immunotherapy involves obtaining NK cells from a healthy donor's immune cell population. These cells are then stimulated and expanded using cytokines and feeder cells, engineered with viral vectors to express CARs, and cryopreserved. Finally, the CAR-NK cells are administered to cancer patients as a therapeutic treatment.

## 1.6 CRISPR-Cas9-mediated genome editing in NK cells

The clustered regularly interspaced short palindromic repeats (CRISPR)-CRISPR-associated protein 9 (Cas9) system revolutionized eukaryotic genome editing, with five landmark papers published by researchers like George M Church, Feng Zhang, Jennifer Doudna, Jin-Soo Kim, and J. Keith Joung in 2013.<sup>151-155</sup> This technology relies on three core components: CRISPR RNA (crRNA), trans-activating CRISPR RNA (tracrRNA), and the Cas9 nuclease. A guide RNA (gRNA) that combines the crRNA and the tracrRNA directs Cas9 to a specific genomic site based on an approximately 20-bp crRNA sequence. Recognition of the targeted site triggers Cas9 activity, inducing a DNA double-strand break (DSB).<sup>156</sup> The DSB can be repaired via two main pathways: non-homologous end joining (NHEJ) and homology-directed repair (HDR). NHEJ, an error-prone but rapid repair mechanism, directly ligates the broken DNA ends without a homologous template, often resulting in small insertions or deletions (indels) that lead to gene knockouts.<sup>157</sup> In contrast, HDR is a high-fidelity process that requires a homologous DNA template for accurate repair, allowing precise incorporation of exogenous DNA sequences at the targeted site.<sup>156</sup> Qi et al. advanced the conventional CRISPR-Cas9 by developing a catalytically dead Cas9 (dCas9) that binds DNA without inducing DSBs, enabling transcriptional interference by blocking RNA polymerase activity.<sup>158</sup> Fusing dCas9 with transcriptional activators like VP64, which allows targeted gene activation, further enhanced the system.<sup>159</sup> Subsequent innovations, including dCas9-based base editing and epigenetic engineering, expanded its utility for precise and programmable genome modifications.<sup>160,161</sup>

Among its groundbreaking applications, CRISPR-Cas9 has been used to address genetic disorders such as sickle cell disease and  $\beta$ -thalassemia, both caused by mutations in the

hemoglobin  $\beta$ -subunit gene.<sup>162,163</sup> Patients with these diseases suffer from sickle-shaped red blood cells that carry less oxygen, traditionally treated through bone marrow transplantation, a method limited by donor matching challenges.<sup>164</sup> A key breakthrough came in 2008 when Sankaran et al. identified the *BCL11A* gene as a critical suppressor of  $\gamma$ -globin expression, contributing to sickle cell pathology in  $\beta$ -globin mutated patients.<sup>165</sup> Building on this, Wu et al. in 2019 successfully used CRISPR-Cas9 to knockout *BCL11A* in CD34+ hematopoietic stem and progenitor cells (HSPCs), resulting in a significant increase in  $\gamma$ -globin expression (47.6% in edited cells vs. 4.5% in unedited cells).<sup>163</sup> The therapeutic potential of this approach lies in the ability of  $\gamma$ -globins to pair with  $\alpha$ -globin chains, forming fetal hemoglobin (HbF). By decreasing the expression of the sickling-related  $\beta^S$ -globin, the formation of HbF effectively inhibits the polymerization of deoxygenated sickling hemoglobin (HbS), thereby preventing red blood cell sickling and improving oxygen transport.<sup>166</sup> This innovation culminated in the FDA approval of CASGEVY, the first CRISPR-Cas9 treatment, in 2023.<sup>167</sup>

Despite its vast potential for various applications, the large size of the *Cas9* gene poses significant challenges for efficient expression, especially in NK cells.<sup>168,169</sup> To address these limitations, electroporation of Cas9-ribonucleoprotein (Cas9-RNP) complexes has become the method of choice, enabling precise and transient gene editing with high efficiency.<sup>168,169</sup> This approach has facilitated key advancements in NK cell engineering for therapeutic applications, including preventing fratricide, enhancing metabolic activity, and improving immune checkpoint targeting. A notable example is the development of CD38 knockout (CD38<sup>KO</sup>) NK cells by Kararoudi et al.<sup>170</sup> In patients treated with daratumumab, a monoclonal antibody targeting CD38, NK cells are often depleted due to fratricide. By knocking out the CD38 gene, CD38<sup>KO</sup> NK cells evade self-recognition via daratumumab

while enhancing their ability to target CD38<sup>+</sup> cancer cells. Hasan et al. applied a similar strategy, knocking out T cell immunoreceptor with immunoglobulin and ITIM domain (TIGIT) in NK cells to leverage TIGIT-targeting antibodies for improved therapeutic outcomes.<sup>171</sup> Another promising target for CRISPR editing is *CISH*, a gene encoding the CIS protein, which directly suppresses cell activity by inhibiting JAK1 and impairing STAT5 signaling. *CISH* knockout (*CISH*<sup>KO</sup>) NK cells demonstrated robust expansion under a low IL-15 concentration (1 ng/mL), achieving a more than 10-fold increase, whereas CIS-positive cells failed to proliferate under the same conditions.<sup>172</sup> *CISH*<sup>KO</sup> cells also exhibited superior cytotoxicity both *in vitro* and *in vivo*. Similarly, targeting NKG2A, an inhibitory receptor frequently expressed in NK cells, has proven effective in enhancing NK cell cytotoxicity.<sup>173</sup> NKG2A expression often enables the evasion of HLA-E-positive cancer cells. By knocking out NKG2A, NK cells improved cytotoxic activity.<sup>173</sup> Although the use of Cas9 is limited due to the requirement of electroporation, these Cas9-driven modifications collectively underscore the potential of gene-edited NK cells for enhanced adoptive immunotherapy.

## 1.7 Viral particles loaded with CRISPR-Cas9

Virus-like particles (VLPs) are self-assembling, non-infectious nanostructures derived from viral proteins that mimic the size and exterior shape of viruses but lack genetic material, preventing them from replicating or causing disease.<sup>174</sup> This makes them safe and highly attractive for medical applications. VLPs are categorized into two main types: non-enveloped and enveloped.<sup>175</sup> Non-enveloped VLPs are formed by assembling viral capsid proteins into structured layers, varying from single to multiple layers, depending on the origin of the virus. In contrast, enveloped VLPs acquire a lipid membrane from the host cell during budding, incorporating viral glycoproteins onto their surface, which enhances their resemblance to live

viruses. This structural diversity allows VLPs to effectively induce robust immune responses, mimicking pathogen-associated molecular patterns (PAMPs), thereby enabling vaccine development.<sup>176</sup>

Recently, VLPs have been increasingly recognized as powerful carriers for delivering therapeutic proteins, nucleic acids, and small molecules.<sup>177-179</sup> Their internal cavities allow for the encapsulation of bioactive substances, while surface modifications enable precise targeting of specific cells.<sup>180</sup> In 2019, Mangeot et al. introduced Nanoblades (NB), a retroviral VLP-based platform for Cas9 delivery.<sup>178</sup> By conjugating Cas9 with the retroviral structural protein Gag (Gag-Cas9), the complex co-localized at the producer cell membrane, enabling Cas9 packaging into VLPs. These VLPs delivered Cas9 into target cells via viral glycoprotein-mediated host receptor interactions.<sup>178</sup> Including a protease-sensitive sequence between Gag and Cas9 facilitated the precise release of Cas9 during viral maturation, ensuring efficient localization of Cas9 to the nucleus.<sup>178</sup> Furthermore, a key component for the Cas9 system, single-guide RNA (sgRNA), was introduced into the NB production mixture.<sup>178</sup> This process enabled the loading of sgRNA onto Cas9, forming RNP complexes for precise genome editing (**Figure 1.5**).<sup>178</sup> Since the first nanoblade discovery, Gutierrez-Guerrero et al. generated a lentiviral nanoblade in 2021 and tested it in multiple cell types.<sup>181</sup>

Nanoblades have shown remarkable precision and efficiency in genome editing across diverse experimental systems. For instance, targeting the empty spiracles homeobox 1 (EMX1) locus in iPSCs achieved an impressive 67% editing efficiency while maintaining pluripotency. In mouse bone marrow cells, nanoblades reduced GFP expression by approximately 75% without impairing differentiation potential.<sup>178</sup> They also demonstrated versatility in delivering both Cas9-RNP and DNA templates for HDR, with DNA delivery

optimized by loading templates onto the viral surface using polybrene, a charge-neutralizing agent, enabling streamlined “all-in-one” HDR using single- or double-stranded DNA.<sup>178</sup> Furthermore, recent studies have demonstrated that nanoblades allowed high-level genome editing in murine and human organoids, achieving up to 75% gene knockout without causing toxicity.<sup>182</sup> Nanoblades were also coupled with HDR-containing adeno-associated virus (AAV) vectors and integrase-deficient lentiviral vector genomes to enable site-directed genetic insertion.<sup>181</sup> The most recent breakthrough was reported in 2024 by Hamilton et al., who used T cell-targeting lentiviral nanoblades to deliver CAR transgene-containing Cas9-RNP viral particles *in vivo*, successfully generating *TRAC* gene-edited CAR-T cells directly *in vivo*.<sup>180</sup> This breakthrough highlights the potential of nanoblades for precise and efficient genome editing in multiple cell types.

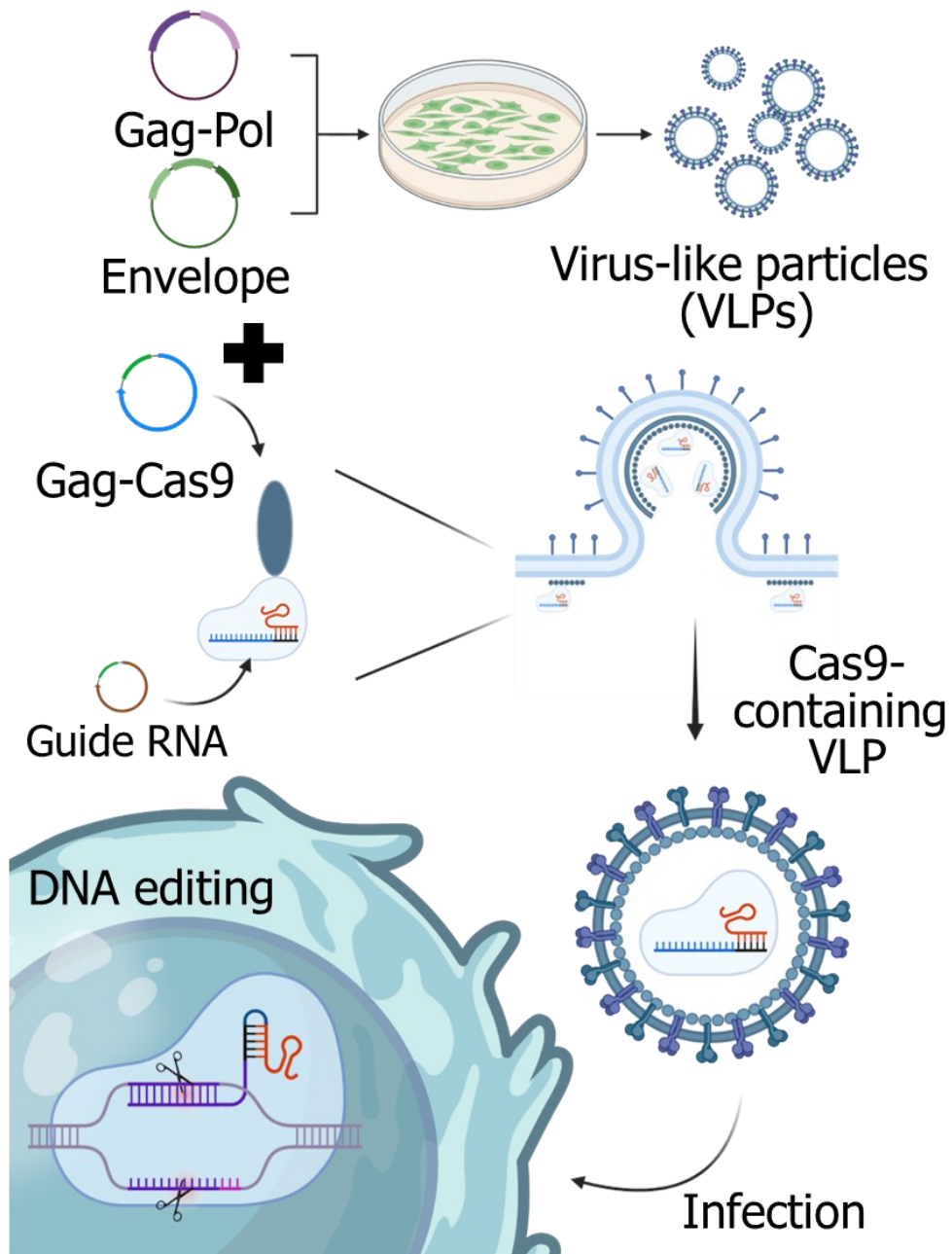


**Figure 1.5 Production of VLPs containing Cas9-RNPs using lentiviral or retroviral systems.** Producer cells transfected with viral structural proteins (Gag-Pol) and envelope glycoproteins naturally generate transgene-lacking VLPs. By incorporating a Gag-Cas9 fusion construct into the VLP production system, Cas9-containing VLPs are formed. These Cas9-VLPs utilize the same infection mechanisms as conventional viral particles through envelope glycoproteins, enabling efficient delivery of Cas9 to target cells. Upon delivery, Cas9 induces DSBs at the targeted genomic location.

## 1.8 Histone deacetylase inhibitors and immunotherapy

Epigenetic regulation, mediated by DNA methylation and histone modification mechanisms, governs gene expression without altering the underlying genetic sequence.<sup>183</sup> Among these regulatory processes, histone acetylation and deacetylation play a pivotal role in chromatin remodeling and transcriptional regulation, controlled by histone acetyltransferases (HATs) and histone deacetylases (HDACs).<sup>184-186</sup> HATs function within multi-protein complexes, such as CREB-binding protein (CBP)/p300 and general control non-repressible 5-related N-acetyltransferases (GNAT), catalyzing the acetylation of histone residues. This modification neutralizes the positive charge on histones, weakening histone-DNA interactions and promoting a relaxed chromatin state conducive to transcriptional activation.<sup>186</sup> HAT complexes often interact with transcriptional coactivators, ensuring the precise regulation of gene expression.<sup>187</sup> Conversely, HDACs counteract this process by catalyzing the removal of acetyl groups, increasing chromatin compaction, and inducing transcriptional repression.<sup>188</sup> HDACs are integral to the formation of nuclear repressive complexes such as nucleosome remodeling and deacetylase (NuRD), switch-independent 3 (Sin3), and corepressor for element-1-silencing transcription factor (CoREST), which contribute to gene silencing and chromatin remodeling.<sup>184</sup> This dynamic equilibrium between HATs and HDACs extends beyond histones to non-histone proteins, including transcriptional factors such as p53 and early region 2 binding factor (E2F), which are crucial for cell cycle progression, differentiation, and apoptosis.<sup>189,190</sup>

Due to their ability to modulate chromatin structure and gene expression, histone deacetylase inhibitors (HDACis) have been explored in various therapeutic applications, with one of the most compelling being cancer treatment, particularly in overcoming tumor

resistance to radiotherapy.<sup>190</sup> A major challenge in radiotherapy is the ability of cancer cells to repair radiation-induced DNA damage and sustain proliferation, a process in which HDACs play a pivotal role by regulating epigenetic mechanisms that influence DNA repair, cell cycle progression, and apoptosis.<sup>190</sup> Poly(ADP-ribose) polymerase 1 (PARP1), a key player in DNA repair, is not only upregulated by HDACs but also directly activated through deacetylation by sirtuins (SIRT) such as SIRT1 and SIRT6, thereby enhancing tumor cell survival following radiation-induced DNA damage.<sup>191</sup> Supporting this, Moertl et al. demonstrated that HDAC inhibition downregulated PARP1, impairing DNA repair and heightened radiosensitivity in tumor cells.<sup>192</sup> Besides strengthening DNA repair, HDACs suppress apoptosis by downregulating pro-apoptotic proteins like Bax and Fas while facilitating cell cycle progression by inhibiting critical regulators such as p21 and p53.<sup>189,190</sup> By counteracting these resistance mechanisms, HDACis induce chromatin relaxation, disrupt DNA repair pathways, arrest cells in the radiation-sensitive G2/M phase, and amplify apoptotic signaling, collectively enhancing the efficacy of radiotherapy.<sup>190,193</sup>

Beyond radiosensitization, HDACis play a pivotal role in modulating antitumor immune responses. HDACis influence the activity of NK cells and T-cell-based immunotherapies both passively and actively.<sup>194-196</sup> HDACis promote the overexpression of stress ligands such as MICA and MICB on tumor cells, increasing their susceptibility to immune-mediated destruction by NKG2D-positive immune cells.<sup>194</sup> Liu et al. demonstrated that panobinostat treatment and HDAC4 knockdown in hepatocellular carcinoma (HCC) increased NKG2DL expression, sensitizing HCC cells to NK cell-mediated lysis.<sup>197</sup> However, their direct effects on NK cells are complex and sometimes contradictory. Broad-spectrum HDACis, such as trichostatin A (TSA), valproic acid (VPA), and sodium butyrate (NaB), impaired NK cell

viability and reduced effector functions, including IFN- $\gamma$  production and the expression of activating receptors like NKG2D and NKp46.<sup>198,199</sup> These inhibitory effects were linked to HDACi-mediated modulation of STAT3 signaling, a critical pathway for NK cell receptor expression, as highlighted by Ni et al.<sup>195</sup> HDACis also bolster the efficacy of T-cell therapies by directly modulating tumor cells.<sup>196</sup> For instance, panobinostat and entinostat upregulated phorbol-12-myristate-13-acetate-induced protein 1 (PMAIP1, also known as NOXA), a pro-apoptotic member of the BCL2 family, sensitizing tumor cells to CD19 CAR T-cell-mediated cytotoxicity without compromising cell viability. This finding was demonstrated by Yan et al. in studies on Raji and Daudi cells.<sup>196</sup>

## **1.9 Histone deacetylase inhibitors in viral promoter activity**

Cell and gene therapy has emerged as a transformative approach in cancer treatment, leveraging viral vectors to deliver therapeutic genes.<sup>200,201</sup> Despite its potential, clinical implementation has been hindered by suboptimal transgene expression, inefficiencies in viral delivery, and challenges in maintaining the expression of therapeutic genes in engineered immune cells.<sup>202,203</sup> HDACis have demonstrated the ability to address these limitations by augmenting the transcriptional activity of transgenes delivered through viral systems and preserving transgene expression, including cytomegalovirus (CMV) and murine stem cell virus (MSCV) promoters, adenoviral (Ad) and AAV systems, and immune cell engineering strategies, offering a versatile solution to enhance the efficacy and durability of gene-based therapies.<sup>200,201,204-207</sup>

A notable example is the HDAC inhibitor FK228, which markedly enhanced adenoviral gene expression in tumor cells without inducing viral replication.<sup>201</sup> This

highlights a mechanism centered on transcriptional enhancement rather than modifications to viral delivery.<sup>201</sup> In prostate cancer cell lines (LNCaP, PC-346C, and TRAMP-C2) transduced with adenoviral vector encoding Ad[CMV-GFP], FK228 not only amplified GFP expression but also elevated transgene mRNA levels.<sup>201</sup> Similarly, VPA, an inhibitor targeting HDAC1 and HDAC3, increased GFP expression in Ad[CMV-GFP]-transduced cells in a promoter-specific manner.<sup>201</sup> While CMV promoters showed heightened activity, prostate-specific PSMA enhancer and the TARP (PPT) promoters exhibited diminished expression when treated with HDACis.<sup>201</sup> HDACis also demonstrated efficacy in enhancing transgene expression from recombinant adeno-associated viruses (rAAV).<sup>200</sup> For instance, FR901228 robustly increased CMV-GFP expression in glioma cell lines (U-251MG) transduced with AAV2EGFP, with no observed changes in AAV genome copy numbers.<sup>200</sup> Mechanistically, this upregulation was linked to increased histone acetylation at the promoter, promoting an open chromatin configuration conducive to higher transcriptional activity.<sup>200</sup> Moreover, in a mouse model of human epidermal growth factor receptor 2 (HER2)-positive tumors, co-administration of the HDAC inhibitor OSU-HDAC42 with a CMV promoter-driven DNA vaccine elicited an enhanced antitumor response compared to the vaccine alone.<sup>208</sup>

Beyond viral vectors, HDACis showed promise in maintaining transgene expression in TCR-engineered T cells.<sup>204</sup> In adoptive cell therapies, a progressive decline in therapeutic gene expression often causes poor treatment outcomes. Moore et al. demonstrated that sodium butyrate, an HDAC inhibitor, preserved gene expression and functional longevity in TCR-transduced T cells.<sup>204</sup> Notably, these effects persisted under cytokine-deprived conditions.<sup>204</sup> These findings suggest that HDACis could sustain the therapeutic efficacy of

engineered immune cells by mitigating epigenetic silencing and preserving transgene expression (**Figure 1.6**).

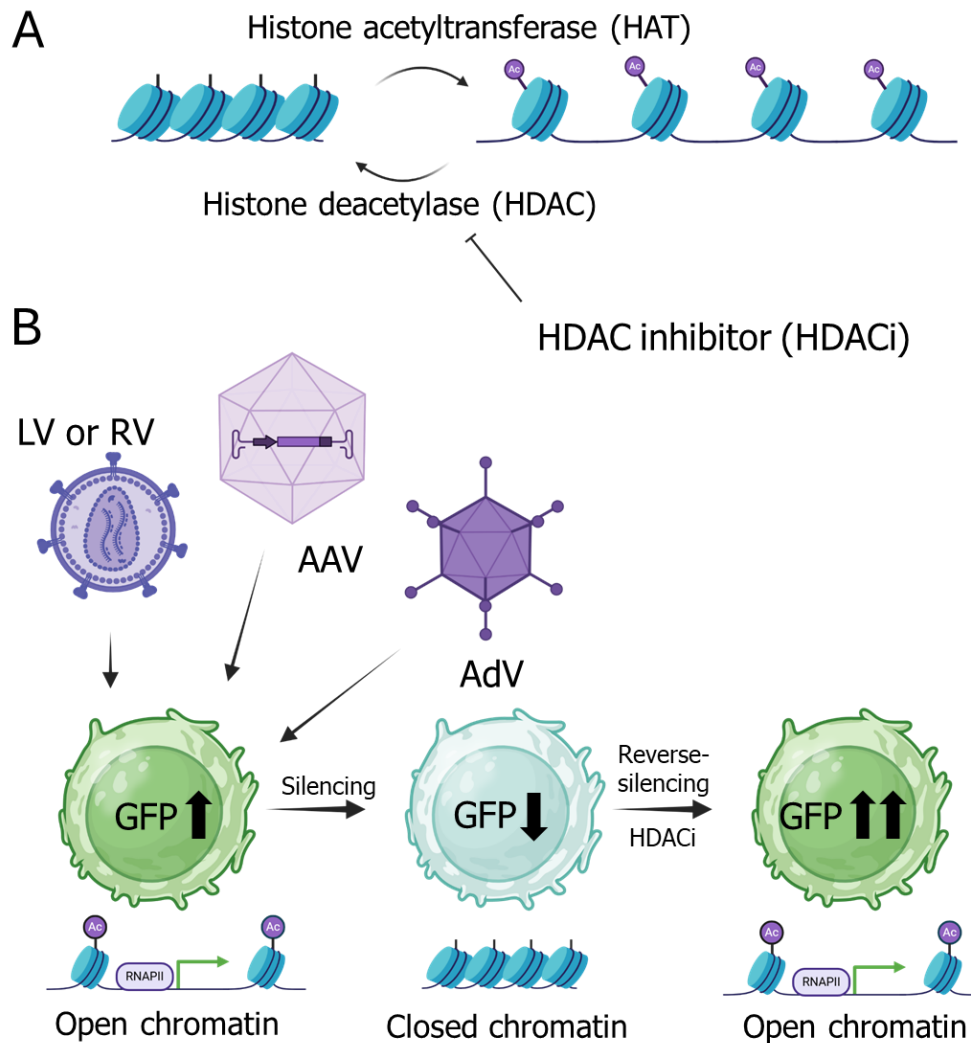


**Figure 1.6 HDAC inhibitor (HDACi) effects on chromatin relaxation and application in viral vector-mediated transgene delivery.** (A) Chromatin structure is dynamically regulated through epigenetic modifications, including histone acetylation and deacetylation. HDACis block histone deacetylase activity, leading to chromatin relaxation and an open chromatin structure. (B) Chromatin structure can contribute to transgene silencing in viral vector-mediated transgene delivery. Treatment with HDACis mitigates this silencing, enabling reactivation and, in some cases, overexpression of transgenes in recipient cells.

## 1.10 Rationale and Research Objectives

NK cells hold great promise for cancer immunotherapy, yet their clinical translation remains limited by challenges in CRISPR-Cas9 gene editing, suboptimal cryopreservation, and transgene silencing. My thesis aims to overcome these hurdles and establish a foundation for next-generation NK cell engineering.

To enhance CRISPR-Cas9 editing in NK cells, I will evaluate novel Cas9-RNP-loaded retroviral particles. This innovative approach aims to simplify NK cell engineering, overcoming the limitations imposed by the large size of the Cas9 protein. This study will be the first to describe a novel and efficient approach using virus-like particles for Cas9 delivery to NK cells.

Additionally, I will optimize cryopreservation protocols to improve NK cell viability and clinical readiness. By investigating the impact of cryopreservation timing during early proliferation, I aim to enhance post-thaw survival and functionality. Further, integrating cryopreservation with genetic engineering strategies will maximize NK cell therapeutic efficacy.

I will explore the application of HDACis to sustain long-term gene expression in NK cells. HDACis have the potential to preserve transgene expression and maintain NK cell cytotoxicity. In particular, I will evaluate anti-CD138 CAR-expressing NK cells for their ability to target multiple myeloma, assessing whether HDACi-mediated CAR maintenance enhances their therapeutic performance.

By integrating these strategies, my work aims to develop a scalable, clinically viable NK cell platform with improved gene-editing efficiency, enhanced post-thaw NK cell use,

and sustained transgene expression, ultimately advancing the field of engineering-based NK cell immunotherapy.

## Chapter 2. Simultaneous Engineering of Natural Killer Cells for CAR Transgenesis and CRISPR-Cas9 Knockout Using Retroviral Particles

### Chapter 2 related authors:

Dong-Hyeon Jo<sup>1,2</sup>, Shelby Kaczmarek<sup>1,2</sup>, Oksu Shin<sup>1</sup>, Lisheng Wang<sup>1,2</sup>, Juthaporn Cowan<sup>1,3,4</sup>, Scott McComb<sup>1,2,5</sup>, and Seung-Hwan Lee<sup>1,2</sup>

<sup>1</sup>Department of Biochemistry, Microbiology, and Immunology, Faculty of Medicine, University of Ottawa, Ottawa, ON, Canada.

<sup>2</sup>The University of Ottawa Centre for Infection, Immunity, and Inflammation, Ottawa, ON, Canada.

<sup>3</sup>Division of Infectious Diseases, Department of Medicine, Faculty of Medicine, University of Ottawa, Ottawa, Ontario, Canada,

<sup>4</sup>Clinical Epidemiology Program, Ottawa Hospital Research Institute, Ottawa, Ontario, Canada

<sup>5</sup>Human Health Therapeutics Research Centre, National Research Council of Canada, Ottawa, ON, Canada

### Publication History:

Received September 26, 2022; Accepted March 11, 2023; Published online March 16, 2023

This paper was published in *Molecular Therapy Methods and Clinical Development* (open access)

This paper is published under the Creative Commons Attribution–NonCommercial–NoDerivatives (CC BY-NC-ND 4.0) license, which restricts reuse and modification by others. However, as the author, I retain the right to reuse and adapt the work for my purposes based on Elsevier’s author rights policy. Chapter 2 includes a slightly modified version of the original paper, reformatted to match the style of this thesis.

The published version of this chapter is available. DOI: [10.1016/j.omtm.2023.03.006](https://doi.org/10.1016/j.omtm.2023.03.006)

## Author Contributions

D.H.J., S.K., O.S., S.M., and S.H.L. contributed to designing and performing the experiments and analyzing the data. D.H.J., S.K., and S.H.L. wrote the manuscript. D.H.J., S.K., L.W., J.C., S.M., and S.H.L. contributed to the discussion. S.H.L. obtained funding. D.H.J. performed 95% of the experiments.

## Acknowledgments

We thank CYTOSEN for kindly providing the K562 feeder cells expressing 4-1BBL (CD137L) and membrane-bound IL-21 (mIL-21). The rhIL-2 cytokine was obtained from NCI Preclinical Repository. We thank Vera Tang from the University of Ottawa flow cytometry core for the help with the flow virometry. We appreciate Nusrah Rajabalee and Jim Sun for their insight into the CRISPR-Cas9 technique. Lastly, we acknowledge the StemCore Laboratories Genomics Core Facility (OHRI) and Preclinical Imaging Core (PCIC) (RRID: SCR\_012601 and SCR\_021832). **Illustrations were created with Biorender.com.** This work was funded by the National Research Council Canada Disruptive Technology Solutions for Cell and Gene Therapy Challenge Program (CGT-501-2) and the Canadian Institutes of Health Research (PJT-178197).

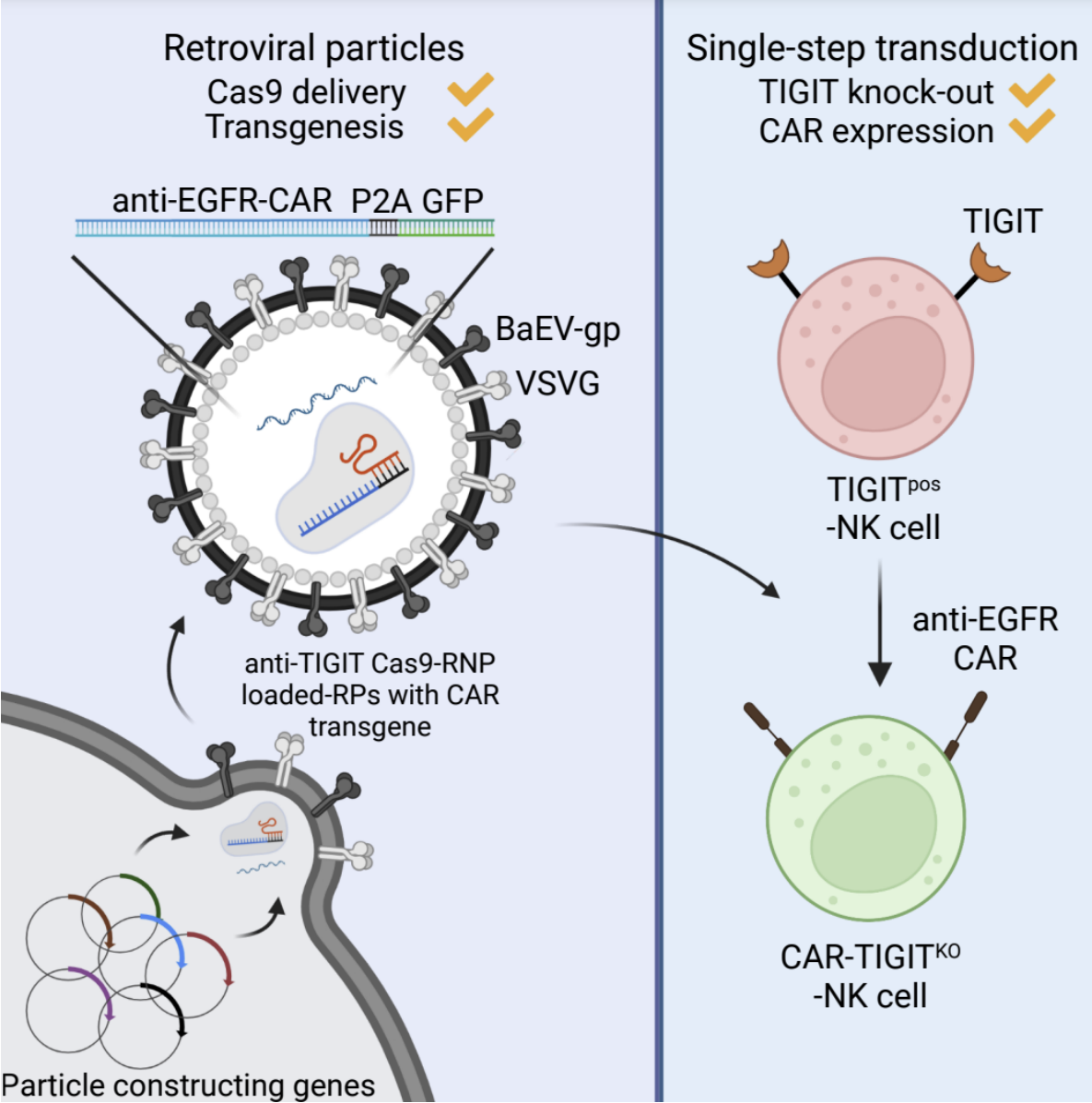


Figure 2.1 Graphical abstract for Chapter 2

## 2.1 Abstract

NK cells are potent cytotoxic innate lymphocytes that can be used for cancer immunotherapy. Since the balance of signals from activating and inhibitory receptors determines the activity of NK cells, their anti-tumor activity can be potentiated by overexpressing activating receptors or knocking out inhibitory receptors via genome engineering, such as CAR transgenesis and CRISPR-Cas9-mediated gene editing, respectively. Here, we report the development of a one-step strategy for CRISPR-Cas9-mediated gene knockout and CAR transgenesis in NK cells using retroviral particles. We generated NK cells expressing anti-epidermal growth factor receptor (EGFR)-CAR with simultaneous *TIGIT* gene knockout using single transduction and evaluated the consequence of the genetic modifications *in vitro* and *in vivo*. Taken together, our results demonstrate that retroviral particle-mediated engineering provides a strategy readily applicable to simultaneous genetic modifications of NK cells for efficient immunotherapy.

## 2.2 Introduction

CAR is a hybrid antigen receptor composed of an extracellular antigen-binding domain and intracellular signaling domains.<sup>209,210</sup> Even though CAR-T therapies have shown dramatic efficacy in treating B-cell malignancies, strong CAR-T cell responses against tumors can drive the production of an overwhelming amount of cytokines, known as CRS.<sup>210</sup> In addition, the threat of GvHD in allogeneic T cell infusions impedes the enthusiasm for an off-the-shelf CAR-T immunotherapy. NK cells are an ideal cell type for CAR therapy without causing severe GvHD or CRS.<sup>211-215</sup> Unlike CAR-T cells, CAR-NK cells retain diverse tumor-specific activating receptors, which decrease the likelihood of tumor cell immunoevasion through downregulation of the CAR target antigen.<sup>212,216</sup> Furthermore, NK cells spare healthy cells by using inhibitory receptors that recognize the MHC class I.<sup>216,217</sup> Recent publications have demonstrated that CAR-NK cells could be a highly effective anti-tumor therapy in an allogeneic setting,<sup>215,218</sup> thereby decreasing cost and increasing the accessibility of CAR therapies. Therefore, these characteristics make CAR-NK cells one of the most promising cell immunotherapies for cancer.

Many studies of cancer cells have shown that overexpression of EGFR is one of the most common cancer-associated factors, making it one of the most frequently targeted antigens in CAR therapy.<sup>219</sup> Activation of EGFR recruits a series of downstream signaling pathways, such as phosphoinositide 3-kinase (PI3K)/protein kinase B (AKT) and Ras/Raf/mitogen-activated protein kinase (MEK)/extracellular signal-regulated kinase (ERK), responsible for mediating cell proliferation, apoptosis, angiogenesis, and tumorigenesis.<sup>220</sup> Specifically, EGFR levels are relatively high on triple-negative breast cancer (TNBC) cells in 45%-70% of patients with poor prognoses.<sup>221-224</sup> Moreover, EGFR

mutations rarely occur in TNBC patients, which further promotes the testing of several immunotherapies such as anti-EGFR monoclonal antibodies.<sup>219,223,224</sup> While EGFR is a proven target for immunotherapy, balancing activity and toxicity remains a critical consideration because of the EGFR expression on many healthy cells. Since NK cells can dismiss healthy cells based on the missing self hypothesis,<sup>18,225</sup> EGFR-targeted CAR-NK cells may have potential benefits over an EGFR-targeting CAR-T therapy.<sup>40,81,215</sup>

T cell immunoglobulin and immunoreceptor tyrosine-based inhibitory motif (ITIM) domain (TIGIT) is a receptor of the Ig superfamily specifically expressed in immune cells where it functions as a co-inhibitory receptor.<sup>226</sup> TIGIT binds to two ligands, CD155 (PVR) and CD112 (PVRL2), which are expressed on antigen-presenting cells, T cells, and a variety of non-hematopoietic cell types, including tumor cells.<sup>227</sup> TIGIT is a checkpoint receptor expressed by both T cells and NK cells and was originally found to induce T cell exhaustion in tumor microenvironments.<sup>208,228</sup> Emerging studies have shown that the blockade of TIGIT might be a promising complement to existing immunotherapies.<sup>229,230</sup> Blocking TIGIT prevents NK cell exhaustion and elicits potent anti-tumor immunity.<sup>160</sup> Therefore, genetically engineering NK cells for the overexpression of anti-EGFR-CAR and the knockout of TIGIT can serve as a logical strategy for which CAR-NK cells can be designed to elicit potent anti-tumor activity.

The CRISPR-Cas9 system has revolutionized biomedical research by providing a powerful genome-editing tool.<sup>152,231</sup> Nonetheless, engineering has been hindered in NK cells due to the inefficient delivery of the large-sized CRISPR-Cas9 plasmid.<sup>169,169</sup> To overcome this, delivery of Cas9-sgRNA complexes by electroporation has been established in NK cells<sup>169-215</sup>; however, electroporation of the Cas9-sgRNA complex requires a convoluted

technique. Recently, delivering Cas9-sgRNA complexes using VLPs has shown efficient genetic knockout in CD4<sup>+</sup>, CD8<sup>+</sup>, CD34<sup>+</sup>, and mouse bone marrow cells.<sup>178,181</sup> Moreover, the VLP system can induce transient Cas9-mediated recombination and reduce off-target effects from the constitutive expression of the Cas9-sgRNA. Such a gene knockout technology is valuable for removing genes responsible for inhibitory signaling, thereby creating a robust NK cell response in immunotherapy.<sup>232</sup> Although the overexpression of CAR molecules and the knockout of inhibitory receptors seem promising to enhance NK cell recognition and cytotoxicity, recurring genetic engineering in primary NK cells is challenging and undesirable due to the limited window for genetic modification of primary NK cells. Here, we took advantage of retroviral particles loaded with Cas9-sgRNA complexes to induce efficient anti-EGFR-CAR transgenesis and *TIGIT* gene knockout simultaneously in NK cells. Retroviral particles efficiently delivered Cas9-sgRNA complexes along with the CAR transgene, proving that this dual engineering technology can effectively support CAR-NK cell immunotherapy.

## 2.3 Materials and Methods

### 2.3.1 Culture of human cell lines

TNBC cell lines, MDA-MB-231, and SUM149PT cells, and ER<sup>+</sup> breast cancer cell line, MCF7 cells, were obtained from ATCC and cultured in DMEM/F12 media (319-075-CL; Wisent) containing 10% heat-inactivated fetal bovine serum (HI-FBS) (12484028; Gibco) and 100 U/mL Penicillin and 100 µg/mL Streptomycin (Pen/Strep) (SV30010; HyClone). Raji cells were obtained from ATCC and cultured with RPMI-1640 medium (350-000-CL; Wisent) containing 10% HI-FBS, 100 µg/mL Pen/Strep, 55 µM β-Mercaptoethanol

(21985023; Gibco), and 20 mM HEPES (CA12001-708; VWR) (RP10 medium). Lenti-X 293T cells were purchased from Takara (632180) and cultured with 10% HI-FBS and 100 µg/mL Pen/Strep supplemented High-Glucose DMEM medium (319-005-CL; Wisent). NK92 cells were cultured with RP10 medium supplemented with 200 U/mL human recombinant IL-2 (NCI Preclinical Repository, USA).

### **2.3.2 Isolation and culture of human pNK cells**

Healthy adult whole blood collection was approved by the Ottawa Health Science Network Research Ethics Board (# 20200527-01H) and the University of Ottawa (# H-01-21-6568). Peripheral blood mononuclear cells (PBMC) were isolated by Ficoll (45001750; Cytiva) gradient centrifugation. Briefly, 35 mL whole blood was layered gently over 15 mL Ficoll and centrifuged at  $1,250 \times g$ , acceleration 1, and brake 0 at room temperature, followed by pipette separation of the PBMC layer. CD56-positive primary NK cells were isolated by negative magnetic selection using a MojoSort human NK cell isolation kit (480054; Biolegend). Isolated pNK cells were immediately cultured with 1: 2 irradiated membrane-bound IL-21 and 4-1BBL expressing K562 feeder cells (gifted from CYTOSEN) and 100 U/mL IL-2 based on the previously reported protocol for 5 days,<sup>146</sup> and the partially expanded pNK cells were frozen at -80 °C with freezing medium containing 90% FBS and 10% DMSO (BP231-100; FisherBioReagents).

### **2.3.3 Plasmid construction**

BaEV-TR and BaEVRless sequences were previously published.<sup>135</sup> Codon-optimized EcoRI-flanking BaEV-TR and BaEVRless were purchased from Thermo Fisher Scientific (GeneArt) and digested with EcoRI (FD0274; Thermo Fisher Scientific). The fragment was

cloned into an EcoRI-digested pMD2.G plasmid (gifted from Didier Trono; 12259; Addgene). To generate a retroviral pMIG-anti-EGFR-CAR-mNeonGreen plasmid, the EcoRI-anti-EGFR-CAR-mNeonGreen-PacI fragment was amplified from the pSLQC5-anti-EGFR-CAR-mNeonGreen plasmid and digested with EcoRI and PacI (FD2204; Thermo Fisher Scientific). The fragment was then cloned into an EcoRI and PacI-treated pMIG plasmid (gifted from William Hahn; 9044; Addgene). The anti-*TIGIT* sgRNA (TCCTCCTGATCTGGGCCAG) containing plasmid was generated using an Esp3I (FD0454; Thermo Fisher Scientific) digested Superblade5 plasmid<sup>178</sup> (gifted from Philippe Mangeot, Théophile Ohlmann & Emiliano Ricci; 134913; Addgene), based on the Zhang lab Golden Gate cloning protocol.<sup>233</sup>

### 2.3.4 BaEV pseudotyped lentiviral vector production

To produce lentiviral vectors,  $1.5 \times 10^6$  Lenti-X 293T cells were plated per well on a 6-well plate in 2 mL Opti-MEM medium (31985070; Gibco) containing 5% HI-FBS and 100  $\mu\text{g}/\text{mL}$  Pen/Strep. The next day, the Lenti-X 293T cells were transfected using Lipofectamine 3000 (L3000015; Invitrogen). Briefly, 1,200 ng of transfer plasmids, pLenti-CMV-MCS-GFP-SV-puro<sup>234</sup> (for EGFP-NK92) (gifted from Paul Odgren; 73582; Addgene) or pSLQC5-anti-EGFR-CAR-mNeonGreen (for CAR-NK92 cells) (gifted from National Research Council of Canada), 1,200 ng of pSPAX2 (gifted from Didier Trono; 12260; Addgene), and 200ng of BaEV-TR were combined with Lipofectamine 3000 (6  $\mu\text{L}$  P3000 and 7  $\mu\text{L}$  Lipofectamine 3000) in 500  $\mu\text{L}$  serum-free Opti-MEM. 1 mL of media was removed from each well and replaced with the Lipofectamine/plasmid mix. After 4 hours of incubation, all medium was removed from each well and replaced with fresh, complete Opti-MEM medium.

Without concentrating the lentiviral particles, viral supernatant was collected at 48 and 96 hours, filtered using a low protein-binding PES filter (83.1826; Sarstedt), and kept at -80 °C.

### **2.3.5 Cas9-RNP and transgene-loaded RP production**

To produce Cas9-RNP retroviral particles,  $1.2 \times 10^6$  Lenti-X 293T cells were plated per well on a 6-well plate in 2 mL of serum-containing Opti-MEM medium. The next day, the cells received 600 ng BIC-Gag-Cas9<sup>178</sup> (gifted from Philippe Mangeot, Théophile Ohlmann & Emiliano Ricci; 119942; Addgene), 1,200 ng MLV-gag-pol (gifted from Marceline Côté, University of Ottawa), 1,200 ng anti-EGFP sgRNA (BLADE-182)<sup>178</sup> (gifted from Philippe Mangeot, Théophile Ohlmann & Emiliano Ricci; 134914; Addgene) or anti-TIGIT sgRNA, 100 ng pMD2.G, and 100 ng BaEV-TR using Lipofectamine 3000 (6  $\mu$ L P3000 and 7  $\mu$ L Lipofectamine 3000). To optimize the envelope combinations, a total of 200 ng envelope plasmids were used (200 ng for a single envelope or 100 ng + 100 ng for two envelopes). For simultaneous CAR transgenesis and TIGIT knockout, 1,200 ng pMIG-anti-EGFR-CAR-mNeouGreen was also added with additional Lipofectamine 3000 (7.7  $\mu$ L P3000 and 9  $\mu$ L Lipofectamine 3000). After 4 hours of incubation, the transfection medium was removed from each well and replaced with fresh, complete Opti-MEM medium. Without concentrating the retroviral particles, the supernatant was collected at 48 hours, filtered using a low protein-binding PES filter, and kept at -80 °C.

### **2.3.6 Flow virometry**

For the mock control,  $1.2 \times 10^6$  Lenti-X 293T cells were plated, and the Cas9-RNP RP production procedure without plasmids was followed. 50  $\mu$ L of the produced RP supernatants and mock control were fixed with 50  $\mu$ L 2% paraformaldehyde (PFA) for 25

min at room temperature. Fixed particles (30  $\mu\text{L}$ ) were diluted with  $1 \times \text{PBS}$  (20012050; Thermo Fisher Scientific) to obtain a  $5 \times 10^{-3}$  dilution. A total of 10  $\mu\text{L}$  of each sample was acquired using the Cytoflex (Beckman) with a violet SSC (VSSC) laser at the Flow Virometry Core, University of Ottawa, and analyzed using Kaluza 2.1 Analysis software (Beckman Coulter). For addressing viral particle sizes, analyzed data were further normalized using the FCMPASS v4.1.6 software (National Cancer Institute) to create a new axis (nm).<sup>235</sup> The MFI (VSSC) of various sizes of polystyrene beads (Thermo Fisher Scientific) and a previously validated refractive index of MLV, 1.455, were applied to convert the VSSC signal from RPs to a new axis (nm).

### **2.3.7 NK92 cell transduction**

For the functional titer calculation,  $5 \times 10^4$  NK92 cells were incubated on a 96-well U-bottom plate with serially diluted RP supernatants, 4  $\mu\text{g}/\text{mL}$  polybrene (TR-1003-G; MilliporeSigma), and 200 U/mL IL-2. The cells were centrifuged for 30 min at  $1500 \times g$ , 32  $^{\circ}\text{C}$ , followed by a 3-day incubation at 37  $^{\circ}\text{C}$  and 5%  $\text{CO}_2$ . After 3 days of incubation, transgene expression or protein reduction was acquired using the Attune NxT flow cytometer (Thermo Fisher Scientific). A functional titer was calculated by using an equation from Addgene (<https://www.addgene.org/protocols/fluorescence-titering-assay/>).

For NK92 transduction, NK92 cells were plated on a 96-well flat-bottom plate coated with 20  $\mu\text{g}/\text{mL}$  Retronectin (T100B, Takara), viral supernatant, 4  $\mu\text{g}/\text{mL}$  polybrene, and 200 U/mL IL-2. The cells were spun down for 30 min at  $1,500 \times g$  and 32  $^{\circ}\text{C}$ . The cells were incubated overnight at 37  $^{\circ}\text{C}$  and 5%  $\text{CO}_2$ . The next day, the viral supernatant was removed, and the cells were resuspended in RP10 medium containing 200 U/mL IL-2. Post-

transduction, GFP expression was observed using the Attune NxT flow cytometer (Thermo Fisher Scientific) and ZOE fluorescent cell imager (Bio-Rad).

To obtain single-copy integrated EGFP-NK92 cells for the EGFP knockout study, less than 10% of NK92 cells were transduced, and the EGFP<sup>+</sup> cells were sorted by the SH800 sorter (SONY) at the Flow core, University of Ottawa.

### **2.3.8 Human primary NK cell transduction**

Five-day expanded and previously frozen pNK cells were thawed and rested overnight in RP10 medium containing 100 U/mL IL-2. The next day, the pNK cells were transduced in a 48-well flat-bottom plate coated with 20 µg/mL Retronectin, RP supernatant (MOI 1 for 40% or MOI 2 for 60% transduction efficiencies), and 100 U/mL IL-2. The cells were spun down at 1200 × g for 90 min at 32 °C and cultured overnight at 37 °C and 5% CO<sub>2</sub>. The next day, the cells were stimulated with irradiated feeder cells in a 1:5 ratio and 100 U/mL IL-2. The pNK cells were further expanded for 9 more days by replacing the culture medium every 2 days without an additional feeder cell stimulation. Expanded NK cells were used for phenotyping, functional assays, genomic analysis, and *in vivo* studies.

### **2.3.9 Flow cytometry and antibodies**

The following monoclonal antibodies (Abs) were used: anti-TIGIT (PerCP-710; 46-9500-42), anti-CTLA4 (FITC; 11-1529-42), anti-NKG2D (PerCP-710; 46-5878-42), anti-CD112 (PE; 12-1128-42), anti-CD155 (FITC; 11-1550-41) and Live/Dead Fixable Aqua Dead Cell Stain (L34966) from Invitrogen; anti-CD56 (BV421; 318328), anti-NKG2A (APC; 375108), anti-KIR3DL1 (BV421; 312713), anti-CD107a (PE; 328608), and anti-EGFR (PE; 352904) from BioLegend; anti-CD56 (BV786; 564058), anti-IL18Rα (PE; 564675), anti-

TIM3 (BV421; 565562), and anti-CD107a (APC; 560664) from BD Biosciences. An anti-sdCAR antibody was generated at the National Research Council.<sup>118</sup> For surface antigen staining, cells were washed once with 150  $\mu$ L of staining buffer (SB) (PBS containing 2% HI FBS). The cells were then resuspended in 50  $\mu$ L SB and incubated with fluorophore-conjugated antibodies for 25 min at 4 °C. After the incubation, the cells were washed once with 150  $\mu$ L SB and fixed with 100  $\mu$ L 2% PFA for 10 min at 4 °C. The PFA was washed using 200  $\mu$ L SB. The cells were resuspended in 200  $\mu$ L SB. Data were acquired using the Attune NxT flow cytometer (Thermo Fisher Scientific) and analyzed using Kaluza 2.1 Analysis software (Beckman Coulter). Intracellular staining of IFN- $\gamma$  was carried out using an anti-IFN- $\gamma$  antibody (BV785; 502542; Biolegend) and a BD Cytotfix/Cytoperm kit (554714). Briefly, cells were fixed with 100  $\mu$ L of BD Cytotfix/Cytoperm buffer after the surface staining procedure. The cells were washed once with 200  $\mu$ L Wash Buffer (WB) (554714) and resuspended in 50  $\mu$ L WB containing an IFN- $\gamma$  antibody. Intracellular staining was performed for 25 min at 4 °C. The cells were then washed once with 200  $\mu$ L SB. For the data acquisition, the cells were resuspended in 200  $\mu$ L SB.

### **2.3.10 NK cell functional assay**

Approximately  $3 \times 10^4$  target cells were plated on a 96-well U-bottom plate and rested overnight at 37 °C and 5% CO<sub>2</sub>. The next day,  $3 \times 10^4$  pNK cells were added to the target cell-containing wells with an anti-CD107a antibody (1  $\mu$ L) and 1  $\times$  brefeldin A (00-4506-51; Invitrogen). After 4 hours of co-incubation, the cells were washed with SB and stained with an anti-CD56 antibody and a live/dead fixable Aqua dye. Intracellular IFN- $\gamma$  was stained according to the manufacturer's protocol with an anti-IFN $\gamma$  antibody as previously described.

### 2.3.11 Genomic analysis

Genomic DNA (gDNA) was isolated from expanded primary NK cells using a Monarch Genomic DNA Purification Kit (T3010S) from New England Biolab (NEB). The *TIGIT* fragment was amplified using a forward *TIGIT* primer (*TIGIT-For*) (TCTTGTGGCTCACCTATGC) and reverse *TIGIT* primer (*TIGIT-Rev*) (AAGCTGGAGCAGGAATGAGC) from the prepared gDNA and analyzed by Sanger sequencing. The sequencing files from *TIGIT* fragments were further analyzed by ICE (Synthego) by comparing non-RP-treated controls with Cas9-RNP-RP-received cells.<sup>236</sup> For integration analysis, a portion of the pMIG fragment was amplified using a pMIG forward primer (pMIG-For) (TGACGAGTTCTGAACACCCG) and a pMIG reverse primer (pMIG-Rev) (CAGTCAGACAGAGACAACAC). For targeted integration analysis, *TIGIT*-5'LTR was amplified using the forward *TIGIT* primer and reverse 5'LTR primer (5'LTR-Rev) (CAGCAAGAGGCTTTATTGGGAA). A bacterial library was generated by putting the amplicons into a plasmid using a PCR cloning kit (E1202S; NEB). All PCR was performed using a Q5 high-fidelity polymerase (NEB), and primers were annealed at 67 °C for 20 sec. PCR amplicons were analyzed by Sanger sequencing. All sequencing data were obtained from the Ottawa Hospital Research Institute (OHRI) DNA sequencing facility. Snapgene (Dotmatics) was used to check the sequencing results.

### 2.3.12 *In vivo* tumor control

NOD.Cg-Prkdc<sup>scid</sup> Il2rg<sup>tm1Wjl</sup>/SzJ (NSG) mice were used for the injection of TNBC cancer xenografts and NK cell treatment studies. A breeding pair of NSG mice was purchased from Jackson Laboratories, and the colony was maintained in the specific-pathogen-free

animal facility at the University of Ottawa in agreement with the guidelines and regulations of the Canadian Council on Animal Care. NSG female mice (8 to 14 weeks old) received  $1 \times 10^5$  firefly luciferase-expressing MDA-MB-231 cells intraperitoneally, and the mice were randomized to each group ( $n = 5/\text{group}$ ). On days 3 and 5 post-target cell injection, the mice received  $1 \times 10^7$  GFP-pNK, CAR-pNK, or CAR-TIGIT<sup>KO</sup>-pNK cells with 2000 U IL-2 intraperitoneally. Luciferase signal was measured once a week using an animal imaging system, IVIS (PerkinElmer), and the data were analyzed using Aura software 3.2 (Spectral Instruments Imaging). Mouse weight was measured once per week. Mice were sacrificed based on the luminescence, movement ability, reactivity, and weight loss. All procedures were approved by and conducted in accordance with the animal guidelines of the University of Ottawa.

### **2.3.13 Statistical analysis and graph generation**

The mean values were tested using two-way ANOVA by comparing cell means regardless of rows and columns. For two-sample comparisons, the mean values were tested by t-test using GraphPad Prism 9 (Dotmatics) (\* $p < 0.05$ , \*\* $p < 0.01$ , \*\*\* $p < 0.001$ , \*\*\*\* $p < 0.0001$ ). Data represent mean  $\pm$  SD. All graphs were generated and analyzed using GraphPad Prism 9.

## **2.4 Results**

### **2.4.1 Efficient Cas9-sgRNA delivery to NK cells through BaEV-TR and VSV-G envelope glycoprotein pseudotyped retroviral particles**

We adopted the RP system, called Nanoblades, from an original report.<sup>178</sup> Production of RPs requires plasmids coding for murine leukemia virus (MLV) structural proteins (Gag-

Pol), viral envelope glycoprotein (G), gag-conjugated Cas9 (Gag-Cas9), and sgRNA. NK cells were found refractory to transduction with vesicular stomatitis virus glycoprotein (VSV-G, herein referred to as V) pseudotyped LVs because they lack the LDL-R.<sup>128</sup> Recently, BaEV pseudotyped lentiviral vectors greatly enhanced the transduction of NK cells.<sup>128,136</sup> Two types of synthetic BaEVs, non-syncytia-forming BaEV-TR (T) and syncytia-forming BaEVRless (R), were previously applied for improving lentiviral vector production and transduction in NK cells.<sup>128,135,136</sup> Interestingly, a combination of V and R enhanced the packaging of Cas9 proteins in RPs compared to individual V or R pseudotyped RPs.<sup>178,181</sup> Thus, we reasoned that efficient delivery of RPs to NK cells might also be achieved by optimizing the viral envelope combinations.

To test this, Lenti-X 293T cells were transfected with plasmids encoding Gag-Pol, Gag-Cas9, sgRNA, and various envelope glycoproteins (V, R, and T envelopes alone, along with their combinations). RPs were harvested 48 hours post-transfection and used for transducing NK cells. As a proof of concept, we decided to use an immortalized human NK cell line (NK92) expressing EGFP (EGFP-NK92 cells) and perform knockout of EGFP using RPs pseudotyped with V, R, T, V + R, V + T, and R + T envelopes. We used a plasmid coding for anti-EGFP-sgRNA, which was previously validated for effectively knocking out EGFP in EGFP<sup>+</sup> mouse bone marrow cells.<sup>178</sup> EGFP-NK92 cells were transduced with various preparations of RPs, and the efficiency of EGFP knockout was evaluated by flow cytometry 5 days post-transduction. Consistent with the previous paper,<sup>178,181</sup> we observed that the efficiency of EGFP knockout was higher in V + R pseudotyped RPs (up to 45% EGFP negative populations) compared to V alone (up to 8%) and R alone (up to 15%). Interestingly, T alone showed similar EGFP knockout efficiency (up to 49%) to the V + R RPs. Furthermore,

the efficiency was greatly improved using V + T, resulting in up to 78% EGFP loss by flow cytometry (**Figure 2.2 A, B**). Therefore, this result suggests that RP-mediated Cas9-sgRNA-RNP delivery is efficient in NK92 cells.

To investigate the differences in the knockout efficiency among RPs pseudotyped with distinct envelope glycoproteins, we performed flow virometry to characterize and quantify RPs.<sup>237</sup> To discern background signals, we included PBS and supernatant from cells that received transfection reagents without plasmids (mock transfection). The supernatant was 200-fold diluted, and 10  $\mu$ L was acquired by flow virometry. We identified distinguishable particle populations from background noise and measured the total number of particles in a gated area. Interestingly, although EGFP was slightly reduced in EGFP-NK92 cells transduced with V-pseudotyped RPs, we found that most particles were from the V-pseudotyped RPs ( $\approx$  121,000 RPs/gate). This inconsistency may be due to the lack of LDL-R expression on NK cells, as previously described.<sup>128</sup> Although R and V + R-pseudotyped RPs were found in a similar amount ( $\approx$  52,000 RPs/gate), pseudotyping with the combination of V and R enhanced the formation of a distinct population in the dot-plot. Notably, T-pseudotyped RPs showed clear separation from background signals observed in PBS and Mock controls. Moreover, the number of V + T-pseudotyped RPs ( $\approx$  115,000 RPs/gate) was increased compared to the T-pseudotyped RPs ( $\approx$  85,000 RPs/gate). The number of T + R-pseudotyped RPs was found to be the lowest ( $\approx$  51,000 RPs/gate) (**Figure 2.2 C**). Overall, the results from flow virometry were consistent with the knockout efficiencies in EGFP-NK92 cells by RPs.

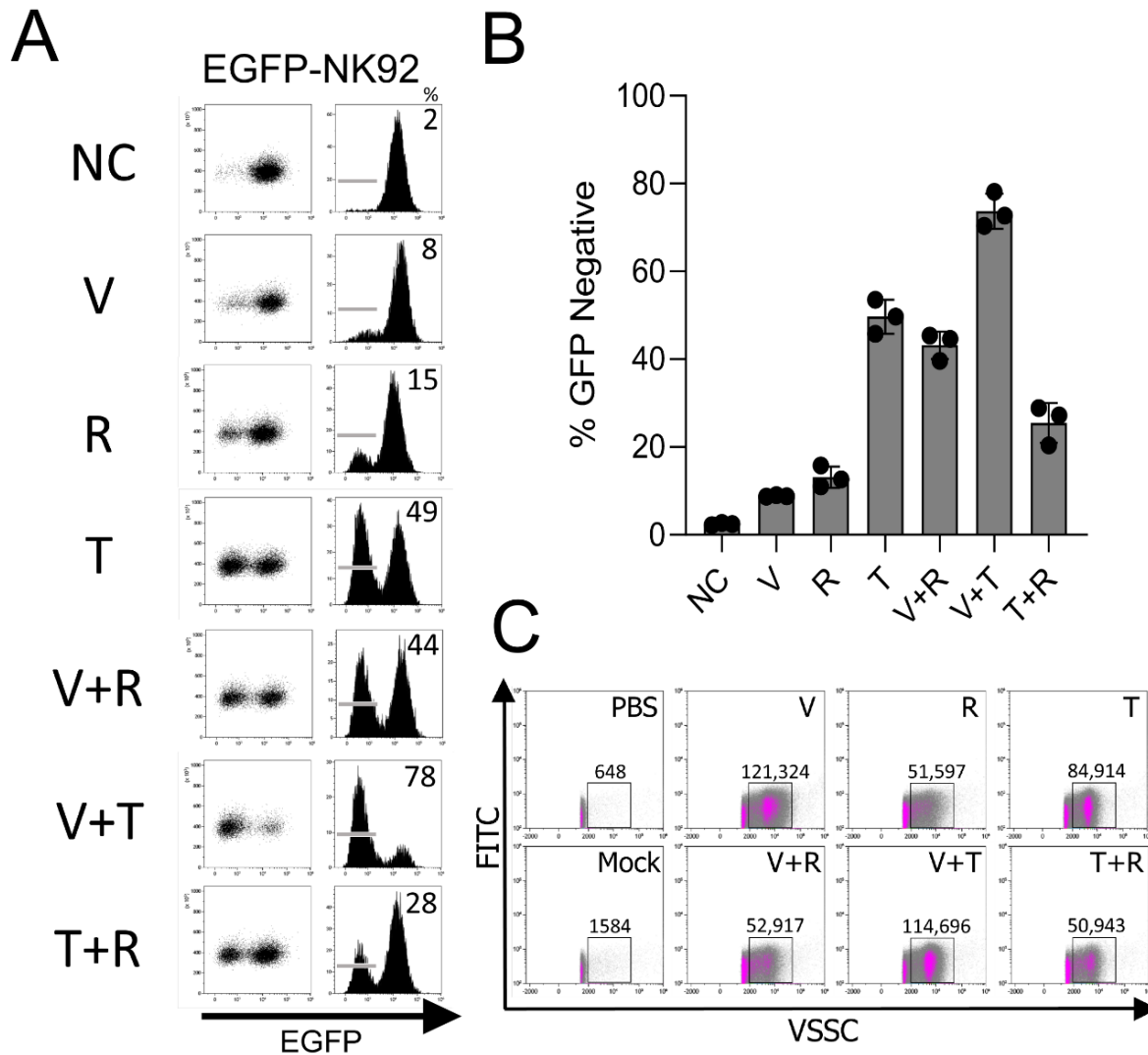


**Figure 2.2 VSV-G and BaEV-TR envelopes pseudotyped RPs efficiently targeted the EGFP gene in EGFP-NK92 cells. (A)** Representative flow cytometry of EGFP expression in EGFP-NK92 cells transduced with RPs pseudotyped with various envelope glycoproteins. **(B)** The EGFP knockout efficiency in EGFP-NK92 cells transduced by RPs pseudotyped with various envelope glycoproteins ( $n = 3$ ). **(C)** Flow virometry analysis of variously pseudotyped RPs. The numbers indicate the total number of viral particles in the gated area. NC, negative control; V, VSV-G; T, BaEV-TR; R, BaEVrless; VSSC, violet side scatter.

### 2.4.2 Cas9-sgRNA delivery to pNK cells using RPs efficiently abrogates TIGIT expression

To test whether RP-mediated delivery of the Cas9-sgRNA-RNP is also effective in human primary NK (pNK) cells, we decided to knock out TIGIT, an inhibitory receptor, using a previously validated sgRNA targeting the first exon of the *TIGIT* gene (CCDS2980) in *ex vivo* expanded human pNK cells.<sup>168</sup> pNK cells were enriched from human PBMCs and further expanded by *ex vivo* co-culture with irradiated K562 feeder cells expressing membrane-bound IL-21 and 4-1BBL.<sup>146</sup> pNK cells were transduced with anti-*TIGIT* V + T pseudotyped RPs, and TIGIT expression was evaluated by flow cytometry. Anti-*EGFP* RPs were used as a negative control. NK cells transduced with anti-*TIGIT* RPs showed reduced TIGIT expression almost to the basal levels based on TIGIT MFIs by flow cytometry (**Figure 2.3 A**). No abnormal expression of other NK cell surface receptors was observed, supporting that RPs specifically targeted genes guided by the Cas9-loaded sgRNAs (**Figure 2.3 B**). To further determine the number of RPs required for primary NK cell modification, we performed volume-based transduction to correlate the number of RPs for each volume and the knockout efficiency. We observed that  $2.7 \times 10^8$  RPs modified  $\approx 89.02\%$  of the pNK cells (**Figure S1 A, B**). Additionally, we calculated the size of anti-*TIGIT* RPs by flow virometry. We normalized the data based on MFIs of violet side scatter signals from different-sized polystyrene beads and the previously validated MLV refractive index (1.455) using FCMPASS software.<sup>235</sup> The average size of the RPs was  $120.7 \text{ nm} \pm 9.8 \text{ nm}$  (**Figure S2**).

Cas9-sgRNA induces targeted DSB, leading to error-prone NHEJ DNA repair and creating indels at the target site.<sup>238</sup> To confirm gene editing caused by the Cas9-sgRNA-RNP complex at the genomic level, we PCR-amplified the targeted genomic region from a pool of

NK cells treated with RPs containing either anti-*EGFP*-sgRNA or anti-*TIGIT*-sgRNA and analyzed the sequence of amplicons. As a non-treated control, amplicons from wild-type NK cells were used. From the sequencing results, we confirmed gene mutations in the sgRNA-targeted *TIGIT* locus (**Figure 2.3 C**). Additionally, we analyzed the sequenced *TIGIT* PCR fragments using Inference of CRISPR Edits (ICE; Synthego) to validate editing efficiencies computationally.<sup>236</sup> As expected, we found a series of indels and aberrant sequences from all *TIGIT*<sup>KO</sup>-pNK samples (**Figure 2.3 D**). On average, 89% of pNK cells were modified. Thus, these results indicate that Cas9-loaded RPs can be used for efficient gene knockout in primary NK cells.



### 2.4.3 Cas9-RNP-loaded RPs can induce *TIGIT* gene knockout and anti-EGFR-CAR transgenesis simultaneously

Since RPs efficiently delivered Cas9-sgRNA-RNP complexes into NK cells, we reasoned that combining Cas9-RNP RPs with a transgene could induce transgenesis and genetic knockout in NK cells simultaneously. We used a CAR structure containing an anti-EGFR nanobody, a hinge, a CD28 transmembrane and intracellular domain, and a CD3 $\zeta$  intracellular domain (**Figure 2.4 A**). This camelid nanobody-based anti-EGFR-CAR has previously been shown to have strong activity in CAR-T cells but has not yet been tested in NK cells.<sup>118</sup> Surface expression of the anti-EGFR-CAR was confirmed using a broadly cross-reactive anti-nanobody to stain NK cells.<sup>118</sup> To test the anti-tumor functionality of the anti-EGFR CAR in NK cells, we generated NK92 cells expressing the CAR using BaEV-TR pseudotyped lentiviral vectors, resulting in CAR expression in  $\approx 38\%$  of NK92 cells (CAR-NK92 cells) (**Figure 2.4 B**). The CAR-NK92 cells were co-cultured with either the triple-negative breast cancer cell line, MDA-MB-231 (EGFR<sup>high</sup>), or an estrogen receptor-positive (ER<sup>+</sup>) breast cancer cell line. MCF7 (EGFR<sup>low</sup>)<sup>239</sup> (**Figure S3 A**), for 4 hours and analyzed for expression of CD107a, a degranulation marker, by flow cytometry. CAR negative (CAR<sup>neg</sup>) and CAR positive (CAR<sup>pos</sup>) NK92 cells showed  $< 6\%$  CD107a expression when co-incubated with EGFR<sup>low</sup> MCF7 cells, while robust CD107a expression ( $\approx 67.6\%$ ) was observed only in CAR<sup>pos</sup> NK92 cells when co-incubated with EGFR<sup>high</sup> MDA-MB-231 cells (**Figure 2.4 B**).

To enhance the anti-tumor activity of the CAR, we simultaneously knocked out *TIGIT*. Since Cas9-RNP RPs were established in the retroviral system, we cloned anti-EGFR-CAR into the pMIG retroviral backbone. Lenti-X 293T cells were transfected with

plasmids encoding Gag-Pol, Gag-Cas9, anti-*TIGIT* sgRNA, VSV-G, BaEV-TR, and anti-EGFR-CAR to prepare V + T pseudotyped RPs (**Figure 2.4 C**). As controls, RPs targeting only *TIGIT* or *CAR* were also prepared and used for NK cell modification. Notably, pNK cells transduced with RPs simultaneously targeting *TIGIT* and delivering a *CAR* gene showed significantly reduced *TIGIT* and induced *CAR* expression post-transduction (**Figure 2.4 D**).

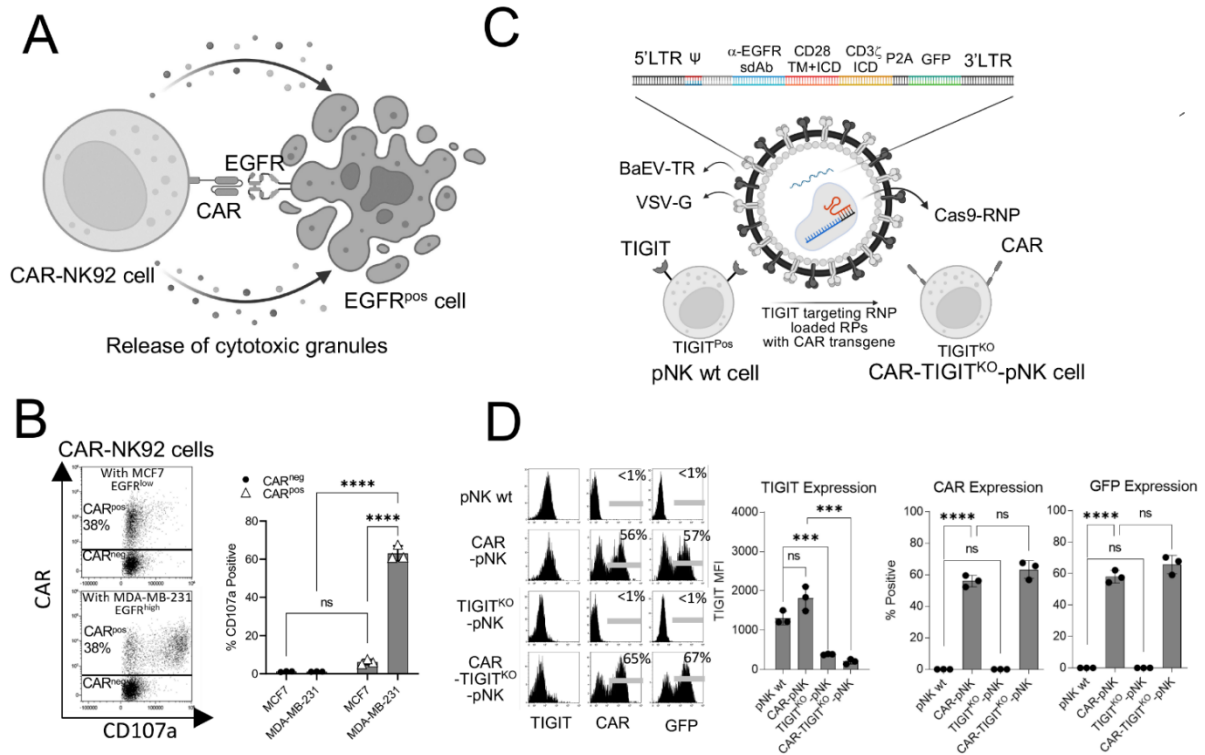


**Figure 2.4 Simultaneous *TIGIT* gene knockout and CAR integration into an NK cell genome by Cas9-RNP-loaded RPs.** (A) Graphical summary depicting anti-EGFR CAR-mediated NK cell functional activation. (B) Representative dot plots and bar graphs showing the enhanced anti-tumor activity of CAR-NK92 cells against the EGFR<sup>high</sup> triple-negative breast cancer cell line MDA-MB-231. (C) Graphical summary illustrating the strategy by which RPs engineer NK cells with anti-EGFR-CAR transgenesis and *TIGIT* gene knockout. (D) TIGIT, CAR, and GFP expression on primary NK cells from three different donors transduced by RPs. ns, non-significant; \*\*\*p < 0.001; \*\*\*\*p < 0.0001.

#### 2.4.4 TIGIT knockout does not improve human NK cell function *in vitro* and *in vivo*

We next investigated whether TIGIT knockout in pNK cells enhances NK cell degranulation. TIGIT recognizes CD112 and CD155 proteins and inhibits NK cells through ITIM and immunoglobulin tail tyrosine (ITT)/ITT-like domains.<sup>227,240</sup> We first assessed the

expression of TIGIT ligands, CD112 and CD155, on EGFR<sup>high</sup> TNBC cells (MDA-MB-231 and SUM149PT), EGFR<sup>low</sup> ER<sup>+</sup> breast cancer cells (MCF7), and EGFR<sup>neg</sup> B cell lymphoma cells (Raji). All three breast cancer cell lines showed surface expression of CD112 and CD155 (**Figure S3 B**). Neither CD112 nor CD155 was observed on EGFR<sup>neg</sup> Raji cells. To investigate the effect of TIGIT knockout on anti-tumor activity, CAR-pNK and CAR-TIGIT<sup>KO</sup>-pNK cells were prepared from three different donors and co-cultured with various target cells. After 4 hours of co-incubation, we measured CD107a and IFN- $\gamma$  expression in GFP-positive (CAR<sup>pos</sup>) and GFP-negative (CAR<sup>neg</sup>) cells (**Figure 2.5 A**). As expected, CAR<sup>pos</sup> cells showed higher CD107a and IFN- $\gamma$  expression than CAR<sup>neg</sup> cells when stimulated with EGFR<sup>high</sup> target cells, MDA-MB-231 and SUM149PT, in all three donors. CAR expression did not enhance NK cell effector function against EGFR<sup>low</sup> and EGFR<sup>neg</sup> target cells, MCF-7 and Raji cells. Unexpectedly, we did not observe enhanced NK cell function in TIGIT<sup>KO</sup> CAR<sup>pos</sup> cells compared to TIGIT<sup>Pos</sup> CAR<sup>pos</sup> NK cells (**Figure 2.5 B**).

To further investigate whether TIGIT knockout might enhance the anti-tumor activity of CAR-NK cells over an extended period that may not be apparent in our short-term *in vitro* assessments, we proceeded to an *in vivo* model of human breast cancer. We first injected  $1 \times 10^5$  EGFR<sup>high</sup> MDA-MB-231 cells expressing firefly luciferase (MDA-MB-231-Fluc) intraperitoneally (i.p.) into immunocompromised NSG mice. Three days after post-tumor engraftment, the mice received two doses of  $1 \times 10^7$  engineered pNK cells, administered at a two-day interval. Luciferase signals were measured weakly using IVIS to assess tumor growth *in vivo* (**Figure 2.5 C, D**). Consistent with our *in vitro* data, CAR expression on pNK cells significantly enhanced tumor control in both groups receiving CAR or CAR-TIGIT<sup>KO</sup> pNK cells. However, TIGIT knockout did not further improve tumor control *in vivo* (**Figure**

2.5 E, F). These results indicate that TIGIT knockout in CAR-NK cells does not improve anti-tumor activity against TNBC cells.

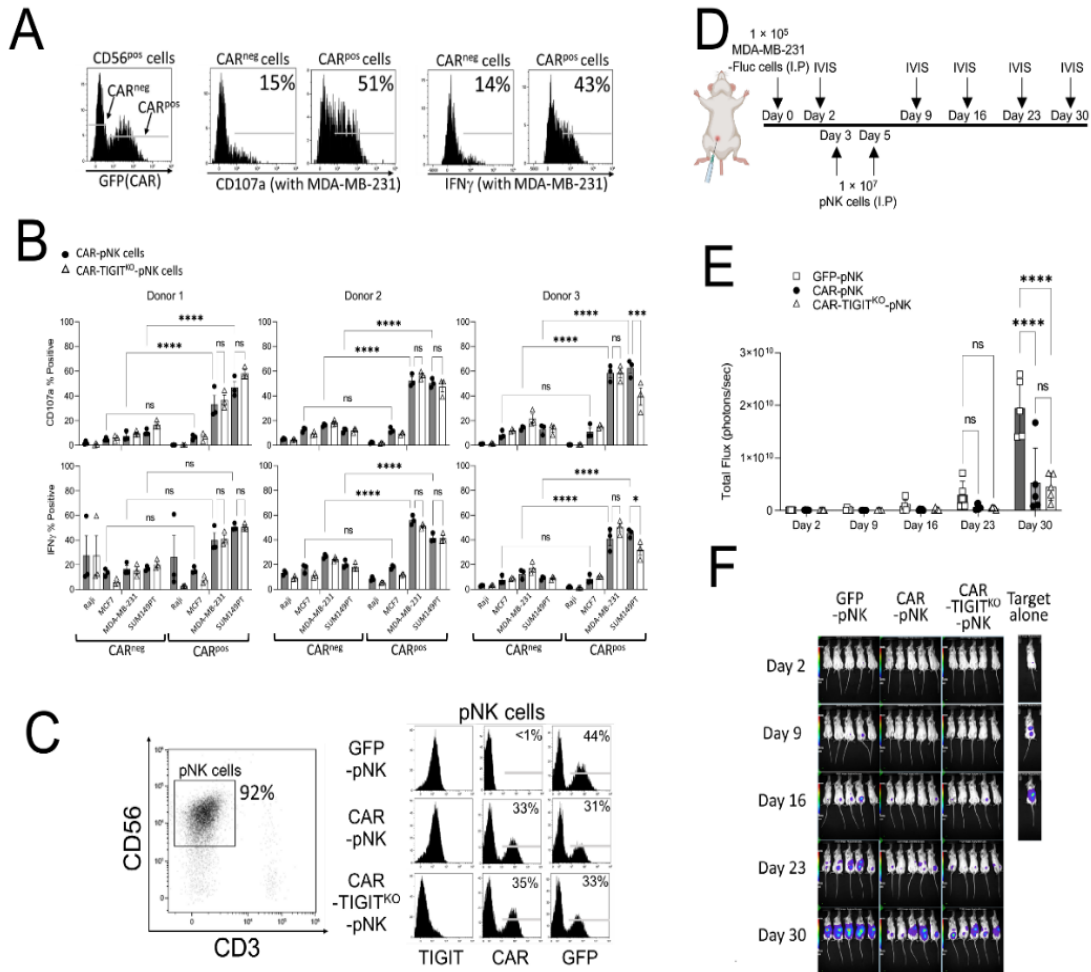


**Figure 2.5 TIGIT knockout failed to enhance the anti-tumor activity of human NK cell function *in vitro* and *in vivo*.** (A) Representative histograms show the gating strategy to measure CD107a and IFN- $\gamma$  expression on NK cells based on CAR expression. (B) The proportions of CD107a<sup>+</sup> and IFN- $\gamma$ <sup>+</sup> cells among the total NK cell population upon stimulation with various target cells (n = 3). Expanded primary NK cells from three donors were analyzed. Data represent mean  $\pm$  SD. (C) TIGIT, CAR, and GFP expression in the first dose of NK cells. (D) Schematic of experimental procedures for evaluating the anti-tumor activity of genetically modified pNK cells *in vivo* using a MDA-MB-231 intraperitoneal xenograft mouse model (n = 5). (E) The tumor burden of each group was measured using total bioluminescence values from control pNK, CAR-pNK, or CAR-TIGIT<sup>KO</sup>-pNK cells. (F) Bioluminescence images were acquired on days 2, 9, 16, 23, and 30 by IVIS. ns, non-significant; \*\*\*p < 0.001; \*\*\*\*p < 0.0001. I.P.: intraperitoneal injection.

### 2.4.5 Cas9-RNP containing RPs allow site-specific CAR integration into the NK cell genome

CRISPR-Cas9 genetic modification is mediated by a cellular DNA repair mechanism caused by DSBs, which has been shown to insert a lentiviral genome at the DSB site when combined with Cas9 and transgene-loaded lentiviral particles.<sup>241</sup> Thus, we assessed whether site-specific CAR integration into the genome also occurred in our CAR-TIGIT<sup>KO</sup> NK cells (**Figure 2.6 A**). To investigate DSB-mediated genome insertion in NK cells, we extracted genomic DNA from primary NK cells transduced with RPs and amplified the region surrounding the sgRNA binding site using PCR (Set 1; TIGIT-For and TIGIT-Rev), as shown in Figure 2.6 A. All DNA extracted from parental and transduced pNK cells showed the presence of a *TIGIT* amplicon in three different donors. To assess integrated viral genomes, we amplified a portion of pMIG and pMIG-anti-EGFR-CAR from transduced NK cells using pMIG-targeting primers (Set 2; pMIG-F and pMIG-R). This part of the transgene was found in all NK cells modified with pMIG backbones. To determine whether anti-EGFR-CAR specifically integrated into the anti-*TIGIT* sgRNA targeting site, we amplified gene fragments using the *TIGIT*-specific primer and a 5'*LTR*-specific primer (Set 3; TIGIT-For and 5'*LTR*-Rev). Notably, amplicons from PCR with TIGIT-For and 5'*LTR*-Rev primers were observed only in the genomic DNA from the CAR-TIGIT<sup>KO</sup>-pNK cells, suggesting targeted CAR transgene insertion into the *TIGIT* locus (**Figure 2.6 B**). The amplicons generated by primer set 2 were more abundant than those from primer set 3, indicating that random CAR integrations predominantly occurred. To further validate the site-specific CAR integration, we cloned the PCR amplicons and Sanger-sequenced seven individual PCR clones. We confirmed the presence of site-specific transgene insertions from all clones. Interestingly, due

to the NHEJ-induced indels, various genomic modifications such as nucleotide deletion and insertion were observed (**Figure 2.6 C, D**). Taken together, our RPs utilizing Cas9-RNP against the *TIGIT* locus enable simultaneous site-specific anti-EGFR-CAR integration in primary NK cells.

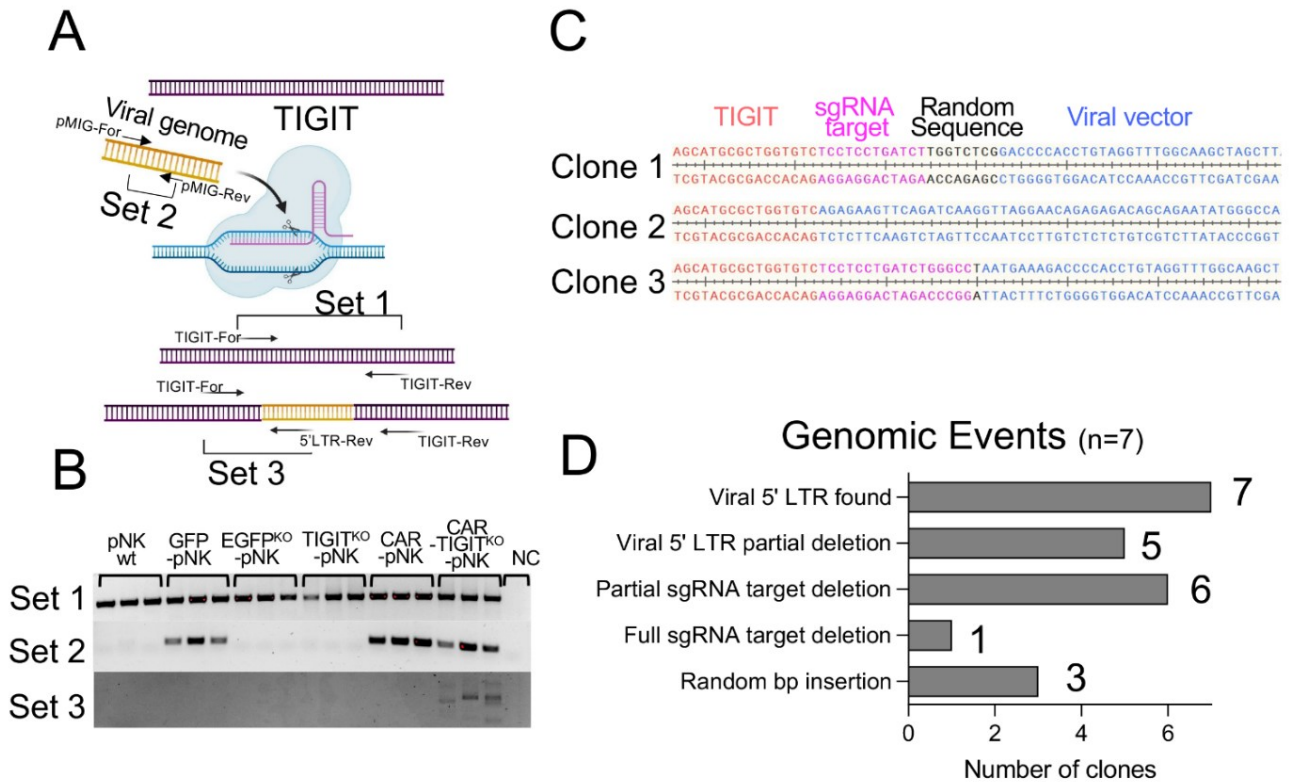


**Figure 2.6 Site-specific CAR integration into an NK cell genome by Cas9-sgRNA RPs.** (A) Illustrative concept of a site-specific CAR integration into the genome by Cas9-sgRNAs. The bottom DNA indicates the genomic modification after engineering with Cas9-RNP loaded RPs. Arrows indicate the locations and directions of primers for PCR. (B) PCR amplicons from primer set 1, set 2, and set 3. Note that the amplicons from PCR with primer set 3 indicate possible site-specific CAR integration into the *TIGIT* locus. (C) Representative Sanger sequencing results of three independent amplicons from PCR with primer set 3. (D) Summary of various genomic events in seven independent amplicons from PCR with primer set 3.

## 2.5 Discussion

This work aimed to test whether the delivery of Cas9-sgRNA RNP complexes via RPs is effective in knocking out genes in NK cells. This technology has been successful in engineering mouse bone marrow cells, human T cells, and human B cells.<sup>178,241</sup>, but has not yet been reported for NK cells, which are known to be more refractory to genetic modification than other immune cells.<sup>128</sup> By adopting the retroviral particle system called Nanoblade, from the original report,<sup>178</sup> we clearly demonstrated that RP-based technology is applicable to NK cell engineering. We established a protocol by which not only Cas9-sgRNA RNP complexes but also CAR transgene could be concurrently delivered to primary NK cells by RPs without a convoluted virus precipitation process. The engineered NK cells clearly showed target gene knockout and CAR expression, and were further used to investigate the outcome of the genetic modification in the *ex vivo* and *in vivo* responses of the anti-tumor response.

BaEV-G allowed successful modifications in NK cells.<sup>135,181</sup> BaEV binds amino acid transporters, ASCT1 and ASCT2, which are highly expressed on activated NK cells, facilitating the entry of BaEV pseudotyped vectors into NK cells.<sup>128,136</sup> In the earlier report, BaEVRless was used to pseudotype retroviral particles.<sup>242,243</sup> BaEVRless benefited the production of BaEV pseudotyped viral vectors compared to the wild-type BaEV.<sup>135</sup> BaEVRless increased the titer of viral particles in combination with VSV-G pseudotyping.<sup>178,181</sup> Despite these reported advantages of the BaEVRless, we observed a highly cytotoxic effect from syncytium formation among RP-producing Lenti-X 293T cells post-transfection. Fusion-mediated producer cell death led us to test non-syncytium-forming BaEV (BaEV-TR). Previously, the RD114 retroviral envelope was modified to contain a transmembrane domain and R peptide from MLV, which benefited viral vector production.<sup>244</sup>

The same strategy was applied to BaEV and increased the scale of viral vector production without inducing syncytia.<sup>135</sup> In this study, we tested whether the BaEV-TR benefits RP production. In addition, we applied a novel flow virometry technique to characterize and quantify RP particles. Since violet lasers are much stronger than blue lasers, violet laser-based side scatter (SSC) calibration was used to measure small retroviral particles.<sup>245,246</sup> Our EGFP knockout data reproduced the results previously reported using VSV-G and BaEVRless pseudotyped Cas9-loaded RPs.<sup>178,181</sup> Interestingly, we found that VSV-G and BaEV-TR RPs were more abundantly produced compared to those RPs with VSV-G and BaEVRless pseudotyping and showed the greatest knockout efficiency. RPs produced with BaEV-TR alone could also form a clear retroviral particle population and induce EGFP knockout at high efficiencies.

Although primary NK cells expanded from PBMCs can be an excellent source of NK cells for CAR transduction, performing multiple rounds of genetic manipulation may not be plausible due to the limitations of NK cell expansion. Therefore, a novel strategy, as we have developed here, to simultaneously modify primary NK cells with CAR overexpression and suppressive gene knockout would be desirable. We combined the RP delivery system and successfully achieved anti-EGFR-CAR overexpression and TIGIT knockout in primary NK cells using single transduction, leading to an innovative strategy to generate a large number of gene-edited CAR-NK cells. A recent report showed a similar approach in T cells using lentiviral particles.<sup>241</sup> Our report is the first to demonstrate the double delivery of a CAR construct and a Cas9-sgRNA-RNP complex to primary NK cells. In addition, we also showed evidence of site-specific CAR transgene integration into the site targeted by the Cas9-sgRNA RPs. Since the concern of random genomic integration of the CAR transgene is serious in

engineering-based immunotherapy due to accidental oncogenesis, the site-specific integration by RPs could greatly address this safety concern if used with an integrase-deficient viral vector. It should also be possible to leverage endogenous genetic regulatory machinery to drive gene expression of CARs or other transgenes utilizing this approach, similar to what has been done with targeted CAR-knockin at the *T cell receptor alpha chain (TRAC)* locus of human T cells.<sup>247</sup>

In earlier studies, titration of Cas9-loaded RPs was performed by conventional western blot and enzyme-linked immunosorbent assay (ELISA).<sup>241,178</sup> Moreover, obtaining the functionality of the gene-targeting Cas9 protein requires the incorporation of sgRNAs.<sup>248</sup> Therefore, confirming the Cas9 proteins from the RPs does not ensure the quantity of sgRNA-loaded Cas9 complexes, which are the functional RNP structures. Due to the concern of empty Cas9 proteins, the functional RPs in this study were confirmed by reduced TIGIT expression of post-transduction of NK cells by flow cytometry in combination with the number of particles determined by flow virometry. For transgene and knockout combinational modifications, CAR expression was the primary consideration in NK cells. Therefore, the titer was mainly estimated based on the expression of GFP and CAR in NK cells. Even though our method could assess the total number of RPs, advanced methods may be required to quantify the number of empty RPs.

For the method development work performed here, we decided to knock out the *TIGIT* gene in NK cells due to the robust tumor control previously observed in a *TIGIT*<sup>KO</sup> mouse model.<sup>249</sup> *TIGIT* controls NK cell function by competing with CD226 and CD96.<sup>227</sup> A previous study investigating this *TIGIT* blockade showed increased NK cell degranulation and IFN- $\gamma$  production in targeting ovarian cancer cells.<sup>250</sup> Our results suggest that breast

cancer cells do not enhance TIGIT<sup>KO</sup> NK cell function *in vitro* and *in vivo*. In contrast to our expectations and previous literature, we found that TIGIT<sup>KO</sup> was not beneficial in further improving the function of EGFR-targeting CAR-NK cells against both the triple-negative and the ER-positive breast cancer cells *in vitro* and *in vivo*. While these results should not be too broadly interpreted, TIGIT may not have a strong inhibitory effect on NK cell function in the context of CAR-NK cells. Given the efficiency of our approach, it would be interesting to combine multiple sgRNAs targeting NK-inhibitory receptors (including TIGIT) to assess their combinatorial effect in the future.

In conclusion, CRISPR-Cas9 is a powerful tool for studying NK cell biology at the genomic and proteomic levels. Here, we demonstrated that Cas9-sgRNA complex-loaded RPs can greatly enhance Cas9 delivery into NK cells in a cost-effective and reproducible manner. Furthermore, Cas9-sgRNA complex RPs loaded with transgenic cargo enabled simultaneous genome editing in combination with possible transgene integration at a targeted site, giving therapeutic potential.

# Chapter 3: Entinostat, a Histone Deacetylase Inhibitor, Enhances CAR-NK Cell Anti-Tumor Activity by Sustaining CAR Expression

## Chapter 3 authors:

Dong-Hyeon Jo<sup>1,3</sup>, Shelby Kaczmarek<sup>1,3</sup>, Abrar Ul Haq Khan<sup>1,3</sup>, Jannat Pervin<sup>1,3</sup>, Diana M Clark<sup>1</sup>, Suresh Gadde<sup>2,3,4</sup>, Lisheng Wang<sup>1,3,4</sup>, Scott McComb<sup>1,3,4,7</sup>, Alissa Visram<sup>1,5,6</sup>, and Seung-Hwan Lee<sup>1,3,4,\*</sup>

<sup>1</sup>Department of Biochemistry, Microbiology, and Immunology, Faculty of Medicine, University of Ottawa, Ottawa, ON, Canada

<sup>2</sup>Department of Cellular and Molecular Medicine, Faculty of Medicine, University of Ottawa, Ottawa, ON, Canada

<sup>3</sup>The University of Ottawa Centre for Infection, Immunity, and Inflammation, Faculty of Medicine, Ottawa, ON, Canada

<sup>4</sup>Ottawa Institute of Systems Biology, Faculty of Medicine, Ottawa, ON, Canada

<sup>5</sup>Division of Infectious Diseases, Department of Medicine, Faculty of Medicine, University of Ottawa, Ottawa, ON, Canada,

<sup>6</sup>Clinical Epidemiology Program, Ottawa Hospital Research Institute, Ottawa, ON, Canada

<sup>7</sup>Human Health Therapeutics Research Centre, National Research Council of Canada, Ottawa, ON, Canada

## Publication History:

Accepted on Feb 21, 2025, in the *Frontiers in Immunology*

This is an open-access article distributed under the terms of the Creative Commons Attribution License (CC BY). The use, distribution, or reproduction in other forums is permitted. Chapter 3 contains a slightly modified version of the paper. The published version of this chapter can be found:

<https://doi.org/10.3389/fimmu.2025.1533044>

### **Author Contributions**

D.H.J. and S.H.L. performed molecular cloning, designed experiments, analyzed data, and wrote the manuscript. S.K. optimized NK cell media. A.K. and J.P. performed puromycin staining. D.C. tested different promoters. S.M. generated backbone plasmids and a cloning strategy. D.H.J., A.V., S.G., S.M., L.W., and S.H.L. contributed to the discussion during the study. S.H.L. obtained funding. D.H.J. performed 95% of the experiments.

### **Acknowledgments**

We appreciate CYTOSEN for generously supplying the K562 feeder cells that express 4-1BBL-mbIL-21. The rhIL-2 cytokine was sourced from the NCI Preclinical Repository. We also acknowledge the StemCore Laboratories Genomics Core Facility (OHRI) and the Preclinical Imaging Core (PCIC) (RRID: SCR\_012601 and SCR\_021832) for their contributions. **Illustrations were created using BioRender.com.**

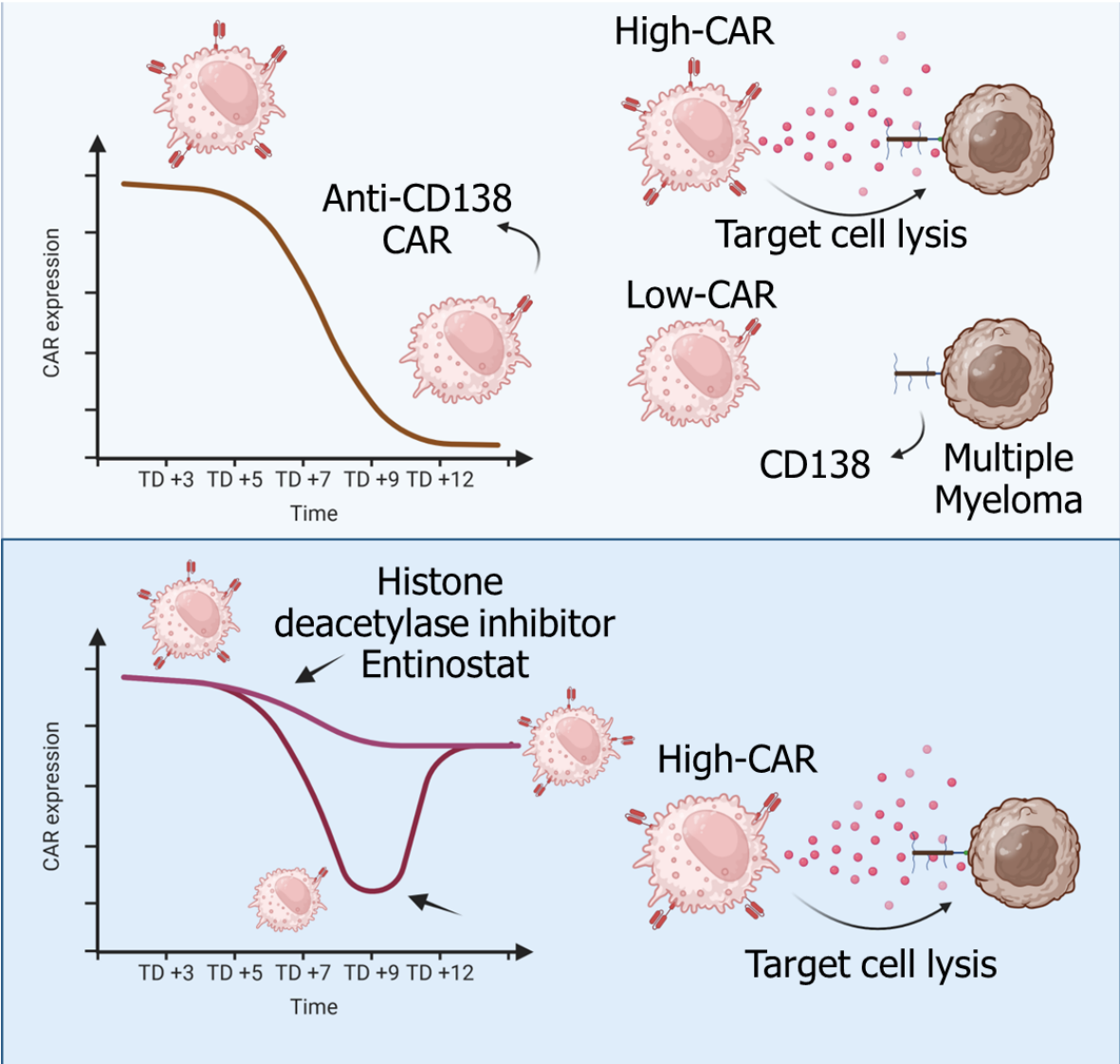


Figure 3.1 Graphical abstract for Chapter 3

### 3.1 Abstract

NK cell therapy has demonstrated significant potential in cancer immunotherapy by harnessing NK cells to target malignancies. CD138-targeting CAR-engineered NK cells offer a promising therapeutic option for multiple myeloma (MM). However, sustaining CAR expression on CAR-NK cells during *ex vivo* expansion poses a challenge to developing effective immunotherapies. In this study, primary NK cells were isolated, cryopreserved, and modified to express anti-CD138 CARs through retroviral transduction. HDACis, particularly entinostat (ENT), were applied to enhance CAR expression stability in CAR-NK cells. Our findings indicate that ENT treatment significantly improves and maintains CAR expression, thereby enhancing the cytotoxic activity of CAR-NK cells against CD138-positive multiple myeloma cells. ENT-treated CAR-NK cells exhibited prolonged CAR persistence and more significant tumor reduction in an MM tumor-bearing mouse model, highlighting the therapeutic potential of ENT-treated CAR-NK cells. This study provides the first evidence that ENT can sustain CAR expression in CAR-NK cells in a promoter-dependent manner, potentially enhancing anti-tumor efficacy in multiple myeloma and underscoring the possible need for further clinical evaluation.

## 3.2 Introduction

Allogeneic NK cell therapy holds promising potential in cancer immunotherapy by utilizing NK cells from healthy donors to treat patients.<sup>211,251,252</sup> These cells can be readily expanded and stored for "off-the-shelf" use, making the therapy more scalable and accessible.<sup>211</sup> NK cells can be engineered with CARs to enhance their cytotoxic effects.<sup>137,253,254</sup> Ongoing research and clinical trials continue to demonstrate the potential of allogeneic CAR-NK therapies, particularly in treating hematological malignancies, where they have shown notable anti-tumor efficacy with a lower risk of complications like GvHD and CRS, which are common in T cell-based therapies.<sup>120,255</sup>

Multiple myeloma (MM) is a clonal plasma cell malignancy characterized by the buildup of malignant plasma cells in the bone marrow, leading to complications such as bone destruction, anemia, and renal impairment.<sup>256</sup> Despite advancements in treatments, including proteasome inhibitors, immunomodulatory drugs, CD38-targeting monoclonal antibodies, and more recently, BCMA-targeting CAR-T cells, MM remains largely incurable, with most patients eventually experiencing relapse.<sup>257,258</sup> Targeting CD138 (syndecan-1), a transmembrane proteoglycan highly expressed in myeloma cells and certain epithelial cells, has emerged as a therapeutic strategy, including using a drug-conjugated anti-CD138 antibody (BT026).<sup>259</sup> Additionally, anti-CD138 CAR-T cells have shown promise in preclinical studies, and a phase 1 clinical trial is underway for patients with relapsed and refractory multiple myeloma (NCT03672318). In NK cell therapy, anti-CD138 CAR has been tested in the NK immortalized cell line, NK92 cells.<sup>260</sup> Although on-target, off-tumor effects remain a concern due to CD138 expression in normal tissues, ongoing optimization in these

approaches could lead to significant advances in cell therapies for multiple myeloma, potentially improving survival outcomes for this difficult-to-treat malignancy.<sup>261</sup>

Viral transduction-mediated gene delivery is a widely used technique in immune cell engineering to introduce therapeutic genes, such as CARs, into T and NK cells.<sup>254,262</sup> However, one challenge is the potential for transgene silencing after integration into the host genome.<sup>263</sup> Gene expression is tightly regulated by histone acetylation, a process controlled by HATs and HDACs.<sup>188</sup> High levels of histone acetylation result in a more open chromatin structure, improving the accessibility of RNA polymerases and facilitating gene expression.<sup>188</sup> Recently, HDACi have increased histone acetylation, resulting in more relaxed chromatin and enhanced promoter accessibility.<sup>188,264</sup> HDAC inhibitors like ENT and VPA have shown promise in increasing transgene expression in cancer cell lines.<sup>205-207</sup> In T cells, TCR engineered cells have demonstrated enhanced expression following HDACi treatment.<sup>204</sup> While TCR-T cells have demonstrated HDACi-mediated transgene overexpression, it is noteworthy that prior studies involving anti-CD19 CAR-T cells treated with HDAC inhibitors, such as panobinostat and ENT, did not show enhanced CAR expression.<sup>196</sup> This discrepancy may be linked to differences in promoter responsiveness to HDACis, as demonstrated by a study on adenoviral vectors containing CMV and PPT promoters.<sup>201</sup> CMV promoter exhibited responsiveness to HDACis, resulting in GFP overexpression, whereas the PPT promoter showed no such effect.

In this study, we investigated the anti-tumor activity of anti-CD138 CAR-engineered NK cells against multiple myeloma, including the option for cryopreservation. After the CAR transduction of NK cells, we observed a progressive decrease in CAR expression in CAR-NK cells during *ex vivo* expansion. Notably, HDACi treatment restored CAR expression,

thereby enhancing effector function both *in vitro* and *in vivo*. To our knowledge, this is the first report to assess the impact of HDACi treatment on transgene overexpression in CAR-NK cells in a promoter-dependent manner. Overall, this study highlights the potential of HDACi, especially ENT, treatment to enhance the efficacy of CAR-NK cell therapy by upregulating CAR expression.

### **3.3 Materials and Methods**

#### **3.3.1 Cancer cell line culture**

Multiple myeloma cell lines, MM1.R and MM1.S, as well as B cell lymphoma cell lines, Ramos and Raji, were obtained from ATCC and cultured in RPMI-1640 medium (350-000-CL; Wisent) supplemented with 10% HI-FBS (12484028; Gibco), 100 U/mL Penicillin and 100 µg/mL Streptomycin (Pen/Strep) (SV30010; HyClone), 55 µM β-Mercaptoethanol (21985023; Gibco), and 20 mM HEPES (CA12001-708; VWR) (hereafter called RP10 medium). MDA-MB-231 cells were also obtained from ATCC, while Lenti-X 293T cells were purchased from Takara (632180), and both were cultured in high-glucose DMEM (319-005-CL; Wisent) supplemented with 10% HI-FBS and 100 µg/mL Pen/Strep. NK92 cells were cultured in RP10 medium supplemented with 200 U/mL human recombinant IL-2 (NCI Preclinical Repository, USA). Two different MM1.S-firefly luciferase (FLUC) cells, MM1.S-FLUC-red fluorescent protein (RFP) and MM1.S-FLUC-blasticidin cells, were utilized for *in vivo* experiments.

### 3.3.2 Generation of master stocks of human primary NK cells

The Ottawa Health Science Network Research Ethics Board (#20200527-01H) and the University of Ottawa (#H-01-21-6568) authorized the collection of whole blood from healthy adults. Peripheral blood mononuclear cells (PBMCs) were extracted using Ficoll (45001750; Cytiva) gradient centrifugation, and NK cells were isolated as previously demonstrated.<sup>137</sup> The isolated primary NK (pNK) cells were immediately cultured with two times the number of irradiated K562 feeder cells, which expressed membrane-bound IL-21 and 4-1BBL (a kind gift from CYTOSEN), along with 100 U/mL of IL-2 in RP-10 medium for three days.<sup>265</sup> After three days, half of the medium was replaced with NKMACS medium (130-114-429; Miltenyi Biotech), and the cells were expanded for 2 additional days. On day 5, an equal volume of NKMACS medium was added. By day 6, the partially expanded pNK cells were frozen at -80 °C using a freezing medium containing 90% FBS and 10% DMSO (BP231-100; FisherBioReagents).

### 3.3.3 Molecular Cloning

To generate a retroviral pMIG-Green fluorescent protein (GFP)-IL-15 plasmid, EcoRI-GFP-IL-15-PacI fragments were produced and digested with EcoRI (FD0274; Thermo Fisher Scientific) and PacI (FD2204; Thermo Fisher Scientific). The resulting fragment was cloned into an EcoRI- and PacI-treated pMIG plasmid (gifted by William Hahn; 9044; Addgene). To create the pMIG-GFP-IL-15-EFS-CAR construct, the FMC63-28Z CAR plasmid was obtained from Addgene (#135991, deposited by Scott McComb; <http://n2t.net/addgene:135991>; RRID: Addgene\_135991).<sup>266</sup> The anti-CD138 single-chain variable fragment (scFv) gene fragment, purchased from GeneArt String (Thermo Fisher

Scientific), was cloned into the FMC63-28Z CAR by replacing FMC63 with anti-CD138 scFv using BpiI-Golden Gate cloning, as described in previous studies (FD1014; Thermo Fisher Scientific).<sup>266</sup> The entire construct, including the EFS promoter and the anti-CD138 CAR, was amplified by PCR and cloned into the pMIG-GFP-IL-15 plasmid using PacI and Sall (FD0644; Thermo Fisher Scientific) restriction sites. For the generation of different promoter-containing CAR constructs, the CMV promoter was extracted from the pLenti-CMV-GFP-SV40-puro plasmid using CMV-F (AGTCGTACCGGTCGTTACATAACTTACGGTAA) and CMV-R (AACATCGGATCCCGCGTCACGACACAGCTCTGCTTATATAGACCT) primers and the MSCV promoter (MSCV-F: AGTCGTACCGGTAATGAAAGACCCACCTGTA and MSCV-R: AACATCGGATCCCGCGTCACGACACGGCGCGCCGAGTGAGGGGTT) was transferred from the pMIG-GFP-IL-15 plasmid to a QC5-EFS-anti-EGFR CAR-IL-15 construct by replacing the EFS promoter using BshTI and BamHI. To generate CD138-positive Ramos cells, the SV40-puro from the pLenti-CMV-GFP-SV40-puro plasmid was replaced with an EFS-multiple cloning site (MCS) using MluI (FD0564; Thermo Fisher Scientific) and Eco91I (FD0394; Thermo Fisher Scientific). The EFS-MCS fragment was purchased from Thermo Fisher Scientific (GeneArt String). The CD138 fragment (GeneArt String, Thermo Fisher Scientific) was then inserted into the pLenti-CMV-GFP-EFS-MCS plasmid using Bsp119I (FD0124; Thermo Fisher Scientific) and NheI (FD0974; Thermo Fisher Scientific). PCR was performed using Platinum™ SuperFi™ PCR Master Mix (12358050; Thermo Fisher Scientific). All cloning was confirmed by sequencing conducted at the Ottawa Hospital Research Institute (OHRI) DNA sequencing facility, and sequencing results were analyzed using SnapGene (Dotmatics).

### 3.3.4 Retroviral and lentiviral vector production

To produce retroviral vectors, we followed a previously published method with slight modifications.<sup>137</sup> A total of  $1.2 \times 10^6$  Lenti-X 293T cells were plated per well on a 6-well plate (83.3920, Sarstedt) in 2 mL of serum-containing Opti-MEM medium (51985091, Gibco). The next day, the cells were transfected with 1,200 ng of retroviral transgene plasmids, 1,200 ng of MLV-gag-pol, 500 ng of pMD2.G (deposited by Didier Trono, Addgene #12259; <http://n2t.net/addgene:12259>; RRID: Addgene\_12259), and 100 ng of BaEV-TR<sup>135</sup> using Lipofectamine 3000 (L3000015, Invitrogen) (6  $\mu$ L P3000 and 7  $\mu$ L Lipofectamine 3000). After a 4-hour incubation, the medium was completely removed and replaced with 2 mL of fresh Opti-MEM medium. The first viral supernatant was collected the day after, followed by a fresh medium replacement for the second harvest on day 2. Viral supernatants were filtered using a low protein-binding PES filter (83.1826, Sarstedt) and stored at -80 °C. To produce lentiviral vectors and the functional titer calculation, we followed the method previously published.<sup>137</sup>

### 3.3.5 Primary NK cell transduction and expansion

Cryopreserved primary NK (pNK) cells of master stocks were thawed and rested overnight in a DMEM/F-12 + supplement (DS) medium,<sup>267</sup> containing 10% HI-FBS and 100 U/mL IL-2. The following day, the pNK cells were transduced in a flat-bottom plate pre-coated with 20  $\mu$ g/mL Retronectin (T100B, Takara Bio). Viral supernatant and 100 U/mL IL-2 were added to the plate. The cells were centrifuged at  $1,000 \times g$  for 30 minutes at 32 °C and cultured overnight at 37 °C and 5% CO<sub>2</sub>. The next day, the engineered pNK cells were stimulated with irradiated feeder cells at a 1:5 ratio and 100 U/mL IL-2. The pNK cells were

then expanded by replacing the culture medium every 2 to 3 days with fresh DS medium containing 100 U/mL IL-2. For experiments involving HDACis, NKMACS medium containing 10% HI-FBS and gentamicin (10 µg/mL, 15710-064, Gibco) was used.

### 3.3.6 Immunostaining

Antibody-based cell immunostaining was performed as previously described<sup>137</sup> with the following antibodies, reagents, and beads. Data were analyzed by Kaluza Analysis 2.1 (Beckman Coulter) and Flowjo v10.8.1 (BD Life Sciences). Jackson ImmunoResearch Laboratories Inc: anti-human Fab(ab')<sub>2</sub> (109-605-006, AF647), anti-Alpaca's VHH (128-605-230, AF647). Invitrogen™ : NKp46 (53-3359-42, AF488), CTLA4 (11-1529-42, FITC), NKp30 (12-3379-42, PE), NKG2D (46-5878-42, PerCP-eFluor710), CD16 (46-0118-42, PerCP-eFluor710), IgG1k (46-4714-82, PerCP-eFluor710), LAG3 (56-2239-41, APC), CD38 (67-0389-42, SB702). BD Biosciences: CD57 (560844, PE). Biolegend: IgG2k (400506, FITC), KIR2DL2/3 (312604, FITC), NKp44 (325108, PE), NKG2C (375003, PE), murine CD45 (110708, PE), IgG1k (400112, PE), TNF-α (557068, PE) CD138 (356514, PE/Cyanine7), IgG1k (400125, PE/Cyanine7), CD107a (328620, APC), NKG2A (375108, APC), KIR3DL1 (312716, APC), IgG1k (400120, APC), IFN-γ (502548, APC/Fire710), CD56 (318328, BV421), CD3 (317332, BV510), CD138 (356520, BV605), IgG1k (562652, BV605), human CD45 (304048, BV785), IFN-γ (502542, BV785). LIVE/DEAD™ Fixable Viability dyes: Yellow (L34959, Invitrogen), Aqua (L34957, Invitrogen), Near-IR (L34976, Invitrogen), Green (L23101, Invitrogen). UltraComp eBeads™ Plus Compensation Beads (01-3333-42, Invitrogen).

### **3.3.7 Puromycin staining**

Puromycin staining was performed based on the previously published paper.<sup>268</sup> Briefly, NK cells were plated on a 48-well plate (83.3923, Sarstedt) with or without 100 mM 2-Deoxy-D-Glucose (2DG) (D8375-5G, MilliporeSigma) and 1  $\mu$ M oligomycin (O4876-5MG, MilliporeSigma) for 45 minutes at 37 °C. Then, the cells received 10  $\mu$ g/ml puromycin (450-162-XL, Wisent) and incubated for 45 minutes at 37 °C. The cells were washed with ice-cold PBS and stained with a live-dead dye and an anti-puromycin antibody (381508, AF647, Biolegend). A Cyto-Fast™ Fix/Perm Buffer Set (426803, Biolegend) was used for the intracellular puromycin staining by following the manufacturer's instructions.

### **3.3.8 *In vitro* CD107a, IFN- $\gamma$ and TNF- $\alpha$ assays**

For CD107a, IFN- $\gamma$ , and TNF- $\alpha$  assays, effector and target cells were plated at a 1:1 ratio on a 96-well plate, with an anti-CD107a antibody (if required) added to each well. The plate was incubated at 37 °C and 5% CO<sub>2</sub>. After 1 hour of incubation, brefeldin A (00-4506-51; Invitrogen) was added to the culture. NK cells and target cells were co-incubated for an additional 3 hours. Following the incubation, the cells were washed with PBS (10010049, Gibco) containing 2% HI-FBS and stained with appropriate antibodies for flow cytometric analysis.

### **3.3.9 *In vitro* killing assay**

For short-term killing assay, target cells were labeled with cell-trace violet (CTV) dye (C34571, Invitrogen™) according to the manufacturer's instructions. The CTV-labeled target cells were then co-cultured with NK cells for 4 hours at varying effector-to-target cell ratios.

The percentage of dead cells within the CTV-positive target cell population was subsequently analyzed by flow cytometry.

For long-term killing assays, FLUC-expressing target cells were used based on the previously published studies.<sup>269</sup> Primary NK cells were co-cultured overnight with FLUC-expressing target cells at varying effector-to-target ratios in a 96-well assay plate (31113, Labselect). Following incubation, D-Luciferin (122799-5, Revvity) was added to the wells to reach a final 150 µg/mL concentration. Luminescence was measured using the Synergy H1 Multi-Mode Plate Reader (Biotek) to assess the cytotoxic activity of the pNK cells against the target cells. Cytotoxicity was calculated based on the equation below. (Lum: Luminescence)

$$\left(1 - \frac{Lum^{Target+NK\ cells}}{Lum^{Target\ alone} - Lum^{medium}}\right) \times 100$$

### 3.3.10 Histone deacetylase inhibitor treatment

Entinostat (A8171-5.1, Labclinics), Valproic acid (P4543-10G, MilliporeSigma), and RGFP966 (16917-1, Cayman Chemical) were obtained from commercial sources. For short-term exposure and dosage evaluation, overnight-rested pNK cells were transduced with CAR-IL-15 retroviral vectors at an MOI of 3, following the standard pNK cell transduction protocol. The transduced cells were stimulated and expanded for 5 days (TD + 5). After 5 days, the modified NK cells were cryopreserved at -80 °C using a freezing medium. The engineered and cryopreserved NK cells were later thawed and rested overnight for HDACi titration. The resting NK cells were treated with varying concentrations of HDACis (as indicated in the figures), incubated for 2 days, and then immunostained to validate transgene expression.

For long-term exposure, pNK cells were transduced, stimulated, and expanded for 5 days. Afterward, the cells were divided into two groups: cultured in an HDACi-containing medium and a DMSO-containing (non-treated, NT) medium. The medium was refreshed every 2 to 3 days. Prior to *in vitro* and *in vivo* experiments, ENT-treated cells were washed once with NKMACS medium.

### **3.3.11 *In vivo* tumor control experiments**

A breeding pair of NSG mice was acquired from Jackson Laboratories, and the colony was housed in the specific pathogen-free animal facility at the University of Ottawa, adhering to Canadian Council on Animal Care guidelines. Male NSG mice (8 to 12 weeks old) received  $2.5 \times 10^6$  MM1.S cells expressing firefly luciferase intravenously. The mice were then assigned to groups ( $n = 5$ /group treated with NK cells or  $n = 2$  or  $3$  for a PBS control). Three or seven days post-injection of the target cells, the mice were administered  $1 \times 10^7$  pNK cells intravenously (for the HDACi study, twice at six-day intervals). The luciferase signal was monitored using the IVIS® Spectrum (Perkin Elmer) and Newton animal imaging system (VILBER; in the middle of this project, Newton was purchased). Blood samples were collected from the saphenous vein. All procedures were approved by and conducted in compliance with the animal care guidelines of the University of Ottawa.

### **3.3.12 Statistical analysis**

The mean values for multiple factors were analyzed using two-way ANOVA, comparing the means of the groups. A t-test was used for two-factor comparisons to evaluate the mean values performed in GraphPad Prism 9 (Dotmatics). Statistical significance was

defined as  $p < 0.05$ . Data are presented as mean  $\pm$  SD, and all graphs were generated and analyzed using GraphPad Prism 9.

## 3.4 Results

### 3.4.1 NK cells from a cryopreserved master stock are expandable *ex vivo* and suitable for CAR engineering

Traditional NK cell engineering involves a continuous process of NK cell isolation, expansion, engineering, and further expansion, where the efficiency of NK cell expansion and engineering is highly donor-dependent. To streamline this process and minimize redundant NK cell isolations, we hypothesized that cryopreserving NK cells at the early stages of expansion could improve NK cell readiness for CAR-NK cell production. pNK cells from three donors were expanded using irradiated K562 cells expressing 4-1BBL and mbIL-21 in the presence of IL-2.<sup>265</sup> After 6 days of expansion, master stocks were prepared by cryopreserving NK cells in FBS containing 10% DMSO. After 2 days of cryopreservation, a vial was thawed, and the pNK cells were further expanded (**Figure 3.2 A**). Their expansion rates were slightly lower than those of pNK cells without cryopreservation. pNK cells that had not been frozen achieved an average 1,609-fold expansion over 12 days. pNK cells from the frozen master stock showed a transient delay in expansion but eventually reached similar growth rates to those of unfrozen pNK cells, achieving an average 846-fold expansion (D6 + 6). Although the total expansion was 1.9-fold lower after 12 days, the expansion rates at two-day intervals following cryopreservation were comparable (**Figure 3.2 B**). Phenotypes of the expanded cells were similar and showed high purity (**Figure 3.2 C, Figure S4**).

To explore the potential for engineering pNK cells from the master stock, we generated a lentiviral vector encoding 4-1BB and CD3 $\zeta$  signaling-based CAR and human IL-15. We thawed pNK cells that had been cryopreserved for one week or three months in a DS medium<sup>267</sup> containing 100 U/mL IL-2 and rested them overnight to remove damaged cells. The following day,  $5 \times 10^4$  pNK cells were transduced with lentiviral vectors at an MOI of 2. After overnight transduction, the viral supernatant was replaced with fresh medium containing  $2.5 \times 10^5$  (5 $\times$ ) irradiated feeder cells (**Figure 3.2 D**). The medium was changed every two days. Fold-expansion and CAR expression were assessed five days post-transduction (TD + 5) and up to 12 days (TD + 12). pNK expansion from cells cryopreserved for either one week or three months was comparable for both unmodified and CAR-engineered pNK cells (**Figure 3.2 E**). CAR expression in CAR-transduced NK cells decreased similarly over time in NK cells cryopreserved for one week or three months when measured on TD + 5 and TD + 12 (**Figure 3.2 F**). Taken together, primary NK cells from a cryopreserved master stock are expandable *ex vivo* and are suitable for engineering via viral transduction.

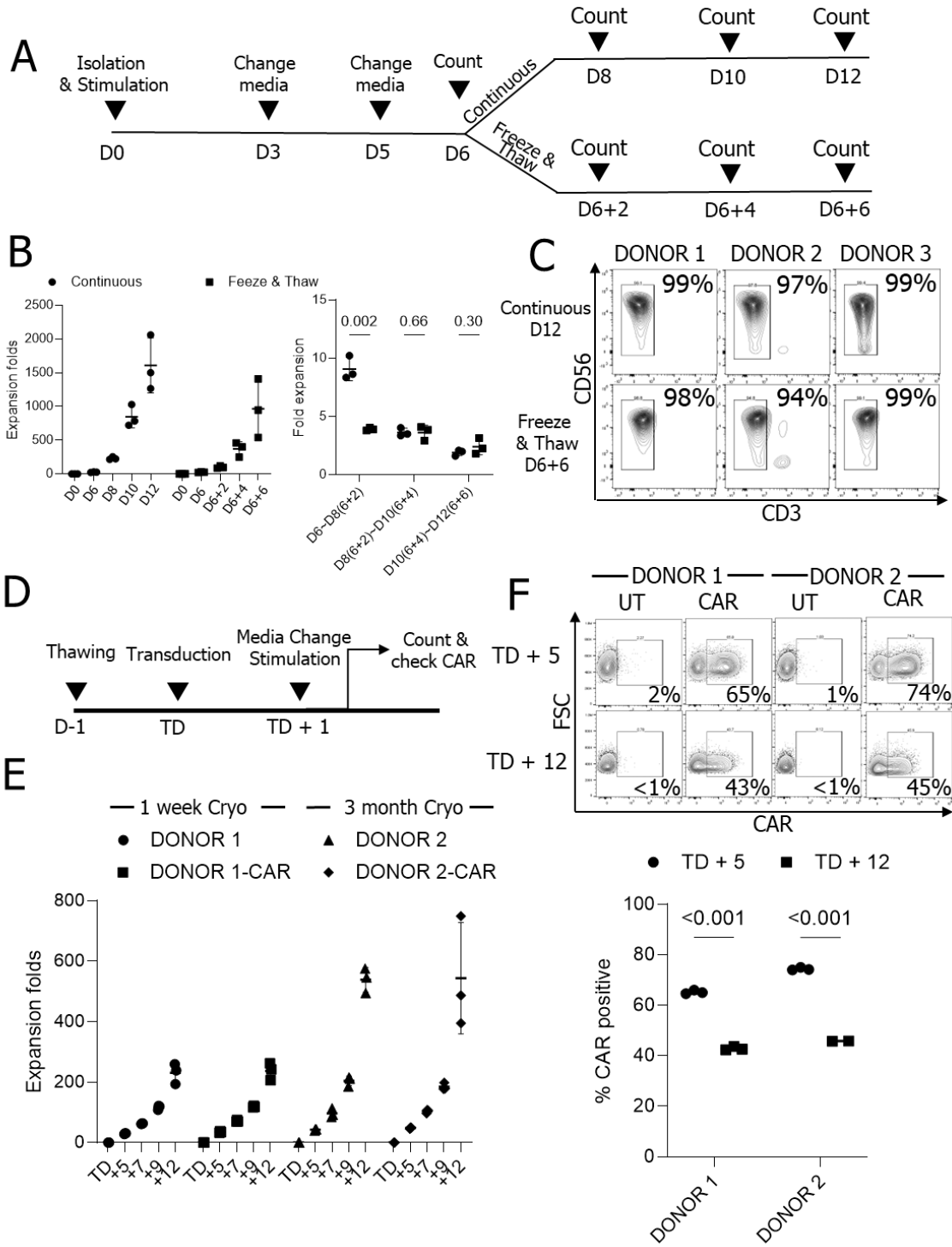


**Figure. 3.2 Cryopreserved master stock NK cells can be expanded and engineered for CAR therapy.** (A) Schematic diagram showing the expansion of cryopreserved NK cells. (B) NK cell expansion folds measured at two-day intervals (n=3 donors' NK cells) (C) NK cell purity analysis from expanded NK cells (n=3 donors' NK cells). (D) Timeline for NK cell engineering and expansion. (E) Expansion folds in UT and CAR engineered NK cells. (n=2 donors' NK cells with triplicate transduction) (F) CAR expression on days 5 and 12 after the transduction (TD + 5 and TD + 12). (n=2 donors' NK cells with triplicate transduction); UT: Untransduced, Cryo: Cryopreserved NK cells.

### 3.4.2 Anti-CD138 CAR enhances NK cell function *in vitro*; however, CAR expression decreases during expansion *ex vivo*

To enhance the ability of expanded NK cells to kill multiple myeloma cells, we designed an anti-CD138 CAR using a BpI-based type II restriction enzyme cloning approach.<sup>266</sup> This CAR construct includes a CD8 hinge, a CD28 transmembrane domain, and CD28-CD3 $\zeta$  intracellular signaling domains in a lentiviral vector. The anti-CD138-CAR sequence was integrated into the retroviral vector pMIG-GFP-IL-15 to generate a retroviral CAR transgene plasmid (**Figure 3.3 A**). This transfer was done due to the use of the GFP-IL-15 backbone. NK92 cells were transduced with retroviral vectors containing GFP-IL-15 and GFP-IL-15-CAR (CAR-IL-15) constructs, and surface CAR expression was assessed using an anti-human Fab(ab')<sub>2</sub> antibody.<sup>270</sup> NK92 cells transduced with GFP-IL-15 showed 71% GFP expression with minimal background anti-Fab(ab')<sub>2</sub> signals, whereas CAR-IL-15-NK92 cells displayed 69% GFP expression and over 50% CAR-positive populations (**Figure 3.3 B**).

To assess NK cell functionality and cytotoxicity, GFP-IL-15-NK92 and CAR-IL-15-NK92 cells were co-cultured with CD138-positive multiple myeloma cell lines (MM1.R and MM1.S) and CD138-negative cell lines (Ramos and MDA-MB-231) (**Figure S5 A**). CD138-

positive targets, MM1.R and MM1.S, induced an average of 67% and 48% CD107a expression and 34% and 17% IFN- $\gamma$  production in CAR-IL-15-NK92 cells, respectively, compared to 28% and 21% CD107a and 7% and 3% IFN- $\gamma$  in UT-NK92 cells. In contrast, negative controls (Ramos, MDA-MB-231) or NK cells alone did not enhance NK cell responses in CAR-IL-15-NK92 cells beyond those seen in UT-NK92 cells (**Figure 3.3 C, D**). CAR-IL-15-NK92 cells demonstrated enhanced cytotoxicity against MM1.R and MM1.S compared to the GFP-IL-15-NK92 cells, while cytotoxicity against Ramos and MDA-MB-231 cells was limited, regardless of CAR expression (**Figure 3.3 E**).

To evaluate the functionality of the anti-CD138 CAR in expanded pNK cells derived from cryopreserved stocks, we thawed frozen pNK cells, genetically modified the pNK cells with retroviral vectors encoding either GFP-IL-15 or CAR-IL-15, and expanded them for 5 days. All three CAR-IL-15-pNK cell cultures exhibited positive staining for CAR, while GFP-IL-15-pNK and UT-pNK cells showed no CAR signals. Both GFP-IL-15 and CAR-IL-15-pNK cells exhibited GFP-positive signals (**Figure S5 B**). Next, we assessed the anti-tumor activity of CAR-IL-15-pNK cells. pNK cell cytotoxicity was evaluated against CD138-positive MM1.S cells and CD138-negative Raji cells. Notably, CAR-IL-15-pNK cells from two donors exhibited significantly higher cytotoxicity against CD138-positive MM1.S but not CD138-negative Raji cells (**Figure 3.3 F**). To address CAR specificity, we generated Ramos cells expressing CD138 (Ramos-CD138). Ramos-CD138 cells induced stronger CD107a and IFN- $\gamma$  signals than Ramos cells (**Figure S5 C**). We also evaluated the *in vivo* cytotoxicity of CAR-IL-15-pNK cells by injecting  $2.5 \times 10^6$  MM1.S cells into NSG mice, followed three days later by  $1 \times 10^7$  pNK cells (**Figure 3.3 G**). In line with our *in vitro* findings, CAR-IL-15-pNK cells demonstrated significantly enhanced eradication of multiple

myeloma cells compared to GFP-IL-15-pNK and UT-pNK controls (**Figure 3.3 H**). Although our anti-CD138 CAR construct improved the anti-tumor function *in vivo*, we also observed a marked decline in CAR expression during *ex vivo* expansion, with expression dropping from 51% (average, avg) on TD + 5 to 15% (avg) on TD + 12, leading to the limited use of CAR-pNK cells within a short expansion time (**Figure 3.3 I**).

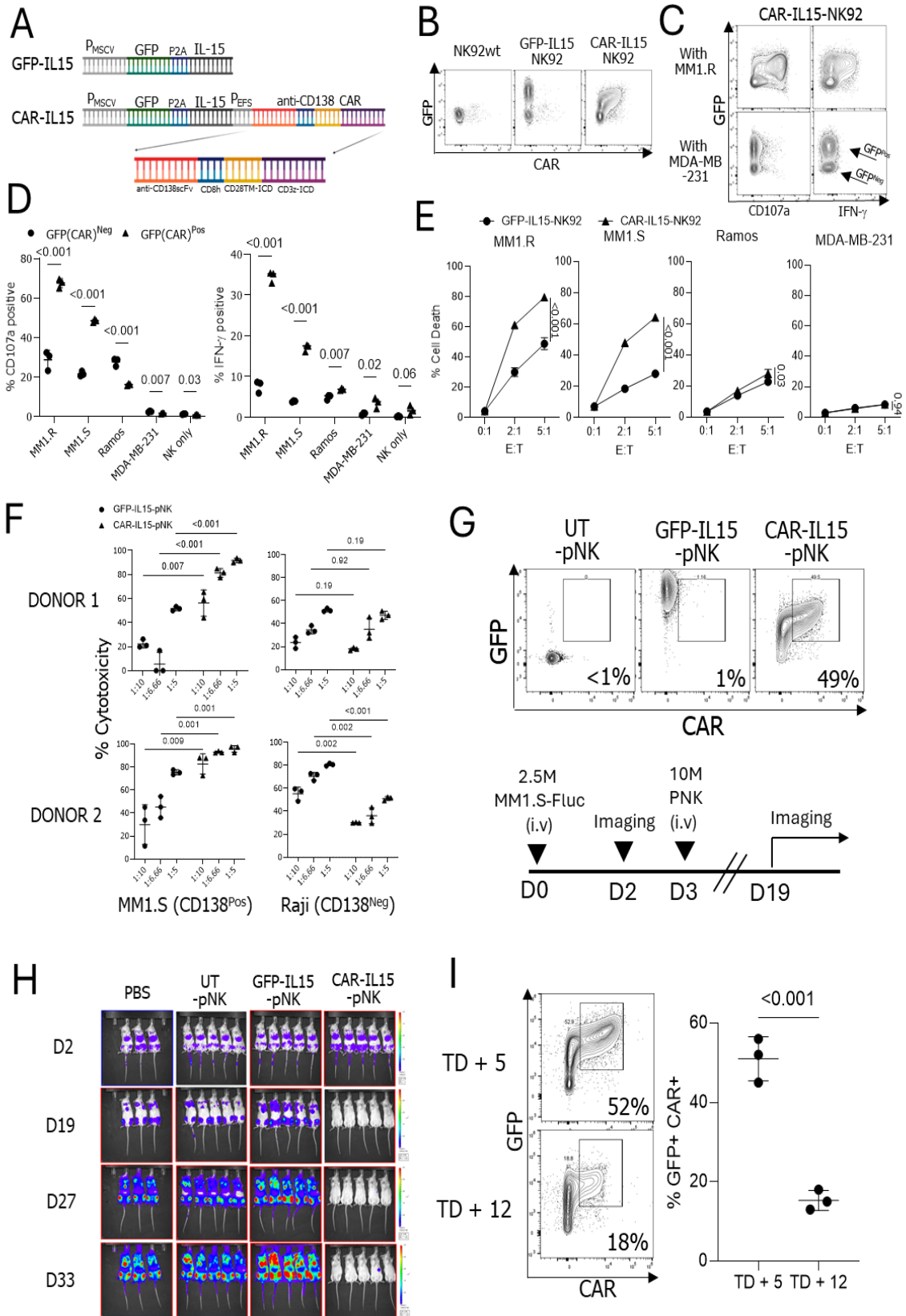


**Figure. 3.3 Functionality and CAR expression of anti-CD138-CAR engineered NK cells.** (A) Design of the anti-CD138 CAR construct. (B) GFP and CAR expression in engineered NK92 cells. (C) The CD107a and IFN- $\gamma$ -expression patterns in modified NK92 cells co-cultured with CD138-positive target MM1.R and CD138-negative target MDA-MB-231 cells. (D) CD107a and IFN- $\gamma$  expression in NK92 cells with or without target cells. (E) NK92 cell killing assay with CD138-positive and negative target cells (F) Killing assay using engineered pNK cells with MM1.S (CD138-positive, CD138<sup>Pos</sup>) and Raji (CD138-negative, CD138<sup>Neg</sup>) cells. (n = 2 donors' NK cells) (G) Injected NK cell GFP and CAR expression, and timeline of the performed the *in vivo* experiment. (H) *In vivo* imaging. Signal intensity indicate firefly luciferase-expressing MM1.S cells. (I) CAR expression in NK cells on TD + 5 and TD + 12 (n = 3 cryopreserved donors' NK cells).

### 3.4.3 Histone deacetylase inhibitors enhance GFP and CAR expression in NK cells in a dose- and promoter-dependent manner

To explore whether this CAR downmodulation can be overcome by adding small-molecule inhibitors targeting epigenetic machinery, we employed HDACi. Specifically, we chose to use Entinostat (ENT, an HDAC class I and IV inhibitor),<sup>271</sup> Valproic Acid (VPA, an HDAC class I and IIa inhibitor),<sup>272</sup> and RGFP966 (RGFP, an HDAC 3 inhibitor)<sup>273</sup> since ENT and VPA previously showed improved transgene regulations.<sup>205-207</sup> For consistency, we cryopreserved anti-CD138 CAR-expressing pNK cells on TD + 5, then thawed, rested overnight, and cultured them with HDAC inhibitors for 2 days. Remarkably, all HDAC inhibitors significantly increased the GFP<sup>+</sup> CAR<sup>+</sup> populations in a dose-dependent manner. Without HDAC inhibitors, the GFP<sup>+</sup> CAR<sup>+</sup> NK cell population averaged 31.6%. However, this population increased to 60.6% with ENT, 57.1% with VPA, and 57.9% with RGFP966 at the highest concentrations tested without significant toxicity (**Figure 3.4 A, Figure S6**). When the MFI of CAR and GFP was assessed, CAR expression generally improved with HDACi treatment; however, the treatment had a stronger effect on GFP expression (**Figure 3.4 B**). Given that GFP and CAR expression were controlled by two distinct promoters in the

GFP-CAR-IL-15 construct, we hypothesized differential effects of HDAC inhibitors on these promoters. Since all three HDAC inhibitors produced similar effects in NK cells, we primarily used ENT in subsequent experiments.

To determine if ENT exerts different effects on various promoters, we generated lentiviral vectors containing an unrelated anti-EGFR CAR construct<sup>118</sup> driven by three distinct promoters: The MSCV promoter, EF1 $\alpha$  small (EFS) promoter, and CMV promoter. Since the MSCV and CMV promoters have shown improved expression after HDACi treatment,<sup>205,208</sup> we anticipated that ENT in NK cells would significantly enhance MSCV and CMV promoter activities. Consistent with our hypothesis, ENT significantly boosted CAR expression driven by both the MSCV and CMV promoters but had a minimal effect on the EFS promoter. Interestingly, after ENT treatment, CAR expression driven by the CMV promoter exhibited a higher MFI than the EFS promoter despite lower baseline expression in the absence of ENT (**Figure 3.4 C**). Notably, we observed enhanced CAR expression in the treatment of ENT, even though the CAR expression is under the EFS promoter in our retroviral CAR construct. Currently, we reason that the leaky upstream MSCV promoter influences the downstream EFS promoter, as reported.<sup>274,275</sup> To determine whether the increased GFP<sup>+</sup> CAR<sup>+</sup> population resulted from enhanced protein translation, we treated NK cells with puromycin and measured puromycin signals using flow cytometry as a surrogate marker for actively translating polypeptides.<sup>268</sup> Puromycin staining revealed that ENT reduced protein translation in pNK cells (**Figure 3.4 D**). Despite reduced translation, GFP expression was still higher in the presence of ENT, indicating that ENT-mediated transgene overexpression is not linked to general protein synthesis in NK cells (**Figure 3.4 E**). Taken

together, histone deacetylase inhibitors enhance CAR expression in NK cells in a promoter-specific manner.

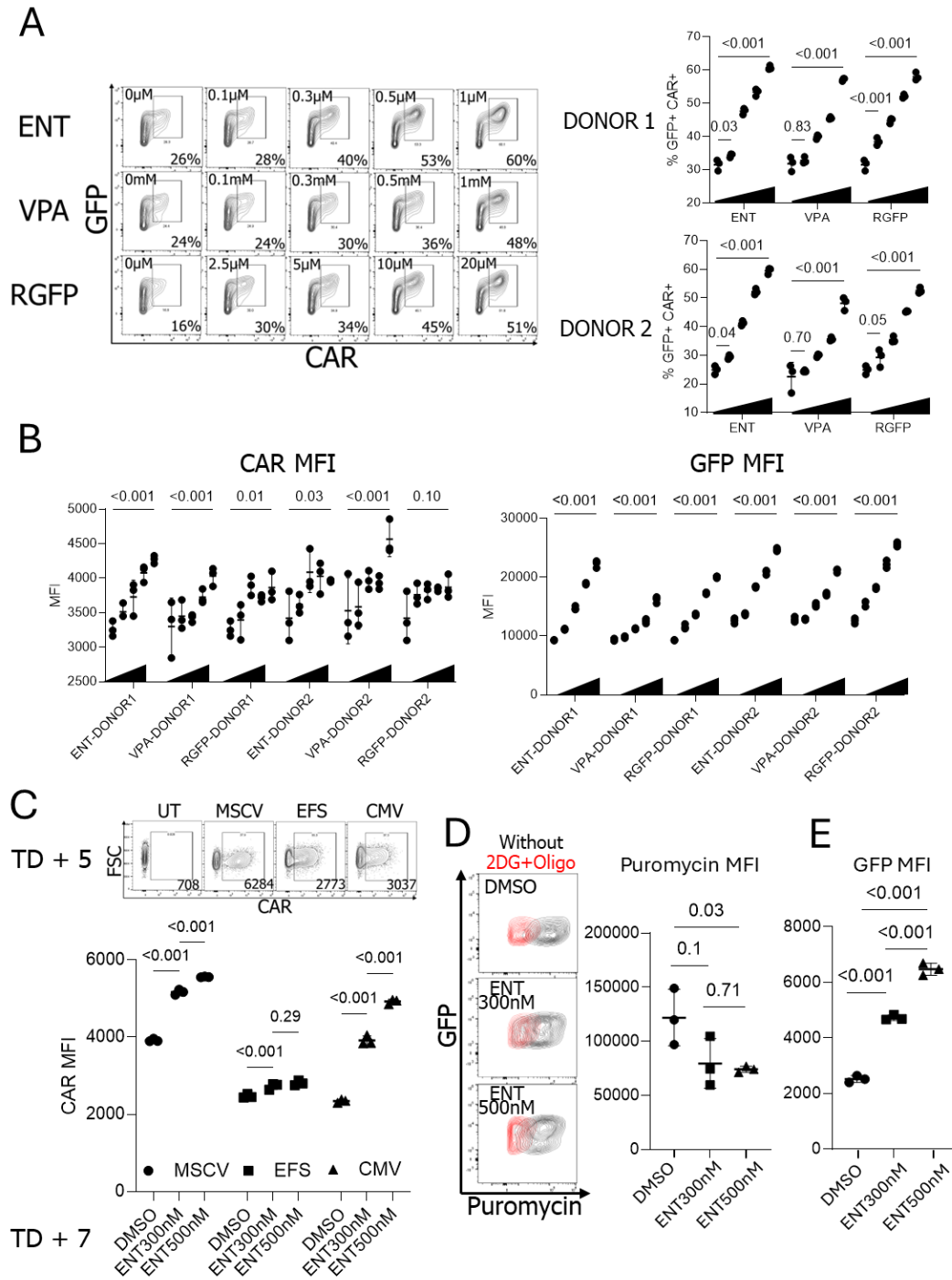


**Figure. 3.4 Enhanced CAR expression in NK cells by treating with histone deacetylase inhibitors.** (A) Effects of different concentrations of HDACi in GFP<sup>+</sup> CAR<sup>+</sup> population. (n = 2 donors' NK cells) (B) CAR and GFP MFIs in HDACi-treated pNK cells. (n = 2 donors' NK cells) (C) ENT 300 nM and 500 nM-treated MSCV, EFS, and CMV-CAR-engineered pNK cells. (n = 1 donor's NK cells, triplicate transductions) (D) Puromycin-based NK cell translation capacity confirmation. Puromycin staining was performed with or without metabolic inhibitors, 2DG, and oligomycin. (n = 1 donor's NK cells) (E) GFP expression in the cells tested for the puromycin staining; ENT: Entinostat, VPA: Valproic acid, RGFP: RGFP966, MSCV: Murine stem cell virus promoter, EFS: EF1- $\alpha$  small promoter, CMV: Cytomegalovirus promoter, 2DG: 2-Deoxy-D-glucose.

#### 3.4.4 Entinostat treatment reduces NK cell degranulation but does not affect CAR-mediated NK cell functionality

We evaluated the kinetics of CAR expression following ENT removal and resting NK cells overnight. The GFP<sup>+</sup> CAR<sup>+</sup> population was maintained after resting with reduced CAR MFIs (**Figure 3.5 A**). We further tested the resting effect for five days. GFP<sup>+</sup> CAR<sup>+</sup> populations continued to decline following ENT withdrawal. Nonetheless, pNK cells maintained higher CAR expression 5 days post-ENT removal than DMSO-treated CAR-pNK cells (**Figure 3.5 B**). To assess the functionality of ENT-treated CAR-IL-15-pNK cells against multiple myeloma cells, we treated cryopreserved NK cells with 500 nM ENT. Considering previous observations of a slight reduction in overall MFIs following overnight resting, we also compared degranulation with that of NK cells rested overnight. Treatment with 500 nM ENT significantly reduced degranulation in response to CD138-negative Ramos cells and NK cells alone. In contrast, CD107a expression remained mostly intact when targeting CD138-positive MM1.S cells. Notably, allowing NK cells to rest overnight partially restored their function against Ramos cells but slightly diminished degranulation against MM1.S cells. (**Figure 3.5 C**). The slight reduction in degranulation may be attributed to the modest

decrease in CAR MFIs post-resting. Therefore, our data suggest that CAR-mediated cytotoxicity remains functional despite ENT treatment.

Next, we evaluated NK cell survival following 500 nM ENT treatment. Given that GFP is linked to IL-15 via the P2A sequence under the MSCV promoter, we hypothesized that ENT-treated NK cells with increased GFP expression would demonstrate improved survival without IL-2. NK cells were cultured with 500 nM ENT for two days, after which IL-2 and ENT were withdrawn. As hypothesized, non-treated NK cells experienced substantial cell death with 78% mortality after four days without IL-2. In contrast, ENT-treated GFP overexpressing NK cells exhibited enhanced survival, with only 39.4% cell death *in vitro* (**Figure 3.5 D**). Altogether, our data demonstrate that ENT treatment enhances transgene expression without compromising CAR-mediated NK cell degranulation.



**Figure. 3.5 CAR maintenance, degranulation, and survival of ENT-treated NK cells *in vitro*.** (A) GFP<sup>+</sup> CAR<sup>+</sup> population and CAR MFI analysis after overnight resting. (n = 2 donors' NK cells treated with ENT 500 nM) (B) GFP<sup>+</sup> CAR<sup>+</sup> population maintenance analysis for 5 days following ENT removal. (n = 2 donors' ENT 500 nM-treated NK cells) (C) CD107a assay using ENT 500 nM-treated NK cells. (n = 2 donors' NK cells) (D) NK cell survival without IL-2. NK cells were treated with IL-2, with or without ENT 500 nM; IL-2 and ENT were then withdrawn to assess their survival. (n=2 donors' NK cells)

### 3.4.5 ENT treatment of CAR-pNK cells during expansion *ex vivo* upregulates CAR expression and improves target cell lysis.

To assess the possible application of ENT during NK cell expansion, we transduced NK cells and expanded CAR-IL-15-pNK cells for 5 days (TD + 5), followed by treatment with either 300 nM or 500 nM ENT for 7 days (TD + 12). The 300 nM and 500 nM were selected due to the CAR maintenance from the HDACi dosage assay. Without ENT, the GFP<sup>+</sup> CAR<sup>+</sup> NK cell population steadily decreased; however, this population was better maintained in the 300 nM and 500 nM ENT treatment groups (**Figure 3.6 A**). NK cells treated with 500 nM ENT exhibited reduced expansion, while those treated with 300 nM ENT continued to proliferate (17.97-fold for 300 nM vs. 7.64-fold for 500 nM) (**Figure 3.6 B**).

To confirm NK cell cytotoxicity following long ENT treatment, we incubated both unmodified and CAR-modified NK cells treated with or without 300 nM ENT. Subsequently,  $1 \times 10^5$  NK cells were co-incubated overnight with  $1 \times 10^6$  MM1.S-FLUC cells at a 1:10 ratio. The results showed that CAR-expressing NK cells significantly outperformed unmodified NK cells in eradicating MM1.S cells. Interestingly, Donors 1 and 2, used in this experiment, exhibited comparable cytotoxicity levels without CAR but differed when CAR expression was present. To explore this further, we assessed CAR expression levels in both donors. Donor 1 demonstrated 59% CAR positivity, whereas Donor 2 exhibited 45%, confirming that

the enhanced cytotoxicity was predominantly driven by CAR expression (**Figure 3.6 C**). By assessing unmodified NK cells, we verified that this enhanced cytotoxicity was not attributed to ENT treatment. DMSO- or ENT-treated unmodified NK cells were co-incubated with the general NK cell target K562 cells. ENT treatment slightly reduced NK cell cytotoxicity and cytokine production, further supporting that CAR expression is the primary factor of ENT-treated NK cell cytotoxicity (**Figure 3.6 D, E**).

The reduced NK cell proliferation in the presence of ENT during expansion limits its applicability. To overcome this limitation, we assessed whether ENT could increase the GFP<sup>+</sup> CAR<sup>+</sup> population in NK cells after TD + 12 days. The DMSO-treated TD + 12 NK cells were treated with 500 nM ENT (brief treatment, bENT) for two days. Notably, this brief ENT treatment upregulated CAR expression, resulting in high CAR expression (**Figure 3.6 F**). We also validated whether the ENT treatment changes NK cell phenotypes. ENT-treated NK cells showed reduced expression of activating receptors, including NKp30, NKp44, NKp46, and NKG2D (**Figure S7**).

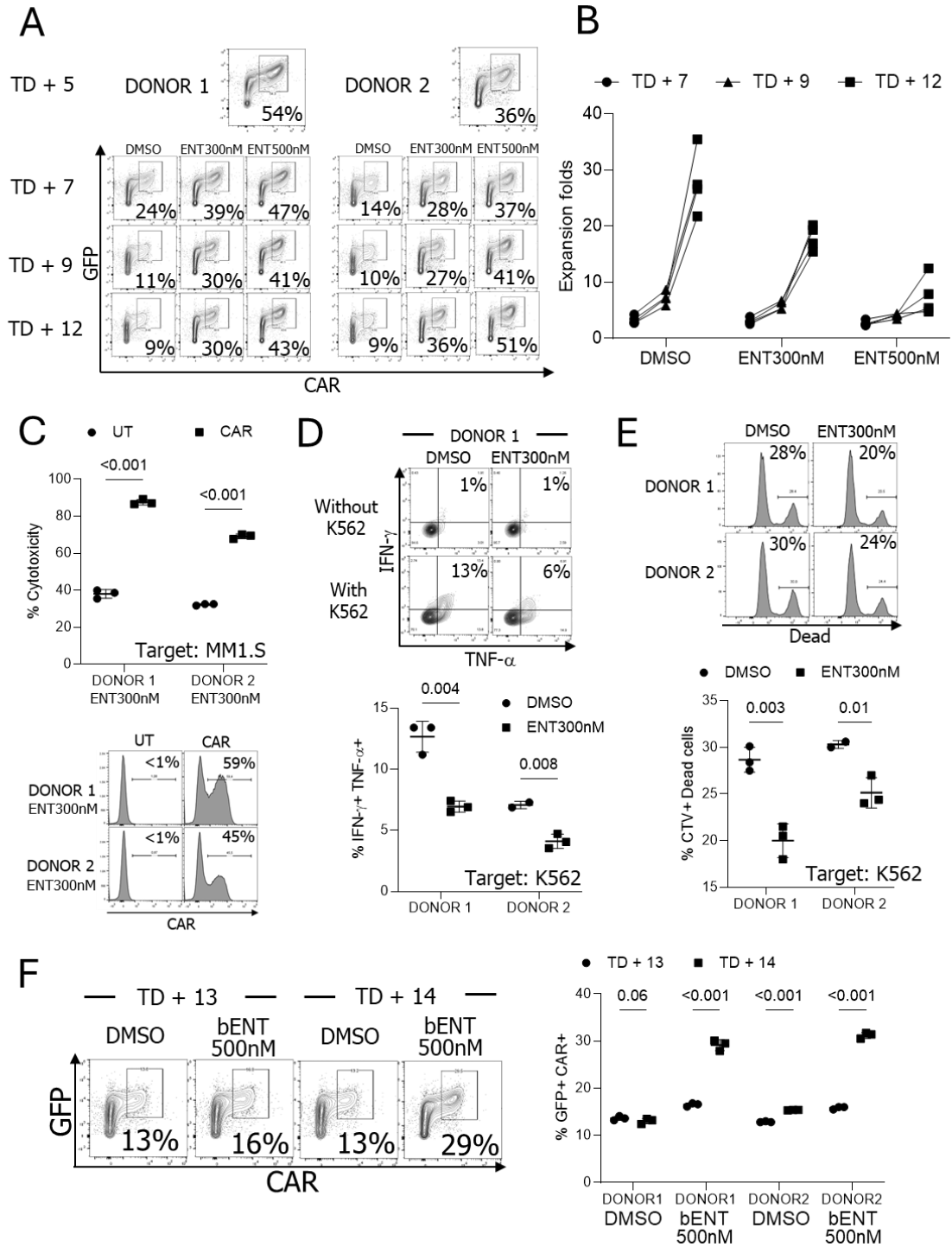


**Figure 3.6 The CAR and NK cell phenotypes and functionalities after long-term ENT treatment.** (A) CAR expression analysis during *ex vivo* expansion following CAR transduction in the presence of ENT (n = 2 donors' NK cells). (B) NK cell expansion for seven days with ENT. (n = 4, 2 donors' NK cells with or without engineering). NK cells were transduced, stimulated, and expanded for five days (TD + 5). The modified NK cells were then cultured with or without ENT. (C) Comparison of NK cell cytotoxicity between ENT 300 nM-treated CAR-NK cells and UT-NK cells *in vitro*. (n = 2 donors' NK cells) (D) Cytokine production analysis in DMSO or ENT 300 nM-treated UT-NK cells. (n = 2 donors' NK cells) (E) Target cell killing activity of the UT-NK cells. (n = 2 donors' NK cells) (F) DMSO-treated TD + 12 NK cells were treated with 500 nM ENT for two days (brief stimulation, bENT). NK cells showed improved GFP<sup>+</sup> CAR<sup>+</sup> populations (n=2 donors' NK cells).

### 3.4.6 ENT-treated CAR-overexpressing pNK cells show enhanced anti-myeloma activity *in vitro* and *in vivo*

To evaluate whether ENT-treated NK cells could improve *in vivo* tumor elimination, we transduced and expanded CAR-pNK cells for 5 days, followed by further expansion with 300 nM ENT for 7 days. A bENT group was also included, where CAR-pNK cells were exposed to 500 nM ENT for 3 days after TD + 9 to assess whether short-term treatment could improve tumor control *in vivo*. In the *in vivo* model,  $2.5 \times 10^6$  MM1.S-FLUC cells were injected intravenously into mice. Based on prior *in vivo* experiments demonstrating that CAR-pNK cells effectively eliminated tumor burdens developed for 3 days, we delayed the first NK cell dose to 7 days post-tumor injection to induce higher tumor burdens. On the day of NK cell injection (TD + 12), the GFP<sup>+</sup> CAR<sup>+</sup> populations were 17%, 44%, and 49% for the DMSO control, 300 nM ENT, and 500 nM bENT groups, respectively (**Figure 3.7 A**). Before *in vivo* injection, the cytotoxicity of ENT-treated pNKs was tested *in vitro*. ENT-treated CAR-IL-15-pNK cells demonstrated superior *in vitro* cytotoxicity against MM1.S cells compared to the DMSO-treated pNK cells (**Figure 3.7 B**). After the first dose, the

remaining NK cells were further expanded for 6 more days with 300 nM ENT or without ENT, followed by another brief stimulation with 500 nM ENT. The second dose of CAR-pNK cells was administered to the mice 6 days after the first injection (TD + 18) (**Figure 3.7 C**). After long-term expansion, ENT treatment showed significantly higher GFP<sup>+</sup> CAR<sup>+</sup> NK cell populations (21%, 58%, and 46% for DMSO, 300nM ENT, and 500nM bENT, respectively) (**Figure 3.7 A**). *In vivo* imaging data demonstrated that the 300 nM and 500 nM bENT-treated NK cells provided superior tumor control compared to the DMSO-treated NK cells (**Figure 3.7 D, E**).

Peripheral blood analysis from ENT-treated mice indicated improved NK cell survival. GFP expression in NK cells suggested that ENT treatment temporarily increased GFP-IL-15 gene expression, contributing to short-term NK cell persistence and enhanced tumor control *in vivo* (**Figure 3.7 F, G**). After 29 days of tumor engraftment, mice were euthanized, and tumor burdens in the bone marrow and spleen were analyzed. Consistent with luminescence data, the percentage of multiple myeloma was significantly lower in mice that received 300 nM or brief-500 nM ENT-treated NK cells (**Figure 3.7 H**). In conclusion, CAR-IL-15-pNK cells treated with ENT during *ex vivo* expansion demonstrated enhanced CAR and IL-15 expression, resulting in superior anti-myeloma activity *in vivo*.

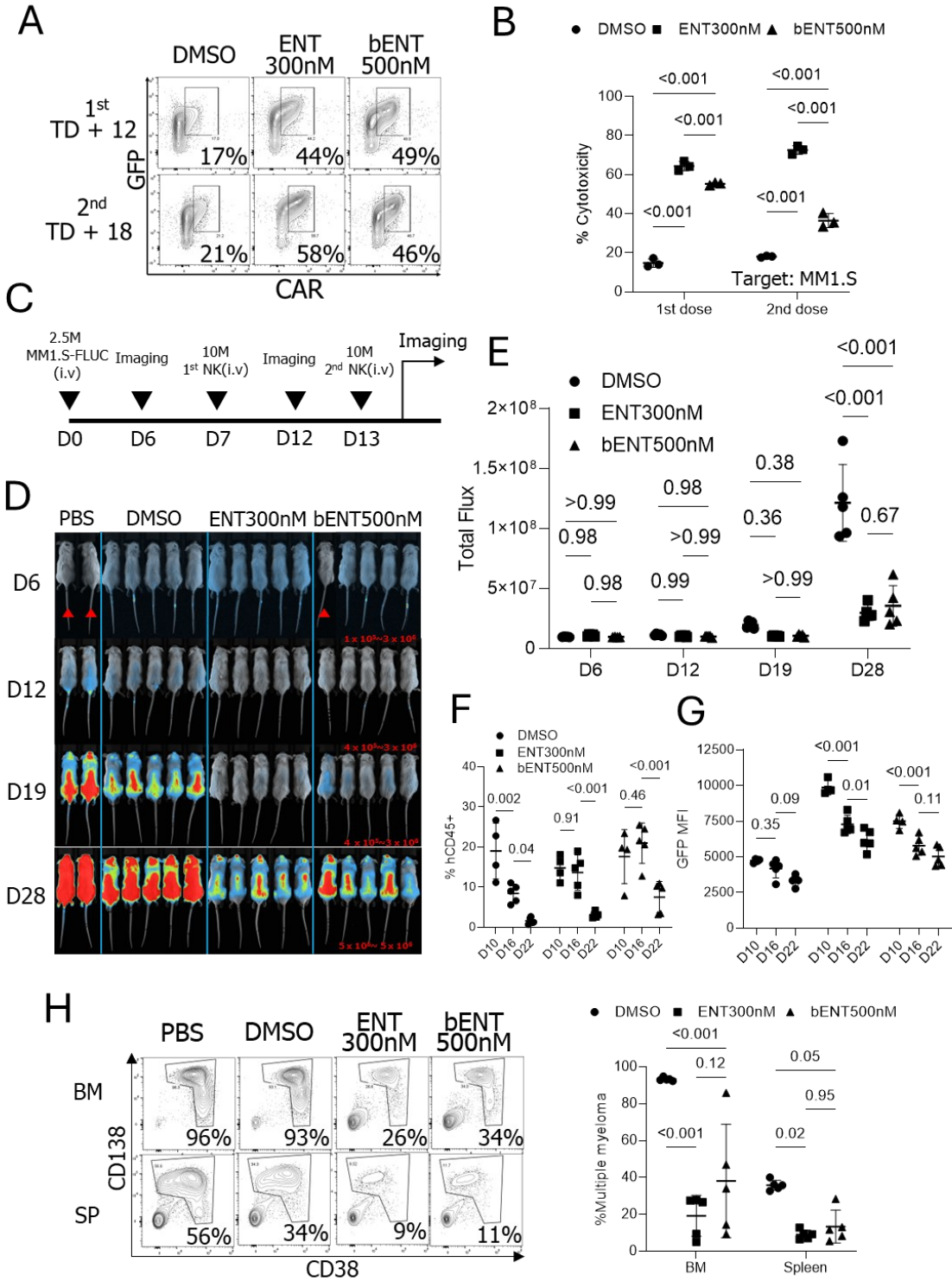


**Figure. 3.7 Anti-tumor activity of CAR-NK cells treated with ENT *in vitro* and *in vivo*.** (A) GFP and CAR expression in NK cells used for *in vivo* injection. (n = 1 donor's NK cells) (B) *In vitro* cytotoxicity assay of the expanded NK cells. Cytotoxicity was assessed on the day of the NK cell injection. (C) Schematic diagram of the *in vivo* experiment. (D) Newton imaging. The brighter colors (blue to red) indicate stronger luminescence signals from MM1.S-FLUC cells. Marked mice were exposed for 30 seconds and not included in the statistical analysis. Other mice received 2 minutes of exposure. Red numbers indicate the analysis scale for the 2-minute exposed mice. (n = 5 mice for NK cell treatments and n = 2 mice for PBS control). (E) Analysis of total flux from each mouse. (F) Percentages of human CD45-positive populations in the blood on days 10, 16, and 22 post-MM1.S-FLUC cell injection. (G) GFP MFIs from the hCD45-positive cells. (H) Multiple myeloma tumor burden on day 29 in bone marrow (BM) and spleen (SP).; FLUC: Firefly luciferase, bENT 500nM: three days ENT 500nM treated NK cells, BM: Bone marrow. The days in Figures D to H indicate the timeline post-MM1.S-FLUC cell injection.

### 3.5 Discussion

MM is characterized by the uncontrolled proliferation of highly differentiated malignant plasma cells.<sup>256</sup> The clonal diversity and differentiation of these plasma cells contribute to high relapse rates in MM patients treated with antibody- or proteasome inhibitor-based therapies.<sup>258</sup> This study investigated CAR-NK cells targeting CD138, a marker highly expressed in multiple myeloma cells.<sup>261</sup> While anti-CD138 CAR-NK cells effectively eradicated target myeloma cells *in vitro*, CAR surface expression on NK cells declined over time during *ex vivo* NK cell expansion, limiting their therapeutic efficacy. To overcome the progressive loss of CAR expression, we assessed the feasibility of using cryopreserved NK cells engineered with an anti-CD138 CAR, combined with HDACis, thereby improving treatment outcomes for multiple myeloma.

One critical component in NK cell research is the expansion process, which can be influenced by factors such as blood donors, irradiated feeder cells, and NK cell isolation methods.<sup>144,276</sup> The importance of the NK cell expansion becomes more significant when NK cells are engineered, for example, with CAR transgenes, as shown in this study. In this research, we tested the feasibility of using primary NK cells cryopreserved at early stimulation stages for engineering and subsequently expanding them after a freeze/thaw cycle. We observed that NK cells generally reached the exponential growth phase around 5 days after the first feeder cell stimulation. Cryopreserving NK cells at this stage consistently yielded high survival rates after thawing. Additionally, NK cells, thawed after being stored at -80°C for three months, still exhibited successful CAR engineering and robust expansion with feeder cell stimulation post-transduction. This cryopreservation strategy provides

flexibility in CAR-NK cell preparation for preclinical experiments and presents a potential advantage for the clinical application of off-the-shelf CAR-NK cell immunotherapy.

Due to the frontline intracellular epigenetic modification pathways, foreign transgenes are prone to gene silencing in various cell types.<sup>263</sup> In particular, CAR downmodulation during *ex vivo* expansion impacts the efficacy of NK cell-mediated immunotherapy. Our study aimed to boost transient CAR expression during *ex vivo* expansion to support long-term expansion and a multi-dosing strategy. To address this issue of CAR downregulation, we decided to test HDAC inhibitors, which are epigenetic modifiers due to the previously reported papers showing HDACi-induced transgene overexpression.<sup>204-207</sup> Remarkably, HDACi treatment was able to restore transgene expression, sustaining CAR expression during *ex vivo* expansion. This sustained expression allowed for more effective and durable CAR-NK cell function, significantly reducing CAR downregulation. Furthermore, HDACi can be applied during the final two days of the *ex vivo* expansion phase to restore CAR expression. Typically, NK cell expansion is limited to 2-3 weeks, as CAR expression diminishes beyond this period. However, brief treatment of CAR-NK cells with HDACi at the end of expansion may extend this duration to 4-5 weeks, addressing a critical bottleneck in CAR-NK cell production. This extended expansion strategy will improve the availability of CAR-NK cells for repeated dosing, enhancing their off-the-shelf potential for more effective therapeutic outcomes and relapse prevention.

In investigating the promoter-specific effects of ENT, we observed that ENT-mediated CAR overexpression driven by the MSCV and CMV promoters in the lentiviral vector system was significantly higher than the effect in the EFS promoter, highlighting the differential regulation of transgene expression in NK cells based on promoter selection. This

promoter effect brings an interesting question. The recent advancements in CAR-NK cell generation, such as targeted gene insertion via AAV vectors, which is considered superior to lentiviral systems for CAR expression, often utilize the MND promoter (myeloproliferative sarcoma virus enhancer, negative control region deleted, dl587rev primer-binding site substituted promoter) in NK cells.<sup>277</sup> Given that our data indicate varied CAR expression and differential responses to epigenetic inhibitors across different promoters in NK cells, it would be worthwhile to investigate whether the MND promoter can achieve high CAR expression in NK cells with a lentiviral system and respond to HDACi.

In conclusion, our study demonstrated that applying HDAC inhibitors, especially ENT, could effectively upregulate the CAR transgene in a promoter-specific manner. It showed sustained CAR and IL-15 transgene expression in NK cells during ex vivo expansion. In the presence of ENT, CAR expression remained stable, allowing for prolonged expansion and supporting the feasibility of multi-dosing CAR-NK cells. This combinational approach of CAR-NK cells with ENT offers significant therapeutic potential for advancing off-the-shelf CAR-NK cell immunotherapy.

# **Chapter 4: CD38 Knockout Using CRISPR-Cas9-Loaded Retroviral Particles Reduces Daratumumab-Mediated NK Cell Fratricide, Leading to Improved Multiple Myeloma Clearance**

## **Chapter 4 related authors:**

Dong-Hyeon Jo<sup>1,2</sup> and Seung-Hwan Lee<sup>1,2</sup>

<sup>1</sup>Department of Biochemistry, Microbiology, and Immunology, Faculty of Medicine, University of Ottawa, Ottawa, ON, Canada.

<sup>2</sup>The University of Ottawa Centre for Infection, Immunity, and Inflammation, Ottawa, ON, Canada.

## **Chapter history:**

This is an ongoing project.

## **Acknowledgement:**

Alissa Visram kindly provided daratumumab for this project. **Figures were generated using Biorender.com.**

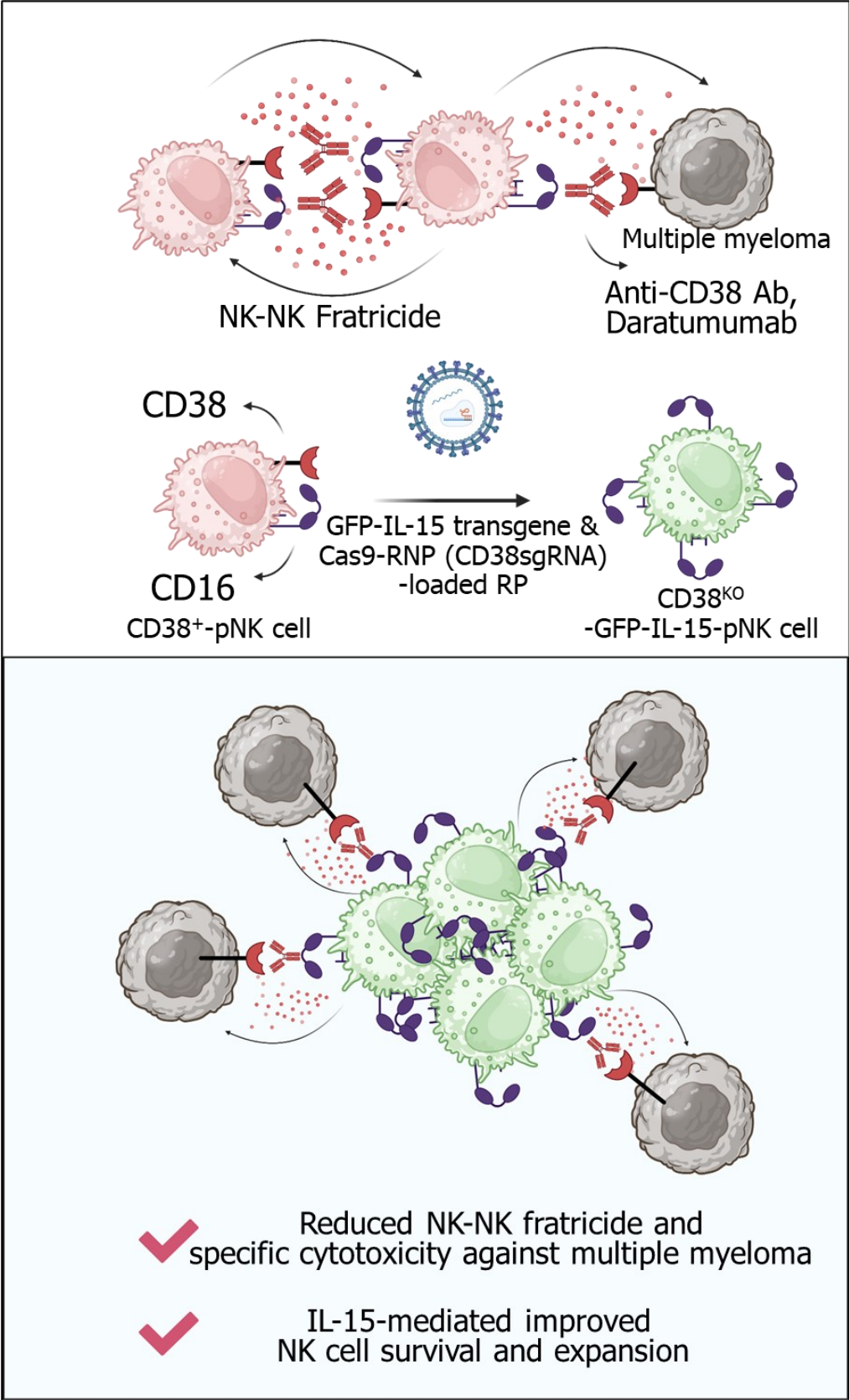


Figure 4.1 Graphical abstract for Chapter 4

## 4.1 Abstract

Treating multiple myeloma continues to be challenging due to the clonal diversity of highly differentiated B-cell populations, which leads to heterogeneous phenotypic profiles and therapeutic resistance. Despite this complexity, CD38 is consistently expressed in multiple myeloma, making it a vital therapeutic target. Among the CD38-targeting agents, the monoclonal antibody daratumumab has emerged as one of the most effective treatments; however, daratumumab frequently depletes natural killer (NK) cells due to CD38 expression on NK cells. To enhance the combinatorial use of NK cells with daratumumab, previous studies utilized CD38 knockout (CD38<sup>KO</sup>) via electroporation, demonstrating improved NK cell functionality and reduced fratricide. Building on the previous findings, in this study, we explore an alternative approach using CRISPR-Cas9-loaded retroviral particles to generate CD38<sup>KO</sup> NK cells. Our method successfully knocked out CD38, reducing NK cell fratricide while enhancing multiple myeloma clearance. Additionally, we simultaneously engineered NK cells to express GFP-IL-15 while removing CD38 to promote their survival and expansion *in vivo*. Our findings support that Cas9-loaded-retroviral particle-mediated NK cell engineering provides a novel strategy to generate CD38<sup>KO</sup> NK cells and a combinational therapy using daratumumab and NK cells.

## 4.2 Introduction

Multiple myeloma is a clonal plasma cell malignancy characterized by uncontrolled proliferation within the bone marrow, leading to excessive immunoglobulin production and subsequent complications such as osteolytic bone lesions, renal failure, and anemia.<sup>256</sup> The pathogenesis of multiple myeloma is driven by a combination of genetic and epigenetic alterations, including chromosomal translocations such as t(4;14), t(11;14), and t(14;16), as well as mutations in key oncogenic pathways including rat sarcoma (RAS)/ mitogen-activated protein kinase (MAPK), nuclear factor kappa B (NF- $\kappa$ B), and tumor protein p53 (TP53).<sup>278,279</sup> These aberrations promote tumor growth, survival, and immune evasion by altering transcriptional programs, cell signalings, and metabolic pathways. The tumor microenvironment also plays a critical role in multiple myeloma progression, with bone marrow stromal cells (BMSCs), regulatory T cells (Tregs), and myeloid-derived suppressor cells (MDSCs) fostering immune suppression and therapy resistance.<sup>280</sup> Furthermore, alterations in metabolic reprogramming, particularly in glycolysis and oxidative phosphorylation, contribute to myeloma cell adaptation and drug resistance, underscoring the need for novel therapeutic strategies.<sup>281</sup>

CD38, a type II transmembrane glycoprotein, and ectoenzyme, is highly expressed in malignant plasma cells and plays a crucial role in multiple myeloma pathophysiology.<sup>282</sup> CD38 catalyzes the conversion of nicotinamide adenine dinucleotide (NAD<sup>+</sup>) into cyclic ADP-ribose (cADPR) and ADP-ribose (ADPR), regulating calcium signaling, cell metabolism, and immune function.<sup>283</sup> Overexpression of CD38 in multiple myeloma has been linked to disease progression, immune escape, and metabolic reprogramming; therefore, targeting CD38 has been a compelling strategy.<sup>284,285</sup> Daratumumab, a human IgG1 $\kappa$  anti-

CD38 monoclonal antibody, has demonstrated efficacy in multiple myeloma treatment. Daratumumab induces multiple killing mechanisms, including direct apoptosis, ADCC, antibody-dependent cellular phagocytosis (ADCP), and complement-dependent cytotoxicity (CDC).<sup>286-288</sup> Due to its therapeutic effect, daratumumab was granted accelerated approval by the FDA in 2015 for patients who received three prior treatments.<sup>289</sup>

While daratumumab effectively eliminates multiple myeloma cells, daratumumab treatment is associated with the depletion of CD38-expressing immune cells, particularly NK cells.<sup>170</sup> NK cells are crucial for innate immune surveillance and tumor control, exerting cytotoxic effects through perforin/granzyme secretion and cytokine-mediated immune modulation.<sup>21,33,287</sup> Importantly, NK cells mediate ADCC, a key mechanism for daratumumab efficacy, by engaging CD16 (FcγRIIIa) to recognize and kill antibody-bound target cells. However, clinical trials such as GEN501 and SIRIUS have reported significant depletion of NK cells following daratumumab treatment due to the CD38-mediated NK cell fratricide.<sup>290-292</sup> This loss of NK cells may contribute to reduced long-term efficacy of daratumumab by impairing innate immune responses. Strategies to mitigate NK cell depletion include genetic engineering approaches such as CD38<sup>KO</sup> to prevent fratricide.<sup>170,292</sup> Preclinical studies have demonstrated that CD38<sup>KO</sup> NK cells retain cytotoxic function while resisting daratumumab-induced depletion, offering a promising strategy to enhance the therapeutic potential of an NK cell and daratumumab combinational immunotherapy.

CRISPR-Cas9 genome editing has revolutionized the field of immune cell engineering, enabling precise gene modifications to enhance therapeutic efficacy.<sup>156</sup> The CRISPR-Cas9 system introduces targeted DSBs at specific genomic loci, which are repaired via NHEJ or HDR, allowing for targeted gene disruption or insertion. Electroporation of Cas9

RNPs is a commonly used method for CD38<sup>KO</sup> NK cell generation; however, it requires significant optimization to improve NK cell viability.<sup>168-170</sup> Alternative strategies, such as VLPs, have been developed for efficient genome editing with minimal cytotoxicity. Retroviral-based VLP-containing Cas9-RNP have demonstrated high efficiency in NK cell engineering, specifically TIGIT<sup>KO</sup> NK cells, and allowed simultaneous engineering to generate CAR and TIGIT<sup>KO</sup> NK cells using a single-step modification.<sup>137</sup>

In this study, we applied Cas9-loaded retroviral particles to generate CD38<sup>KO</sup> NK cells and assessed their cytotoxicity and fratricide with daratumumab. Additionally, we introduced GFP-IL-15 transgenesis to enhance NK cell persistence *in vivo*. Our findings demonstrate that CD38<sup>KO</sup> NK cells resist daratumumab-induced depletion while maintaining anti-myeloma cytotoxicity. This approach provides a novel strategy to generate CD38<sup>KO</sup> NK cells for multiple myeloma treatment with daratumumab.

## 4.3 Materials and Methods

### 4.3.1 Cancer cell line culture

Multiple myeloma cell lines, U266, MM1.R, and MM1.S, were obtained from ATCC and cultured in RPMI-1640 medium (350-000-CL; Wisent) supplemented with 10% HI-FBS (12484028; Gibco), 100 U/mL Penicillin and 100 µg/mL Streptomycin (Pen/Strep) (SV30010; HyClone), 55 µM β-Mercaptoethanol (21985023; Gibco), and 20 mM HEPES (CA12001-708; VWR) (RP10 medium). Lenti-X 293T cells were purchased from Takara (632180) and were cultured in high-glucose DMEM (319-005-CL; Wisent) supplemented with 10% HI-FBS and 100 µg/mL Pen/Strep.

### 4.3.2 Generation of master stocks of human primary NK cells

Chapter 3 focused on the cryopreservation process of primary NK (pNK) cells derived from peripheral blood. Initially, these cells were cultured for 3 days in an RP-10 medium containing 100 U/mL of IL-2 alongside irradiated K562 feeder cells at a 1:2 ratio. CYTOSEN generously provided the feeder cells. Following this initial phase, half of the culture medium was replaced with NKMACS medium (130-114-429; Miltenyi Biotech), enabling further expansion for an additional 2 days. Between days 5 and 6, the partially expanded pNK cells were cryopreserved at -80 °C using a freezing solution (90% FBS and 10% DMSO; BP231-100; FisherBioReagents).

### 4.3.3 Retroviral and lentiviral vector production

To produce Cas9-RNP retroviral particles, we slightly modified the previously published protocol.<sup>137</sup> In summary, we plated  $1.2 \times 10^6$  Lenti-X 293T cells per well in a 6-well plate using 2 mL of serum-containing Opti-MEM media. The next day, cells were transfected with 7  $\mu$ L of Lipofectamine 3000 along with 900 ng of BIC-Gag-Cas9, 1,200 ng of MLV-gag-pol, 1,200 ng of either anti-EGFP<sup>137</sup> or anti-CD38 sgRNA plasmid (AGTGTATGGGATGCTTTCAA),<sup>293</sup> 500 ng of pMD2.G, and 100 ng of BaEV-TR. For simultaneous engineering, we co-transfected 1,200 ng of the retroviral transgene plasmid (pMIG-GFP or pMIG-GFP-IL-15; detailed in the previous chapter) with an additional 9  $\mu$ L of Lipofectamine 3000. After four hours, we replaced the medium with fresh serum-containing Opti-MEM. Supernatants were collected at 24 hours, and fresh medium was added. A second collection was done at 48 hours, combining both harvests. The viral supernatant

was filtered through a low protein-binding PES filter and stored at -80 °C. Virus titration was performed as previously described.<sup>137</sup>

#### **4.3.4 Primary NK cell transduction and expansion**

Cryopreserved pNK cells from master stocks were thawed and rested overnight in NKMACS medium with 10% HI-FBS, and 100 U/mL IL-2, and NK cell modification was performed as previously described in Chapter 3. Briefly, thawed pNK cells were modified on a retronectin-coated 48-well flat-bottom with the viral particle supernatant overnight. Then, the cells were cultured by replacing the medium with a fresh NKMACS medium every 2 to 3 days.

#### **4.3.5 Immunostaining**

Antibody-based cell immunostaining was performed as previously described<sup>137</sup> with the following antibodies, reagents, and beads. Data were analyzed by Kaluza Analysis 2.1 (Beckman Coulter). CD38 (67-0389-42, SB702) CD16 (360728, BV605) NKG2D (46-5878-42, PerCP-eFluor710) CD56 (318328, BV421) hCD45 (304048, BV785) mCD45.1 (110708, PE) NKG2A (375108, APC) CD3 (317332, BV510) CXCR4 (12-9991-81, PE) Fixable Yellow (L34959, Invitrogen) Fixable Near-IR (L34976, Invitrogen). UltraComp eBeads™ Plus Compensation Beads (01-3333-42, Invitrogen).

#### **4.3.6 *In vitro* apoptosis assay**

To assess daratumumab-mediated NK cell apoptosis, a commercially available PE Annexin V apoptosis assay kit was used (640934, Biolegend). NK cells were co-cultured with or without 1 µg/mL daratumumab for 3 hours. The cells were washed twice with Staining

Buffer (SB, PBS + 2% HI-FBS) and then resuspended in 50  $\mu$ L Annexin V Binding Buffer containing 1  $\mu$ L of PE-conjugated Annexin V and 0.25  $\mu$ L 7-AAD. The cells were incubated for 15 min at room temperature. 200  $\mu$ L Annexin V Binding Buffer was added, and data were directly acquired using Attune Flow Cytometry (Thermo Fisher Scientific).

#### **4.3.7 *In vitro* killing assay**

Target cells were labeled with cell-trace violet (CTV) dye (C34571, Invitrogen™) according to the manufacturer's instructions. The CTV-labeled target cells were then co-cultured with NK cells at a 1:2 ratio for four hours with or without 1  $\mu$ g/mL daratumumab. The cells were stained with 7-AAD, and the percentage of 7-AAD-positive cells within the CTV-positive target cell population was subsequently analyzed by flow cytometry.

#### **4.3.8 *In vivo* NK cell survival experiments**

A breeding pair of NSG mice was acquired and maintained as previously described.<sup>137</sup> The NSG mice (8 to 12 weeks old) received  $5 \times 10^6$  NK cells intravenously. If necessary, 2000 U of IL-2 was administered with the NK cells. On the day of NK cell injection, daratumumab-control mice received 8 mg/kg of daratumumab intraperitoneally (n = 2 or 3/group). Seven days after the injection of the NK cells, the mice were euthanized, and their organs were harvested. Blood samples were collected from the tail vein and diluted in SB (2% HI-FBS in PBS) containing 2 mM ethylenediaminetetraacetic acid (EDTA). All procedures were approved by and conducted following the animal care guidelines of the University of Ottawa.

### 4.3.9 Statistical analysis

The mean values for multiple factors were analyzed using two-way ANOVA, comparing the means of the groups. A t-test was used for two-factor comparisons to evaluate the mean values performed in GraphPad Prism 9 (Dotmatics). Data are presented as mean  $\pm$  SD, and all graphs were generated and analyzed using GraphPad Prism 9 (\* $p < 0.05$ , \*\* $p < 0.01$ , \*\*\* $p < 0.001$ , \*\*\*\* $p < 0.0001$ ).

## 4.4 Results

### 4.4.1 CRISPR-Cas9-loaded retroviral particles successfully abrogate CD38 expression in NK cells.

Previous studies have indicated that CD38 expression in NK cells is a key driver in their susceptibility to daratumumab-induced fratricide.<sup>170,292</sup> To investigate this further, we employed CRISPR-Cas9 gene editing using Cas9-RNP-loaded RPs targeting the *CD38* gene with a 20 bp single-guide RNA (sgRNA) containing AGTGTATGGGATGCTTTCAA.<sup>293</sup> We produced Cas9-RNP-RPs using Lenti-X 293T cells via conventional plasmid transfection. These RPs were harvested and tested on NK cells from three independent donors, which had been cryopreserved at an early expansion phase. Cas9-RNP-loaded RPs successfully generated an average of 42% CD38-negative NK cell populations, whereas the negative control (EGFP-targeting sgRNA) did not affect CD38 expression (**Figure 4.2 A**). Post-modification phenotypic analysis confirmed a significant reduction in CD38 protein expression without altering other membrane proteins (**Figure 4.2 B**).

While we previously utilized flow virometry to quantify viral particle production, its reliance on specialized instrumentation limits its accessibility. To standardize NK cell

engineering using RPs, we implemented a simultaneous engineering strategy and titrated produced RPs based on transgene expression.<sup>137</sup> By calculating transduction units and testing MOIs of 1, 3, and 5, we observed a dose-dependent increase in CD38<sup>KO</sup> and GFP expression. We achieved 83% GFP-positive NK cells with 46% CD38<sup>KO</sup> efficiency using an MOI of 5 RPs (**Figure 4.2 C**). To further increase the CD38-negative NK cell population, we introduced a CD38-negative selection step using a CD38-targeting biotin-conjugated antibody coupled with streptavidin magnetic beads. This additional step increased the proportion of CD38-negative NK cells from 49% to 88% (**Figure 4.2 D**).

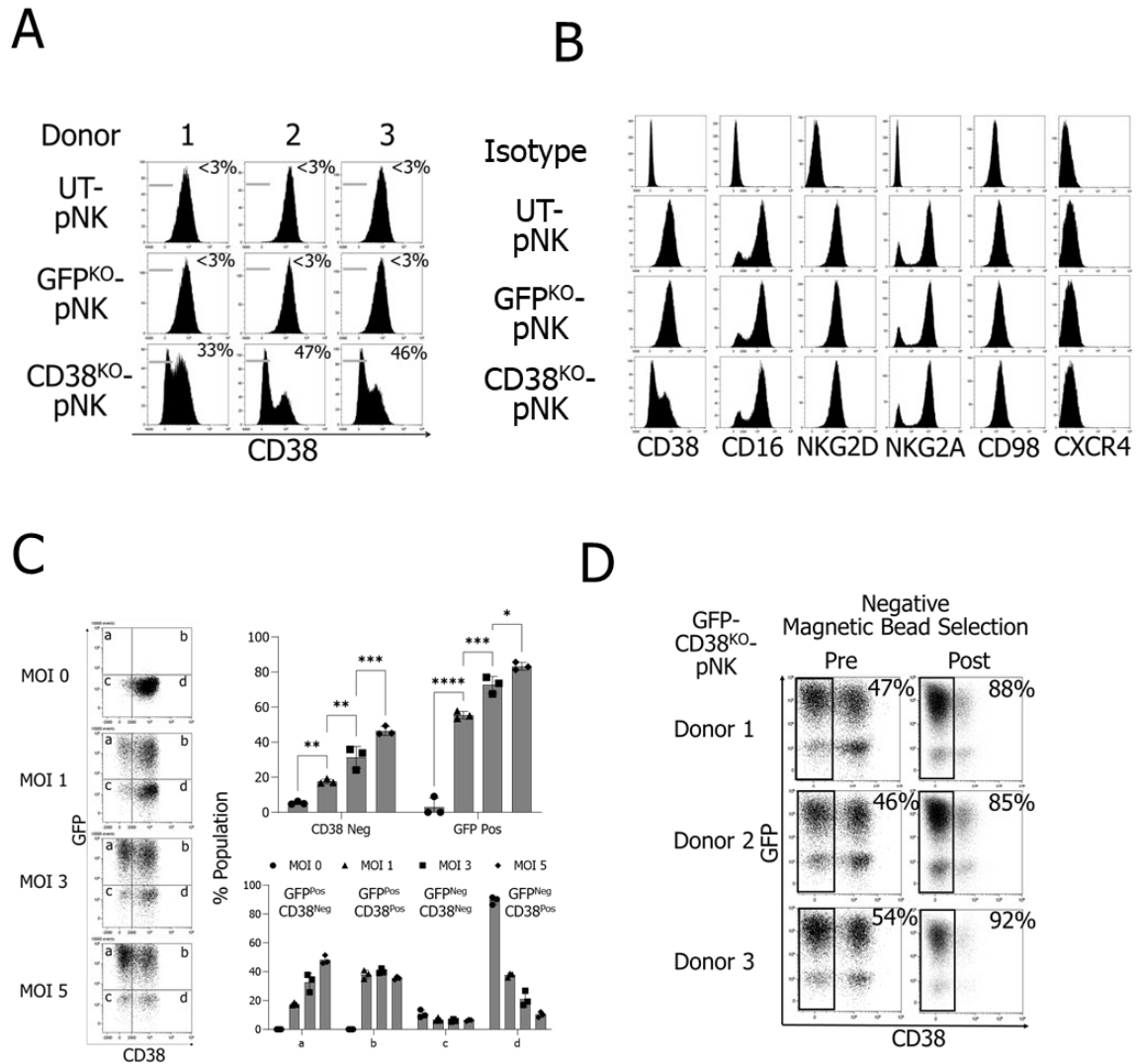


**Figure 4.2 Efficient CD38 knockout in NK cells using Cas9-RNP-loaded retroviral particles and electroporation.** (A) Flow cytometry analysis of CD38 expression in NK cells from three independent donors following EGFP<sup>KO</sup> and CD38<sup>KO</sup>. (B) NK cell phenotyping post-engineering (C) Dose-dependent CD38<sup>KO</sup> and GFP expression in simultaneously engineered NK cells (D) CD38-negative selection using a biotin-conjugated anti-CD38 antibody and streptavidin magnetic beads increased the proportion of CD38-negative NK cells. Data represent mean values  $\pm$  SD; \* $p < 0.05$ ; \*\* $p < 0.01$ ; \*\*\* $p < 0.001$ ; \*\*\*\* $p < 0.0001$ .

#### 4.4.2 CD38<sup>KO</sup> improves NK cell cytotoxicity against multiple myeloma while reducing NK cell fratricide

To assess whether CD38<sup>KO</sup> enhances NK cell-mediated cytotoxicity in the presence of daratumumab, we first characterized CD38 expression in multiple myeloma cell lines, including U266, MM1.S, and MM1.R. Consistent with previous findings, U266 cells lacked CD38 expression, whereas MM1.S and MM1.R exhibited CD38-positive populations (**Figure 4.3 A**).<sup>294,295</sup> We used these cell lines to evaluate CD38<sup>KO</sup> NK cell cytotoxicity with daratumumab. Notably, compared to CD38-positive NK cells, CD38<sup>KO</sup> NK cells demonstrated enhanced cytolytic activity against CD38-positive MM1.S and MM1.R cells (24% versus 41% and 38% versus 46%) but showed no improvement in cytotoxicity against CD38-negative U266 cells (10% versus 8%). Without daratumumab, NK cells, whether CD38<sup>KO</sup> or unmodified, exhibited no significant differences in cytotoxicity against any of the multiple myeloma cell lines tested (**Figure 4.3 B**). These results indicate that CD38<sup>KO</sup> enhances daratumumab-mediated targeting of CD38-positive multiple myeloma cells.

We next examined whether daratumumab induces NK cell death *in vitro*. We incubated NK cells with 1 µg/mL daratumumab for three hours. An Annexin V-based apoptosis assay revealed a significant increase in apoptotic NK cells from 4% to 58% following daratumumab treatment, confirming NK cell fratricide. Notably, CD38<sup>KO</sup> NK cell apoptosis averaged 24% with daratumumab, suggesting that CD38<sup>KO</sup> protects NK cells from daratumumab-induced fratricide (**Figure 4.3 C**). This finding aligns with the ADCC mechanism, where daratumumab targets CD38-expressing cells, including NK cells. Without CD38 expression, NK cells resist fratricide while maintaining their cytotoxic function against CD38-positive multiple myeloma cells.

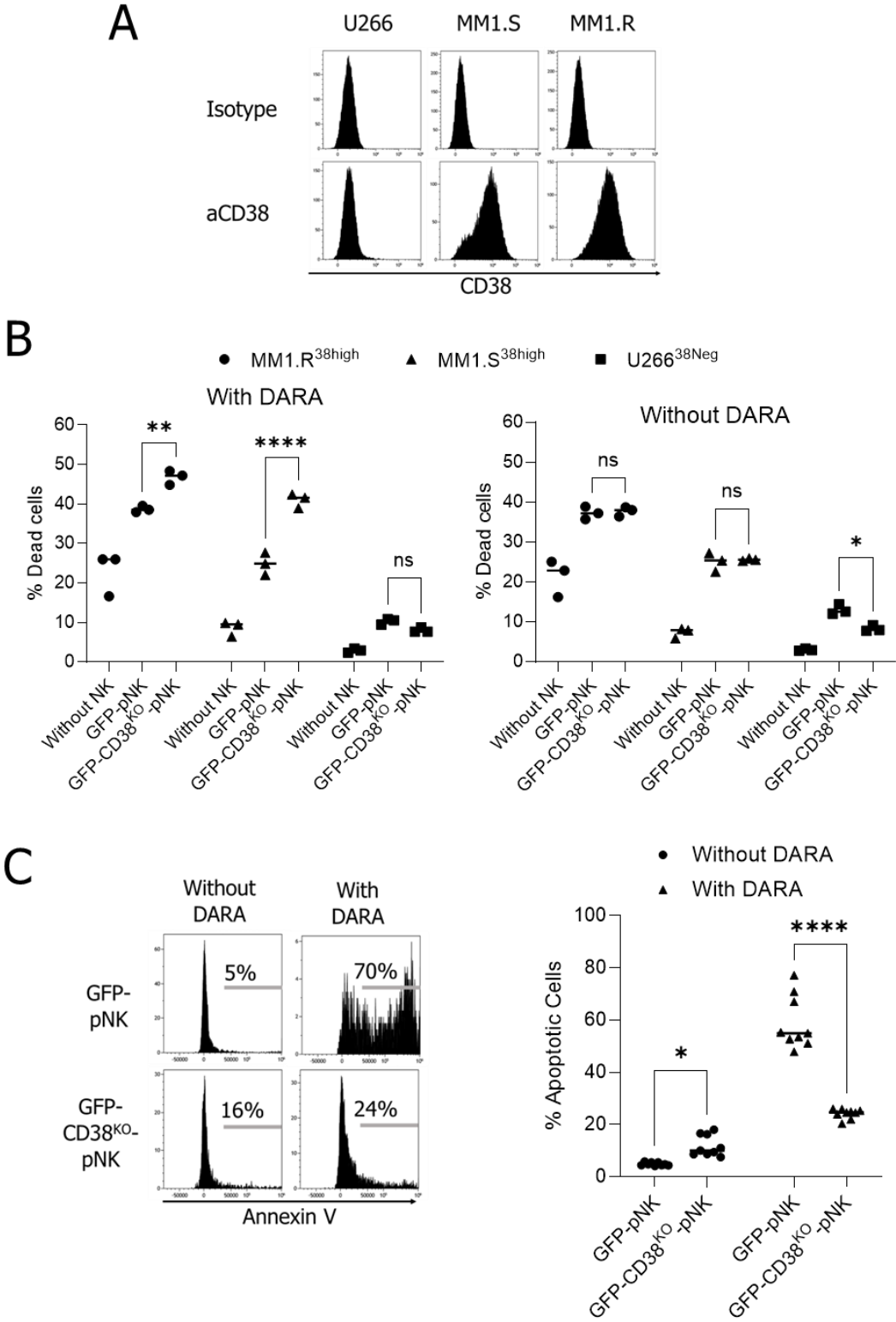


**Figure 4.3 CD38<sup>KO</sup> enhances daratumumab-mediated NK cell cytotoxicity while preventing NK cell fratricide. (A)** CD38 expression in the target multiple myeloma cells. **(B)** Cytotoxicity assay comparing CD38<sup>KO</sup> and wild-type NK cells against multiple myeloma cell lines (U266, MM1.S, and MM1.R) with or without daratumumab. **(C)** Annexin V-based apoptosis assay assessing daratumumab-induced NK cell fratricide. Data are presented as mean  $\pm$  SD; Dara, daratumumab. ns, non-significant; \* $p < 0.05$ ; \*\* $p < 0.01$ ; \*\*\*\* $p < 0.0001$ .

#### **4.4.3 CD38<sup>KO</sup> NK cells improve NK cell survival in the presence of daratumumab, while IL-15 engineering facilitates NK cell expansion *in vivo*.**

To evaluate whether CD38<sup>KO</sup> enhances NK cell survival *in vivo* in the presence of daratumumab, we first generated CD38<sup>KO</sup> NK cells and injected both CD38-positive and CD38<sup>KO</sup> NK cells into NSG mice intravenously (**Figure 4.4 A**). The mice also received 8 mg/kg daratumumab intraperitoneally on the same day. After 7 days, spleens were harvested, and human CD45-positive populations were analyzed by flow cytometry. Consistent with our *in vitro* findings, CD38<sup>KO</sup> NK cells demonstrated improved survival in the presence of daratumumab. Without CD38<sup>KO</sup> and with daratumumab, human CD45-positive populations were observed at 0.05% and 0.15%, whereas with CD38<sup>KO</sup>, these values increased to 0.72% and 2.38%. Without daratumumab, CD38<sup>KO</sup> NK cells exhibited 2.36% and 1.66% ( $n = 2$  mice/group) (**Figure 4.4 B**). Despite the improvements, overall NK cell survival remained poor with the 2000 U IL-2 support. This raised concerns about whether CD38<sup>KO</sup> alone is sufficient to enhance NK cell persistence *in vivo*, highlighting the need for additional engineering.

Given the previous success of IL-15-engineered NK cells in improving survival, we further investigated IL-15-mediated NK cell survival and expansion *in vivo*.<sup>213</sup> To assess this, we intravenously injected GFP-IL-15-expressing NK cells and monitored GFP-positive populations in the blood collected via the tail vein. 2  $\mu$ L of blood was diluted in SB containing

EDTA and analyzed directly using flow cytometry (**Figure 4.4 C**). As hypothesized, GFP-IL-15-expressing NK cells demonstrated enhanced NK cell persistence and promoted significant expansion over time. Fourteen days post-injection, GFP<sup>+</sup> cells constituted 0.17% of the blood population, dramatically increasing to 11.02% by day 50, indicating a sustained and potent IL-15-driven NK cell expansion *in vivo* (**Figure 4.4 D**).

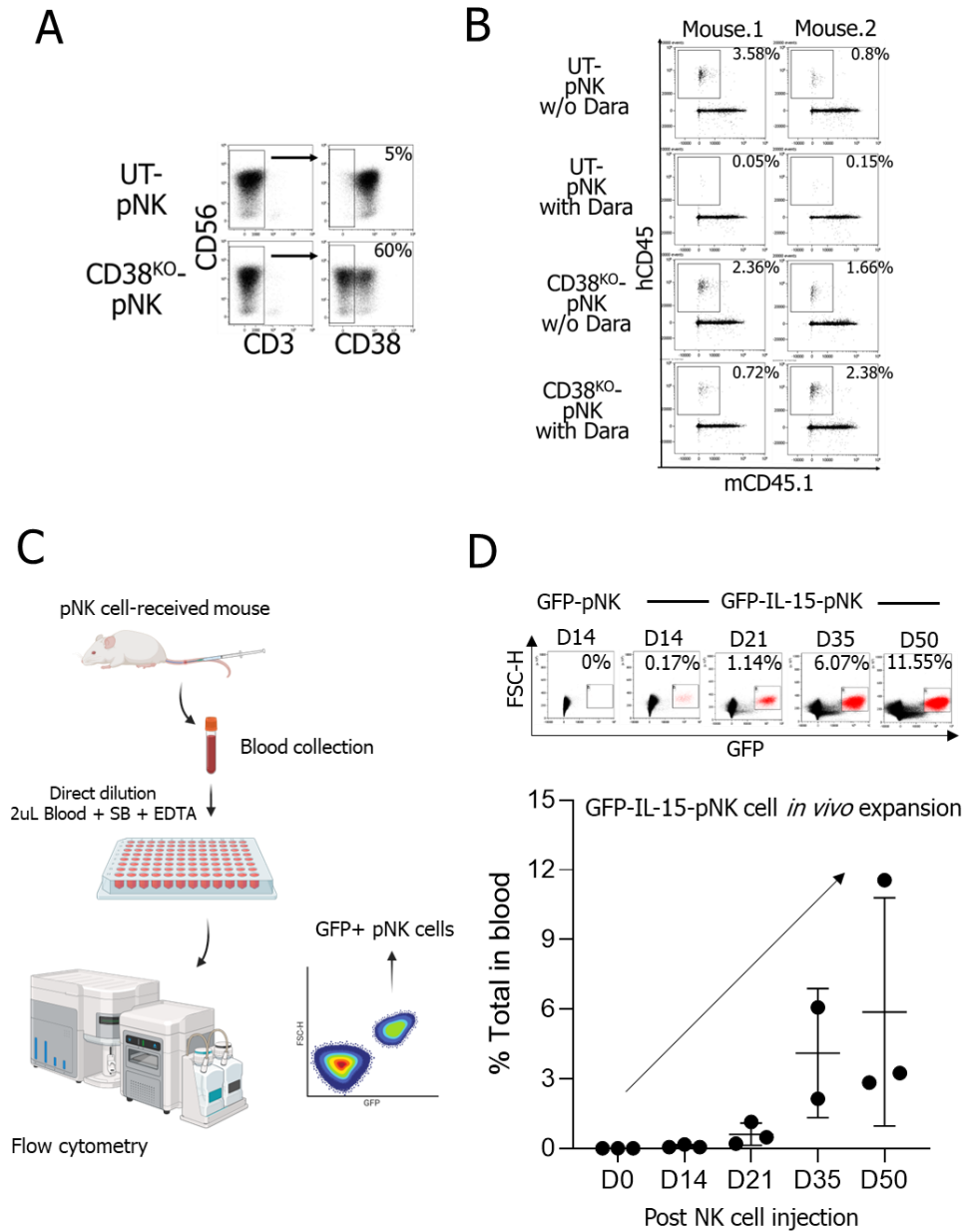


**Figure 4.4 CD38<sup>KO</sup> and IL-15 enhance NK cell survival *in vivo*.** (A) Injected NK cell purity and CD38 expression (B) Flow cytometry analysis of human CD45-positive populations in spleens seven days post-injection, with or without daratumumab. (C) Graphical summary of the performed *in vivo* NK cell tracking experiment. (D) GFP-IL-15 engineered NK cell expansion over time *in vivo*. GFP-positive populations represent injected modified NK cells. Data represent mean  $\pm$  SD; Dara, daratumumab.

#### 4.4.4 Simultaneous engineering of NK cells with GFP-IL-15 and CD38<sup>KO</sup> significantly reduces NK cell fratricide and enhances NK cell expansion *in vivo*.

Since both CD38 knockout and IL-15 transgenesis are favorable modifications, we opted to achieve both genetic edits through a single transduction approach, as previously demonstrated.<sup>137</sup> We generated GFP-IL-15- and anti-*CD38* Cas9-RNP-loaded RPs and transduced NK cells. NK cells that received only GFP-IL-15 exhibited 98% GFP expression and 9% CD38-negative phenotype. In contrast, NK cells that received GFP-IL-15 and *CD38*-targeting Cas9-RNP demonstrated 96% GFP expression and a significantly higher 64% CD38-negative population (**Figure 4.5 A**). These findings confirm the successful simultaneous engineering of NK cells for CD38 knockout and IL-15 transgenesis.

To evaluate the *in vivo* persistence of CD38<sup>KO</sup> and GFP-IL-15 NK cells, as well as their resistance to daratumumab-induced fratricide, we intravenously injected GFP-IL-15 and CD38<sup>KO</sup> GFP-IL-15-NK cells, followed by intraperitoneal administration of daratumumab (8 mg/kg). Seven days post-injection, spleens were harvested for analysis. As expected, GFP-IL-15 significantly enhanced NK cell populations compared to the previous experiments lacking IL-15. CD38<sup>KO</sup> substantially improved NK cell survival in the presence of daratumumab (w/o CD38<sup>KO</sup>, <1%; with CD38<sup>KO</sup>, 12%) (**Figure 4.5 B**). We further analyzed whether the hCD45-positive cells are CD3-negative CD56-positive NK cells. Flow cytometric analysis of murine CD45.1-negative and human CD45-positive populations confirmed the presence of CD56-positive and CD3-negative NK cells expressing GFP, demonstrating that CD38<sup>KO</sup> NK cells effectively survived and GFP-IL-15 significantly enhanced NK cell numbers (**Figure 4.5 C**).

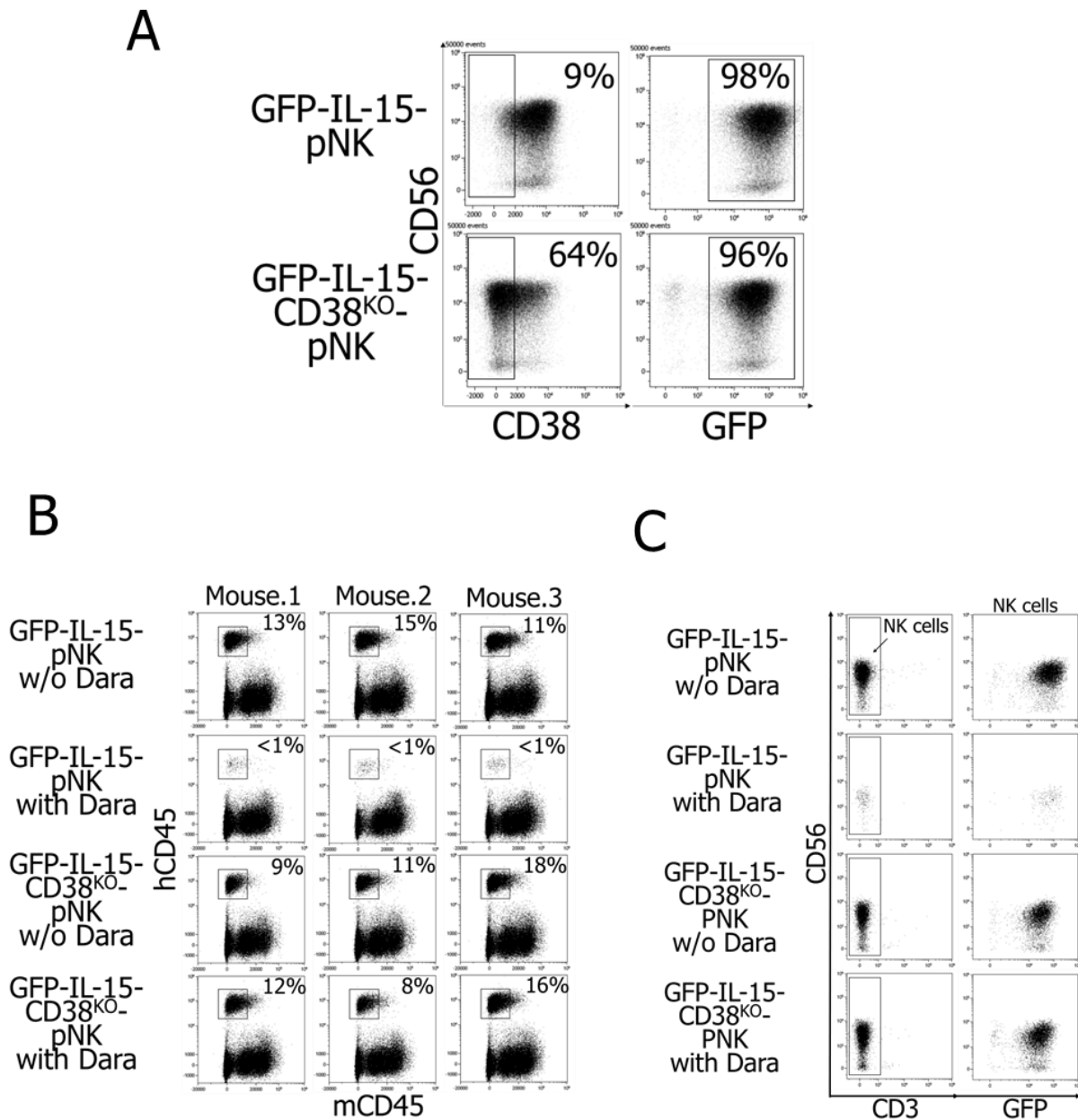


**Figure 4.5 Simultaneous engineering of NK cells with GFP-IL-15 and CD38<sup>KO</sup> enhances survival and expansion. (A)** Flow cytometry analysis showing successful co-engineering of NK cells with GFP-IL-15 and CD38<sup>KO</sup>. **(B)** *In vivo* survival of engineered NK cells following intravenous injection and daratumumab treatment. CD38<sup>KO</sup> improved NK cell survival in the presence of daratumumab. **(C)** The human CD45-positive immune cell population that survived. CD3, CD56, and GFP signals were used to phenotype the cells; Dara, daratumumab.

## 4.5 Discussion

Daratumumab, a monoclonal antibody targeting CD38, has revolutionized multiple myeloma treatment since its accelerated FDA approval in 2015.<sup>289</sup> Its potent anti-CD38 activity facilitates the elimination of multiple myeloma cells through ADCC, ADCP, and CDC.<sup>286-288</sup> However, a major limitation of daratumumab therapy is the significant depletion of NK cells, as CD38 is also expressed on NK cells, leading to their rapid fratricidal loss and subsequent impairment of ADCC.<sup>292</sup> To address this challenge, CD38<sup>KO</sup> NK cells have been developed, preserving NK cell viability while maintaining their cytotoxic function against multiple myeloma cells.<sup>170</sup> Studies have demonstrated that CD38<sup>KO</sup> reduced daratumumab-induced fratricide. CD38<sup>KO</sup> also enhanced persistence, expansion, and metabolic fitness in NK cells.<sup>170</sup> By mitigating NK cell depletion and optimizing NK cell effector functions, CD38<sup>KO</sup> NK cells represent a viable approach to overcoming the current limitations of daratumumab-based multiple myeloma therapy.<sup>203</sup>

Despite the therapeutic benefits of CD38<sup>KO</sup> NK cells, their generation has relied predominantly on the electroporation-mediated delivery of Cas9-RNP, a method known to compromise NK cell viability due to the associated electrical stress.<sup>168-170</sup> While optimization of electroporation has improved knockout efficiency and cell survival, the technique remains challenging to implement broadly in NK cell engineering.<sup>168,169</sup> To overcome these limitations, we previously demonstrated a novel Cas9-RNP delivery system using retroviral particles, which successfully mediated TIGIT knockout in NK cells.<sup>137</sup> In this study, we applied Cas9-RNP-loaded retroviral particles to generate CD38<sup>KO</sup> NK cells, demonstrating that this method is a highly effective alternative to electroporation. Post-transduction analysis confirmed that CD38<sup>KO</sup> NK cells reduced daratumumab-mediated fratricide and improved

functionality against multiple myeloma, validating the feasibility of this system. Furthermore, we implemented a simultaneous engineering strategy to enhance NK cell modification, survival, and expansion. By generating GFP- and anti-*CD38*-Cas9-RNP-loaded retroviral particles, we successfully produced  $CD38^{KO}$  GFP-positive NK cells. Additionally, by incorporating an IL-15 transgene alongside  $CD38^{KO}$ , we generated  $CD38^{KO}$  GFP-IL-15-expressing NK cells, which exhibited enhanced *in vivo* proliferation and persistence. This streamlined approach significantly simplified the conventional multi-step process required for CRISPR-Cas9 knockout and transgenesis, offering an efficient and scalable strategy for NK cell engineering.

Our findings demonstrated that  $CD38^{KO}$  NK cells exhibited improved survival and resistance to fratricide in the presence of daratumumab, while IL-15 transgenesis further enhanced their persistence and expansion *in vivo*. To maximize therapeutic efficacy, combining  $CD38^{KO}$  NK cells with anti-CD138 CAR may be ideal for therapeutic engineering. This dual-targeting strategy could potentiate multiple myeloma clearance by leveraging both CD138-directed cytotoxicity and the ADCC mediated by daratumumab. Additionally, the incorporation of HDACis, such as ENT, could further enhance anti-CD138 CAR expression and sustain IL-15 transgene expression, thereby optimizing the cytotoxic potential of  $CD38^{KO}$  anti-CD138 CAR-NK cells. This multi-strategic NK cell engineering is expected to exhibit stabilized transgene expression, increased CAR-mediated cytotoxicity, and improved ADCC in combination with daratumumab, ultimately leading to more robust multiple myeloma eradication. Future studies should explore the synergistic potential of this combinational approach to maximize therapeutic outcomes.

While CD38<sup>KO</sup> NK cells offer a promising strategy for improving daratumumab efficacy, another compelling alternative involves FcεRI-γ-negative NK cells, known as g-NK (gamma-negative NK) cells.<sup>34</sup> This subset naturally exhibits a CD38-low or CD38-negative phenotype, rendering them resistant to daratumumab-induced fratricide while displaying superior ADCC activity.<sup>35</sup> In human samples, g-NK cells are commonly found in human cytomegalovirus (HCMV)-seropositive donors, but their therapeutic applicability remains constrained by donor variability and limited *ex vivo* expansion following the current protocols for primary NK cells.<sup>34</sup> However, recent advancements in NK cell expansion techniques have enabled the robust proliferation of g-NK cells, demonstrating potent multiple myeloma clearance with daratumumab.<sup>35</sup> Given their low CD38 expression, g-NK cells represent an intriguing alternative to CD38<sup>KO</sup> NK cells for combination therapies. Future research should investigate the efficacy of anti-CD138 CAR-engineered g-NK cells with daratumumab as a potential strategy for optimizing multiple treatments.

In conclusion, our study highlighted the effectiveness of CD38<sup>KO</sup> NK cells generated via Cas9-RNP-loaded retroviral particles in mitigating daratumumab-mediated fratricide and enhancing multiple myeloma clearance. By integrating CD38<sup>KO</sup> with IL-15 transgenesis, we achieved robust NK cell survival and expansion even in daratumumab-treated conditions. This combinational engineering approach lays the foundation for future investigations into CAR-NK therapies and will be critical in refining the engineered NK cell-based immunotherapies for treating multiple myeloma patients.

## **Chapter 5: Discussion and Future Directions**

**Figures were generated using Biorender.com.**

## 5.1 NK cell engineering and immunotherapy

NK cells are vital components of the innate immune system, serving as frontline defenders in the surveillance and elimination of stressed or abnormal cells.<sup>1</sup> Their functional strategies comprise two key mechanisms: direct cytotoxicity of target cells and the secretion of pro-inflammatory cytokines, including TNF- $\alpha$ , GM-CSF, and IFN- $\gamma$ .<sup>1,3,296</sup> These cytokines amplify immune responses by recruiting and activating neutrophils, macrophages, and dendritic cells, fostering communication between innate and adaptive immunity.<sup>1,4-7</sup> A balance between activating and inhibitory receptors orchestrates the precise effector functions of NK cells, enabling selective targeting of stressed or malignant cells while sparing healthy tissue.<sup>17</sup> This regulation is essential for maintaining immune tolerance and preventing autoimmunity.

NK cells have emerged as promising agents in cancer immunotherapy, driven by their innate capacity to recognize and eliminate malignant cells without prior antigen sensitization and with minimal off-target effects.<sup>1,76</sup> Unlike T cell-based therapies, NK cell immunotherapy is associated with a significantly lower risk of GvHD, CRS, and neurotoxicity, complications frequently observed in CAR-T cell treatments.<sup>79-81</sup> This favorable safety profile stems from NK cells' intrinsic regulatory mechanisms, which mitigate the risk of excessive inflammatory responses and immune-mediated tissue damage.<sup>82</sup> Additionally, the low immunopathogenicity of NK cells allows for their use from allogeneic donors, paving the way for scalable "off-the-shelf" therapies that enhance accessibility and streamline production.<sup>82</sup>

Despite their immense therapeutic potential, the clinical deployment of NK cells is hindered by biological and technical challenges that constrain their efficacy. Compared to T cells, NK cells often exhibit inconsistent expansion *ex vivo*, and gene editing efficiency remains variable, posing obstacles to large-scale manufacturing and reproducible therapeutic outcomes.<sup>94,126-128,297</sup> Moreover, NK cells are particularly vulnerable to cryo-damage, resulting in diminished viability and function post-thaw, complicating the development of reliable "off-the-shelf" products.<sup>149</sup> Although CRISPR-Cas9 technology offers exciting possibilities for genetic enhancement, low transfection rates and inconsistent Cas9 expression frequently impede successful gene modification in NK cells.<sup>168,169</sup> Transgene silencing over time further undermines the durability and persistent functions of engineered NK cells, restricting their long-term effectiveness in clinical settings.

To mitigate these challenges, I investigated optimized cryopreservation protocols for NK cells during early proliferation, the utilization of CRISPR/Cas9-loaded retroviral particles to enhance genome editing in NK cells, and the application of HDACis to sustain transgene expression in CAR-NK cells. Collectively, my thesis advanced the workflow for NK cell generation and gene editing and extended the functional longevity of NK cells. These advancements represent a significant step toward more effective and durable NK cell immunotherapies, ultimately contributing to the next generation of cancer treatment options.

## **5.2 NK cell expansion, cryopreservation, and population diversity**

The growing interest in NK cells for clinical application is largely driven by their potential for allogeneic NK cell transfer.<sup>82</sup> In cancer patients, the immune system is often severely weakened, resulting in immune cells that are less effective at combating tumors.<sup>147</sup>

This weakened state limits the efficacy of immunotherapy when relying on the patient's immune cells.<sup>147</sup> As a result, NK cells sourced from unrelated healthy donors become particularly valuable, providing a robust and reliable alternative.<sup>82</sup> One major advantage of this approach is the ability to cryopreserve selected and expanded NK cells as a master stock, facilitating their uniform use across multiple patients. Although cryopreserving fully expanded NK cells has traditionally posed significant difficulties, recent advancements, such as mitigating granzyme B-mediated cryo-damage with IL-15 and IL-18, have dramatically improved NK cell survival following cryopreservation, leading to enhanced preclinical outcomes.<sup>148,150</sup>

While most research emphasized cryopreserving fully expanded NK cells, I investigated the potential for cryopreservation during the early proliferation phase. By closely analyzing NK cell expansion dynamics, I identified an optimal window for cryopreservation at 5 to 7 days post-expansion. This occurs during the exponential growth phase when proliferation potential peaks. NK cells preserved at this stage were successfully recovered, remaining viable for subsequent viral vector modifications. This approach streamlines NK cell expansion by mitigating the risk of delays associated with expansion failures from uncharacterized donor-derived NK cells. Consequently, this method provides a reliable master stock of selected NK cells that can be utilized for future clinical and research purposes.

Despite the improvement of cryopreservation, NK cell therapy has predominantly utilized a single type of approach (IL-2 with feeder cells) for NK cell expansion, which often leads to the expansion of a homogeneous NK cell population, presumably characterized by FcεRI-γ-positive NK cells (**Figure 5.1 A and B**). Since human blood contains diverse NK cell subsets, this simplified expansion strategy may not fully utilize the therapeutic potential

of diverse NK cell subsets for immunotherapy. To address this, I explored various expansion strategies, including creating hypoxic and acidic culture environments using glucose oxidase/catalase (GOX/CAT) systems and using HLA-E-positive feeder cells to stimulate NKG2C-positive NK cells selectively.<sup>298,299</sup> Although data from these approaches are still under investigation, preliminary results have revealed the expansion of NK cells with promising phenotypes, such as tumor-infiltrating (CD11b negative) and NKG2C<sup>+</sup> CD57<sup>+</sup> NK cells, compared to the conventionally expanded CD11b<sup>+</sup> NKG2C<sup>-</sup> CD57<sup>-</sup> NK cells (**Figure 5.1 C and D**).<sup>144,300,301</sup> Continued investigation into these novel NK cell expansion protocols with various culture conditions will be critical for developing advanced therapies incorporating diverse NK cell subsets.

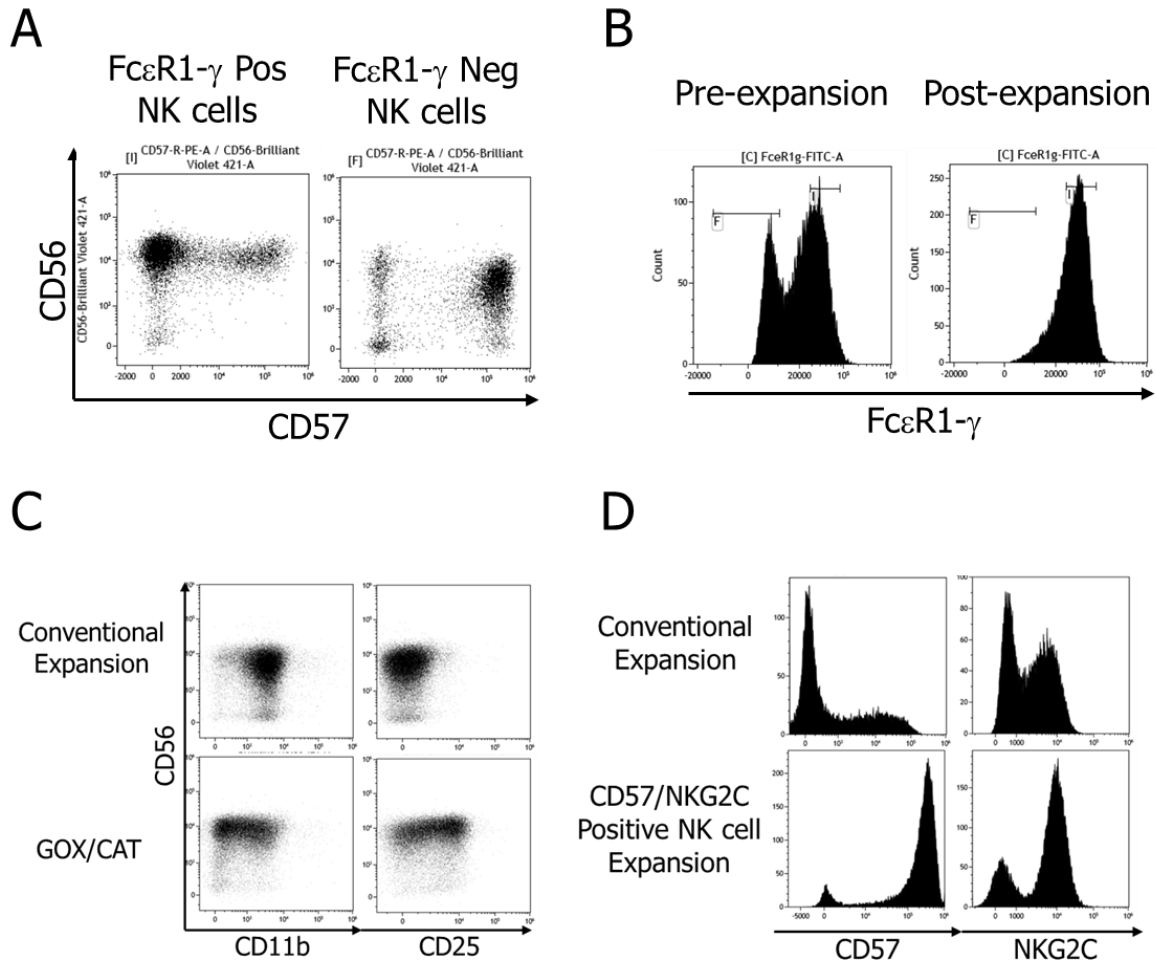


**Figure 5.1 Post-NK cell expansion phenotypes using various culture conditions. (A)** Fc $\epsilon$ R1- $\gamma$ -negative and positive NK cell representative phenotype. **(B)** NK cell expansion often leads to the preferential proliferation of specific subsets, such as Fc $\epsilon$ R1 $\gamma$ -positive NK cells. **(C)** Glucose oxidase/catalase (GOX/CAT)-mediated cultural hypoxic condition expanded a novel subset of NK cells. **(D)** A preferential culture strategy for CD57 and NKG2C-positive NK cells successfully expanded a novel subset of NK cells.

### 5.3 CRISPR-Cas9-loaded retroviral particles for NK cell engineering

CRISPR/Cas9 technology has significantly advanced cell engineering by enabling precise gene editing through targeted DNA DSBs. Guided by RNA, the Cas9 protein can induce gene knockout via NHEJ or facilitate precise transgene insertion through HDR.<sup>156</sup>

<sup>157</sup>While viral vectors have traditionally been used for CRISPR-Cas9 delivery, the application in NK cells is limited by due to the poor Cas9 expression.<sup>168,169</sup> Alternatively, electroporation of Cas9-RNP has emerged as a preferred approach, overcoming these challenges and enabling effective gene knockouts in NK cells.

Despite this, the application of CRISPR-Cas9 in NK cells remains relatively underexplored compared to its use in T cells. For example, while CRISPR screening in T cells is well-documented, comprehensive and large-scale CRISPR-Cas9 screens have never been conducted on NK cells.<sup>302</sup> This gap likely stems from the limitations of conventional CRISPR-Cas9 methods, which rely heavily on viral vector delivery and often result in suboptimal expression in NK cells. To address this, I introduced a novel strategy employing CRISPR-Cas9-loaded retroviral particles to deliver RNP complexes into NK cells. This approach demonstrated high delivery efficiency and successfully achieved TIGIT and CD38 knockout, reinforcing the feasibility of viral particle-based RNP delivery in NK cells.

However, while effective sgRNAs were identified for TIGIT and CD38, inconsistencies between genomic mutations and protein depletion remain challenging. This discrepancy likely reflects the variability in DNA repair and randomly inserted or deleted DNA following Cas9-induced DSB. As CRISPR-Cas9-loaded retroviral particle technology is relatively new, first developed in 2019, with applications in NK cells emerging in 2023, comprehensive sgRNA pools designed for efficient protein depletion are still lacking. Moving forward, collaborative efforts to identify and share validated sgRNA sequences will be crucial in advancing CRISPR-Cas9-based NK cell engineering and ensuring reproducible results across laboratories.

To further refine viral particle-mediated protein delivery, I employed flow virometry, a specialized form of flow cytometry optimized for analyzing nanometer-scale small particles, to address questions regarding retroviral particle production during Cas9-loaded retroviral particle studies. Similar to conventional flow cytometry, flow virometry uses laser-based detection to measure scattered and emitted light from particles, permitting the analysis of nano-sized particles.<sup>303</sup> This technique allows for analyzing viral supernatants, quantifying the number and size of Cas9-loaded particles with high precision. These measurements successfully indicated particle sizes of approximately 120 nm, aligning with the known size of retroviruses and thereby confirming the accuracy of flow virometry in detecting and characterizing viral particles.

A significant advantage of flow virometry lies in its potential to directly measure Cas9 protein presence within viral particles without viral particle destruction. By conjugating fluorochromes such as GFP to Cas9 proteins, I could load the fluorescently tagged complexes into viral particles and detect Cas9-GFP through flow virometry (**Figure 5.2**). This non-destructive approach eliminates the need for traditional viral disruption or fixation methods, which often compromise particle integrity.<sup>304-306</sup> As a result, flow virometry offers a streamlined and highly sensitive method for validating proteins within viral particles, presenting a valuable tool for advancing viral vector research and optimizing CRISPR-Cas9 delivery systems for NK cell engineering. Future research should emphasize the importance of flow virometry-based viral particle analysis.

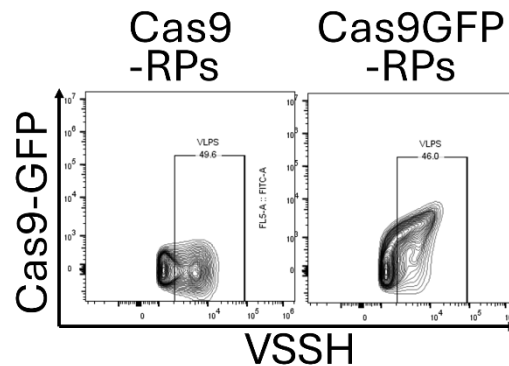


**Figure 5.2 Flow virometry-based detection of Cas9 in viral particles.** Flow virometry is a novel technique that enables fluorescent protein detection, benefiting the detection of engineered viral particles, such as Cas9-loaded retroviral particles. By conjugating a fluorescent protein (GFP) to Cas9, flow virometry allows the detection of Cas9 in VLPs without disrupting their native structure. VSSH: violet-side scatter-height

## 5.4 Histone deacetylase inhibitors in NK cell engineering and transgene expression

HDACis have recently gained attention in cancer treatment. Traditionally, HDACis have been combined with radiotherapy due to the HDAC involvement in DNA repair, and inhibitors can prevent the repair mechanism in the damaged cancer cells upon radiation treatment.<sup>190</sup> In addition, HDACis showed improvement in CAR-T cell therapy for their ability to enhance target cell sensitivity to immune-mediated killing. HDACis, by increasing NOXA signaling, heighten susceptibility to granzyme-mediated apoptosis in target cancer cells.<sup>196</sup> In addition, HDACis upregulate the ligands for NK cell activating receptor NKG2D, such as MICA/B and ULBPs, potentially increasing target cell sensitivity to NK cell-mediated cytotoxicity.<sup>197</sup> Therefore, HDACis can be an attractive therapeutic agent in cancer treatment.

Intriguingly, HDACis have been shown to improve the transcriptional ability of viral transgenes.<sup>200,201,204-207</sup> To address the possible use of HDACis in NK cell engineering, I tested HDACis in CAR- and IL-15-engineered NK cells. Although engineered CAR-NK cells experienced a decline in transgene expression over time, HDACis preserved CAR and IL-15 expression and efficiently eradicated target cells *in vitro* and *in vivo*. Importantly, the effects of HDACis on transgene expression were promoter-dependent. Among the tested promoters, EFS, commonly used in clinical trials, showed the lowest expression in the presence of HDACis, while the virus-driven CMV and MSCV promoters exhibited robust transgene overexpression with HDACis, following previous findings that viral promoters were more regulated than endogenous promoters.<sup>263</sup> The CMV promoter, in particular, showed remarkable upregulation in response to HDACis, presenting opportunities for transient overexpression of genes that might otherwise pose risks, such as those causing severe CRS, but essential for immune activation, allowing for controlled short-term expression.

Due to the improved transgene expression in NK cells achieved through HDACis and promoter engineering, there is a unique opportunity to combine these methods with CRISPR-Cas9 and HDACis. The major challenge for transgene encoding Cas9 delivery in NK cells lies in the size of the *Cas9* gene, which results in size-mediated poor Cas9 expression in NK cells.<sup>168,169</sup> Traditionally, Cas9 proteins have been tested with the EFS promoter.<sup>307,308</sup> This finding suggests that switching the EFS promoter to the CMV and MSCV promoter may transiently increase Cas9 expression in NK cells with HDACis. This strategy may address the conventional challenges related to large CRISPR-Cas9 proteins and allow for efficient Cas9-based genome screening in NK cells.

The optimization of transgene expression through HDACis and promoter engineering also presents possible new research strategies, particularly for expressing complex or large transgenes, such as dual CAR constructs and synNotch receptors. Traditionally, increasing the size of viral transgenes has reduced gene expression, mirroring the challenges encountered with CRISPR-Cas9 delivery in NK cells.<sup>309,310</sup> However, the findings demonstrated in this thesis suggest that leveraging HDACis, in combination with MSCV and CMV promoter-driven constructs, may overcome these limitations. This could enable the testing and implementation of large genes in NK cells, broadening the scope of next-generation NK cell immunotherapies (**Figure 5.3**).

A particularly exciting prospect is the application of synNotch receptors, synthetic proteins that have been extensively studied in T cells but remain largely underexplored in NK cells.<sup>310,311</sup> SynNotch receptors contain transcriptional activators, such as Gal4/VP64, released upon target antigen engagement, triggering downstream expression of genes from responder promoters.<sup>311</sup> Given the large size and complexity of synNotch systems, which have been major barriers to their application in NK cells. Engineering NK cells with MSCV and CMV-driven synNotch, in combination with HDACis, can be a promising area for further investigation. This approach could unlock novel avenues for NK cell therapies.

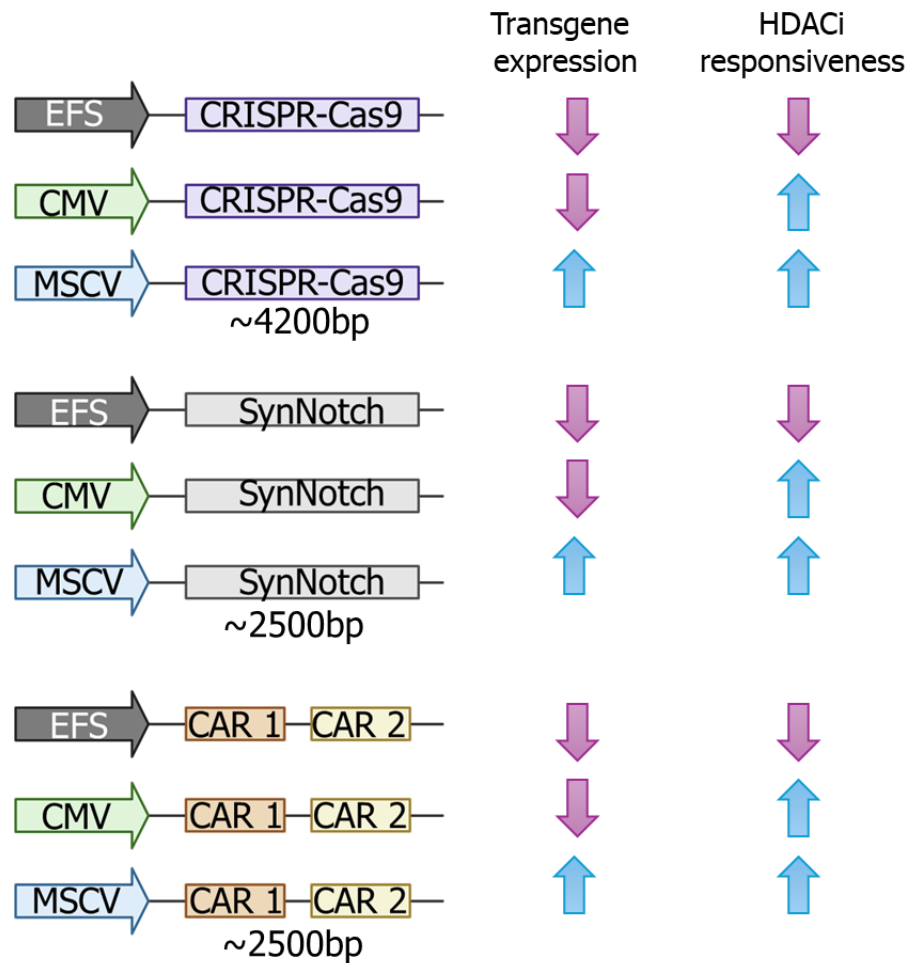


**Figure 5.3 Future directions for NK cell engineering using MSCV and CMV promoters and HDACi.** NK cell engineering has traditionally been limited by poor transgene expression. The MSCV and CMV promoter significantly enhances transgene expression in NK cells with HDACi. This advancement would be particularly valuable for experiments involving large transgenes, such as CRISPR-Cas9, SynNotch, and double/triple CAR constructs.

# **Final Chapter: Concluding Remarks with Graphical Synopsis**

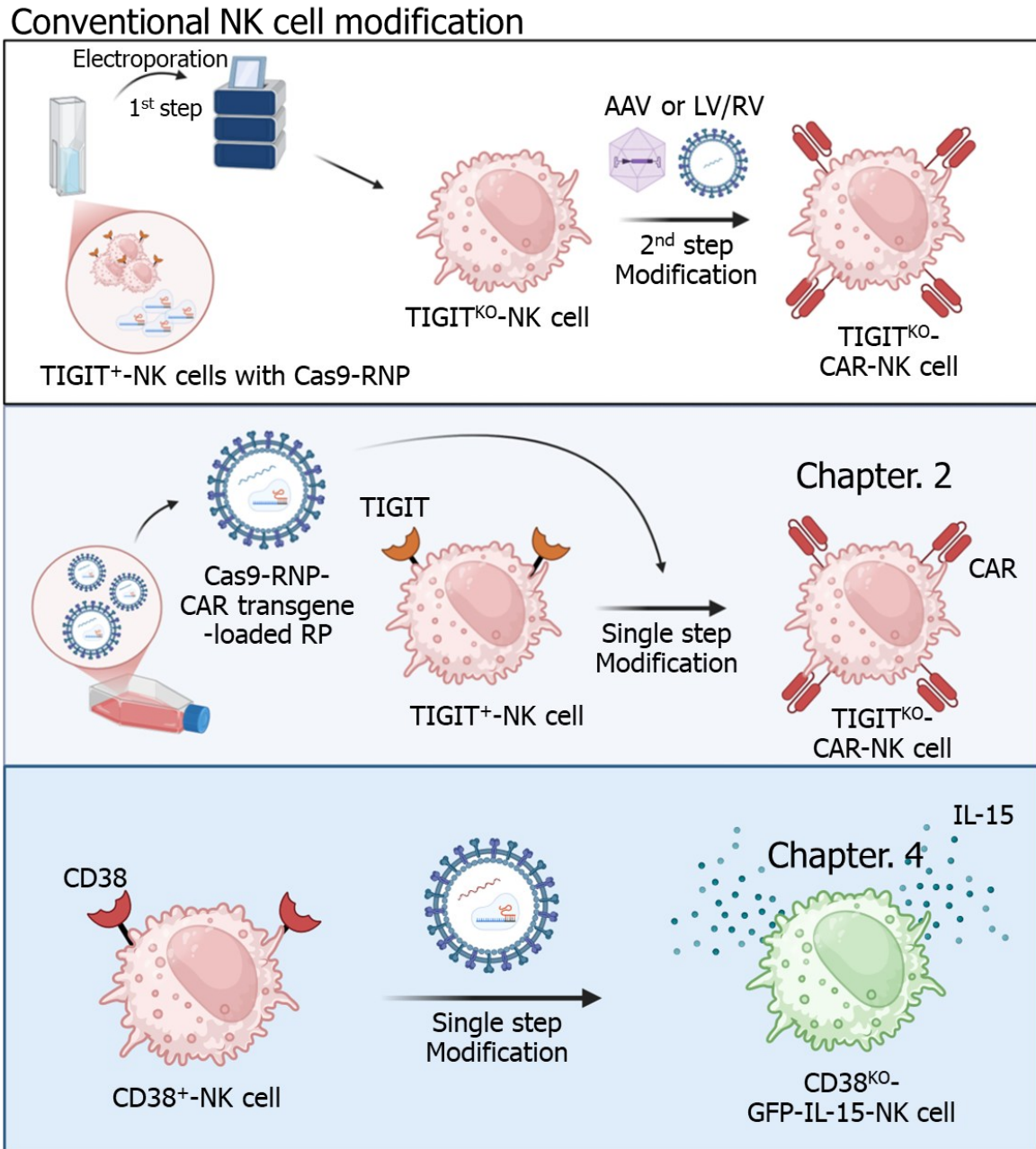
**Figures were generated using Biorender.com.**

NK cells are potent innate immune effectors with intrinsic self-regulatory mechanisms and tumor-killing capabilities, making them attractive candidates for allogeneic immunotherapy.<sup>1,21</sup> Clinical studies, such as those from MD Anderson Cancer Center and FT596 trials, have shown promising results, with CR rates of 37.8% and 37%, respectively, and minimal adverse effects.<sup>99,120,121</sup> Despite their potential, the genetic modification of NK cells has long been challenging.<sup>126-128</sup> The introduction of BaEV-G in 2014 and its application to NK cells in 2019 have markedly accelerated the development of CAR- and cytokine-engineered NK cells.<sup>128,135</sup> Nevertheless, key hurdles remain in cryopreservation, CRISPR-Cas9-mediated genome editing, and long-lasting transgene expression.

The most significant achievement in my thesis is establishing an NK cell cryopreservation method to overcome common laboratory challenges.<sup>149</sup> By cryopreserving NK cells early in the expansion, I successfully generated a master stock and eliminated the need for repeated NK cell isolations and stimulations. These cryopreserved NK cells were effectively re-expanded with only a brief delay. These cells remained suitable for CAR engineering and maintained consistent expansion even with genetic modification. By developing a methodology for NK cell cryo-master stock generation, my thesis established a more efficient and reproducible platform for future preclinical and clinical studies.

While CRISPR-Cas9 has been transformative in T cell research, its potential in NK cells remains largely under-evaluated.<sup>302,312,313</sup> My thesis introduced Cas9-RNP-loaded retroviral particles as a novel gene-editing strategy for NK cells, demonstrating high-efficiency knockouts of TIGIT and CD38. This system also enabled simultaneous CAR and cytokine gene editing in a single step, an advancement over traditional multi-step modifications in NK cells. My thesis is the first to establish the feasibility of Cas9-RNP-

retroviral particle technology in NK cells, paving the way for advanced future CRISPR-Cas9 engineering research for NK cell-based cancer immunotherapy (**Figure 6.1**).



Dong-Hyeon Jo's thesis

**Figure 6.1** Graphical summary of Chapters 2 and 4. Simultaneous engineering of natural killer cells using CRISPR-Cas9- and transgene-loaded retroviral particles.

To overcome limitations in transgene expression, I investigated HDACis to sustain CAR expression in NK cells. While previous studies suggested that HDACis could improve transgene expression, their effects in NK cell engineering remained underexplored.<sup>200,201,204-208</sup> I focused on testing ENT in anti-CD138 CAR NK cells and demonstrated significantly sustained CAR expression without compromising viability. This ENT-mediated CAR overexpression was promoter-dependent, increasing MSCV- and CMV-driven CARs but not EFS-driven CARs. This enhanced CAR expression led to better clearance of multiple myeloma *in vitro* and *in vivo* (**Figure 6.2**).

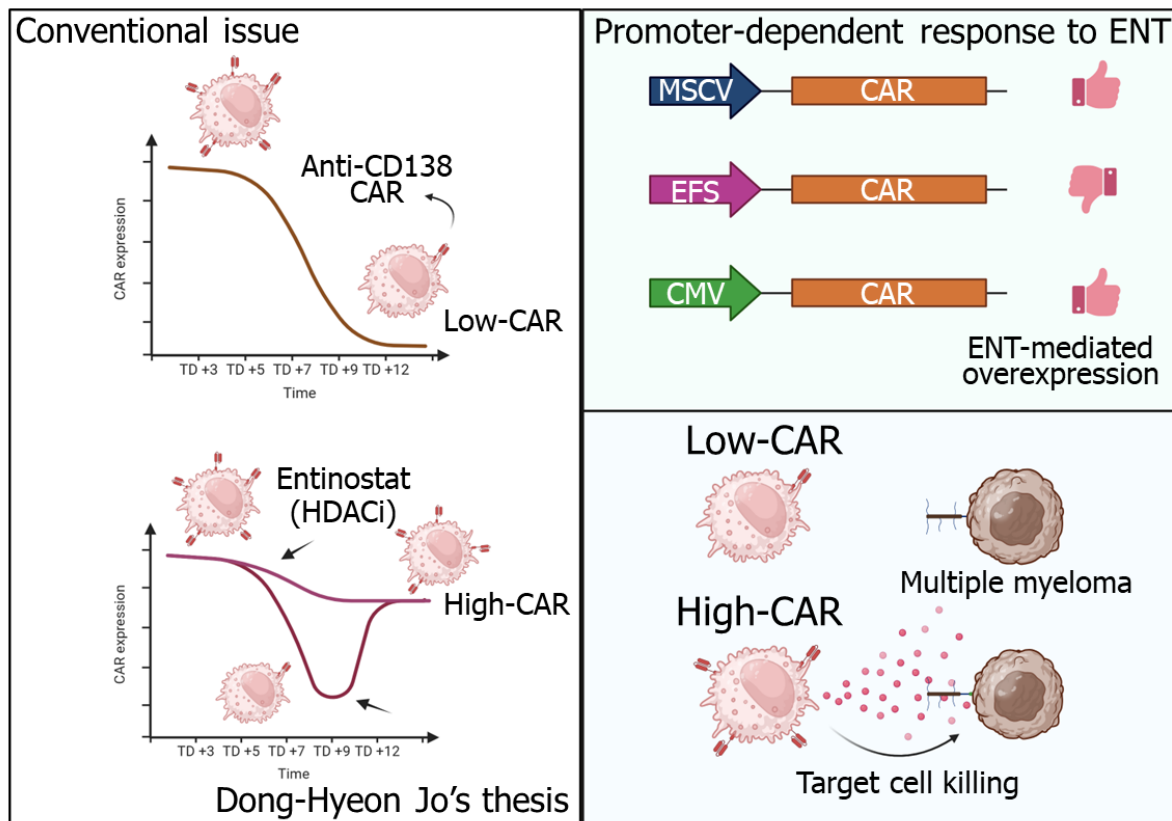


**Figure 6.2 Graphical summary of Chapter 3: Entinostat, a histone deacetylase inhibitor, enhances CAR-NK cell anti-tumor activity by sustaining CAR expression.**

In conclusion, my thesis lays a strong foundation for future studies, demonstrating that integrating multiple genetic modification strategies can enhance the effectiveness of NK cell therapies and improve preclinical outcomes. By addressing key challenges in cryopreservation, CRISPR-Cas9 engineering, and long-lasting transgene expression, my thesis contributes to the rapidly evolving field of engineering-based NK cell immunotherapy and developing next-generation cancer treatments using NK cells.

## References

1. Huntington, N.D., Vosshenrich, C.A., and Di Santo, J.P. (2007). Developmental pathways that generate natural-killer-cell diversity in mice and humans. *Nat Rev Immunol* 7, 703-714. 10.1038/nri2154.
2. Voskoboinik, I., Whisstock, J.C., and Trapani, J.A. (2015). Perforin and granzymes: function, dysfunction and human pathology. *Nat Rev Immunol* 15, 388-400. 10.1038/nri3839.
3. Louis, C., Souza-Fonseca-Guimaraes, F., Yang, Y., D'Silva, D., Kratina, T., Dagley, L., Hediye-Zadeh, S., Rautela, J., Masters, S.L., Davis, M.J., Babon, J.J., et al. (2020). NK cell-derived GM-CSF potentiates inflammatory arthritis and is negatively regulated by CIS. *J Exp Med* 217. 10.1084/jem.20191421.
4. Palano, M.T., Gallazzi, M., Cucchiara, M., De Lerma Barbaro, A., Gallo, D., Bassani, B., Bruno, A., and Mortara, L. (2021). Neutrophil and Natural Killer Cell Interactions in Cancers: Dangerous Liaisons Instructing Immunosuppression and Angiogenesis. *Vaccines (Basel)* 9. 10.3390/vaccines9121488.
5. Zhou, J., Zhang, S., and Guo, C. (2021). Crosstalk between macrophages and natural killer cells in the tumor microenvironment. *Int Immunopharmacol* 101, 108374. 10.1016/j.intimp.2021.108374.
6. Guerriero, J.L. (2019). Macrophages: Their Untold Story in T Cell Activation and Function. *Int Rev Cell Mol Biol* 342, 73-93. 10.1016/bs.ircmb.2018.07.001.
7. Suchanek, O., Ferdinand, J.R., Tuong, Z.K., Wijeyesinghe, S., Chandra, A., Clauder, A.K., Almeida, L.N., Clare, S., Harcourt, K., Ward, C.J., Bashford-Rogers, R., et al. (2023). Tissue-resident B cells orchestrate macrophage polarisation and function. *Nat Commun* 14, 7081. 10.1038/s41467-023-42625-4.
8. Lanier, L.L., Testi, R., Bindl, J., and Phillips, J.H. (1989). Identity of Leu-19 (CD56) leukocyte differentiation antigen and neural cell adhesion molecule. *J Exp Med* 169, 2233-2238. 10.1084/jem.169.6.2233.
9. Lanier, L.L., Le, A.M., Civin, C.I., Loken, M.R., and Phillips, J.H. (1986). The relationship of CD16 (Leu-11) and Leu-19 (NKH-1) antigen expression on human peripheral blood NK cells and cytotoxic T lymphocytes. *J Immunol* 136, 4480-4486.
10. Moretta, L. (2010). Dissecting CD56dim human NK cells. *Blood* 116, 3689-3691. 10.1182/blood-2010-09-303057.
11. Schwane, V., Huynh-Tran, V.H., Vollmers, S., Yakup, V.M., Sauter, J., Schmidt, A.H., Peine, S., Altfeld, M., Richert, L., and Korner, C. (2020). Distinct Signatures in the Receptor Repertoire Discriminate CD56bright and CD56dim Natural Killer Cells. *Front Immunol* 11, 568927. 10.3389/fimmu.2020.568927.
12. Cooper, M.A., Fehniger, T.A., Turner, S.C., Chen, K.S., Ghaheri, B.A., Ghayur, T., Carson, W.E., and Caligiuri, M.A. (2001). Human natural killer cells: a unique innate

- immunoregulatory role for the CD56(bright) subset. *Blood* *97*, 3146-3151. 10.1182/blood.v97.10.3146.
13. Rodriguez-Mogeda, C., van Ansenwoude, C.M.J., van der Molen, L., Strijbis, E.M.M., Mebius, R.E., and de Vries, H.E. (2024). The role of CD56(bright) NK cells in neurodegenerative disorders. *J Neuroinflammation* *21*, 48. 10.1186/s12974-024-03040-8.
  14. Michel, T., Poli, A., Cuapio, A., Briquemont, B., Iserentant, G., Ollert, M., and Zimmer, J. (2016). Human CD56bright NK Cells: An Update. *J Immunol* *196*, 2923-2931. 10.4049/jimmunol.1502570.
  15. Chan, A., Hong, D.L., Atzberger, A., Kollnberger, S., Filer, A.D., Buckley, C.D., McMichael, A., Enver, T., and Bowness, P. (2007). CD56bright human NK cells differentiate into CD56dim cells: role of contact with peripheral fibroblasts. *J Immunol* *179*, 89-94. 10.4049/jimmunol.179.1.89.
  16. Rebuffet, L., Melsen, J.E., Escaliere, B., Basurto-Lozada, D., Bhandoola, A., Bjorkstrom, N.K., Bryceson, Y.T., Castriconi, R., Cichocki, F., Colonna, M., Davis, D.M., et al. (2024). High-dimensional single-cell analysis of human natural killer cell heterogeneity. *Nat Immunol* *25*, 1474-1488. 10.1038/s41590-024-01883-0.
  17. Borrego, F. (2006). The first molecular basis of the "missing self" hypothesis. *J Immunol* *177*, 5759-5760. 10.4049/jimmunol.177.9.5759.
  18. Ljunggren, H.G., and Karre, K. (1990). In search of the 'missing self': MHC molecules and NK cell recognition. *Immunol Today* *11*, 237-244. 10.1016/0167-5699(90)90097-s.
  19. Pende, D., Falco, M., Vitale, M., Cantoni, C., Vitale, C., Munari, E., Bertaina, A., Moretta, F., Del Zotto, G., Pietra, G., Mingari, M.C., et al. (2019). Killer Ig-Like Receptors (KIRs): Their Role in NK Cell Modulation and Developments Leading to Their Clinical Exploitation. *Front Immunol* *10*, 1179. 10.3389/fimmu.2019.01179.
  20. Wang, X., Xiong, H., and Ning, Z. (2022). Implications of NKG2A in immunity and immune-mediated diseases. *Front Immunol* *13*, 960852. 10.3389/fimmu.2022.960852.
  21. Sivori, S., Vacca, P., Del Zotto, G., Munari, E., Mingari, M.C., and Moretta, L. (2019). Human NK cells: surface receptors, inhibitory checkpoints, and translational applications. *Cell Mol Immunol* *16*, 430-441. 10.1038/s41423-019-0206-4.
  22. Kumar, S. (2018). Natural killer cell cytotoxicity and its regulation by inhibitory receptors. *Immunology* *154*, 383-393. 10.1111/imm.12921.
  23. Connelley, T.K., Longhi, C., Burrells, A., Degnan, K., Hope, J., Allan, A.J., Hammond, J.A., Storset, A.K., and Morrison, W.I. (2014). NKp46+ CD3+ cells: a novel nonconventional T cell subset in cattle exhibiting both NK cell and T cell features. *J Immunol* *192*, 3868-3880. 10.4049/jimmunol.1302464.
  24. Correia, M.P., Stojanovic, A., Bauer, K., Juraeva, D., Tykocinski, L.O., Lorenz, H.M., Brors, B., and Cerwenka, A. (2018). Distinct human circulating

- NKp30(+)FcepsilonRIgamma(+)CD8(+) T cell population exhibiting high natural killer-like antitumor potential. *Proc Natl Acad Sci U S A* *115*, E5980-E5989. 10.1073/pnas.1720564115.
25. Vitale, M., Bottino, C., Sivori, S., Sanseverino, L., Castriconi, R., Marcenaro, E., Augugliaro, R., Moretta, L., and Moretta, A. (1998). NKp44, a novel triggering surface molecule specifically expressed by activated natural killer cells, is involved in non-major histocompatibility complex-restricted tumor cell lysis. *J Exp Med* *187*, 2065-2072. 10.1084/jem.187.12.2065.
  26. Sen Santara, S., Lee, D.J., Crespo, A., Hu, J.J., Walker, C., Ma, X., Zhang, Y., Chowdhury, S., Meza-Sosa, K.F., Lewandrowski, M., Zhang, H., et al. (2023). The NK cell receptor NKp46 recognizes ecto-calreticulin on ER-stressed cells. *Nature* *616*, 348-356. 10.1038/s41586-023-05912-0.
  27. Pogge von Strandmann, E., Simhadri, V.R., von Tresckow, B., Sasse, S., Reiners, K.S., Hansen, H.P., Rothe, A., Boll, B., Simhadri, V.L., Borchmann, P., McKinnon, P.J., et al. (2007). Human leukocyte antigen-B-associated transcript 3 is released from tumor cells and engages the NKp30 receptor on natural killer cells. *Immunity* *27*, 965-974. 10.1016/j.immuni.2007.10.010.
  28. Vivier, E., Nunes, J.A., and Vely, F. (2004). Natural killer cell signaling pathways. *Science* *306*, 1517-1519. 10.1126/science.1103478.
  29. de Kruijf, E.M., Sajet, A., van Nes, J.G., Putter, H., Smit, V.T., Eagle, R.A., Jafferji, I., Trowsdale, J., Liefers, G.J., van de Velde, C.J., and Kuppen, P.J. (2012). NKG2D ligand tumor expression and association with clinical outcome in early breast cancer patients: an observational study. *BMC Cancer* *12*, 24. 10.1186/1471-2407-12-24.
  30. Billadeau, D.D., Upshaw, J.L., Schoon, R.A., Dick, C.J., and Leibson, P.J. (2003). NKG2D-DAP10 triggers human NK cell-mediated killing via a Syk-independent regulatory pathway. *Nat Immunol* *4*, 557-564. 10.1038/ni929.
  31. Wang, J., Li, C.D., and Sun, L. (2020). Recent Advances in Molecular Mechanisms of the NKG2D Pathway in Hepatocellular Carcinoma. *Biomolecules* *10*. 10.3390/biom10020301.
  32. Chen, X., Bai, F., Sokol, L., Zhou, J., Ren, A., Painter, J.S., Liu, J., Sallman, D.A., Chen, Y.A., Yoder, J.A., Djeu, J.Y., et al. (2009). A critical role for DAP10 and DAP12 in CD8+ T cell-mediated tissue damage in large granular lymphocyte leukemia. *Blood* *113*, 3226-3234. 10.1182/blood-2008-07-168245.
  33. Capuano, C., Pighi, C., Battella, S., De Federicis, D., Galandrini, R., and Palmieri, G. (2021). Harnessing CD16-Mediated NK Cell Functions to Enhance Therapeutic Efficacy of Tumor-Targeting mAbs. *Cancers (Basel)* *13*. 10.3390/cancers13102500.
  34. Hammer, Q., Ruckert, T., Borst, E.M., Dunst, J., Haubner, A., Durek, P., Heinrich, F., Gasparoni, G., Babic, M., Tomic, A., Pietra, G., et al. (2018). Peptide-specific recognition of human cytomegalovirus strains controls adaptive natural killer cells. *Nat Immunol* *19*, 453-463. 10.1038/s41590-018-0082-6.

35. Bigley, A.B., Spade, S., Agha, N.H., Biswas, S., Tang, S., Malik, M.H., Dai, L., Masoumi, S., Patino-Escobar, B., Hale, M., DiPierro, G., et al. (2021). FcepsilonRIgamma-negative NK cells persist *in vivo* and enhance efficacy of therapeutic monoclonal antibodies in multiple myeloma. *Blood Adv* 5, 3021-3031. 10.1182/bloodadvances.2020002440.
36. Zhang, T., Scott, J.M., Hwang, I., and Kim, S. (2013). Cutting edge: antibody-dependent memory-like NK cells distinguished by FcRgamma deficiency. *J Immunol* 190, 1402-1406. 10.4049/jimmunol.1203034.
37. Koene, H.R., Kleijer, M., Algra, J., Roos, D., von dem Borne, A.E., and de Haas, M. (1997). Fc gammaRIIIa-158V/F polymorphism influences the binding of IgG by natural killer cell Fc gammaRIIIa, independently of the Fc gammaRIIIa-48L/R/H phenotype. *Blood* 90, 1109-1114.
38. Hatjiharissi, E., Xu, L., Santos, D.D., Hunter, Z.R., Ciccarelli, B.T., Verselis, S., Modica, M., Cao, Y., Manning, R.J., Leleu, X., Dimmock, E.A., et al. (2007). Increased natural killer cell expression of CD16, augmented binding and ADCC activity to rituximab among individuals expressing the FcgammaRIIIa-158 V/V and V/F polymorphism. *Blood* 110, 2561-2564. 10.1182/blood-2007-01-070656.
39. Imsirovic, V., Wensveen, F.M., Polic, B., and Jelencic, V. (2024). Maintaining the Balance: Regulation of NK Cell Activity. *Cells* 13. 10.3390/cells13171464.
40. Liu, M., Liang, S., and Zhang, C. (2021). NK Cells in Autoimmune Diseases: Protective or Pathogenic? *Front Immunol* 12, 624687. 10.3389/fimmu.2021.624687.
41. Barrow, A.D., Martin, C.J., and Colonna, M. (2019). The Natural Cytotoxicity Receptors in Health and Disease. *Front Immunol* 10, 909. 10.3389/fimmu.2019.00909.
42. Bialoszewska, A., Baychelier, F., Niderla-Bielinska, J., Czop, A., Debre, P., Vieillard, V., Kieda, C., and Malejczyk, J. (2013). Constitutive expression of ligand for natural killer cell NKp44 receptor (NKp44L) by normal human articular chondrocytes. *Cell Immunol* 285, 6-9. 10.1016/j.cellimm.2013.08.005.
43. Moretta, A., Vitale, M., Bottino, C., Orengo, A.M., Morelli, L., Augugliaro, R., Barbaresi, M., Ciccone, E., and Moretta, L. (1993). P58 molecules as putative receptors for major histocompatibility complex (MHC) class I molecules in human natural killer (NK) cells. Anti-p58 antibodies reconstitute lysis of MHC class I-protected cells in NK clones displaying different specificities. *J Exp Med* 178, 597-604. 10.1084/jem.178.2.597.
44. Colonna, M., and Samaridis, J. (1995). Cloning of immunoglobulin-superfamily members associated with HLA-C and HLA-B recognition by human natural killer cells. *Science* 268, 405-408. 10.1126/science.7716543.
45. Lorenz, U. (2009). SHP-1 and SHP-2 in T cells: two phosphatases functioning at many levels. *Immunol Rev* 228, 342-359. 10.1111/j.1600-065X.2008.00760.x.

46. Ben-Shmuel, A., Sabag, B., Puthenveetil, A., Biber, G., Levy, M., Jubany, T., Awwad, F., Roy, R.K., Joseph, N., Matalon, O., Kivelevitz, J., et al. (2022). Inhibition of SHP-1 activity by PKC-theta regulates NK cell activation threshold and cytotoxicity. *Elife* *11*. 10.7554/eLife.73282.
47. Hao, F., Wang, C., Sholy, C., Cao, M., and Kang, X. (2021). Strategy for Leukemia Treatment Targeting SHP-1,2 and SHIP. *Front Cell Dev Biol* *9*, 730400. 10.3389/fcell.2021.730400.
48. Patsoukis, N., Duke-Cohan, J.S., Chaudhri, A., Aksoylar, H.I., Wang, Q., Council, A., Berg, A., Freeman, G.J., and Boussiotis, V.A. (2020). Interaction of SHP-2 SH2 domains with PD-1 ITSM induces PD-1 dimerization and SHP-2 activation. *Commun Biol* *3*, 128. 10.1038/s42003-020-0845-0.
49. Binstadt, B.A., Brumbaugh, K.M., Dick, C.J., Scharenberg, A.M., Williams, B.L., Colonna, M., Lanier, L.L., Kinet, J.P., Abraham, R.T., and Leibson, P.J. (1996). Sequential involvement of Lck and SHP-1 with MHC-recognizing receptors on NK cells inhibits FcR-initiated tyrosine kinase activation. *Immunity* *5*, 629-638. 10.1016/s1074-7613(00)80276-9.
50. Plas, D.R., Johnson, R., Pingel, J.T., Matthews, R.J., Dalton, M., Roy, G., Chan, A.C., and Thomas, M.L. (1996). Direct regulation of ZAP-70 by SHP-1 in T cell antigen receptor signaling. *Science* *272*, 1173-1176. 10.1126/science.272.5265.1173.
51. Schmied, L., Luu, T.T., Sondergaard, J.N., Hald, S.H., Meinke, S., Mohammad, D.K., Singh, S.B., Mayer, C., Perinetti Casoni, G., Chrobok, M., Schlums, H., et al. (2023). SHP-1 localization to the activating immune synapse promotes NK cell tolerance in MHC class I deficiency. *Sci Signal* *16*, eabq0752. 10.1126/scisignal.abq0752.
52. Konjevic, G.M., Vuletic, A.M., Mirjadic Martinovic, K.M., Larsen, A.K., and Jurisic, V.B. (2019). The role of cytokines in the regulation of NK cells in the tumor environment. *Cytokine* *117*, 30-40. 10.1016/j.cyto.2019.02.001.
53. Becknell, B., and Caligiuri, M.A. (2005). Interleukin-2, interleukin-15, and their roles in human natural killer cells. *Adv Immunol* *86*, 209-239. 10.1016/S0065-2776(04)86006-1.
54. Miyazaki, T., Kawahara, A., Fujii, H., Nakagawa, Y., Minami, Y., Liu, Z.J., Oishi, I., Silvennoinen, O., Witthuhn, B.A., Ihle, J.N., and et al. (1994). Functional activation of Jak1 and Jak3 by selective association with IL-2 receptor subunits. *Science* *266*, 1045-1047. 10.1126/science.7973659.
55. Lord, J.D., McIntosh, B.C., Greenberg, P.D., and Nelson, B.H. (1998). The IL-2 receptor promotes proliferation, bcl-2 and bcl-x induction, but not cell viability through the adapter molecule Shc. *J Immunol* *161*, 4627-4633.
56. Vuletic, A., Jovanic, I., Jurisic, V., Milovanovic, Z., Nikolic, S., Spurnic, I., and Konjevic, G. (2020). IL-2 And IL-15 Induced NKG2D, CD158a and CD158b Expression on T, NKT- like and NK Cell Lymphocyte Subsets from Regional Lymph Nodes of Melanoma Patients. *Pathol Oncol Res* *26*, 223-231. 10.1007/s12253-018-0444-2.

57. Lusty, E., Poznanski, S.M., Kwofie, K., Mandur, T.S., Lee, D.A., Richards, C.D., and Ashkar, A.A. (2017). IL-18/IL-15/IL-12 synergy induces elevated and prolonged IFN-gamma production by *ex vivo* expanded NK cells which is not due to enhanced STAT4 activation. *Mol Immunol* 88, 138-147. 10.1016/j.molimm.2017.06.025.
58. Bacon, C.M., McVicar, D.W., Ortaldo, J.R., Rees, R.C., O'Shea, J.J., and Johnston, J.A. (1995). Interleukin 12 (IL-12) induces tyrosine phosphorylation of JAK2 and TYK2: differential use of Janus family tyrosine kinases by IL-2 and IL-12. *J Exp Med* 181, 399-404. 10.1084/jem.181.1.399.
59. Ma, X., Yan, W., Zheng, H., Du, Q., Zhang, L., Ban, Y., Li, N., and Wei, F. (2015). Regulation of IL-10 and IL-12 production and function in macrophages and dendritic cells. *F1000Res* 4. 10.12688/f1000research.7010.1.
60. Tomura, M., Zhou, X.Y., Maruo, S., Ahn, H.J., Hamaoka, T., Okamura, H., Nakanishi, K., Tanimoto, T., Kurimoto, M., and Fujiwara, H. (1998). A critical role for IL-18 in the proliferation and activation of NK1.1+ CD3- cells. *J Immunol* 160, 4738-4746.
61. Khan, A.U.H., Almutairi, S.M., Ali, A.K., Salcedo, R., Stewart, C.A., Wang, L., and Lee, S.H. (2021). Expression of Nutrient Transporters on NK Cells During Murine Cytomegalovirus Infection Is MyD88-Dependent. *Front Immunol* 12, 654225. 10.3389/fimmu.2021.654225.
62. Muroi, M., and Tanamoto, K. (2008). TRAF6 distinctively mediates MyD88- and IRAK-1-induced activation of NF-kappaB. *J Leukoc Biol* 83, 702-707. 10.1189/jlb.0907629.
63. Leong, J.W., Chase, J.M., Romee, R., Schneider, S.E., Sullivan, R.P., Cooper, M.A., and Fehniger, T.A. (2014). Preactivation with IL-12, IL-15, and IL-18 induces CD25 and a functional high-affinity IL-2 receptor on human cytokine-induced memory-like natural killer cells. *Biol Blood Marrow Transplant* 20, 463-473. 10.1016/j.bbmt.2014.01.006.
64. Mailliard, R.B., Alber, S.M., Shen, H., Watkins, S.C., Kirkwood, J.M., Herberman, R.B., and Kalinski, P. (2005). IL-18-induced CD83+CCR7+ NK helper cells. *J Exp Med* 202, 941-953. 10.1084/jem.20050128.
65. Khan, A.U.H., Ali, A.K., Marr, B., Jo, D., Ahmadvand, S., Fong-McMaster, C., Almutairi, S.M., Wang, L., Sad, S., Harper, M.E., and Lee, S.H. (2023). The TNFalpha/TNFR2 axis mediates natural killer cell proliferation by promoting aerobic glycolysis. *Cell Mol Immunol* 20, 1140-1155. 10.1038/s41423-023-01071-4.
66. Wang, R., Jaw, J.J., Stutzman, N.C., Zou, Z., and Sun, P.D. (2012). Natural killer cell-produced IFN-gamma and TNF-alpha induce target cell cytolysis through up-regulation of ICAM-1. *J Leukoc Biol* 91, 299-309. 10.1189/jlb.0611308.
67. Min, B., Yang, B., Kim, Y.S., Park, G.M., Kim, H., Kim, H., Kim, E.J., Hwang, Y.K., Shin, E.C., and Cho, S. (2022). Harnessing novel engineered feeder cells expressing activating molecules for optimal expansion of NK cells with potent antitumor activity. *Cell Mol Immunol* 19, 296-298. 10.1038/s41423-021-00759-9.

68. Viel, S., Marcais, A., Guimaraes, F.S., Loftus, R., Rabilloud, J., Grau, M., Degouve, S., Djebali, S., Sanlaville, A., Charrier, E., Bienvenu, J., et al. (2016). TGF-beta inhibits the activation and functions of NK cells by repressing the mTOR pathway. *Sci Signal* 9, ra19. 10.1126/scisignal.aad1884.
69. Slattery, K., and Gardiner, C.M. (2019). NK Cell Metabolism and TGFbeta - Implications for Immunotherapy. *Front Immunol* 10, 2915. 10.3389/fimmu.2019.02915.
70. Schmierer, B., and Hill, C.S. (2007). TGFbeta-SMAD signal transduction: molecular specificity and functional flexibility. *Nat Rev Mol Cell Biol* 8, 970-982. 10.1038/nrm2297.
71. Alvarez, M., Dunai, C., Khuat, L.T., Aguilar, E.G., Barao, I., and Murphy, W.J. (2020). IL-2 and Anti-TGF-beta Promote NK Cell Reconstitution and Anti-tumor Effects after Syngeneic Hematopoietic Stem Cell Transplantation. *Cancers (Basel)* 12. 10.3390/cancers12113189.
72. Zaiatz-Bittencourt, V., Finlay, D.K., and Gardiner, C.M. (2018). Canonical TGF-beta Signaling Pathway Represses Human NK Cell Metabolism. *J Immunol* 200, 3934-3941. 10.4049/jimmunol.1701461.
73. Regis, S., Dondero, A., Caliendo, F., Bottino, C., and Castriconi, R. (2020). NK Cell Function Regulation by TGF-beta-Induced Epigenetic Mechanisms. *Front Immunol* 11, 311. 10.3389/fimmu.2020.00311.
74. Gao, Y., Souza-Fonseca-Guimaraes, F., Bald, T., Ng, S.S., Young, A., Ngiow, S.F., Rautela, J., Straube, J., Waddell, N., Blake, S.J., Yan, J., et al. (2017). Tumor immunoevasion by the conversion of effector NK cells into type 1 innate lymphoid cells. *Nat Immunol* 18, 1004-1015. 10.1038/ni.3800.
75. Cortez, V.S., Ulland, T.K., Cervantes-Barragan, L., Bando, J.K., Robinette, M.L., Wang, Q., White, A.J., Gilfillan, S., Cella, M., and Colonna, M. (2017). SMAD4 impedes the conversion of NK cells into ILC1-like cells by curtailing non-canonical TGF-beta signaling. *Nat Immunol* 18, 995-1003. 10.1038/ni.3809.
76. Liu, S., Galat, V., Galat, Y., Lee, Y.K.A., Wainwright, D., and Wu, J. (2021). NK cell-based cancer immunotherapy: from basic biology to clinical development. *J Hematol Oncol* 14, 7. 10.1186/s13045-020-01014-w.
77. Song, F., Hu, Y., Zhang, Y., Zhang, M., Yang, T., Wu, W., Huang, S., Xu, H., Chang, A.H., Huang, H., and Wei, G. (2023). Safety and efficacy of autologous and allogeneic humanized CD19-targeted CAR-T cell therapy for patients with relapsed/refractory B-ALL. *J Immunother Cancer* 11. 10.1136/jitc-2022-005701.
78. Lupo, K.B., and Matosevic, S. (2019). Natural Killer Cells as Allogeneic Effectors in Adoptive Cancer Immunotherapy. *Cancers (Basel)* 11. 10.3390/cancers11060769.
79. Morris, E.C., Neelapu, S.S., Giavridis, T., and Sadelain, M. (2022). Cytokine release syndrome and associated neurotoxicity in cancer immunotherapy. *Nat Rev Immunol* 22, 85-96. 10.1038/s41577-021-00547-6.

80. Chen, S., Zhu, H., and Jounaidi, Y. (2024). Comprehensive snapshots of natural killer cells functions, signaling, molecular mechanisms and clinical utilization. *Signal Transduct Target Ther* 9, 302. 10.1038/s41392-024-02005-w.
81. Sanber, K., Savani, B., and Jain, T. (2021). Graft-versus-host disease risk after chimeric antigen receptor T-cell therapy: the diametric opposition of T cells. *Br J Haematol* 195, 660-668. 10.1111/bjh.17544.
82. Heipertz, E.L., Zynda, E.R., Stav-Noraas, T.E., Hungler, A.D., Boucher, S.E., Kaur, N., and Vemuri, M.C. (2021). Current Perspectives on "Off-The-Shelf" Allogeneic NK and CAR-NK Cell Therapies. *Front Immunol* 12, 732135. 10.3389/fimmu.2021.732135.
83. Eisenhauer, E.A., Therasse, P., Bogaerts, J., Schwartz, L.H., Sargent, D., Ford, R., Dancey, J., Arbuck, S., Gwyther, S., Mooney, M., Rubinstein, L., et al. (2009). New response evaluation criteria in solid tumours: revised RECIST guideline (version 1.1). *Eur J Cancer* 45, 228-247. 10.1016/j.ejca.2008.10.026.
84. Dohner, H., Wei, A.H., Appelbaum, F.R., Craddock, C., DiNardo, C.D., Dombret, H., Ebert, B.L., Fenaux, P., Godley, L.A., Hasserjian, R.P., Larson, R.A., et al. (2022). Diagnosis and management of AML in adults: 2022 recommendations from an international expert panel on behalf of the ELN. *Blood* 140, 1345-1377. 10.1182/blood.2022016867.
85. Hallek, M., Cheson, B.D., Catovsky, D., Caligaris-Cappio, F., Dighiero, G., Dohner, H., Hillmen, P., Keating, M., Montserrat, E., Chiorazzi, N., Stilgenbauer, S., et al. (2018). iwCLL guidelines for diagnosis, indications for treatment, response assessment, and supportive management of CLL. *Blood* 131, 2745-2760. 10.1182/blood-2017-09-806398.
86. Yang, Y., Lim, O., Kim, T.M., Ahn, Y.O., Choi, H., Chung, H., Min, B., Her, J.H., Cho, S.Y., Keam, B., Lee, S.H., et al. (2016). Phase I Study of Random Healthy Donor-Derived Allogeneic Natural Killer Cell Therapy in Patients with Malignant Lymphoma or Advanced Solid Tumors. *Cancer Immunol Res* 4, 215-224. 10.1158/2326-6066.CIR-15-0118.
87. Modak, S., Le Luduec, J.B., Cheung, I.Y., Goldman, D.A., Ostrovnaya, I., Doubrovina, E., Basu, E., Kushner, B.H., Kramer, K., Roberts, S.S., O'Reilly, R.J., et al. (2018). Adoptive immunotherapy with haploidentical natural killer cells and Anti-GD2 monoclonal antibody m3F8 for resistant neuroblastoma: Results of a phase I study. *Oncoimmunology* 7, e1461305. 10.1080/2162402X.2018.1461305.
88. Lin, M., Luo, H., Liang, S., Chen, J., Liu, A., Niu, L., and Jiang, Y. (2020). Pembrolizumab plus allogeneic NK cells in advanced non-small cell lung cancer patients. *J Clin Invest* 130, 2560-2569. 10.1172/JCI132712.
89. Ciurea, S.O., Kongtim, P., Srour, S., Chen, J., Soebbing, D., Shpall, E., Rezvani, K., Nakkula, R., Thakkar, A., Troy, E.C., Cash, A.A., et al. (2024). Results of a phase I trial with Haploidentical mbIL-21 *ex vivo* expanded NK cells for patients with

- multiply relapsed and refractory AML. *Am J Hematol* 99, 890-899. 10.1002/ajh.27281.
90. Leivas, A., Perez-Martinez, A., Blanchard, M.J., Martin-Clavero, E., Fernandez, L., Lahuerta, J.J., and Martinez-Lopez, J. (2016). Novel treatment strategy with autologous activated and expanded natural killer cells plus anti-myeloma drugs for multiple myeloma. *Oncoimmunology* 5, e1250051. 10.1080/2162402X.2016.1250051.
  91. Zhao, X., Cai, L., Hu, Y., and Wang, H. (2020). Cord-Blood Natural Killer Cell-Based Immunotherapy for Cancer. *Front Immunol* 11, 584099. 10.3389/fimmu.2020.584099.
  92. Goldenson, B.H., Hor, P., and Kaufman, D.S. (2022). iPSC-Derived Natural Killer Cell Therapies - Expansion and Targeting. *Front Immunol* 13, 841107. 10.3389/fimmu.2022.841107.
  93. Laskowski, T.J., Biederstadt, A., and Rezvani, K. (2022). Natural killer cells in antitumour adoptive cell immunotherapy. *Nat Rev Cancer* 22, 557-575. 10.1038/s41568-022-00491-0.
  94. Ziblat, A., Iraolagoitia, X.L.R., Nunez, S.Y., Torres, N.I., Secchiari, F., Sierra, J.M., Spallanzani, R.G., Rovegno, A., Secin, F.P., Fuertes, M.B., Domaica, C.I., et al. (2021). Circulating and Tumor-Infiltrating NK Cells From Clear Cell Renal Cell Carcinoma Patients Exhibit a Predominantly Inhibitory Phenotype Characterized by Overexpression of CD85j, CD45, CD48 and PD-1. *Front Immunol* 12, 681615. 10.3389/fimmu.2021.681615.
  95. Jacobson, A., Bell, F., Lejarcegui, N., Mitchell, C., Frenkel, L., and Horton, H. (2013). Healthy Neonates Possess a CD56-Negative NK Cell Population with Reduced Anti-Viral Activity. *PLoS One* 8, e67700. 10.1371/journal.pone.0067700.
  96. Baek, H.J., Kim, D.W., Phan, M.T., Kim, J.S., Yang, J.H., Choi, J.I., Lee, J.J., Shin, M.G., Ryang, D.W., Kim, S.K., Lee, S.H., et al. (2015). Comparison of FcRgamma-Deficient and CD57+ Natural Killer Cells Between Cord Blood and Adult Blood in the Cytomegalovirus-Endemic Korean Population. *Ann Lab Med* 35, 423-428. 10.3343/alm.2015.35.4.423.
  97. Dalle, J.H., Menezes, J., Wagner, E., Blagdon, M., Champagne, J., Champagne, M.A., and Duval, M. (2005). Characterization of cord blood natural killer cells: implications for transplantation and neonatal infections. *Pediatr Res* 57, 649-655. 10.1203/01.PDR.0000156501.55431.20.
  98. Wang, Y., Xu, H., Zheng, X., Wei, H., Sun, R., and Tian, Z. (2007). High expression of NKG2A/CD94 and low expression of granzyme B are associated with reduced cord blood NK cell activity. *Cell Mol Immunol* 4, 377-382.
  99. Liu, E., Marin, D., Banerjee, P., Macapinlac, H.A., Thompson, P., Basar, R., Nassif Kerbauy, L., Overman, B., Thall, P., Kaplan, M., Nandivada, V., et al. (2020). Use of CAR-Transduced Natural Killer Cells in CD19-Positive Lymphoid Tumors. *N Engl J Med* 382, 545-553. 10.1056/NEJMoa1910607.

100. Zhu, H., and Kaufman, D.S. (2019). An Improved Method to Produce Clinical-Scale Natural Killer Cells from Human Pluripotent Stem Cells. *Methods Mol Biol* *2048*, 107-119. 10.1007/978-1-4939-9728-2\_12.
101. Guedan, S., Calderon, H., Posey, A.D., Jr., and Maus, M.V. (2019). Engineering and Design of Chimeric Antigen Receptors. *Mol Ther Methods Clin Dev* *12*, 145-156. 10.1016/j.omtm.2018.12.009.
102. Kuwana, Y., Asakura, Y., Utsunomiya, N., Nakanishi, M., Arata, Y., Itoh, S., Nagase, F., and Kurosawa, Y. (1987). Expression of chimeric receptor composed of immunoglobulin-derived V regions and T-cell receptor-derived C regions. *Biochem Biophys Res Commun* *149*, 960-968. 10.1016/0006-291x(87)90502-x.
103. Mitra, A., Barua, A., Huang, L., Ganguly, S., Feng, Q., and He, B. (2023). From bench to bedside: the history and progress of CAR T cell therapy. *Front Immunol* *14*, 1188049. 10.3389/fimmu.2023.1188049.
104. Eshhar, Z., Waks, T., Gross, G., and Schindler, D.G. (1993). Specific activation and targeting of cytotoxic lymphocytes through chimeric single chains consisting of antibody-binding domains and the gamma or zeta subunits of the immunoglobulin and T-cell receptors. *Proc Natl Acad Sci U S A* *90*, 720-724. 10.1073/pnas.90.2.720.
105. Hwu, P., Shafer, G.E., Treisman, J., Schindler, D.G., Gross, G., Cowherd, R., Rosenberg, S.A., and Eshhar, Z. (1993). Lysis of ovarian cancer cells by human lymphocytes redirected with a chimeric gene composed of an antibody variable region and the Fc receptor gamma chain. *J Exp Med* *178*, 361-366. 10.1084/jem.178.1.361.
106. Krause, A., Guo, H.F., Latouche, J.B., Tan, C., Cheung, N.K., and Sadelain, M. (1998). Antigen-dependent CD28 signaling selectively enhances survival and proliferation in genetically modified activated human primary T lymphocytes. *J Exp Med* *188*, 619-626. 10.1084/jem.188.4.619.
107. Maher, J., Brentjens, R.J., Gunset, G., Riviere, I., and Sadelain, M. (2002). Human T-lymphocyte cytotoxicity and proliferation directed by a single chimeric TCRzeta/CD28 receptor. *Nat Biotechnol* *20*, 70-75. 10.1038/nbt0102-70.
108. Finney, H.M., Akbar, A.N., and Lawson, A.D. (2004). Activation of resting human primary T cells with chimeric receptors: costimulation from CD28, inducible costimulator, CD134, and CD137 in series with signals from the TCR zeta chain. *J Immunol* *172*, 104-113. 10.4049/jimmunol.172.1.104.
109. Goyco Vera, D., Waghela, H., Nuh, M., Pan, J., and Lulla, P. (2024). Approved CAR-T therapies have reproducible efficacy and safety in clinical practice. *Hum Vaccin Immunother* *20*, 2378543. 10.1080/21645515.2024.2378543.
110. Kisielow, P. (2019). How does the immune system learn to distinguish between good and evil? The first definitive studies of T cell central tolerance and positive selection. *Immunogenetics* *71*, 513-518. 10.1007/s00251-019-01127-8.

111. Rosenberg, J., and Huang, J. (2018). CD8(+) T Cells and NK Cells: Parallel and Complementary Soldiers of Immunotherapy. *Curr Opin Chem Eng* *19*, 9-20. 10.1016/j.coche.2017.11.006.
112. Imamura, M., Hashino, S., and Tanaka, J. (1996). Graft-versus-leukemia effect and its clinical implications. *Leuk Lymphoma* *23*, 477-492. 10.3109/10428199609054857.
113. Mailankody, S., Matous, J.V., Chhabra, S., Liedtke, M., Sidana, S., Oluwole, O.O., Malik, S., Nath, R., Anwer, F., Cruz, J.C., Htut, M., et al. (2023). Allogeneic BCMA-targeting CAR T cells in relapsed/refractory multiple myeloma: phase 1 UNIVERSAL trial interim results. *Nat Med* *29*, 422-429. 10.1038/s41591-022-02182-7.
114. Norelli, M., Camisa, B., Barbiera, G., Falcone, L., Purevdorj, A., Genua, M., Sanvito, F., Ponzoni, M., Doglioni, C., Cristofori, P., Traversari, C., et al. (2018). Monocyte-derived IL-1 and IL-6 are differentially required for cytokine-release syndrome and neurotoxicity due to CAR T cells. *Nat Med* *24*, 739-748. 10.1038/s41591-018-0036-4.
115. Kotch, C., Barrett, D., and Teachey, D.T. (2019). Tocilizumab for the treatment of chimeric antigen receptor T cell-induced cytokine release syndrome. *Expert Rev Clin Immunol* *15*, 813-822. 10.1080/1744666X.2019.1629904.
116. Strati, P., Ahmed, S., Kebriaei, P., Nastoupil, L.J., Claussen, C.M., Watson, G., Horowitz, S.B., Brown, A.R.T., Do, B., Rodriguez, M.A., Nair, R., et al. (2020). Clinical efficacy of anakinra to mitigate CAR T-cell therapy-associated toxicity in large B-cell lymphoma. *Blood Adv* *4*, 3123-3127. 10.1182/bloodadvances.2020002328.
117. Parker, K.R., Migliorini, D., Perkey, E., Yost, K.E., Bhaduri, A., Bagga, P., Haris, M., Wilson, N.E., Liu, F., Gabunia, K., Scholler, J., et al. (2020). Single-Cell Analyses Identify Brain Mural Cells Expressing CD19 as Potential Off-Tumor Targets for CAR-T Immunotherapies. *Cell* *183*, 126-142 e117. 10.1016/j.cell.2020.08.022.
118. McComb, S., Nguyen, T., Shepherd, A., Henry, K.A., Bloemberg, D., Marcil, A., Maclean, S., Zafer, A., Gilbert, R., Gadoury, C., Pon, R.A., et al. (2022). Programmable Attenuation of Antigenic Sensitivity for a Nanobody-Based EGFR Chimeric Antigen Receptor Through Hinge Domain Truncation. *Front Immunol* *13*, 864868. 10.3389/fimmu.2022.864868.
119. Castellanos-Rueda, R., Di Roberto, R.B., Bieberich, F., Schlatter, F.S., Palianina, D., Nguyen, O.T.P., Kapetanovic, E., Laubli, H., Hierlemann, A., Khanna, N., and Reddy, S.T. (2022). speedingCARs: accelerating the engineering of CAR T cells by signaling domain shuffling and single-cell sequencing. *Nat Commun* *13*, 6555. 10.1038/s41467-022-34141-8.
120. Marin, D., Li, Y., Basar, R., Rafei, H., Daher, M., Dou, J., Mohanty, V., Dede, M., Nieto, Y., Uprety, N., Acharya, S., et al. (2024). Safety, efficacy and determinants of response of allogeneic CD19-specific CAR-NK cells in CD19(+) B cell tumors: a phase 1/2 trial. *Nat Med* *30*, 772-784. 10.1038/s41591-023-02785-8.

121. Ghobadi, A., Bachanova, V., Patel, K., Park, J.H., Flinn, I., Riedell, P.A., Bachier, C., Diefenbach, C.S., Wong, C., Bickers, C., Wong, L., et al. (2025). Induced pluripotent stem-cell-derived CD19-directed chimeric antigen receptor natural killer cells in B-cell lymphoma: a phase 1, first-in-human trial. *Lancet* *405*, 127-136. 10.1016/S0140-6736(24)02462-0.
122. Shi, Y., Hao, D., Qian, H., and Tao, Z. (2024). Natural killer cell-based cancer immunotherapy: from basics to clinical trials. *Exp Hematol Oncol* *13*, 101. 10.1186/s40164-024-00561-z.
123. Ghosh, S., Brown, A.M., Jenkins, C., and Campbell, K. (2020). Viral Vector Systems for Gene Therapy: A Comprehensive Literature Review of Progress and Biosafety Challenges. *Appl Biosaf* *25*, 7-18. 10.1177/1535676019899502.
124. Labbe, R.P., Vessillier, S., and Rafiq, Q.A. (2021). Lentiviral Vectors for T Cell Engineering: Clinical Applications, Bioprocessing and Future Perspectives. *Viruses* *13*. 10.3390/v13081528.
125. Schmidt, P., Raftery, M.J., and Pecher, G. (2020). Engineering NK Cells for CAR Therapy-Recent Advances in Gene Transfer Methodology. *Front Immunol* *11*, 611163. 10.3389/fimmu.2020.611163.
126. Sutlu, T., Nystrom, S., Gilljam, M., Stellan, B., Applequist, S.E., and Alici, E. (2012). Inhibition of intracellular antiviral defense mechanisms augments lentiviral transduction of human natural killer cells: implications for gene therapy. *Hum Gene Ther* *23*, 1090-1100. 10.1089/hum.2012.080.
127. Chockley, P., Patil, S.L., and Gottschalk, S. (2021). Transient blockade of TBK1/IKKepsilon allows efficient transduction of primary human natural killer cells with vesicular stomatitis virus G-pseudotyped lentiviral vectors. *Cytotherapy* *23*, 787-792. 10.1016/j.jcyt.2021.04.010.
128. Bari, R., Granzin, M., Tsang, K.S., Roy, A., Krueger, W., Orentas, R., Schneider, D., Pfeifer, R., Moeker, N., Verhoeyen, E., Dropulic, B., et al. (2019). A Distinct Subset of Highly Proliferative and Lentiviral Vector (LV)-Transducible NK Cells Define a Readily Engineered Subset for Adoptive Cellular Therapy. *Front Immunol* *10*, 2001. 10.3389/fimmu.2019.02001.
129. Roche, S., Albertini, A.A., Lepault, J., Bressanelli, S., and Gaudin, Y. (2008). Structures of vesicular stomatitis virus glycoprotein: membrane fusion revisited. *Cell Mol Life Sci* *65*, 1716-1728. 10.1007/s00018-008-7534-3.
130. Nikolic, J., Belot, L., Raux, H., Legrand, P., Gaudin, Y., and A, A.A. (2018). Structural basis for the recognition of LDL-receptor family members by VSV glycoprotein. *Nat Commun* *9*, 1029. 10.1038/s41467-018-03432-4.
131. Amirache, F., Levy, C., Costa, C., Mangeot, P.E., Torbett, B.E., Wang, C.X., Negre, D., Cosset, F.L., and Verhoeyen, E. (2014). Mystery solved: VSV-G-LVs do not allow efficient gene transfer into unstimulated T cells, B cells, and HSCs because they lack the LDL receptor. *Blood* *123*, 1422-1424. 10.1182/blood-2013-11-540641.

132. Hu, K. (2014). All roads lead to induced pluripotent stem cells: the technologies of iPSC generation. *Stem Cells Dev* 23, 1285-1300. 10.1089/scd.2013.0620.
133. Abbasalipour, M., Khosravi, M.A., Zeinali, S., Khanahmad, H., Karimipoor, M., and Azadmanesh, K. (2019). Improvement of K562 Cell Line Transduction by FBS Mediated Attachment to the Cell Culture Plate. *Biomed Res Int* 2019, 9540702. 10.1155/2019/9540702.
134. Gong, Y., Klein Wolterink, R.G.J., Janssen, I., Groot, A.J., Bos, G.M.J., and Germeraad, W.T.V. (2020). Rosuvastatin Enhances VSV-G Lentiviral Transduction of NK Cells via Upregulation of the Low-Density Lipoprotein Receptor. *Mol Ther Methods Clin Dev* 17, 634-646. 10.1016/j.omtm.2020.03.017.
135. Girard-Gagnepain, A., Amirache, F., Costa, C., Levy, C., Frecha, C., Fusil, F., Negre, D., Lavillette, D., Cosset, F.L., and Verhoeyen, E. (2014). Baboon envelope pseudotyped LVs outperform VSV-G-LVs for gene transfer into early-cytokine-stimulated and resting HSCs. *Blood* 124, 1221-1231. 10.1182/blood-2014-02-558163.
136. Colamartino, A.B.L., Lemieux, W., Bifsha, P., Nicoletti, S., Chakravarti, N., Sanz, J., Romero, H., Selleri, S., Beland, K., Guiot, M., Tremblay-Laganiere, C., et al. (2019). Efficient and Robust NK-Cell Transduction With Baboon Envelope Pseudotyped Lentivector. *Front Immunol* 10, 2873. 10.3389/fimmu.2019.02873.
137. Jo, D.H., Kaczmarek, S., Shin, O., Wang, L., Cowan, J., McComb, S., and Lee, S.H. (2023). Simultaneous engineering of natural killer cells for CAR transgenesis and CRISPR-Cas9 knockout using retroviral particles. *Mol Ther Methods Clin Dev* 29, 173-184. 10.1016/j.omtm.2023.03.006.
138. Guo, S., Lei, W., Jin, X., Liu, H., Wang, J.Q., Deng, W., and Qian, W. (2024). CD70-specific CAR NK cells expressing IL-15 for the treatment of CD19-negative B-cell malignancy. *Blood Adv* 8, 2635-2645. 10.1182/bloodadvances.2023012202.
139. Guo, C., Chen, H., Yu, J., Lu, H., Xia, Q., Li, X., Guo, X., Wang, T., Zhi, L., Niu, Z., and Zhu, W. (2023). Engagement of an optimized lentiviral vector enhances the expression and cytotoxicity of CAR in human NK cells. *Mol Immunol* 155, 91-99. 10.1016/j.molimm.2023.01.010.
140. Balka, K.R., Louis, C., Saunders, T.L., Smith, A.M., Calleja, D.J., D'Silva, D.B., Moghaddas, F., Tailler, M., Lawlor, K.E., Zhan, Y., Burns, C.J., et al. (2020). TBK1 and IKKepsilon Act Redundantly to Mediate STING-Induced NF-kappaB Responses in Myeloid Cells. *Cell Rep* 31, 107492. 10.1016/j.celrep.2020.03.056.
141. de Rham, C., Ferrari-Lacraz, S., Jendly, S., Schneiter, G., Dayer, J.M., and Villard, J. (2007). The proinflammatory cytokines IL-2, IL-15 and IL-21 modulate the repertoire of mature human natural killer cell receptors. *Arthritis Res Ther* 9, R125. 10.1186/ar2336.
142. Choi, Y.H., Lim, E.J., Kim, S.W., Moon, Y.W., Park, K.S., and An, H.J. (2019). IL-27 enhances IL-15/IL-18-mediated activation of human natural killer cells. *J Immunother Cancer* 7, 168. 10.1186/s40425-019-0652-7.

143. Imai, C., Iwamoto, S., and Campana, D. (2005). Genetic modification of primary natural killer cells overcomes inhibitory signals and induces specific killing of leukemic cells. *Blood* *106*, 376-383. 10.1182/blood-2004-12-4797.
144. Yang, Y., Badeti, S., Tseng, H.C., Ma, M.T., Liu, T., Jiang, J.G., Liu, C., and Liu, D. (2020). Superior Expansion and Cytotoxicity of Human Primary NK and CAR-NK Cells from Various Sources via Enriched Metabolic Pathways. *Mol Ther Methods Clin Dev* *18*, 428-445. 10.1016/j.omtm.2020.06.014.
145. Lapteva, N., Durett, A.G., Sun, J., Rollins, L.A., Huye, L.L., Fang, J., Dandekar, V., Mei, Z., Jackson, K., Vera, J., Ando, J., et al. (2012). Large-scale *ex vivo* expansion and characterization of natural killer cells for clinical applications. *Cytotherapy* *14*, 1131-1143. 10.3109/14653249.2012.700767.
146. Denman, C.J., Senyukov, V.V., Somanchi, S.S., Phatarpekar, P.V., Kopp, L.M., Johnson, J.L., Singh, H., Hurton, L., Maiti, S.N., Huls, M.H., Champlin, R.E., et al. (2012). Membrane-bound IL-21 promotes sustained *ex vivo* proliferation of human natural killer cells. *PLoS One* *7*, e30264. 10.1371/journal.pone.0030264.
147. Blache, U., Popp, G., Dunkel, A., Koehl, U., and Fricke, S. (2022). Potential solutions for manufacture of CAR T cells in cancer immunotherapy. *Nat Commun* *13*, 5225. 10.1038/s41467-022-32866-0.
148. Saultz, J.N., and Otegbeye, F. (2023). Optimizing the cryopreservation and post-thaw recovery of natural killer cells is critical for the success of off-the-shelf platforms. *Front Immunol* *14*, 1304689. 10.3389/fimmu.2023.1304689.
149. Damodharan, S.N., Walker, K.L., Forsberg, M.H., McDowell, K.A., Bouchlaka, M.N., Drier, D.A., Sondel, P.M., DeSantes, K.B., and Capitini, C.M. (2020). Analysis of *ex vivo* expanded and activated clinical-grade human NK cells after cryopreservation. *Cytotherapy* *22*, 450-457. 10.1016/j.jcyt.2020.05.001.
150. Berjis, A., Muthumani, D., Aguilar, O.A., Pomp, O., Johnson, O., Finck, A.V., Engel, N.W., Chen, L., Plachta, N., Scholler, J., Lanier, L.L., et al. (2024). Pretreatment with IL-15 and IL-18 rescues natural killer cells from granzyme B-mediated apoptosis after cryopreservation. *Nat Commun* *15*, 3937. 10.1038/s41467-024-47574-0.
151. Mali, P., Yang, L., Esvelt, K.M., Aach, J., Guell, M., DiCarlo, J.E., Norville, J.E., and Church, G.M. (2013). RNA-guided human genome engineering via Cas9. *Science* *339*, 823-826. 10.1126/science.1232033.
152. Cong, L., Ran, F.A., Cox, D., Lin, S., Barretto, R., Habib, N., Hsu, P.D., Wu, X., Jiang, W., Marraffini, L.A., and Zhang, F. (2013). Multiplex genome engineering using CRISPR/Cas systems. *Science* *339*, 819-823. 10.1126/science.1231143.
153. Jinek, M., East, A., Cheng, A., Lin, S., Ma, E., and Doudna, J. (2013). RNA-programmed genome editing in human cells. *Elife* *2*, e00471. 10.7554/eLife.00471.
154. Hwang, W.Y., Fu, Y., Reyon, D., Maeder, M.L., Tsai, S.Q., Sander, J.D., Peterson, R.T., Yeh, J.R., and Joung, J.K. (2013). Efficient genome editing in zebrafish using a CRISPR-Cas system. *Nat Biotechnol* *31*, 227-229. 10.1038/nbt.2501.

155. Cho, S.W., Kim, S., Kim, J.M., and Kim, J.S. (2013). Targeted genome engineering in human cells with the Cas9 RNA-guided endonuclease. *Nat Biotechnol* *31*, 230-232. 10.1038/nbt.2507.
156. Pacesa, M., Pelea, O., and Jinek, M. (2024). Past, present, and future of CRISPR genome editing technologies. *Cell* *187*, 1076-1100. 10.1016/j.cell.2024.01.042.
157. Rodgers, K., and McVey, M. (2016). Error-Prone Repair of DNA Double-Strand Breaks. *J Cell Physiol* *231*, 15-24. 10.1002/jcp.25053.
158. Qi, L.S., Larson, M.H., Gilbert, L.A., Doudna, J.A., Weissman, J.S., Arkin, A.P., and Lim, W.A. (2021). Repurposing CRISPR as an RNA-guided platform for sequence-specific control of gene expression. *Cell* *184*, 844. 10.1016/j.cell.2021.01.019.
159. Perez-Pinera, P., Kocak, D.D., Vockley, C.M., Adler, A.F., Kabadi, A.M., Polstein, L.R., Thakore, P.I., Glass, K.A., Ousterout, D.G., Leong, K.W., Guilak, F., et al. (2013). RNA-guided gene activation by CRISPR-Cas9-based transcription factors. *Nat Methods* *10*, 973-976. 10.1038/nmeth.2600.
160. Ma, Y., Yu, L., Zhang, X., Xin, C., Huang, S., Bai, L., Chen, W., Gao, R., Li, J., Pan, S., Qi, X., et al. (2018). Highly efficient and precise base editing by engineered dCas9-guide tRNA adenosine deaminase in rats. *Cell Discov* *4*, 39. 10.1038/s41421-018-0047-9.
161. Kwon, D.Y., Zhao, Y.T., Lamonica, J.M., and Zhou, Z. (2017). Locus-specific histone deacetylation using a synthetic CRISPR-Cas9-based HDAC. *Nat Commun* *8*, 15315. 10.1038/ncomms15315.
162. Brandow, A.M., and Liem, R.I. (2022). Advances in the diagnosis and treatment of sickle cell disease. *J Hematol Oncol* *15*, 20. 10.1186/s13045-022-01237-z.
163. Wu, Y., Zeng, J., Roscoe, B.P., Liu, P., Yao, Q., Lazzarotto, C.R., Clement, K., Cole, M.A., Luk, K., Baricordi, C., Shen, A.H., et al. (2019). Highly efficient therapeutic gene editing of human hematopoietic stem cells. *Nat Med* *25*, 776-783. 10.1038/s41591-019-0401-y.
164. Gorur, V., Kranc, K.R., Ganuza, M., and Telfer, P. (2024). Haematopoietic stem cell health in sickle cell disease and its implications for stem cell therapies and secondary haematological disorders. *Blood Rev* *63*, 101137. 10.1016/j.blre.2023.101137.
165. Sankaran, V.G., Menne, T.F., Xu, J., Akie, T.E., Lettre, G., Van Handel, B., Mikkola, H.K., Hirschhorn, J.N., Cantor, A.B., and Orkin, S.H. (2008). Human fetal hemoglobin expression is regulated by the developmental stage-specific repressor BCL11A. *Science* *322*, 1839-1842. 10.1126/science.1165409.
166. Lettre, G., and Bauer, D.E. (2016). Fetal haemoglobin in sickle-cell disease: from genetic epidemiology to new therapeutic strategies. *Lancet* *387*, 2554-2564. 10.1016/S0140-6736(15)01341-0.
167. Philippidis, A. (2024). CASGEVY Makes History as FDA Approves First CRISPR/Cas9 Genome Edited Therapy. *Hum Gene Ther* *35*, 1-4. 10.1089/hum.2023.29263.bfs.

168. Huang, R.S., Shih, H.A., Lai, M.C., Chang, Y.J., and Lin, S. (2020). Enhanced NK-92 Cytotoxicity by CRISPR Genome Engineering Using Cas9 Ribonucleoproteins. *Front Immunol* *11*, 1008. 10.3389/fimmu.2020.01008.
169. Huang, R.S., Lai, M.C., Shih, H.A., and Lin, S. (2021). A robust platform for expansion and genome editing of primary human natural killer cells. *J Exp Med* *218*. 10.1084/jem.20201529.
170. Naeimi Kararoudi, M., Nagai, Y., Elmas, E., de Souza Fernandes Pereira, M., Ali, S.A., Imus, P.H., Wethington, D., Borrello, I.M., Lee, D.A., and Ghiaur, G. (2020). CD38 deletion of human primary NK cells eliminates daratumumab-induced fratricide and boosts their effector activity. *Blood* *136*, 2416-2427. 10.1182/blood.2020006200.
171. Hasan, M.F., Campbell, A.R., Croom-Perez, T.J., Oyer, J.L., Dieffenthaler, T.A., Robles-Carrillo, L.D., Cash, C.A., Eloriaga, J.E., Kumar, S., Andersen, B.W., Naeimi Kararoudi, M., et al. (2023). Knockout of the inhibitory receptor TIGIT enhances the antitumor response of *ex vivo* expanded NK cells and prevents fratricide with therapeutic Fc-active TIGIT antibodies. *J Immunother Cancer* *11*. 10.1136/jitc-2023-007502.
172. Zhu, H., Blum, R.H., Bernareggi, D., Ask, E.H., Wu, Z., Hoel, H.J., Meng, Z., Wu, C., Guan, K.L., Malmberg, K.J., and Kaufman, D.S. (2020). Metabolic Reprogramming via Deletion of CISH in Human iPSC-Derived NK Cells Promotes *In Vivo* Persistence and Enhances Anti-tumor Activity. *Cell Stem Cell* *27*, 224-237 e226. 10.1016/j.stem.2020.05.008.
173. Qin, Y., Cui, Q., Sun, G., Chao, J., Wang, C., Chen, X., Ye, P., Zhou, T., Jeyachandran, A.V., Sun, O., Liu, W., et al. (2024). Developing enhanced immunotherapy using NKG2A knockout human pluripotent stem cell-derived NK cells. *Cell Rep* *43*, 114867. 10.1016/j.celrep.2024.114867.
174. Tariq, H., Batool, S., Asif, S., Ali, M., and Abbasi, B.H. (2021). Virus-Like Particles: Revolutionary Platforms for Developing Vaccines Against Emerging Infectious Diseases. *Front Microbiol* *12*, 790121. 10.3389/fmicb.2021.790121.
175. Gupta, R., Arora, K., Roy, S.S., Joseph, A., Rastogi, R., Arora, N.M., and Kundu, P.K. (2023). Platforms, advances, and technical challenges in virus-like particles-based vaccines. *Front Immunol* *14*, 1123805. 10.3389/fimmu.2023.1123805.
176. Nooraei, S., Bahrulolum, H., Hoseini, Z.S., Katalani, C., Hajizade, A., Easton, A.J., and Ahmadian, G. (2021). Virus-like particles: preparation, immunogenicity and their roles as nanovaccines and drug nanocarriers. *J Nanobiotechnology* *19*, 59. 10.1186/s12951-021-00806-7.
177. Unti, M.J., and Jaffrey, S.R. (2024). Highly efficient cellular expression of circular mRNA enables prolonged protein expression. *Cell Chem Biol* *31*, 163-176 e165. 10.1016/j.chembiol.2023.09.015.
178. Mangeot, P.E., Risson, V., Fusil, F., Marnef, A., Laurent, E., Blin, J., Mournetas, V., Massourides, E., Sohier, T.J.M., Corbin, A., Aube, F., et al. (2019). Genome editing

- in primary cells and *in vivo* using viral-derived Nanoblades loaded with Cas9-sgRNA ribonucleoproteins. *Nat Commun* *10*, 45. 10.1038/s41467-018-07845-z.
179. He, J., Yu, L., Lin, X., Liu, X., Zhang, Y., Yang, F., and Deng, W. (2022). Virus-like Particles as Nanocarriers for Intracellular Delivery of Biomolecules and Compounds. *Viruses* *14*. 10.3390/v14091905.
  180. Hamilton, J.R., Chen, E., Perez, B.S., Sandoval Espinoza, C.R., Kang, M.H., Trinidad, M., Ngo, W., and Doudna, J.A. (2024). *In vivo* human T cell engineering with enveloped delivery vehicles. *Nat Biotechnol* *42*, 1684-1692. 10.1038/s41587-023-02085-z.
  181. Gutierrez-Guerrero, A., Abrey Recalde, M.J., Mangeot, P.E., Costa, C., Bernadin, O., Perian, S., Fusil, F., Froment, G., Martinez-Turtos, A., Krug, A., Martin, F., et al. (2021). Baboon Envelope Pseudotyped "Nanoblades" Carrying Cas9/gRNA Complexes Allow Efficient Genome Editing in Human T, B, and CD34(+) Cells and Knock-in of AAV6-Encoded Donor DNA in CD34(+) Cells. *Front Genome Ed* *3*, 604371. 10.3389/fgeed.2021.604371.
  182. Tiroille, V., Krug, A., Bokobza, E., Kahi, M., Bulcaen, M., Ensinck, M.M., Geurts, M.H., Hendriks, D., Vermeulen, F., Larbret, F., Gutierrez-Guerrero, A., et al. (2023). Nanoblades allow high-level genome editing in murine and human organoids. *Mol Ther Nucleic Acids* *33*, 57-74. 10.1016/j.omtn.2023.06.004.
  183. Jaenisch, R., and Bird, A. (2003). Epigenetic regulation of gene expression: how the genome integrates intrinsic and environmental signals. *Nat Genet* *33 Suppl*, 245-254. 10.1038/ng1089.
  184. Shi, M.Q., Xu, Y., Fu, X., Pan, D.S., Lu, X.P., Xiao, Y., and Jiang, Y.Z. (2024). Advances in targeting histone deacetylase for treatment of solid tumors. *J Hematol Oncol* *17*, 37. 10.1186/s13045-024-01551-8.
  185. Moran, B., Davern, M., Reynolds, J.V., Donlon, N.E., and Lysaght, J. (2023). The impact of histone deacetylase inhibitors on immune cells and implications for cancer therapy. *Cancer Lett* *559*, 216121. 10.1016/j.canlet.2023.216121.
  186. Schneider, A., Chatterjee, S., Bousiges, O., Selvi, B.R., Swaminathan, A., Cassel, R., Blanc, F., Kundu, T.K., and Boutillier, A.L. (2013). Acetyltransferases (HATs) as targets for neurological therapeutics. *Neurotherapeutics* *10*, 568-588. 10.1007/s13311-013-0204-7.
  187. Brown, C.E., Lechner, T., Howe, L., and Workman, J.L. (2000). The many HATs of transcription coactivators. *Trends Biochem Sci* *25*, 15-19. 10.1016/s0968-0004(99)01516-9.
  188. Milazzo, G., Mercatelli, D., Di Muzio, G., Triboli, L., De Rosa, P., Perini, G., and Giorgi, F.M. (2020). Histone Deacetylases (HDACs): Evolution, Specificity, Role in Transcriptional Complexes, and Pharmacological Actionability. *Genes (Basel)* *11*. 10.3390/genes11050556.

189. Kang, M.A., Kim, M.S., Kim, J.Y., Shin, Y.J., Song, J.Y., and Jeong, J.H. (2015). A novel pyrido-thieno-pyrimidine derivative activates p53 through induction of phosphorylation and acetylation in colorectal cancer cells. *Int J Oncol* *46*, 342-350. 10.3892/ijo.2014.2720.
190. Ling, R., Wang, J., Fang, Y., Yu, Y., Su, Y., Sun, W., Li, X., and Tang, X. (2023). HDAC-an important target for improving tumor radiotherapy resistance. *Front Oncol* *13*, 1193637. 10.3389/fonc.2023.1193637.
191. Jokinen, R., Pirnes-Karhu, S., Pietilainen, K.H., and Pirinen, E. (2017). Adipose tissue NAD(+)-homeostasis, sirtuins and poly(ADP-ribose) polymerases -important players in mitochondrial metabolism and metabolic health. *Redox Biol* *12*, 246-263. 10.1016/j.redox.2017.02.011.
192. Moertl, S., Payer, S., Kell, R., Winkler, K., Anastasov, N., and Atkinson, M.J. (2019). Comparison of Radiosensitization by HDAC Inhibitors CUDC-101 and SAHA in Pancreatic Cancer Cells. *Int J Mol Sci* *20*. 10.3390/ijms20133259.
193. Fan, Y., Jia, X., Xie, T., Zhu, L., and He, F. (2020). Radiosensitizing effects of c-myc gene knockdown-induced G2/M phase arrest by intrinsic stimuli via the mitochondrial signaling pathway. *Oncol Rep* *44*, 2669-2677. 10.3892/or.2020.7806.
194. Cho, H., Son, W.C., Lee, Y.S., Youn, E.J., Kang, C.D., Park, Y.S., and Bae, J. (2021). Differential Effects of Histone Deacetylases on the Expression of NKG2D Ligands and NK Cell-Mediated Anticancer Immunity in Lung Cancer Cells. *Molecules* *26*. 10.3390/molecules26133952.
195. Ni, L., Wang, L., Yao, C., Ni, Z., Liu, F., Gong, C., Zhu, X., Yan, X., Watowich, S.S., Lee, D.A., and Zhu, S. (2017). The histone deacetylase inhibitor valproic acid inhibits NKG2D expression in natural killer cells through suppression of STAT3 and HDAC3. *Sci Rep* *7*, 45266. 10.1038/srep45266.
196. Yan, X., Chen, D., Wang, Y., Guo, Y., Tong, C., Wei, J., Zhang, Y., Wu, Z., and Han, W. (2022). Identification of NOXA as a pivotal regulator of resistance to CAR T-cell therapy in B-cell malignancies. *Signal Transduct Target Ther* *7*, 98. 10.1038/s41392-022-00915-1.
197. Liu, Y.F., Chiang, Y., Hsu, F.M., Tsai, C.L., and Cheng, J.C. (2022). Radiosensitization effect by HDAC inhibition improves NKG2D-dependent natural killer cytotoxicity in hepatocellular carcinoma. *Front Oncol* *12*, 1009089. 10.3389/fonc.2022.1009089.
198. Rossi, L.E., Avila, D.E., Spallanzani, R.G., Ziblat, A., Fuertes, M.B., Lapyckyj, L., Croci, D.O., Rabinovich, G.A., Domaica, C.I., and Zwirner, N.W. (2012). Histone deacetylase inhibitors impair NK cell viability and effector functions through inhibition of activation and receptor expression. *J Leukoc Biol* *91*, 321-331. 10.1189/jlb.0711339.
199. Soria-Castro, R., Chavez-Blanco, A.D., Garcia-Perez, B.E., Wong-Baeza, I., Flores-Mejia, R., Flores-Borja, F., Estrada-Parra, S., Estrada-Garcia, I., Serafin-Lopez, J., and Chacon-Salinas, R. (2020). Valproic acid inhibits interferon-gamma production

- by NK cells and increases susceptibility to *Listeria monocytogenes* infection. *Sci Rep* *10*, 17802. 10.1038/s41598-020-74836-w.
200. Okada, T., Uchibori, R., Iwata-Okada, M., Takahashi, M., Nomoto, T., Nonaka-Sarukawa, M., Ito, T., Liu, Y., Mizukami, H., Kume, A., Kobayashi, E., et al. (2006). A histone deacetylase inhibitor enhances recombinant adeno-associated virus-mediated gene expression in tumor cells. *Mol Ther* *13*, 738-746. 10.1016/j.ymthe.2005.11.010.
  201. Danielsson, A., Dzojic, H., Rashkova, V., Cheng, W.S., and Essand, M. (2011). The HDAC inhibitor FK228 enhances adenoviral transgene expression by a transduction-independent mechanism but does not increase adenovirus replication. *PLoS One* *6*, e14700. 10.1371/journal.pone.0014700.
  202. Azcona, M.S.R., and Mussolino, C. (2024). Protocol for Efficient Generation of Chimeric Antigen Receptor T Cells with Multiplexed Gene Silencing by Epigenome Editing. *Methods Mol Biol* *2842*, 209-223. 10.1007/978-1-0716-4051-7\_11.
  203. Gurney, M., Stikvoort, A., Nolan, E., Kirkham-McCarthy, L., Khoruzhenko, S., Shivakumar, R., Zweegman, S., Van de Donk, N., Mutis, T., Szegezdi, E., Sarkar, S., et al. (2022). CD38 knockout natural killer cells expressing an affinity optimized CD38 chimeric antigen receptor successfully target acute myeloid leukemia with reduced effector cell fratricide. *Haematologica* *107*, 437-445. 10.3324/haematol.2020.271908.
  204. Moore, T.V., Scurti, G.M., DeJong, M., Wang, S.Y., Dalheim, A.V., Wagner, C.R., Hutchens, K.A., Speiser, J.J., Godellas, C.V., Fountain, C., Fleiser, J., et al. (2021). HDAC inhibition prevents transgene expression downregulation and loss-of-function in T-cell-receptor-transduced T cells. *Mol Ther Oncolytics* *20*, 352-363. 10.1016/j.omto.2021.01.014.
  205. Kim, Y.E., Park, J.A., Park, S.K., Kang, H.B., Kwon, H.J., and Lee, Y. (2013). Enhancement of Transgene Expression by HDAC Inhibitors in Mouse Embryonic Stem Cells. *Dev Reprod* *17*, 379-387. 10.12717/DR.2013.17.4.379.
  206. Fan, S., Maguire, C.A., Ramirez, S.H., Bradel-Tretheway, B., Sapinoro, R., Sui, Z., Chakraborty-Sett, S., and Dewhurst, S. (2005). Valproic acid enhances gene expression from viral gene transfer vectors. *J Virol Methods* *125*, 23-33. 10.1016/j.jviromet.2004.11.023.
  207. Elmer, J.J., Christensen, M.D., Barua, S., Lehrman, J., Haynes, K.A., and Rege, K. (2016). The histone deacetylase inhibitor Entinostat enhances polymer-mediated transgene expression in cancer cell lines. *Biotechnol Bioeng* *113*, 1345-1356. 10.1002/bit.25898.
  208. Lai, M.D., Chen, C.S., Yang, C.R., Yuan, S.Y., Tsai, J.J., Tu, C.F., Wang, C.C., Yen, M.C., and Lin, C.C. (2010). An HDAC inhibitor enhances the antitumor activity of a CMV promoter-driven DNA vaccine. *Cancer Gene Ther* *17*, 203-211. 10.1038/cgt.2009.65.

209. Rafiq, S., Hackett, C.S., and Brentjens, R.J. (2020). Engineering strategies to overcome the current roadblocks in CAR T cell therapy. *Nat Rev Clin Oncol* *17*, 147-167. 10.1038/s41571-019-0297-y.
210. Roselli, E., Frieling, J.S., Thorner, K., Ramello, M.C., Lynch, C.C., and Abate-Daga, D. (2019). CAR-T Engineering: Optimizing Signal Transduction and Effector Mechanisms. *BioDrugs* *33*, 647-659. 10.1007/s40259-019-00384-z.
211. Berrien-Elliott, M.M., Jacobs, M.T., and Fehniger, T.A. (2023). Allogeneic natural killer cell therapy. *Blood* *141*, 856-868. 10.1182/blood.2022016200.
212. Guillerey, C., Huntington, N.D., and Smyth, M.J. (2016). Targeting natural killer cells in cancer immunotherapy. *Nat Immunol* *17*, 1025-1036. 10.1038/ni.3518.
213. Liu, E., Tong, Y., Dotti, G., Shaim, H., Savoldo, B., Mukherjee, M., Orange, J., Wan, X., Lu, X., Reynolds, A., Gagea, M., et al. (2018). Cord blood NK cells engineered to express IL-15 and a CD19-targeted CAR show long-term persistence and potent antitumor activity. *Leukemia* *32*, 520-531. 10.1038/leu.2017.226.
214. Shimasaki, N., Jain, A., and Campana, D. (2020). NK cells for cancer immunotherapy. *Nat Rev Drug Discov* *19*, 200-218. 10.1038/s41573-019-0052-1.
215. Daher, M., Basar, R., Gokdemir, E., Baran, N., Uprety, N., Nunez Cortes, A.K., Mendt, M., Kerbauy, L.N., Banerjee, P.P., Shanley, M., Imahashi, N., et al. (2021). Targeting a cytokine checkpoint enhances the fitness of armored cord blood CAR-NK cells. *Blood* *137*, 624-636. 10.1182/blood.2020007748.
216. Lee, S.H., Miyagi, T., and Biron, C.A. (2007). Keeping NK cells in highly regulated antiviral warfare. *Trends Immunol* *28*, 252-259. 10.1016/j.it.2007.04.001.
217. Vivier, E., Tomasello, E., Baratin, M., Walzer, T., and Ugolini, S. (2008). Functions of natural killer cells. *Nat Immunol* *9*, 503-510. 10.1038/ni1582.
218. Xiao, L., Cen, D., Gan, H., Sun, Y., Huang, N., Xiong, H., Jin, Q., Su, L., Liu, X., Wang, K., Yan, G., et al. (2019). Adoptive Transfer of NKG2D CAR mRNA-Engineered Natural Killer Cells in Colorectal Cancer Patients. *Mol Ther* *27*, 1114-1125. 10.1016/j.ymthe.2019.03.011.
219. Schaft, N. (2020). The Landscape of CAR-T Cell Clinical Trials against Solid Tumors-A Comprehensive Overview. *Cancers (Basel)* *12*. 10.3390/cancers12092567.
220. Nakajima, H., Ishikawa, Y., Furuya, M., Sano, T., Ohno, Y., Horiguchi, J., and Oyama, T. (2014). Protein expression, gene amplification, and mutational analysis of EGFR in triple-negative breast cancer. *Breast Cancer* *21*, 66-74. 10.1007/s12282-012-0354-1.
221. Hoadley, K.A., Weigman, V.J., Fan, C., Sawyer, L.R., He, X., Troester, M.A., Sartor, C.I., Rieger-House, T., Bernard, P.S., Carey, L.A., and Perou, C.M. (2007). EGFR associated expression profiles vary with breast tumor subtype. *BMC Genomics* *8*, 258. 10.1186/1471-2164-8-258.

222. Masuda, H., Zhang, D., Bartholomeusz, C., Doihara, H., Hortobagyi, G.N., and Ueno, N.T. (2012). Role of epidermal growth factor receptor in breast cancer. *Breast Cancer Res Treat* *136*, 331-345. 10.1007/s10549-012-2289-9.
223. Secq, V., Villeret, J., Fina, F., Carmassi, M., Carcopino, X., Garcia, S., Metellus, I., Boubli, L., Iovanna, J., and Charpin, C. (2014). Triple negative breast carcinoma EGFR amplification is not associated with EGFR, Kras or ALK mutations. *Br J Cancer* *110*, 1045-1052. 10.1038/bjc.2013.794.
224. Tilch, E., Seidens, T., Cocciardi, S., Reid, L.E., Byrne, D., Simpson, P.T., Vargas, A.C., Cummings, M.C., Fox, S.B., Lakhani, S.R., and Chenevix Trench, G. (2014). Mutations in EGFR, BRAF and RAS are rare in triple-negative and basal-like breast cancers from Caucasian women. *Breast Cancer Res Treat* *143*, 385-392. 10.1007/s10549-013-2798-1.
225. Portillo, A.L., Hogg, R., Poznanski, S.M., Rojas, E.A., Cashell, N.J., Hammill, J.A., Chew, M.V., Shenouda, M.M., Ritchie, T.M., Cao, Q.T., Hirota, J.A., et al. (2021). Expanded human NK cells armed with CAR uncouple potent anti-tumor activity from off-tumor toxicity against solid tumors. *iScience* *24*, 102619. 10.1016/j.isci.2021.102619.
226. Anderson, A.C., Joller, N., and Kuchroo, V.K. (2016). Lag-3, Tim-3, and TIGIT: Co-inhibitory Receptors with Specialized Functions in Immune Regulation. *Immunity* *44*, 989-1004. 10.1016/j.immuni.2016.05.001.
227. Chauvin, J.M., and Zarour, H.M. (2020). TIGIT in cancer immunotherapy. *J Immunother Cancer* *8*. 10.1136/jitc-2020-000957.
228. Okwor, C.I.A., Oh, J.S., Crawley, A.M., Cooper, C.L., and Lee, S.H. (2020). Expression of Inhibitory Receptors on T and NK Cells Defines Immunological Phenotypes of HCV Patients with Advanced Liver Fibrosis. *iScience* *23*, 101513. 10.1016/j.isci.2020.101513.
229. Johnston, R.J., Comps-Agrar, L., Hackney, J., Yu, X., Huseni, M., Yang, Y., Park, S., Javinal, V., Chiu, H., Irving, B., Eaton, D.L., et al. (2014). The immunoreceptor TIGIT regulates antitumor and antiviral CD8(+) T cell effector function. *Cancer Cell* *26*, 923-937. 10.1016/j.ccell.2014.10.018.
230. Chauvin, J.M., Pagliano, O., Fourcade, J., Sun, Z., Wang, H., Sander, C., Kirkwood, J.M., Chen, T.H., Maurer, M., Korman, A.J., and Zarour, H.M. (2015). TIGIT and PD-1 impair tumor antigen-specific CD8(+) T cells in melanoma patients. *J Clin Invest* *125*, 2046-2058. 10.1172/JCI80445.
231. Savic, N., and Schwank, G. (2016). Advances in therapeutic CRISPR/Cas9 genome editing. *Transl Res* *168*, 15-21. 10.1016/j.trsl.2015.09.008.
232. Bexte, T., Alzubi, J., Reindl, L.M., Wendel, P., Schubert, R., Salzmann-Manrique, E., von Metzler, I., Cathomen, T., and Ullrich, E. (2022). CRISPR-Cas9 based gene editing of the immune checkpoint NKG2A enhances NK cell mediated cytotoxicity against multiple myeloma. *Oncoimmunology* *11*, 2081415. 10.1080/2162402X.2022.2081415.

233. Konermann, S., Brigham, M.D., Trevino, A.E., Joung, J., Abudayyeh, O.O., Barcena, C., Hsu, P.D., Habib, N., Gootenberg, J.S., Nishimasu, H., Nureki, O., et al. (2015). Genome-scale transcriptional activation by an engineered CRISPR-Cas9 complex. *Nature* *517*, 583-588. 10.1038/nature14136.
234. Witwicka, H., Hwang, S.Y., Reyes-Gutierrez, P., Jia, H., Odgren, P.E., Donahue, L.R., Birnbaum, M.J., and Odgren, P.R. (2015). Studies of OC-STAMP in Osteoclast Fusion: A New Knockout Mouse Model, Rescue of Cell Fusion, and Transmembrane Topology. *PLoS One* *10*, e0128275. 10.1371/journal.pone.0128275.
235. Welsh, J.A., and Jones, J.C. (2020). Small Particle Fluorescence and Light Scatter Calibration Using FCM(PASS) Software. *Curr Protoc Cytom* *94*, e79. 10.1002/cpcy.79.
236. Conant, D., Hsiao, T., Rossi, N., Oki, J., Maures, T., Waite, K., Yang, J., Joshi, S., Kelso, R., Holden, K., Enzmann, B.L., et al. (2022). Inference of CRISPR Edits from Sanger Trace Data. *CRISPR J* *5*, 123-130. 10.1089/crispr.2021.0113.
237. Brittain, G.C.t., Chen, Y.Q., Martinez, E., Tang, V.A., Renner, T.M., Langlois, M.A., and Gulnik, S. (2019). A Novel Semiconductor-Based Flow Cytometer with Enhanced Light-Scatter Sensitivity for the Analysis of Biological Nanoparticles. *Sci Rep* *9*, 16039. 10.1038/s41598-019-52366-4.
238. Ran, F.A., Hsu, P.D., Wright, J., Agarwala, V., Scott, D.A., and Zhang, F. (2013). Genome engineering using the CRISPR-Cas9 system. *Nat Protoc* *8*, 2281-2308. 10.1038/nprot.2013.143.
239. Xiao, T., Li, W., Wang, X., Xu, H., Yang, J., Wu, Q., Huang, Y., Geradts, J., Jiang, P., Fei, T., Chi, D., et al. (2018). Estrogen-regulated feedback loop limits the efficacy of estrogen receptor-targeted breast cancer therapy. *Proc Natl Acad Sci U S A* *115*, 7869-7878. 10.1073/pnas.1722617115.
240. Liu, S., Zhang, H., Li, M., Hu, D., Li, C., Ge, B., Jin, B., and Fan, Z. (2013). Recruitment of Grb2 and SHIP1 by the ITT-like motif of TIGIT suppresses granule polarization and cytotoxicity of NK cells. *Cell Death Differ* *20*, 456-464. 10.1038/cdd.2012.141.
241. Hamilton, J.R., Tsuchida, C.A., Nguyen, D.N., Shy, B.R., McGarrigle, E.R., Sandoval Espinoza, C.R., Carr, D., Blaesche, F., Marson, A., and Doudna, J.A. (2021). Targeted delivery of CRISPR-Cas9 and transgenes enables complex immune cell engineering. *Cell Rep* *35*, 109207. 10.1016/j.celrep.2021.109207.
242. Kubo, Y., Izumida, M., Togawa, K., Zhang, F., and Hayashi, H. (2019). Cytoplasmic R-peptide of murine leukemia virus envelope protein negatively regulates its interaction with the cell surface receptor. *Virology* *532*, 82-87. 10.1016/j.virol.2019.04.005.
243. Melikyan, G.B., Markosyan, R.M., Brener, S.A., Rozenberg, Y., and Cohen, F.S. (2000). Role of the cytoplasmic tail of ecotropic moloney murine leukemia virus Env protein in fusion pore formation. *J Virol* *74*, 447-455. 10.1128/jvi.74.1.447-455.2000.

244. Sandrin, V., Boson, B., Salmon, P., Gay, W., Negre, D., Le Grand, R., Trono, D., and Cosset, F.L. (2002). Lentiviral vectors pseudotyped with a modified RD114 envelope glycoprotein show increased stability in sera and augmented transduction of primary lymphocytes and CD34<sup>+</sup> cells derived from human and nonhuman primates. *Blood* *100*, 823-832. 10.1182/blood-2001-11-0042.
245. McVey, M.J., Spring, C.M., and Kuebler, W.M. (2018). Improved resolution in extracellular vesicle populations using 405 instead of 488 nm side scatter. *J Extracell Vesicles* *7*, 1454776. 10.1080/20013078.2018.1454776.
246. Gardiner, C., Shaw, M., Hole, P., Smith, J., Tannetta, D., Redman, C.W., and Sargent, I.L. (2014). Measurement of refractive index by nanoparticle tracking analysis reveals heterogeneity in extracellular vesicles. *J Extracell Vesicles* *3*, 25361. 10.3402/jev.v3.25361.
247. Eyquem, J., Mansilla-Soto, J., Giavridis, T., van der Stegen, S.J., Hamieh, M., Cunanan, K.M., Odak, A., Gonen, M., and Sadelain, M. (2017). Targeting a CAR to the TRAC locus with CRISPR/Cas9 enhances tumour rejection. *Nature* *543*, 113-117. 10.1038/nature21405.
248. Cofsky, J.C., Soczek, K.M., Knott, G.J., Nogales, E., and Doudna, J.A. (2022). CRISPR-Cas9 bends and twists DNA to read its sequence. *Nat Struct Mol Biol* *29*, 395-402. 10.1038/s41594-022-00756-0.
249. Zhang, Q., Bi, J., Zheng, X., Chen, Y., Wang, H., Wu, W., Wang, Z., Wu, Q., Peng, H., Wei, H., Sun, R., et al. (2018). Blockade of the checkpoint receptor TIGIT prevents NK cell exhaustion and elicits potent anti-tumor immunity. *Nat Immunol* *19*, 723-732. 10.1038/s41590-018-0132-0.
250. Maas, R.J., Hoogstad-van Evert, J.S., Van der Meer, J.M., Mekers, V., Rezaeifard, S., Korman, A.J., de Jonge, P.K., Cany, J., Woestenenk, R., Schaap, N.P., Massuger, L.F., et al. (2020). TIGIT blockade enhances functionality of peritoneal NK cells with altered expression of DNAM-1/TIGIT/CD96 checkpoint molecules in ovarian cancer. *Oncoimmunology* *9*, 1843247. 10.1080/2162402X.2020.1843247.
251. Page, A., Chuvin, N., Valladeau-Guilemond, J., and Depil, S. (2024). Development of NK cell-based cancer immunotherapies through receptor engineering. *Cell Mol Immunol* *21*, 315-331. 10.1038/s41423-024-01145-x.
252. Kilgour, M.K., Bastin, D.J., Lee, S.H., Ardolino, M., McComb, S., and Visram, A. (2023). Advancements in CAR-NK therapy: lessons to be learned from CAR-T therapy. *Front Immunol* *14*, 1166038. 10.3389/fimmu.2023.1166038.
253. Li, Y., Basar, R., Wang, G., Liu, E., Moyes, J.S., Li, L., Kerbauy, L.N., Uprety, N., Fathi, M., Rezvan, A., Banerjee, P.P., et al. (2022). KIR-based inhibitory CARs overcome CAR-NK cell trogocytosis-mediated fratricide and tumor escape. *Nat Med* *28*, 2133-2144. 10.1038/s41591-022-02003-x.
254. Xie, G., Dong, H., Liang, Y., Ham, J.D., Rizwan, R., and Chen, J. (2020). CAR-NK cells: A promising cellular immunotherapy for cancer. *EBioMedicine* *59*, 102975. 10.1016/j.ebiom.2020.102975.

255. Mansouri, V., Yazdanpanah, N., and Rezaei, N. (2022). The immunologic aspects of cytokine release syndrome and graft versus host disease following CAR T cell therapy. *Int Rev Immunol* *41*, 649-668. 10.1080/08830185.2021.1984449.
256. Kyle, R.A., and Rajkumar, S.V. (2008). Multiple myeloma. *Blood* *111*, 2962-2972. 10.1182/blood-2007-10-078022.
257. Lin, Y., Raje, N.S., Berdeja, J.G., Siegel, D.S., Jagannath, S., Madduri, D., Liedtke, M., Rosenblatt, J., Maus, M.V., Massaro, M., Petrocca, F., et al. (2023). Idecabtagene vicleucel for relapsed and refractory multiple myeloma: post hoc 18-month follow-up of a phase 1 trial. *Nat Med* *29*, 2286-2294. 10.1038/s41591-023-02496-0.
258. Rajkumar, S.V. (2022). Multiple myeloma: 2022 update on diagnosis, risk stratification, and management. *Am J Hematol* *97*, 1086-1107. 10.1002/ajh.26590.
259. Jagannath, S., Heffner, L.T., Jr., Ailawadhi, S., Munshi, N.C., Zimmerman, T.M., Rosenblatt, J., Lonial, S., Chanan-Khan, A., Rühle, M., Rharbaoui, F., Haeder, T., et al. (2019). Indatuximab Ravtansine (BT062) Monotherapy in Patients With Relapsed and/or Refractory Multiple Myeloma. *Clin Lymphoma Myeloma Leuk* *19*, 372-380. 10.1016/j.clml.2019.02.006.
260. Luanpitpong, S., Poohadsuan, J., Klaihmon, P., and Issaragrisil, S. (2021). Selective Cytotoxicity of Single and Dual Anti-CD19 and Anti-CD138 Chimeric Antigen Receptor-Natural Killer Cells against Hematologic Malignancies. *J Immunol Res* *2021*, 5562630. 10.1155/2021/5562630.
261. Riccardi, F., Tangredi, C., Dal Bo, M., and Toffoli, G. (2024). Targeted therapy for multiple myeloma: an overview on CD138-based strategies. *Front Oncol* *14*, 1370854. 10.3389/fonc.2024.1370854.
262. Okuma, A. (2021). Generation of CAR-T Cells by Lentiviral Transduction. *Methods Mol Biol* *2312*, 3-14. 10.1007/978-1-0716-1441-9\_1.
263. Cabrera, A., Edelstein, H.I., Glykofrydis, F., Love, K.S., Palacios, S., Tycko, J., Zhang, M., Lensch, S., Shields, C.E., Livingston, M., Weiss, R., et al. (2022). The sound of silence: Transgene silencing in mammalian cell engineering. *Cell Syst* *13*, 950-973. 10.1016/j.cels.2022.11.005.
264. Selim, O., Song, C., Kumar, A., Phelan, R., Singh, A., and Federman, N. (2023). A review of the therapeutic potential of histone deacetylase inhibitors in rhabdomyosarcoma. *Front Oncol* *13*, 1244035. 10.3389/fonc.2023.1244035.
265. Somanchi, S.S., Senyukov, V.V., Denman, C.J., and Lee, D.A. (2011). Expansion, purification, and functional assessment of human peripheral blood NK cells. *J Vis Exp*. 10.3791/2540.
266. Bloemberg, D., Nguyen, T., MacLean, S., Zafer, A., Gadoury, C., Gurnani, K., Chattopadhyay, A., Ash, J., Lippens, J., Harcus, D., Page, M., et al. (2020). A High-Throughput Method for Characterizing Novel Chimeric Antigen Receptors in Jurkat Cells. *Mol Ther Methods Clin Dev* *16*, 238-254. 10.1016/j.omtm.2020.01.012.

267. Koh, S.K., Park, J., Kim, S.E., Lim, Y., Phan, M.T., Kim, J., Hwang, I., Ahn, Y.O., Shin, S., Doh, J., and Cho, D. (2022). Natural Killer Cell Expansion and Cytotoxicity Differ Depending on the Culture Medium Used. *Ann Lab Med* 42, 638-649. 10.3343/alm.2022.42.6.638.
268. Arguello, R.J., Combes, A.J., Char, R., Gigan, J.P., Baaziz, A.I., Bousiquot, E., Camosseto, V., Samad, B., Tsui, J., Yan, P., Boissonneau, S., et al. (2020). SCENITH: A Flow Cytometry-Based Method to Functionally Profile Energy Metabolism with Single-Cell Resolution. *Cell Metab* 32, 1063-1075 e1067. 10.1016/j.cmet.2020.11.007.
269. Brown, C.E., Wright, C.L., Naranjo, A., Vishwanath, R.P., Chang, W.C., Olivares, S., Wagner, J.R., Bruins, L., Raubitschek, A., Cooper, L.J., and Jensen, M.C. (2005). Biophotonic cytotoxicity assay for high-throughput screening of cytolytic killing. *J Immunol Methods* 297, 39-52. 10.1016/j.jim.2004.11.021.
270. Schanda, N., Sauer, T., Kunz, A., Huckelhoven-Krauss, A., Neuber, B., Wang, L., Hinkelbein, M., Sedloev, D., He, B., Schubert, M.L., Muller-Tidow, C., et al. (2021). Sensitivity and Specificity of CD19.CAR-T Cell Detection by Flow Cytometry and PCR. *Cells* 10. 10.3390/cells10113208.
271. Connolly, R.M., Rudek, M.A., and Piekarz, R. (2017). Entinostat: a promising treatment option for patients with advanced breast cancer. *Future Oncol* 13, 1137-1148. 10.2217/fon-2016-0526.
272. Al-Khafaji, A.S.K., Wang, L.M., Alabdei, H.H., and Liloglou, T. (2024). Effect of valproic acid on histone deacetylase expression in oral cancer (Review). *Oncol Lett* 27, 197. 10.3892/ol.2024.14330.
273. Leus, N.G., van der Wouden, P.E., van den Bosch, T., Hooghiemstra, W.T.R., Ourailidou, M.E., Kistemaker, L.E., Bischoff, R., Gosens, R., Haisma, H.J., and Dekker, F.J. (2016). HDAC 3-selective inhibitor RGFP966 demonstrates anti-inflammatory properties in RAW 264.7 macrophages and mouse precision-cut lung slices by attenuating NF-kappaB p65 transcriptional activity. *Biochem Pharmacol* 108, 58-74. 10.1016/j.bcp.2016.03.010.
274. Reichenbach, P., Giordano Attianese, G.M.P., Ouchen, K., Cribioli, E., Triboulet, M., Ash, S., Saillard, M., Vuillefroy de Silly, R., Coukos, G., and Irving, M. (2023). A lentiviral vector for the production of T cells with an inducible transgene and a constitutively expressed tumour-targeting receptor. *Nat Biomed Eng* 7, 1063-1080. 10.1038/s41551-023-01013-5.
275. Giordano Attianese, G.M.P., Ash, S., and Irving, M. (2023). Coengineering specificity, safety, and function into T cells for cancer immunotherapy. *Immunol Rev* 320, 166-198. 10.1111/imr.13252.
276. Maia, A., Tarannum, M., Lerias, J.R., Piccinelli, S., Borrego, L.M., Maeurer, M., Romee, R., and Castillo-Martin, M. (2024). Building a Better Defense: Expanding and Improving Natural Killer Cells for Adoptive Cell Therapy. *Cells* 13. 10.3390/cells13050451.

277. Naeimi Kararoudi, M., Likhite, S., Elmas, E., Yamamoto, K., Schwartz, M., Sorathia, K., de Souza Fernandes Pereira, M., Sezgin, Y., Devine, R.D., Lyberger, J.M., Behbehani, G.K., et al. (2022). Optimization and validation of CAR transduction into human primary NK cells using CRISPR and AAV. *Cell Rep Methods* 2, 100236. 10.1016/j.crmeth.2022.100236.
278. Bianchi, G., and Ghobrial, I.M. (2014). Biological and Clinical Implications of Clonal Heterogeneity and Clonal Evolution in Multiple Myeloma. *Curr Cancer Ther Rev* 10, 70-79. 10.2174/157339471002141124121404.
279. Corre, J., Munshi, N., and Avet-Loiseau, H. (2015). Genetics of multiple myeloma: another heterogeneity level? *Blood* 125, 1870-1876. 10.1182/blood-2014-10-567370.
280. Wang, C., Wang, W., Wang, M., Deng, J., Sun, C., Hu, Y., and Luo, S. (2024). Different evasion strategies in multiple myeloma. *Front Immunol* 15, 1346211. 10.3389/fimmu.2024.1346211.
281. Weir, P., Donaldson, D., McMullin, M.F., and Crawford, L. (2023). Metabolic Alterations in Multiple Myeloma: From Oncogenesis to Proteasome Inhibitor Resistance. *Cancers (Basel)* 15. 10.3390/cancers15061682.
282. Hogan, K.A., Chini, C.C.S., and Chini, E.N. (2019). The Multi-faceted Ecto-enzyme CD38: Roles in Immunomodulation, Cancer, Aging, and Metabolic Diseases. *Front Immunol* 10, 1187. 10.3389/fimmu.2019.01187.
283. Atanackovic, D., Steinbach, M., Radhakrishnan, S.V., and Luetkens, T. (2016). Immunotherapies targeting CD38 in Multiple Myeloma. *Oncoimmunology* 5, e1217374. 10.1080/2162402X.2016.1217374.
284. Costa, F., Dalla Palma, B., and Giuliani, N. (2019). CD38 Expression by Myeloma Cells and Its Role in the Context of Bone Marrow Microenvironment: Modulation by Therapeutic Agents. *Cells* 8. 10.3390/cells8121632.
285. Horenstein, A.L., Bracci, C., Morandi, F., and Malavasi, F. (2019). CD38 in Adenosinergic Pathways and Metabolic Re-programming in Human Multiple Myeloma Cells: In-tandem Insights From Basic Science to Therapy. *Front Immunol* 10, 760. 10.3389/fimmu.2019.00760.
286. Sanchez, L., Wang, Y., Siegel, D.S., and Wang, M.L. (2016). Daratumumab: a first-in-class CD38 monoclonal antibody for the treatment of multiple myeloma. *J Hematol Oncol* 9, 51. 10.1186/s13045-016-0283-0.
287. de Weers, M., Tai, Y.T., van der Veer, M.S., Bakker, J.M., Vink, T., Jacobs, D.C., Oomen, L.A., Peipp, M., Valerius, T., Slootstra, J.W., Mutis, T., et al. (2011). Daratumumab, a novel therapeutic human CD38 monoclonal antibody, induces killing of multiple myeloma and other hematological tumors. *J Immunol* 186, 1840-1848. 10.4049/jimmunol.1003032.
288. Overdijk, M.B., Verploegen, S., Bogels, M., van Egmond, M., Lammerts van Bueren, J.J., Mutis, T., Groen, R.W., Breij, E., Martens, A.C., Bleeker, W.K., and Parren, P.W. (2015). Antibody-mediated phagocytosis contributes to the anti-tumor activity of the

- therapeutic antibody daratumumab in lymphoma and multiple myeloma. *MAbs* 7, 311-321. 10.1080/19420862.2015.1007813.
289. Bhatnagar, V., Gormley, N.J., Luo, L., Shen, Y.L., Sridhara, R., Subramaniam, S., Shen, G., Ma, L., Shord, S., Goldberg, K.B., Farrell, A.T., et al. (2017). FDA Approval Summary: Daratumumab for Treatment of Multiple Myeloma After One Prior Therapy. *Oncologist* 22, 1347-1353. 10.1634/theoncologist.2017-0229.
  290. Usmani, S.Z., Nahi, H., Plesner, T., Weiss, B.M., Bahlis, N.J., Belch, A., Voorhees, P.M., Laubach, J.P., van de Donk, N., Ahmadi, T., Uhlar, C.M., et al. (2020). Daratumumab monotherapy in patients with heavily pretreated relapsed or refractory multiple myeloma: final results from the phase 2 GEN501 and SIRIUS trials. *Lancet Haematol* 7, e447-e455. 10.1016/S2352-3026(20)30081-8.
  291. Usmani, S.Z., Weiss, B.M., Plesner, T., Bahlis, N.J., Belch, A., Lonial, S., Lokhorst, H.M., Voorhees, P.M., Richardson, P.G., Chari, A., Sasser, A.K., et al. (2016). Clinical efficacy of daratumumab monotherapy in patients with heavily pretreated relapsed or refractory multiple myeloma. *Blood* 128, 37-44. 10.1182/blood-2016-03-705210.
  292. Casneuf, T., Xu, X.S., Adams, H.C., 3rd, Axel, A.E., Chiu, C., Khan, I., Ahmadi, T., Yan, X., Lonial, S., Plesner, T., Lokhorst, H.M., et al. (2017). Effects of daratumumab on natural killer cells and impact on clinical outcomes in relapsed or refractory multiple myeloma. *Blood Adv* 1, 2105-2114. 10.1182/bloodadvances.2017006866.
  293. Veliz, K., Shen, F., Shestova, O., Shestov, M., Shestov, A., Sleiman, S., Hansen, T., O'Connor, R.S., and Gill, S. (2024). Deletion of CD38 enhances CD19 chimeric antigen receptor T cell function. *Mol Ther Oncol* 32, 200819. 10.1016/j.omton.2024.200819.
  294. Greenstein, S., Krett, N.L., Kurosawa, Y., Ma, C., Chauhan, D., Hideshima, T., Anderson, K.C., and Rosen, S.T. (2003). Characterization of the MM.1 human multiple myeloma (MM) cell lines: a model system to elucidate the characteristics, behavior, and signaling of steroid-sensitive and -resistant MM cells. *Exp Hematol* 31, 271-282. 10.1016/s0301-472x(03)00023-7.
  295. Nakamura, A., Suzuki, S., Kanasugi, J., Ejiri, M., Hanamura, I., Ueda, R., Seto, M., and Takami, A. (2021). Synergistic Effects of Venetoclax and Daratumumab on Antibody-Dependent Cell-Mediated Natural Killer Cytotoxicity in Multiple Myeloma. *Int J Mol Sci* 22. 10.3390/ijms221910761.
  296. Boivin, W.A., Cooper, D.M., Hiebert, P.R., and Granville, D.J. (2009). Intracellular versus extracellular granzyme B in immunity and disease: challenging the dogma. *Lab Invest* 89, 1195-1220. 10.1038/labinvest.2009.91.
  297. Barnes, S.A., Trew, I., de Jong, E., and Foley, B. (2021). Making a Killer: Selecting the Optimal Natural Killer Cells for Improved Immunotherapies. *Front Immunol* 12, 765705. 10.3389/fimmu.2021.765705.
  298. Mueller, S., Millonig, G., and Waite, G.N. (2009). The GOX/CAT system: a novel enzymatic method to independently control hydrogen peroxide and hypoxia in cell culture. *Adv Med Sci* 54, 121-135. 10.2478/v10039-009-0042-3.

299. Phan, M.T., Kim, J., Koh, S.K., Lim, Y., Yu, H., Lee, M., Lee, J.M., Kang, E.S., Kim, H.Y., Kim, S.K., Hwang, I., et al. (2022). Selective Expansion of NKG2C<sup>+</sup> Adaptive NK Cells Using K562 Cells Expressing HLA-E. *Int J Mol Sci* 23. 10.3390/ijms23169426.
300. Shenouda, M.M., Gillgrass, A., Nham, T., Hogg, R., Lee, A.J., Chew, M.V., Shafaei, M., Aarts, C., Lee, D.A., Hassell, J., Bane, A., et al. (2017). *Ex vivo* expanded natural killer cells from breast cancer patients and healthy donors are highly cytotoxic against breast cancer cell lines and patient-derived tumours. *Breast Cancer Res* 19, 76. 10.1186/s13058-017-0867-9.
301. Kim, G.H., Dang, H.N., Phan, M.T., Kweon, S.H., Chun, S., and Cho, D. (2018). X-ray as Irradiation Alternative for K562 Feeder Cell Inactivation in Human Natural Killer Cell Expansion. *Anticancer Res* 38, 5767-5772. 10.21873/anticancer.12915.
302. Xiang, M., Li, H., Zhan, Y., Ma, D., Gao, Q., and Fang, Y. (2024). Functional CRISPR screens in T cells reveal new opportunities for cancer immunotherapies. *Mol Cancer* 23, 73. 10.1186/s12943-024-01987-z.
303. Maltseva, M., and Langlois, M.A. (2022). Flow Virometry for Characterizing the Size, Concentration, and Surface Antigens of Viruses. *Curr Protoc* 2, e368. 10.1002/cpz1.368.
304. Graham, L., and Orenstein, J.M. (2007). Processing tissue and cells for transmission electron microscopy in diagnostic pathology and research. *Nat Protoc* 2, 2439-2450. 10.1038/nprot.2007.304.
305. Richert-Poggeler, K.R., Franzke, K., Hipp, K., and Kleespies, R.G. (2018). Electron Microscopy Methods for Virus Diagnosis and High Resolution Analysis of Viruses. *Front Microbiol* 9, 3255. 10.3389/fmicb.2018.03255.
306. Yi, H., Strauss, J.D., Ke, Z., Alonas, E., Dillard, R.S., Hampton, C.M., Lamb, K.M., Hammonds, J.E., Santangelo, P.J., Spearman, P.W., and Wright, E.R. (2015). Native immunogold labeling of cell surface proteins and viral glycoproteins for cryo-electron microscopy and cryo-electron tomography applications. *J Histochem Cytochem* 63, 780-792. 10.1369/0022155415593323.
307. Shalem, O., Sanjana, N.E., Hartenian, E., Shi, X., Scott, D.A., Mikkelsen, T., Heckl, D., Ebert, B.L., Root, D.E., Doench, J.G., and Zhang, F. (2014). Genome-scale CRISPR-Cas9 knockout screening in human cells. *Science* 343, 84-87. 10.1126/science.1247005.
308. Sanjana, N.E., Shalem, O., and Zhang, F. (2014). Improved vectors and genome-wide libraries for CRISPR screening. *Nat Methods* 11, 783-784. 10.1038/nmeth.3047.
309. Counsell, J.R., Asgarian, Z., Meng, J., Ferrer, V., Vink, C.A., Howe, S.J., Waddington, S.N., Thrasher, A.J., Muntoni, F., Morgan, J.E., and Danos, O. (2017). Lentiviral vectors can be used for full-length dystrophin gene therapy. *Sci Rep* 7, 44775. 10.1038/srep44775.

310. Cante-Barrett, K., Mendes, R.D., Smits, W.K., van Helsdingen-van Wijk, Y.M., Pieters, R., and Meijerink, J.P. (2016). Lentiviral gene transfer into human and murine hematopoietic stem cells: size matters. *BMC Res Notes* 9, 312. 10.1186/s13104-016-2118-z.
311. Roybal, K.T., Williams, J.Z., Morsut, L., Rupp, L.J., Kolinko, I., Choe, J.H., Walker, W.J., McNally, K.A., and Lim, W.A. (2016). Engineering T Cells with Customized Therapeutic Response Programs Using Synthetic Notch Receptors. *Cell* 167, 419-432 e416. 10.1016/j.cell.2016.09.011.
312. Hu, Y., Zhou, Y., Zhang, M., Ge, W., Li, Y., Yang, L., Wei, G., Han, L., Wang, H., Yu, S., Chen, Y., et al. (2021). CRISPR/Cas9-Engineered Universal CD19/CD22 Dual-Targeted CAR-T Cell Therapy for Relapsed/Refractory B-cell Acute Lymphoblastic Leukemia. *Clin Cancer Res* 27, 2764-2772. 10.1158/1078-0432.CCR-20-3863.
313. Johansen, K.H. (2022). How CRISPR/Cas9 Gene Editing Is Revolutionizing T Cell Research. *DNA Cell Biol* 41, 53-57. 10.1089/dna.2021.0579.

# Appendix

## Supplementary Figures

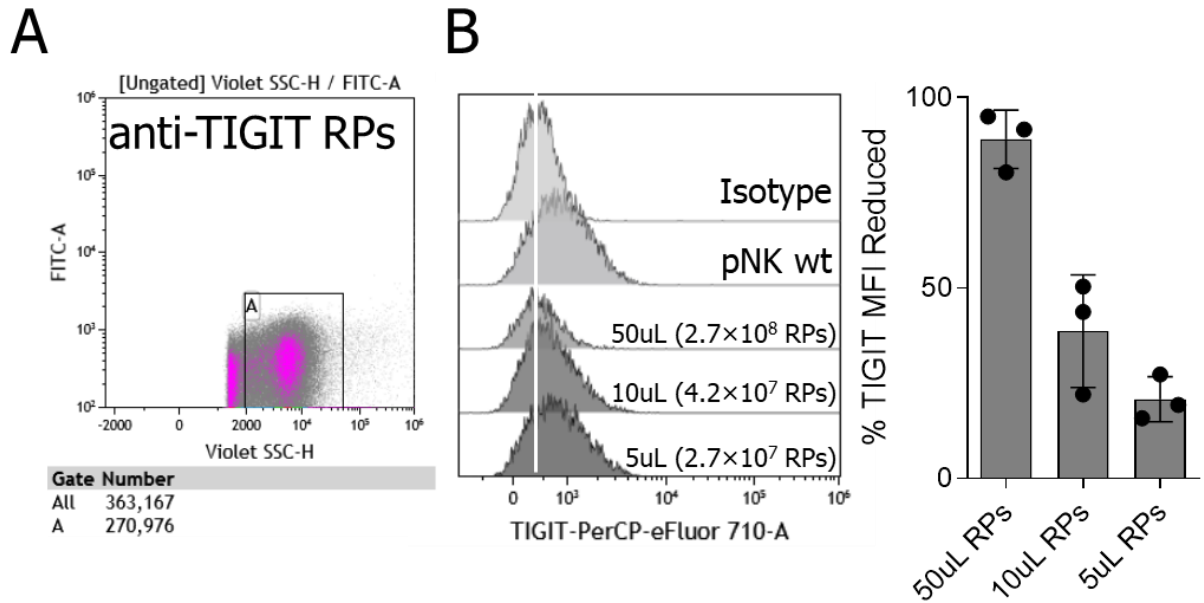


**Figure S1 The number of RPs for human primary NK cell TIGIT knockout. (A)** Representative dot-plot to gate RPs **(B)** Volume-based TIGIT knockout in NK cells and the number of particles in each volume.

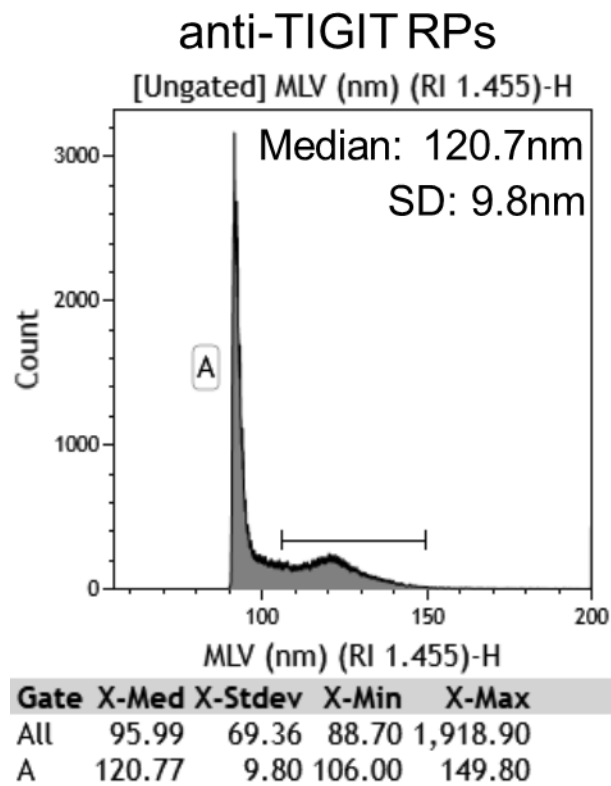


**Figure S2 Size of RPs.** RPs were calculated by FCMPASS based on polystyrene standard beads and the MLV refractive index, 1.455. X-Med; Median, X-Stdev (SD); Standard deviation, X-Min; Minimum, X-Max, Maximum.

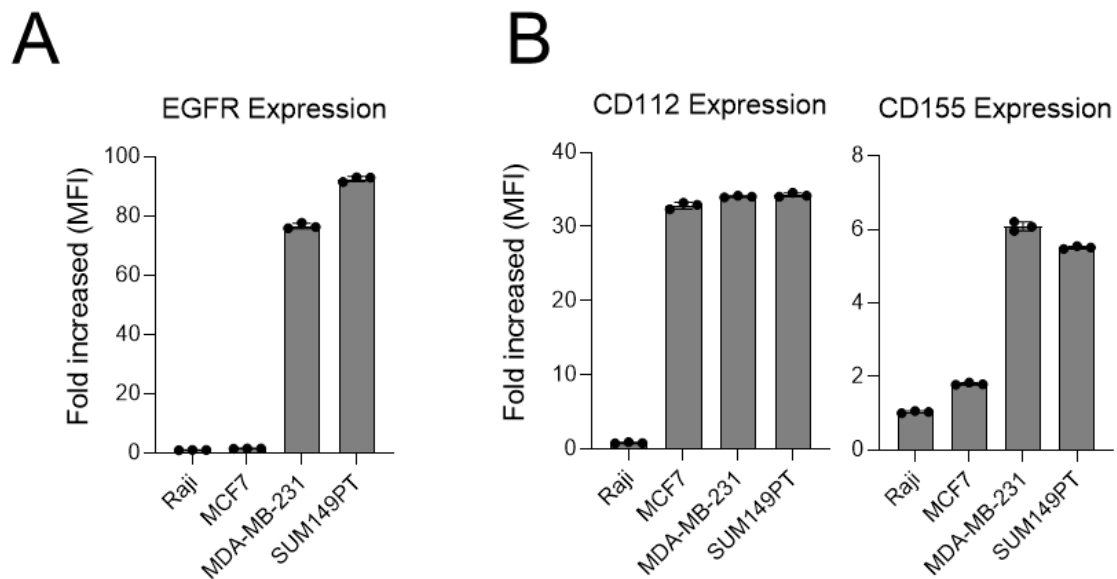


**Figure S3 Determination of EGFR and TIGIT ligand expression (CD112 and CD155) on various cancer cell lines. (A)** Surface EGFR expression on B cell lymphoma, estrogen receptor-positive, and triple-negative breast cancer cell lines. **(B)** Surface expression of TIGIT ligands CD112 and CD155 on the cancer cell lines.

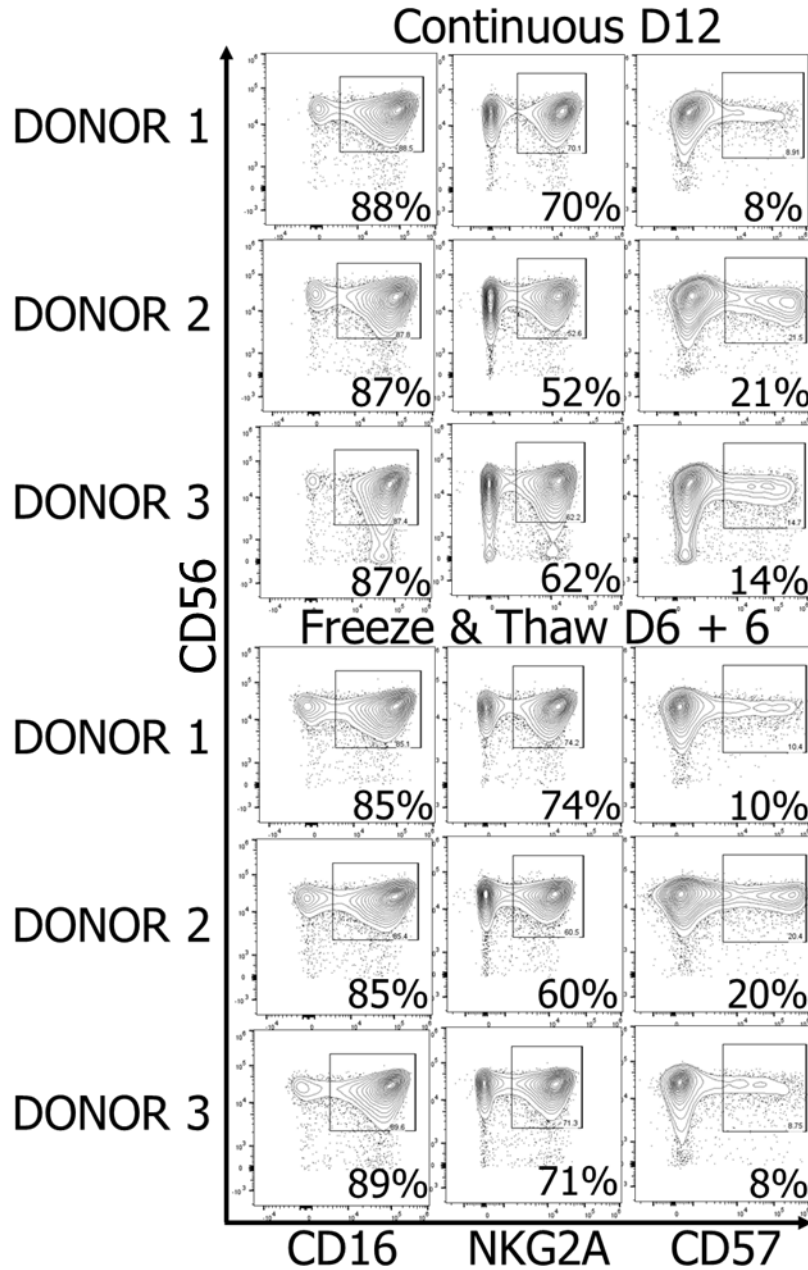


**Figure S4 NK cell population markers in continuously expanded and early cryopreserved-expanded NK cells.** Human primary NK cells were expanded over a period of 12 days. Cryopreservation was performed on day six of the expansion process. NK cells from three different donors (n=3) were used for analysis.

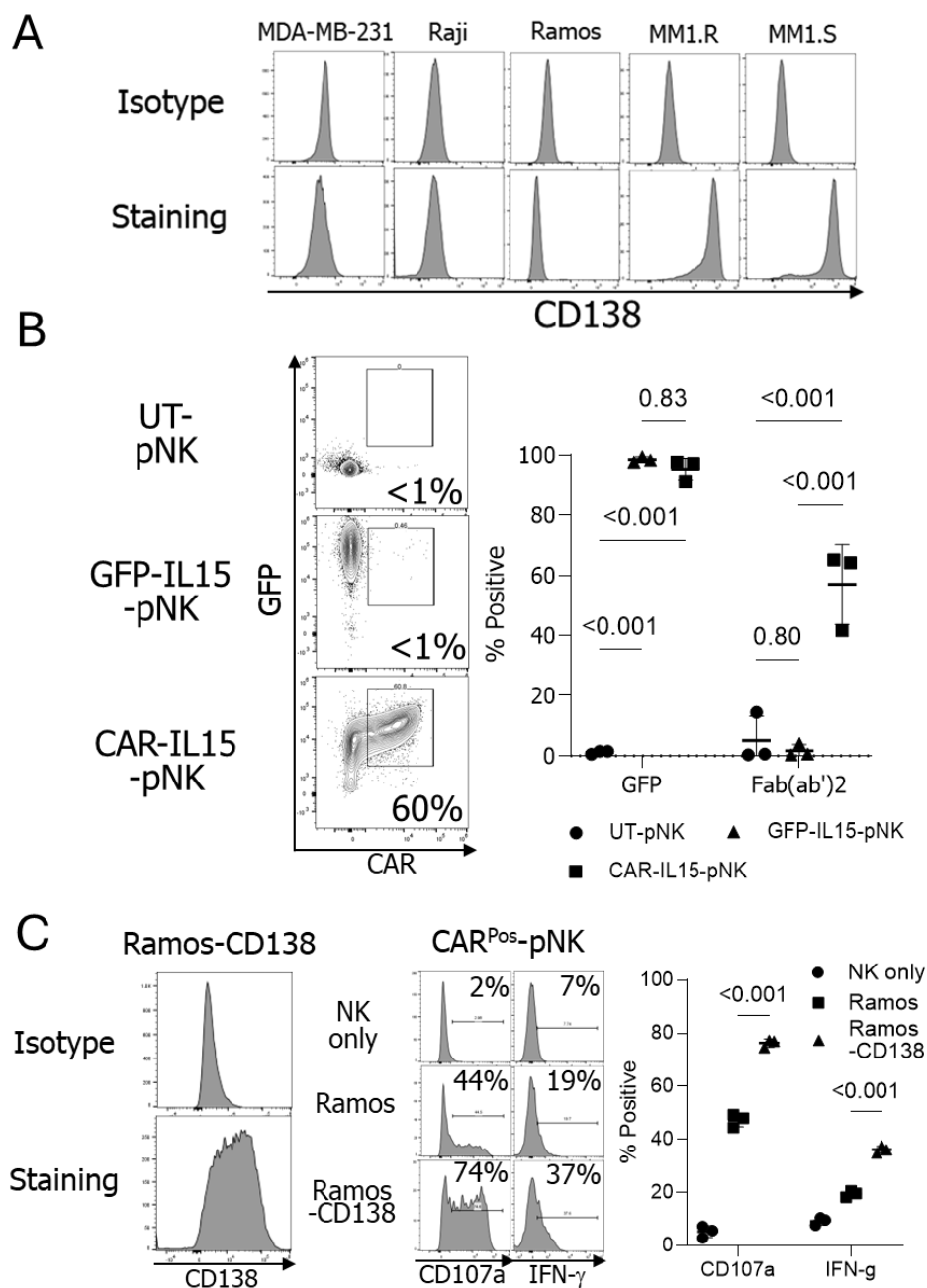


**Figure S5 CD138 expression in target cells and CAR functionality in pNK cells. (A)** CD138 expression in the target cells used in this study was confirmed by flow cytometry. **(B)** GFP and CAR expression in modified pNK cells. (n=3 cryopreserved donors' NK cells) **(C)** CAR activity confirmation using CD138-expressing Ramos cells.

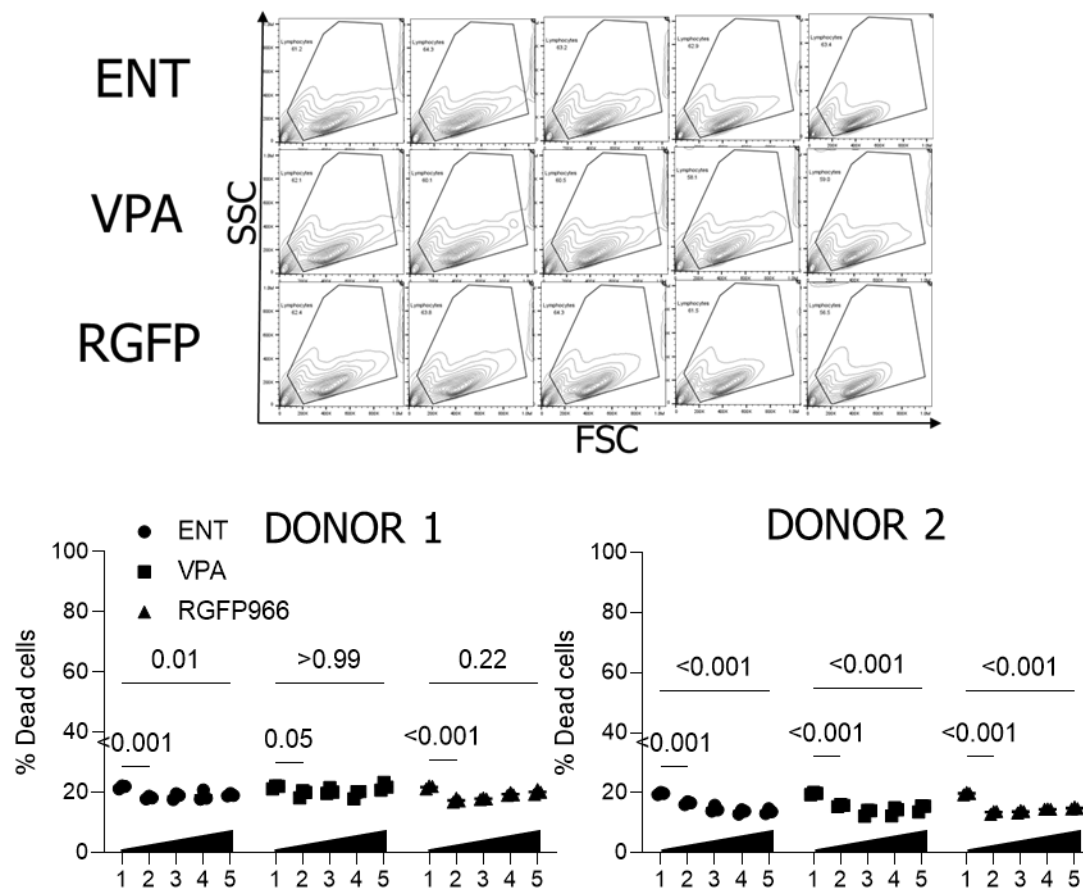


**Figure S6 HDACi toxicity.** HDACi toxicity was assessed using flow cytometry, with dead cells identified within gated areas. Cells were exposed to various concentrations of inhibitors for two days. The concentrations tested were as follows: ENT: 0  $\mu$ M, 0.1  $\mu$ M, 0.3  $\mu$ M, 0.5  $\mu$ M, and 1  $\mu$ M; VPA: 0 mM, 0.1 mM, 0.3 mM, 0.5 mM, and 1 mM; RGFP966: 0  $\mu$ M, 2.5  $\mu$ M, 5  $\mu$ M, 10  $\mu$ M, and 20  $\mu$ M.

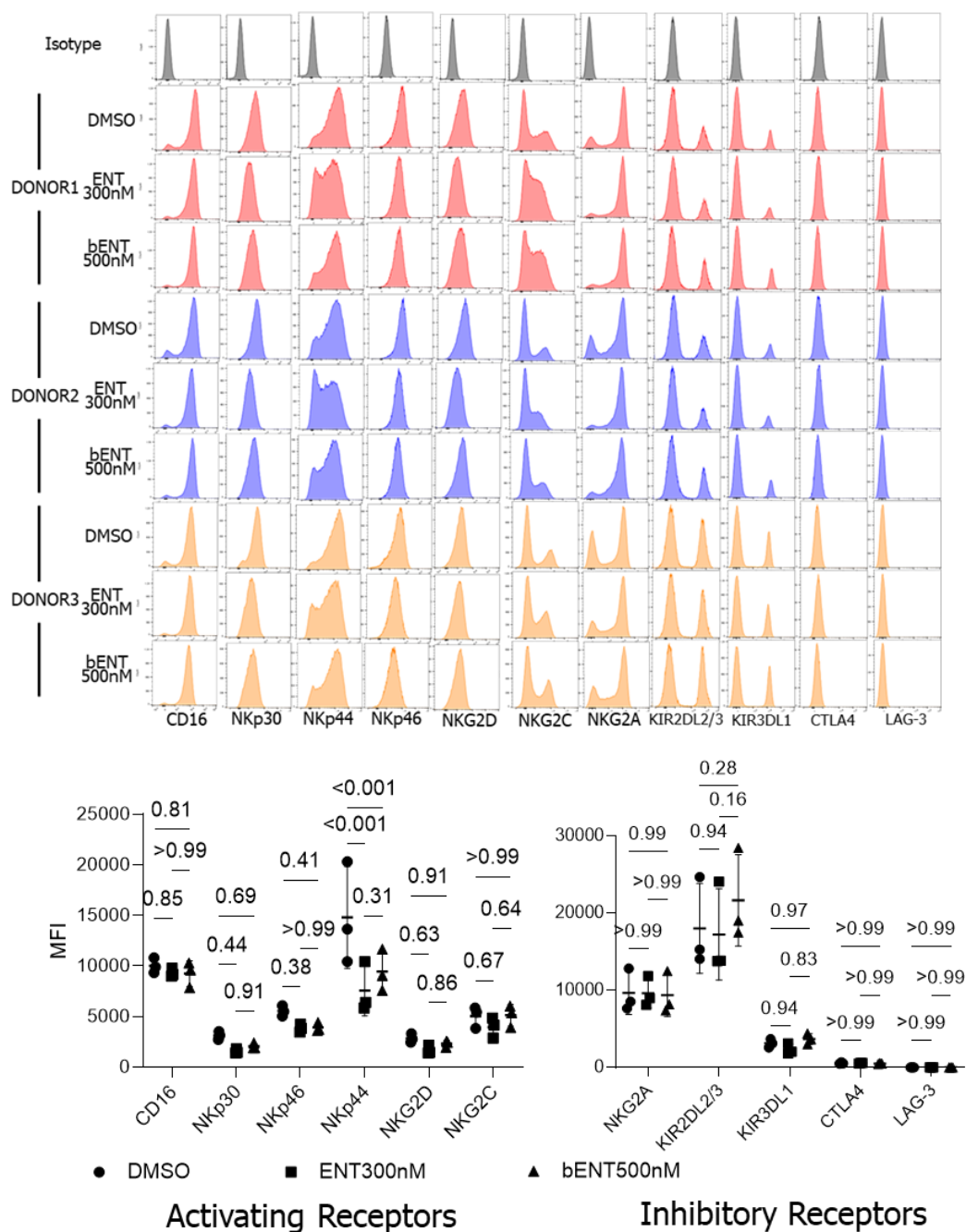


**Figure S7 Phenotypes of ENT-treated NK cells.** NK cells were modified and expanded for five days (TD + 5), followed by further expansion for an additional seven days, either with or without 300 nM ENT. On TD + 9, DMSO-treated NK cells were divided into two conditions: DMSO or 500 nM ENT (bENT500nM). On TD + 12, NK cells were phenotyped by immunostaining.

# Curriculum Vitae: Dong-Hyeon Jo

---

## Educations

**2020/09 ~ 2025/05:** Ph.D. fast-track in Microbiology and Immunology, University of Ottawa, Canada

MIC5100 Pathogen Interactions and Host, **A**

MIC8122 Advanced Topic in Immunology, **A+**

MIC8238 Advanced Topics in Bacteriology – Mechanisms of Pathogenesis, **A+**

BCH8310 Current Topic in RNA Molecular Biology, **A+**

**2012/03 ~ 2019/08:** B.Sc in Microbiology (2 years in the military and 1 year traveling), Chung-Buk National University, South Korea, **GPA 3.51/4.0**

---

## Scholarships and awards

**BMI Seminar Day - Poster Presentation Award** (06/2024)  
150 CAD

**Ontario Graduate Scholarship (OGS)** (05/2024~05/2025)  
15,000 CAD total

**Ontario Graduate Scholarship (OGS)** (05/2023~05/2024)  
15,000 CAD total

**Admission Scholarship** (09/2022~09/2026)  
University of Ottawa (Ph.D.)  
36,000 CAD

**Admission Scholarship** (09/2020~09/2022)  
University of Ottawa (MSc)  
15,000 CAD

---

## Publications

**2025**, Minji Park, Yuree Lim, Yujung Jo, **Dong-Hyeon Jo**, Sang-ki Kim, Hyun-Young Kim, Seung-Hwan Lee, Mijeong Lee, Duck Cho. **BaEV-Pseudotyped Lentiviral Transduction Facilitates Stable CAR expression on NK cells and Sustains Robust CAR-Mediated Cytotoxicity.** *Molecular Therapy Method & Clinical Development*, Submitted in April 2025.

**2025**, Shelby Kaczmarek, **Dong-Hyeon Jo**, Stefania Berton, Safa Ghaziasgar, Bryan Marr, Lisheng Wang, Mihue Jang, Alissa Visram, Scott McComb, and Seung-Hwan Lee. **Anti-BCMA-CAR-IL15 natural killer cells prevent multiple myeloma growth in the bone marrow but allow later emergence of extramedullary disease.** *Journal for Immunotherapy of Cancer*, Submitted in March 2025.

**2025**, Bryan Mar, **Dong-Hyeon Jo**, Mihue Jang, and Seung-Hwan Lee. **Cytokines in Focus: IL-2 and IL-15 in Natural Killer Adoptive Cell Cancer Immunotherapy.** *Immune*

*Network*, doi: <https://doi.org/10.4110/in.2025.25.e17>

**2025, Dong-Hyeon Jo**, Shelby Kaczmarek, Abrar Ul Haq Khan, Jannat Perkin, Diana M Clark, Lisheng Wang, Scott McComb, Alissa Visram, and Seung-Hwan Lee. **Entinostat, a Histone Deacetylase Inhibitor, Enhances CAR-NK Cell Anti-Tumor Activity by Sustaining CAR Expression.** *Frontiers in Immunology*, doi: <https://doi.org/10.3389/fimmu.2025.1533044>

**2023, Dong-Hyeon Jo**, Shelby Kaczmarek, Oksu Shin, Lisheng Wang, Juthaporn Cowan, Scott McComb, and Seung-Hwan Lee. **Simultaneous Engineering of Natural Killer Cells for CAR Transgenesis and CRISPR-Cas9 Knockout using Retroviral Particles** *Molecular Therapy Methods and Clinical Development*, doi: <https://doi.org/10.1016/j.omtm.2023.03.006>

**2023**, Abrar Ul Haq Khan, Alaa Kassim Ali, Bryan Marr, **Dong-Hyeon Jo**, Simin Ahmadvand, Claire Fong-McMaster, Saeedah MUSAED Almutairi, Lisheng Wang, Subash Sad, Mary-Ellen Harper, and Seung-Hwan Lee **The TNF $\alpha$ /TNFR2 axis mediates natural killer cell proliferation by promoting aerobic glycolysis** *Cellular & Molecular Immunology*, doi: <https://doi.org/10.1038/s41423-023-01071-4>

**2021**, Henk van Faassen, **Dong-Hyeon Jo**, Shannon Ryan, Michael J Lowden, Shalini Raphael, C Roger MacKenzie, Seung-Hwan Lee, Greg Hussack, and Kevin A Henry. **Incorporation of a Novel CD16-Specific Single-Domain Antibody into Multispecific Natural Killer Cell Engagers with Potent ADCC** *Molecular Pharmaceutics*, doi: [10.1021/acs.molpharmaceut.1c00208](https://doi.org/10.1021/acs.molpharmaceut.1c00208)

**2020**, Faria Ahmed, **Dong-Hyeon Jo**, and Seung-Hwan Lee. **Can natural killer cells be a principal player in anti-SARS-CoV-2 immunity?** *Frontiers in Immunology*, doi: [10.3389/fimmu.2020.586765](https://doi.org/10.3389/fimmu.2020.586765), 2020.

## Conferences and Seminars

### **The University of Calgary – Recruitment seminar oral presentation**

2024 – NK cell-based cell therapy: Cryopreservation, NK cell engineering, CRISPR-Cas9, and more

### **Canadian Natural Killer Cell Consortium (CanNKC) – Poster presentation**

2024 – CD38 knockout desensitizes Natural Killer Cells from daratumumab-mediated NK cell fratricide

### **Innate Killer Summit – Poster presentation**

2024 – anti-CD138 Chimeric Antigen Receptor Expressing CD38 knock-out NK cell Generation using CRISPR-Cas9-Loaded Retroviral Particles

### **Canadian Natural Killer Cell Consortium (CanNKC) – Poster presentation & Oral presentation**

2023 – Simultaneous Engineering of Natural Killer Cells for CAR Transgenesis and

CRISPR-Cas9 Knock-out using Retroviral Particles

**Canadian Society for Immunology (CSI) – Poster presentation & Oral presentation**

2022 – Efficient Human Natural Killer Cell Genome Editing Using Viral Vector like Cas9-sgRNA Loaded Nanoblades

**Canadian Society for Immunology (CSI) – Poster presentation**

2021 – Hypoxia-inducible cytokine expression in engineered natural killer(NK) cells to target solid tumors

**The American Association of Immunologists (AAI) – Poster presentation**

2020 – Developing natural killer cells producing hypoxia-inducible cytokines for effective immunotherapy against solid tumors

**University of Ottawa Student Seminar – Oral Presentation**

2020 – Hypoxia-inducible cytokine expression in engineered natural killer cells to target solid tumors

**Work in Progress (WIP) Seminar – Oral Presentation**

2020 – Hypoxia-inducible cytokine expression enhances the anti-tumor activity of natural killer cells in the tumor microenvironment

---

**Work and Volunteer Experience**

**Dr. Seung-Hwan Lee's Immunology Laboratory, Canada**

**07.07.2019~ 30.08.2020**

Department of Biochemistry, Microbiology, and Immunology, University of Ottawa  
Junior Technician

- Developed a culturing method to culture Natural Killer (NK) cell lines
- Produced viral vectors to modify NK cells to perform functional assays
- Learned how to use the CRISPR Cas9 system, flow cytometry (Attune), qPCR, PCR
- Optimized transduction and transfection protocols

---

**Training Experience**

I developed most of Dr. Seung-Hwan Lee's laboratory protocols for human NK cells. In doing so, I trained colleagues, alumni, and external scientists, including Shelby Kaczmarek, Bryan Marr, Casey Wang, Daina M. Clark, Safa Ghaziasgar, Dr. Abrar Ul Haq Khan, Oksu Shin, Dr. Sam Kung, and Dr. Alaa Kassim Ali, in key techniques such as general molecular cloning, NK cell expansion, cryopreservation, engineering, and CRISPR-Cas9 applications.

---

**Obtained Skills**

**NK cell engineering and cryopreservation**

CAR-NK cell generation

Antibody-dependent cellular cytotoxicity (ADCC) assay using engineered NK cells  
NK cell cryopreservation

**Molecular cloning**

Restriction enzyme digestion and ligation  
Golden-gate cloning  
Gibson assembly and over-lapping PCR  
Transformation, colony PCR, and sequencing

**Viral vector production and transduction**

Lentiviral and Retroviral vector production  
CRISPR-Cas9 and over-expression  
Primary and cancer cell transduction  
Cell sorting

**Cell culture and Flow cyto and virometry**

Feeder cell irradiation  
Flow cytometer: Attune (Thermofisher)  
Flow virometry: Cytotflex  
Surface and intracellular staining  
Fluorophore selection and compensation

**Mouse handling**

NSG mouse handling, breeding, and weaning  
I.P, I.V, and subcutaneous injection  
Organ extraction and immune cell isolation  
IVIS and Newton, small animal imaging systems  
Saphenous Bleeding

---

**Reference**

**Dr. Seung-Hwan Lee**

Associate Professor  
Department of Biochemistry, Microbiology and Immunology  
University of Ottawa  
Work Email: [Seunglee@uottawa.ca](mailto:Seunglee@uottawa.ca)

**Dr. Sam Kung**

Professor  
Department of Immunology  
University of Manitoba  
Work Email: [sam.kung@umanitoba.ca](mailto:sam.kung@umanitoba.ca)